# ISOLATION AND IDENTIFICATION OF PROTEIN BINDING TO ANION EXCHANGER 1 (AE1) IN HUMAN KIDNEY

**THITIMA KESKANOKWONG**

**A THESIS SUBMITTED IN PARTIAL FULFILLMENT**
**OF THE REQUIREMENTS FOR**
**THE DEGREE OF DOCTOR OF PHILOSOPHY**
**(MOLECULAR GENETICS AND GENETIC ENGINEERING)**
**FACULTY OF GRADUATE STUDIES**
**MAHIDOL UNIVERSITY**
**2007**

Thesis
Entitled

# ISOLATION AND IDENTIFICATION OF PROTEIN BINDING TO ANION EXCHANGER 1 (AE1) IN HUMAN KIDNEY

Thitima Keskanokwong
Mrs. Thitima Keskanokwong
Candidate

V. Akkarapatumwong
Asst. Prof. Varaporn Akkarapatumwong, Ph.D.
Major-Advisor

Witoon Tirasophon
Asst. Prof. Witoon Tirasophon, Ph.D.
Co-Advisor

Pa-thai Yenchitsomanus
Prof. Pa-thai Yenchitsomanus, Ph.D.
Co-Advisor

Asst. Prof. Lily Eurwilaichitr, Ph.D.
Co-Advisor

Sakol Panyim
Prof. Sakol Panyim, Ph.D.
Co-Advisor

Prof. M.R. Jisnuson Svasti, Ph.D.
Dean
Faculty of Graduate Studies

V. Akkarapatumwong
Asst. Prof. Varaporn Akkarapatumwong, Ph.D.
Chair
Doctor of Philosophy Programme in
Molecular Genetics and Genetic Engineering
Institute of Molecular Biology and Genetics

Thesis
Entitled

# ISOLATION AND IDENTIFICATION OF PROTEIN BINDING TO ANION EXCHANGER 1 (AE1) IN HUMAN KIDNEY

was submitted to the Faculty of Graduate Studies, Mahidol University
For the degree of Doctor of Philosophy
(Molecular Genetics and Genetic Engineering)
on
27 June 2007

Thitima Keskanokwong
.....
Mrs. Thitima Keskanokwong
Candidate

Apinunt Udomkit
.....
Asst. Prof. Apinunt Udomkit, Ph.D.
Chair

V. Akkarapatumwong
.....
Asst. Prof. Varaporn Akkarapatumwong, Ph.D.
Member

Sophit Wongkham
.....
Assoc. Prof. Sophit Wongkham, Ph.D.
Member

Pa-thai Yenchitsomanus
.....
Prof. Pa-thai Yenchitsomanus, Ph.D.
Member

Witoon Tirasophon
.....
Asst. Prof. Witoon Tirasophon, Ph.D.
Member

Varanuj Chatsudthipong
.....
Assoc. Prof. Varanuj Chatsudthipong, Ph.D.
Member

.....
Prof. M.R. Jisnuson Svasti, Ph.D.
Dean
Faculty of Graduate Studies
Mahidol University

C. Krittanai
.....
Asst. Prof. Chartchai Krittanai, Ph.D.
Acting Director
Institute of Molecular Biology and Genetics
Mahidol University

# ACKNOWLEDGEMENTS

Most of all I would like to thank my research advisor, Asst. Prof. Varaporn Akkarapatumwong, She has given me enormous freedom to pursue my own interests while at the same time providing guidance, stimulating suggestions and encouragement, then helped me in all the time of research and writing of this thesis. She is not only a great scientist with deep vision but also she is the most importantly a kind person.

Part of the thesis work was done while I worked at the Department of Physiology, University of Alberta. I am also grateful thank to Prof. Joe Casey, my co-advisor, who has shown a large and consistent interested in my project during the times of doing experiments, manuscript preparation and submission.

It is also difficult to overstate my gratitude to Prof. Pa-thai Yenchitsomanus, my co-advisor. His generously for suggestions, guidance and support in part of cDNA library, chemicals and DNA sequencing are meaningful that I will always be grateful.

I would also like to thank the members of my thesis defense examination committee: Asst. Prof. Witoon Tirasophon, and Assoc. Prof. Varanuj Chatsudthipong who contributed and providing me with valuable comments on earlier versions of this thesis. Special thanks go to Assoc. Prof. Sopit Wongkham for coming all the way from the Khon Kean University to serve as my external examiner.

I would like to from Royal Golden Jubilee-Ph.D Program of the Thailand Research Fund (TRF) for their kind financial support which in part funded my tuition fee, stipend, and my stay in Canada.

My special thanks to Prof. Reinhart A. F. Reithmeier for valuable suggestion, Dr. Saranya Kittanakom for pulse chase analysis, immunofluorescence staining in MDCK cells and human kidney tissue, and Haley J. Shandro for doing transport activity assay which are valuable contributing and provided data for publication in Journal of Biological Chemistry, Dr. Wanna Thongnoppakhun for providing human kidney cDNA and Prof. Shoukat Dedhar for ILK cDNA. I am also indebted to all members in Casey's laboratory; particularly Dr. Patricio Morgan for training laboratory skills, Anita Quon for chemical ordering.

Many thanks also to the staffs and students at Institute of Molecular Biology and Genetics whose friendship and support have made it more than a temporary place of study. My best friends while I did my master degree at Department of Biochemistry and friends at MMBU of Siriraj Hospital are acknowledged for all the emotional support, comraderie, entertainment, and caring they provided.

Importantly, I wish to thank my beloved Dr. Nattawat Onlamoon who always offers caring, encouragement, and love which help me to get through the difficult time. Last, but certainly not least, I am forever indebted to my parents, my brother who passed away and my little sister for their love, understanding, endless patience and unconditional support when it was the most required. To them I dedicate this thesis. As always it is impossible to mention everybody who had an impact to this work.

Thitima Keskanokwong

ISOLATION AND IDENTIFICATION OF PROTEIN BINDING TO ANION EXCHANGER 1 (AE1) IN HUMAN KIDNEY

THITIMA KESKANOKWONG 4536651 MBMG/D

Ph.D. (MOLECULAR GENETICS AND GENETIC ENGINEERING)

THESIS ADVISORS: VARAPORN AKKARAPATUMWONG, Ph.D., PA-THAI YENCHIT SOMANUS, Ph.D., SAKOL PANYIM, Ph.D., WITOON TIRASOPHON, Ph.D., LILY EURWILAICHITR, Ph.D.

ABSTRACT

Kidney anion exchanger 1 (kAE1) mediates $Cl^-/HCO_3^-$ exchange at the basolateral membrane of kidney α-intercalated cells. It is an isoform of erythroid AE1 (eAE1) and lacks 65 amino acids at its amino terminus. This may cause some structural changes and altered protein-protein interaction in kAE1. Several mutations in the AE1 gene have been found and associated with Distal Renal Tubular Acidosis (dRTA). The proposed mechanism of the dRTA is involved in defects of protein trafficking or mis-targeting to an appropriate site of the α-intercalated cells. Both the C- and N-termini of kAE1 are required for correct basolateral localization of proteins in polarized epithelial cells. However, the human proteins interacting with the N-terminus have not been identified. Therefore, this study aimed to identify proteins interacting with NkAE1 that may be involved in the kAE1 trafficking. Yeast two-hybrid screening revealed interactions with several proteins including integrin-linked kinase (ILK), glyceraldehyde-3-phosphate dehydrogenase (GAPDH) and pantophysin (PPH). Interaction between kAE1 and the selected proteins was demonstrated in the co-expression experiments including co-immunoprecipitation, affinity co-purification and immunofluorescence staining in human embryonic kidney (HEK 293) cells. Interestingly, cell surface biotinylation results showed that ILK, but not GAPDH and pantophysin, promoted cell surface expression of kAE1. ILK also enhanced $Cl^-/HCO_3^-$ transport activity of kAE1 in line with the observed increase of cell surface expression. Mapping analysis revealed that kAE1 interacts with the C-terminus of ILK through the kAE1 calponin homology (CH) domain. In addition, the ankyrin repeats, PH domain and kinase activity of ILK were not required for binding ability to kAE1 and cell surface expression of kAE1. ILK also interacted with eAE1 suggesting that lack of the 65 amino acids of kAE1 would not alter the folded structure of CH domain in eAE1. However, overexpression of ILK did not significantly increase cell surface expression of eAE1 when compared with that of kAE1 in which ILK might play a role in an isoform specific manner as a key protein to increase the level of kAE1 on the cell surface of the kidney cells. Further investigation found that ILK promotes kAE1 expression at the cell surface in HEK 293 cells by forming kAE1-ILK-paxillin-actopaxin complex links kAE1 to the actin cytoskeleton. This study presents data demonstrating that ILK provides a linkage between kAE1 and the underlying actin cytoskeleton to stabilize kAE1 at the plasma membrane, resulting in the higher level of cell surface expression.

KEY WORDS: kAE1 / PROTEIN TRAFFICKING / YEAST TWO-HYBRID / ILK / CH DOMAIN

186 pp.

การแยกและการค้นหาโปรตีนที่มีปฏิสัมพันธ์กับโปรตีนแอนไอออนเอ็กซ์เชงเจอร์-วันในไตของมนุษย์
(ISOLATION AND IDENTIFICATION OF PROTEIN BINDING TO ANION EXCHANGER 1 (AE1) IN HUMAN KIDNEY)

ฐิติมา เกศกนกวงศ์ 4536651 MBMG/D
ปร.ด. (อณูพันธุศาสตร์และพันธุวิศวกรรมศาสตร์)
คณะกรรมการควบคุมวิทยานิพนธ์ : วราภรณ์ อัครปทุมวงศ์, Ph.D., เพทาย เย็นจิตโสมนัส, Ph.D., สกล พันธุ์ยิ้ม, Ph.D., วิทูรย์ ถิระโสภณ, Ph.D., ลิลี่ เอื้อวิไลจิตร, Ph.D.

บทคัดย่อ

โปรตีน kidney anion exchanger 1 (kAE1) ทำหน้าที่ในการแลกเปลี่ยนคลอไรด์กับไบคาร์บอเนตที่ basolateral membrane ของเซลล์ขับกรดในไต โปรตีนนี้เป็น isoform ของ erythroid anion exchanger 1 (eAE1) โดยมีกรดอะมิโน 65 ตัวที่ปลายอะมิโนน้อยกว่า eAE1 ซึ่งอาจมีผลทำให้โปรตีนทั้งสองมีปฏิสัมพันธ์ต่อโปรตีนที่เกี่ยวข้องแตกต่างกัน มิวเตชั่นของยีน AE1 มีหลายชนิดที่เกี่ยวข้องกับการเกิดโรคไตผิดปกติในการขับกรด ได้มีการตั้งสมมุติฐานว่าการเปลี่ยนแปลงของโปรตีน AE1 จากผลของมิวเตชั่น อาจนำไปสู่ความผิดปกติของการขนส่งโปรตีน หรือการเคลื่อนย้ายของ kAE1 ไปยังตำแหน่งที่ไม่เหมาะสม การศึกษาต่อมาพบว่าทั้งปลายอะมิโน และปลายคาร์บอกซี่ ของ AE1 เป็นส่วนสำคัญในการควบคุมการขนส่งและการเคลื่อนย้ายโปรตีนไปยังตำแหน่งที่ถูกต้อง ปัจจุบันยังไม่พบ โปรตีนที่จับกับปลายอะมิโนของ kAE1 (NkAE1) ตลอดจนความเข้าใจกลไกการขนส่ง kAE1 โดยผ่านโปรตีนตัวอื่นในเซลล์ของไตมนุษย์ยังไม่มีผู้ศึกษามาก่อน วัตถุประสงค์ของการศึกษานี้คือ การค้นหาโปรตีนที่จับกับ NkAE1 ด้วยวิธี yeast two-hybrid จากนั้นคัดเลือกโปรตีนที่ได้ คือ integrin-linked kinase (ILK), glyceraldehydes-3-phosphate dehydrogenase และ pantophysin นำมาวิเคราะห์ในรายละเอียดเพื่อศึกษาปฏิสัมพันธ์กับ kAE1 ด้วยวิธี co-immunoprecipitation, affinity co-purification และ immunofluorescence staining ในเซลล์เพาะเลี้ยง HEK 293 ผลการวิเคราะห์ยืนยันความจำเพาะของการจับของโปรตีนทั้งสามกับ NkAE1 แต่การศึกษาด้วยวิธี cell surface biotinylation แสดงให้เห็นว่าเฉพาะ ILK ที่เพิ่มการแสดงออกของ kAE1 ที่ผิวเซลล์ นอกจากนี้ ILK ยังทำให้มีการเพิ่มการแลกเปลี่ยนไอออนของ kAE1 อย่างชัดเจน ทำให้ได้ข้อสรุปว่า ILK น่าจะมีบทบาทต่อการขนส่ง kAE1 โดยใช้ calponin homology (CH) domain ของ kAE1 ในการจับกับปลายคาร์บอกซี่ของ ILK ในขณะที่ ankyrin repeats, PH domain และ ผลของ phosphorylation ของ ILK ไม่มีส่วนเกี่ยวข้อง นอกจากนี้ยังพบว่า ILK สามารถจับกับ eAE1 ได้ แสดงว่ากรดอะมิโน 65 ตัวที่ปลายด้านอะมิโนของ eAE1 ไม่มีผลต่อการม้วนพับของโครงสร้างของ eAE1 ที่เปลี่ยนแปลงไปโดยเฉพาะในส่วนของ CH domain การศึกษานี้บ่งชี้ว่าการจับกันของ kAE1 และ ILK เป็นส่วนของกลุ่มโปรตีนที่ประกอบด้วย kAE1 ILK paxillin และ actopaxin โดยสรุปการศึกษานี้แสดงให้เห็นว่า ILK เป็นตัวเชื่อมที่สำคัญระหว่าง kAE1 กับ cytoskeleton โดยผ่าน actin ที่สามารถจับกับกลุ่มโปรตีนนี้ได้ ซึ่งทำให้การคงอยู่ของ kAE1 ที่ plasma membrane มีเสถียรภาพเป็นผลให้มีการแสดงออกของ kAE1 ที่ผิวเซลล์ในระดับที่สูงขึ้น

# CONTENTS

# CONTENTS (cont.)

# CONTENTS (cont.)

# CONTENTS (cont.)

# CONTENTS (cont.)

# CONTENTS (cont.)

# CONTENTS (cont.)

# LIST OF TABLES

**Table** **Page**

# LIST OF FIGURES

**Figure** **Page**

# LIST OF FIGURES (cont.)

# LIST OF FIGURES (cont.)



# LIST OF ABBREVIATIONS

| | | |
|---|---|---|
| AD | = | autosomal dominant |
| AE | = | anion exchanger |
| α-Gal | = | alpha galactosidase |
| ANK | = | ankyrin |
| AP | = | adaptor protein |
| AR | = | autosomal recessive |
| AT | = | angiotensin receptor |
| ATP | = | adenosine triphosphate |
| BCECF-AM | = | 2',7'-bis-(2-carboxyethyl)-5 -(6)-carboxyfluorescein-acetoxymethyl ester |
| β-Gal | = | beta galactosidase |
| $\beta_I$ | = | intracellular buffer capacity |
| BLM | = | basolateral membrane |
| bp | = | base pair |
| BSA | = | bovine serum albumin |
| BT | = | bicarbonate transporter |
| CA | = | carbonic anhydrase |
| CD | = | circular dichroism spectroscopy |
| CDK | = | cyclin-dependent kinase |
| CH | = | calponin homology domain |
| $Cl^-/HCO_3^-$ | = | chloride/bicarbonate |
| C | = | carboxyl-terminal |
| DEPC | = | diethyl pyrocarbonate |
| DIDS | = | 4,4'-diisothiocyanostilbene-2,2'-disulfonate |
| DMEM | = | Dulbecco's modified Eagle medium |
| dNTP | = | deoxynucleoside triphosphate |
| dRTA | = | distal renal tubular acidosis |

# LIST OF ABBREVIATIONS (cont.)

| | | |
|---|---|---|
| eAE1 | = | erythroid anion exchanger 1 |
| EDTA | = | ethylenediaminetetraacetic acid |
| Endo H | = | endoglycosidase H |
| ER | = | endoplasmic reticulum |
| FBS | = | fetal bovine serum |
| FITC | = | fluorescine isothiocyanate |
| GAL4-AD | = | GAL4 activation domain |
| GAL4-BD | = | GAL4 binding domain |
| GAPDH | = | glyceradehyde-3-phosphate dehydrogenase |
| GLUT | = | glucose transporter |
| GPA | = | glycophorin A |
| HA | = | hemagglutinin |
| HBSS | = | Hank's balance salt solution |
| $H_2$DIDS | = | 4,4'-diidothiocyanodihydrostilbene-2,2'-disulfonate |
| Hb | = | hemoglobin |
| HEK | = | human embryonic kidney |
| ILK | = | integrin-linked kinase |
| kAE1 | = | kidney anion exchanger 1 |
| LB | = | Luria broth |
| MDCK | = | Madin Darby canine kidney |
| min | = | minute |
| NBC | = | sodium bicarbonate co-transporter |
| NHE | = | sodium proton exchanger |
| N | = | amino-terminal |
| OD | = | optical density |
| PBS | = | phosphate buffer saline |
| PBSs | = | paxillin binding subdomain sequence |
| PCR | = | polymerase chain reaction |
| PDZ | = | PSD-95/Dlg/ZO-1 |

# LIST OF ABBREVIATIONS (cont)

| | | |
|---|---|---|
| PH | = | Pleckstrin homology |
| PINCH | = | particularly interesting new cysteine-histidine-rich protein 1 |
| PKA | = | protein kinase A |
| PPH | = | pantophysin |
| PVDF | = | polyvinylidene difluoride |
| RBCs | = | red blood cell |
| RT | = | reverse transcriptase |
| SAO | = | Southeast Asian ovalocytosis |
| SCAMPs | = | secretory carrier associated membrane proteins |
| SD | = | synthetic dropout medium |
| SDS | = | sodium dodecyl sulfate |
| SDS-PAGE | = | SDS-polyacrylamide gel electrophoresis |
| SITS | = | 4-acetamido-4'-isothiocyanostilbene-2,2'-disulfonate |
| SLC | = | solute carrier family |
| Src | = | non-receptor protein tyrosine kinase |
| TBST | = | Tris buffer saline with Tween-20 |
| TEMED | = | N,N,N',N'-tetramethylethylenediamine |
| TK | = | tyrosine kinase |
| TMs | = | transmembrane segments |
| $V_{max}$ | = | maximum transport rate |
| VAMP | = | vesicle-associated membrane protein |
| YFP | = | yellow fluorescent protein |
| YPDA | = | yeast peptone D-glucose supplemented with adenine |
| WT | = | wild-type |

# CHAPTER I
# INTRODUCTION

Anion exchanger 1 (AE1, band 3) is the prototypical member of bicarbonate transporter superfamily, involved in maintaining acid-base homeostasis in the human body [1, 2]. AE1 is encoded by *AE1* gene (also known as *SLC4A1*), which is located on chromosome 17q21-22. The *AE1* gene comprises 20 exons [3]. It encodes erythroid AE1 (eAE1) and kidney AE1 (kAE1), which arise from differential promoter usage.

eAE1 is the major integral membrane protein of the erythrocyte, which serves the dual roles of chloride/bicarbonate ($Cl^-/HCO_3^-$) exchange and cytoskeletal anchorage to red cell membrane [4]. kAE1 is the basolateral $Cl^-/HCO_3^-$ exchanger of the acid-secreting α-intercalated cell of the kidney collecting duct [5]. Transcription of eAE1 in erythroid precursors is under the control of an erythroid-specific promoter upstream of exon 1, while renal transcription arises from a distinct promoter within intron 3 of the *AE1* gene [6]. Thus, the resultant kidney transcripts encode the kAE1 polypeptide lacking 65 amino acids at the N-terminus present in human eAE1 [3].

eAE1 is composed of 911 amino acids, which form three structurally and functionally distinct domains. The C-terminus constitutes a highly conserved domain that is predicted to transverse the lipid bilayer up to 12-14 times [7]. This domain is responsible for anion transport and remains functional either when translated from cDNA clone encoding the isolated membrane domain or after proteolytic removal of a short cytoplasmic C-terminal tail containing a binding site of carbonic anhydrase (CA) II [8]. The N-terminal cytoplasmic domain is involved in a number of functions unrelated to anion transport, including anchoring the plasma membrane to the cytoskeleton via interactions with ankyrin-1 and proteins 4.1 and 4.2, as well as glycolytic enzymes and hemoglobin [5, 9].

The three-dimensional structure of the N-terminal cytoplasmic domain eAE1 revealed a globular structure, composed of 11 β-strands and 10 helical segments [4].

The first 54 residues at N-terminus contain 20 acidic residues, the strongly anionic region involved in most peripheral protein interactions [9]. Loss of this portion causes deletion of a central strand in the major β-sheet, which may greatly alter the globular structure of eAE1. This alteration causes major functional differences between eAE1 and kAE1. Unlike eAE1, the N-terminal kAE1 no longer binds to ankyrin-1 and proteins 4.1 and 4.2 and glycolytic enzymes [10, 11]. The absence of 65 amino acids at the N-terminus of kAE1 would cause some structural changes and alter protein-protein interactions. However, the identity of kAE1-binding protein(s) in α-intercalated cells remains unknown. A previous study reported that a new protein, called kanadaptin (kidney anion exchanger adaptor protein), has been identified as a protein binding to the N-terminal cytoplasmic domain of mouse kAE1 but not to eAE1 by yeast-two hybrid system [12]. However, human kanadaptin cDNA was identified and protein interaction of this protein with kAE1 was investigated [13]. The result showed that human kanadaptin did not interact with kAE1 in both yeast system and in human embryonic kidney (HEK 293) [13, 14]. This leads the question what protein interacts with the N-terminal cytoplasmic domain of kAE1 in human.

The function of kAE1 is important in the process of bicarbonate reabsorption across basolateral membrane of the α-intercalated cells of the renal collecting duct, which occurs in association with net acid excretion mediated by $H^+$-ATPase pump in the apical membrane of these cells. Failure of either acid excretion or bicarbonate reabsorption by these cells leads to distal renal tubular acidosis (dRTA), the disorder characterized by the incapability of the kidney to acidify urine in the presence of systemic acidosis [15]. Defects in any one of several transporters and enzymes of the α- intercalated cells required for transepithelial acid excretion and bicarbonate reabsorption might cause heritable dRTA [16]. Among these components are the $H^+$-ATPase, AE1 [3], cytoplasmic carbonic anhydrase II (CAII) [17], and at least in conditions of $K^+$ deprivation, $H^+/K^+$-ATPase [18]. Although mutations in vacuolar $H^+$-ATPase have been found in autosomal recessive dRTA through whole-genome linkage mapping followed by candidate screening within the linked region [19], several mutations in *AE1* gene has been associated with both autosomal dominant and autosomal recessive dRTA [20-22]. To date, *AE1* mutations associated with autosomal dominant dRTA are missense mutations in codon 589 (R589H, R589S,

R589C), S613F, G609R and an 11-amino acid deletion at the carboxy terminus (R901X), while *AE1* mutations linked to autosomal recessive dRTA are G701D, ΔV850, A858D, S773P and G701D/SAO.

A current hypothesis is that these mutations cause dRTA either by preventing the movement of mutant and normal proteins to the cell surface (impaired trafficking) or sending the mutant proteins to inappropriate sites (mistargeting), which resulted in impairing bicarbonate movement across the basolateral membrane [23]. Although, no mutation in the N-terminus of kAE1 has been reported to be associated with dRTA, it has recently found that deletion of the N-terminal kAE1 and C-terminal (R901X) resulted in the apical localization of the proteins in Madin Darby canine kidney cells type I (MDCKI), suggesting that a determinant within the kAE1 N-terminus co-operates with the C-terminus for kAE1 basolateral localization [24]. Another study of chicken kidney AE1-4 demonstrated the presence of basolateral localization signal in the N-terminus [25].

Beyond observations that some mutations of kAE1 cause defects in trafficking to basolateral membrane, the precise mechanism to explain kAE1 delivery to basolateral membrane of distal renal tubule cells still has not been defined. To understand kAE1 transport, targeting, and regulation, it will be necessary to identify protein(s) that interact with kAE1. The function of the C-terminus of kAE1 has been extensively studied while little is known about the N-terminal domain of kAE1. Therefore, this study was designed to identify proteins that interacts with the N-terminus of kAE1, using yeast two-hybrid screening of human kidney cDNA library. The interaction between the two proteins was subsequently verified in human kidney cells (HEK 293 cells) using co-immunoprecipitaion, affinity co-purification and immunofluorescence methods. Cell surface biotinylation was carried out to determine effect of interacting proteins on cell surface expression of kAE1. Detailed analysis of interaction between kAE1 and ILK was further investigated. For example, identification of the critical region required for the kAE1-ILK interaction, kAE1-ILK-paxillin-actopaxin complex co-purification, Triton X-100 cytoskeleton extraction and transport activity assay. The results of this study would constitute a new insight into trafficking mechanism of kAE1, which may provide more understanding in the pathogenesis of dRTA.

# CHAPTER II
# OBJECTIVES

The objectives of the studies in this thesis are:

1. To identify proteins expressed in human kidney that interact with the N- terminus of kAE1 using yeast two-hybrid system.
2. To study the interaction of kAE1 and interacting proteins in transfected human embryonic kidney (HEK 293) cells.
3. To study the role of kAE1 interacting proteins on the physiological function of kAE1.

# CHAPTER III
# LITERATURE REVIEW

Since this thesis is involved in the identification of novel proteins that interact with kidney anion exchanger 1 (kAE1), the general current information on bicarbonate transporter superfamily, anion exchangers (AEs), molecular biology of AE1, the role of AE1 in regulation of acid-base balance in red blood cells and kidney, defects of the protein associated with dRTA, kAE1 protein trafficking, and protein interacting with AE1 are reviewed.

## 1. Bicarbonate transporter superfamily

All cell types in human body require the regulation of acid-base balance to maintain the optimal physiological function. Intracellular pH ($pH_i$) regulation is critical for most cellular processes, including cell volume regulation, vesicle trafficking, cellular metabolism, cell membrane polarity, muscular contraction, and cytoskeletal interactions [26-30]. Changes in pH can alter fundamental biological properties in the cell including protein-protein interactions, enzyme kinetics, and fluid osmolarity [26-28, 31]. Intracellular and extracellular pH can be maintained by one of two ways: metabolic generation or consumption of $H^+$ or transport of $H^+$ into or out of the cell. After removal from the cell, protons or proton equivalents are temporarily buffered in the blood, predominantly by $CO_2/HCO_3^-$ and hemoglobin [32]. The regulation of this system requires the control of acid-base transporter protein called bicarbonate transporter. This transporter includes many proteins which can be organized into a large family.

The bicarbonate transporter family belongs to solute linked carrier (SLC) family which consists of at least 2 gene families including the SLC4 and the more recently identified SLC26 family [33]. The SLC4 family includes the products of ten human genes and at least eight members encode bicarbonate transporters [34, 35]. The SLC26 family includes more than ten members which have been shown to transport

one or more of the following substrates: sulfate, chloride, fructose, iodide, oxalate, formate, hydroxyl or bicarbonate [33].

While the SLC26 family is a relatively recently-identified family of transporters, in which individual proteins differs in both anion transport specificity and expression pattern, the SLC4 family has been more intensively studied [34]. The SLC4 family comprises 3 groups with known transport function; 1) three chloride-bicarbonate transporters or anion exchangers (SLC4A1-3); 2) three electrogenic and electroneutral sodium-bicarbonate cotransporters (NBCe1/SLC4A4, NBCe2/SLC4A5 and NBCn1/SLC4A7); 3) two sodium driven chloride-bicarbonate transporters (SLC4A8 and SLC4A10). There are two other gene products with inconclusive function including SLC4A9 and SLC4A11. There are at least three structural or functional similarities among SLC4 family members. Firstly, all members of SLC4 family appear to encode integral membrane proteins consistent with the presence of 10-14 transmembrane segments, a long N-terminal hydrophobic domain and a much shorter C-terminal hydrophobic domain. Secondly, all members are known to be glycosylated. Thirdly, some members are inhibited by disulfonic stibene derivatives such as DIDS. In addition, functional differences were categorized based on nature of transport activity, ability to carry an anion or a cation and electrogenic property of transporter as observed by the movement of net negatively charge across the membrane causing a shift in membrane potential (electrogenic) or no net movement of electrical charge causing no change in membrane potential (electroneutral). AE1-3 exchange monovalent anions from opposite site of the membrane while the SLC4A4, 5 and 7 cotransport some ion together or SLC4A8 and 10 appear to be a hybrid cotransporter/exchanger. Table 1 summarizes the best-characterized bicarbonate transporter superfamily members and their properties.

## 2. Chloride-bicarbonate anion exchanger

The anion exchangers (AEs) mediate the electroneutral exchange of chloride and bicarbonate ($Cl^-/HCO_3^-$) across the plasma membrane. Four AE proteins (AE1-4) share similar membrane organization which composes of three different domains. The major difference between AE proteins are distinguished by the amino acid sequence length at the N-terminal cytoplasmic domain; 400 amino acids for AE1, 700 amino

**Table 1 Bicarbonate transport proteins and their properties.**

| Protein | Other names | Tissue distribution | Mechanism | Net charge flux | References |
|---|---|---|---|---|---|
| AE1 | SLC4A1, Band 3 | erythrocyte, kidney, heart | $Cl^-/HCO_3^-$ exchange | 0 | [36] |
| AE2 | SLC4A2 | widespread | | 0 | [37] |
| AE3 | SLC4A3 | brain, heart, retina, gastrointestinal tract, kidney | | 0 | [38] |
| NBC1a | SLC4A4, kNBC | kidney, cornea | $Na^+/HCO_3^-$ co-transport | -2 or -1 | [39] |
| NBC1b | SLC4A4, hhNBC, pNBC, rb1NBC, splicing variant of NBC1 | heart, pancreas, kidney, cornea, prostate, colon, stomach, glia, thyroid, brain | | -2 or -1 | [40-42] |
| NBC3 | SLC4A7, NBC2, NBCn1a,b,c,d | heart, kidney, skeletal muscle, pulmonary, artery, aorta, submandibular gland | | 0 | [43] |
| NBC4 | SLC4A5, NBC4a,b,c | liver, spleen, epididymis, heart, brain kidney | | -1 or 0 | [44] |
| AE4 | SLC4A9 | kidney, testis | $Cl^-/HCO_3^-$ exchange? $Na^+/HCO_3^-$ co-transport? | ? | [45] |
| NDCBE1 | SLC4A8, NDAE1, NCBE, (NBC3) | neurons, kidney, fibroblasts | $Na^+$-dependent $Cl^-/HCO_3^-$ exchange | 0 or +1 | [46] |
| Btr1 | SLC4A11 | kidney, salivary gland, testis, thyroid, trachea | - | - | [45] |
| DRA | SLC26A3, CLD | colon, ileum, ecrine sweat gland | $Cl^-/HCO_3^-$ exchange | 0 | [47] |
| Pendrin | SLC26A4, PDS | inner ear, thyroid, kidney | $Cl^-/HCO_3^-$ exchange; also $I^-$ | 0 | [48] |
| PAT-1 | SLC26A6, CFEX | kidney, heart, pancreas, liver skeletal muscle, intestine, placenta | $Cl^-/HCO_3^-$ exchange oxalate and formate | 0 | [49] |
| SLC26A7 | SLC26A7 | kidney | $Cl^-$, $SO_4^{2-}$, $HCO_3^-$? | | [50] |
| Tat1 | SLC26A8 | spermatocytes | | | [50] |
| SLC26A9 | SLC26A9 | lung | | | [50] |

acids for AE2 and 3, and an intermediate length for AE4, which described by variation in their N-terminal amino acid sequences derived from alternative promoter usage.

Among these AE proteins, AE1 is the most widely recognized protein in this family. It is also known as band 3 protein in red blood cells based on its position on SDS-polyacrylamide gel electrophoresis of red blood cell membrane proteins. There are two alternative N-terminal variants, known to be expressed in red blood cells and the α-intercalated cells of the collecting duct in kidney. Naturally occurring mutations of AE1 can cause human disease affecting function of red blood cells and/or α-intercalated cells of the distal nephron. AE1 will be described in more detail in the next section.

AE2 was first cloned from human kidney and lymphoma cells shortly after the cloning of AE1 [51]. Both human and mouse AE2 have three alternative promoters (a, b and c) that give five N-terminal variants (a, b1, b2, c1 and c2) [37, 51]. All variants have N-terminal cytoplasmic domain longer than AE1. AE2 widely distribute at the basolateral membranes of most epithelial cells especially in gastric parietal cells where it plays a key role in $H^+$ secretion into the lumen of gastric gland [52].

Similar to AE1, AE3 gene has two alternative promoters encoding two alternative N-terminal variants including the cardiac isoform (cAE3) and the brain isoform (bAE3). However, these two variants can be presented in heart, brain and elsewhere [53]. Both isoforms can be expressed either at basolateral or apical membrane of polarized cells. It has been reported that the substitution polymorphism at A867D provide a small degree of susceptibility to idiopathic generalized epilepsy [54]. AE4 is the most recent chloride-bicarbonate anion exchanger that was cloned in 2001 from rabbit kidney [55]. The sequence analysis of cDNA shows that it is more closely related to the sodium driven chloride-bicarbonate transporter. However, it appeared to behave like chloride-bicarbonate exchanger when expressed in COS cells which leading to the name AE4. Immunocytochemistry staining showed that the AE4 is present in the apical membranes of α-intercalated cells in the rabbit renal cortex [55]. Although the results showed AE4 seems to be a chloride-bicarbonate exchanger, the functional study of human AE4 in *Xenopus* oocytes failed to demonstrate this effect [56]. Thus additional study is required to establish the function of AE4.

## 3. Human anion exchanger 1 (AE1)

AE1 was firstly described as band 3, the major integral membrane protein of human red blood cells. To date eAE1 has been sequenced from a various organisms including chicken, rat, mouse, cow, trout as well as human [36, 38, 57-60].

### 3.1 Organization of human AE1 gene

Human AE1 gene locates on chromosome 17q21-22 [61]. It spans approximately 20 kb containing 20 exons and separated by 19 introns [62]. The exon sizes are relatively small with the length from 62 to 254 bp except exon 20 is 2153 bp while the intron sizes range from 86 to 5123 bp. All exon-intron boundaries conform to the consensus found in other human gene. The region in gene upstream of exon 1 contains an erythroid specific promotor that control transcription of erythroid isoform of AE1 (eAE1). This promotor region does not have TATA or CCAAT box but contains the consensus sequences of the binding sites for variety of transcription factors [6]. However, TATA and CCAAT boxes of AE1 gene are found downstream in the intron 3. There are two initiation codons downstream of this TATA box, one is in intron 3 and another one in exon 5. The exon designed as K1 is non-erythroid and contributes to the 5' end of the truncated AE1 transcript for kidney isoform (kAE1) expressed in the α-intercalated cells (Figure 1). The downstream end of exon 20 is defined as the RNA cleavage site or poly A addition site. Nine Alu repeat elements approximately 300 bp identified within the human AE1 gene are the same as those commonly found in other primates [62]. Northern blot analysis of human reticulocyte suggested that human eAE1 mRNA was approximately 4.7 kb [57, 58]. The 20 exons eAE1 transcript encode for 911 amino acids.

### 3.2 AE1 structure

AE1 is polytopic membrane protein composed of three structurally and functionally distinct domains including a long N-terminal cytoplasmic domain, a 12-14 transmembrane domains, and a short C-terminal cytoplasmic domain (Figure 2).

#### 3.2.1 N-terminal cytoplasmic domain

A large 40 kDa of N-terminal cytoplasmic domain of AE1 (residues 1-403) is

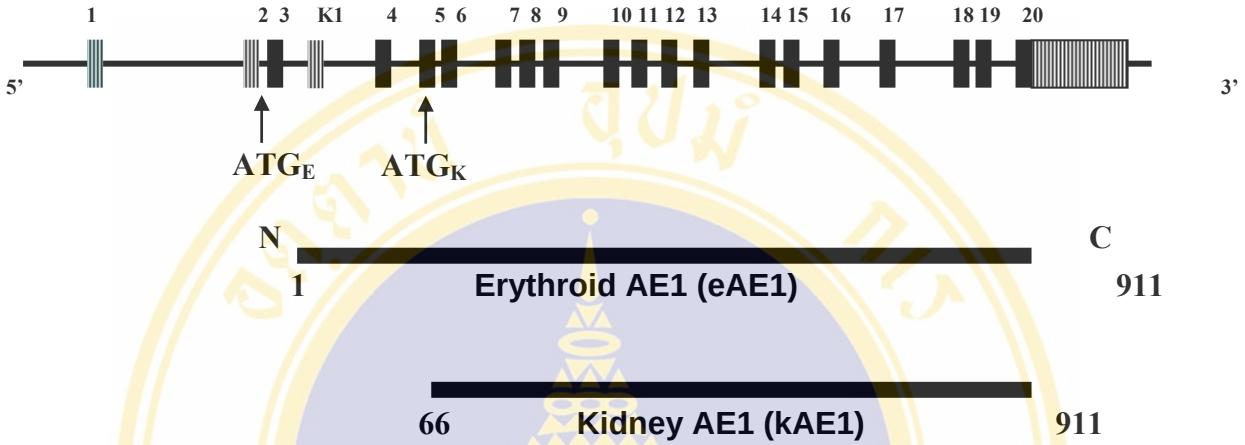


**Figure 1 Diagramatic representation of human *AE1* gene and its two protein isoforms (eAE1 and kAE1).**

Human *AE1* gene is shown in the upper part. Exons are represented by open and filled boxes. Their sizes are not scaled. Exon numbers are indicated each exons. The protein coding region shown as solid boxes and the 5' and 3' noncoding regions shown as lined boxed. The same gene encodes both erythroid (eAE1) and kidney (kAE1) isoforms of AE1 protein by using alternative promoters, splicing patterns and start codons ($ATG_E$ and $ATG_K$), resulting in different lengths of polypeptides (lower). The eAE1 contains 911 amino acids whereas the kAE1 consists of 846 amino acids.

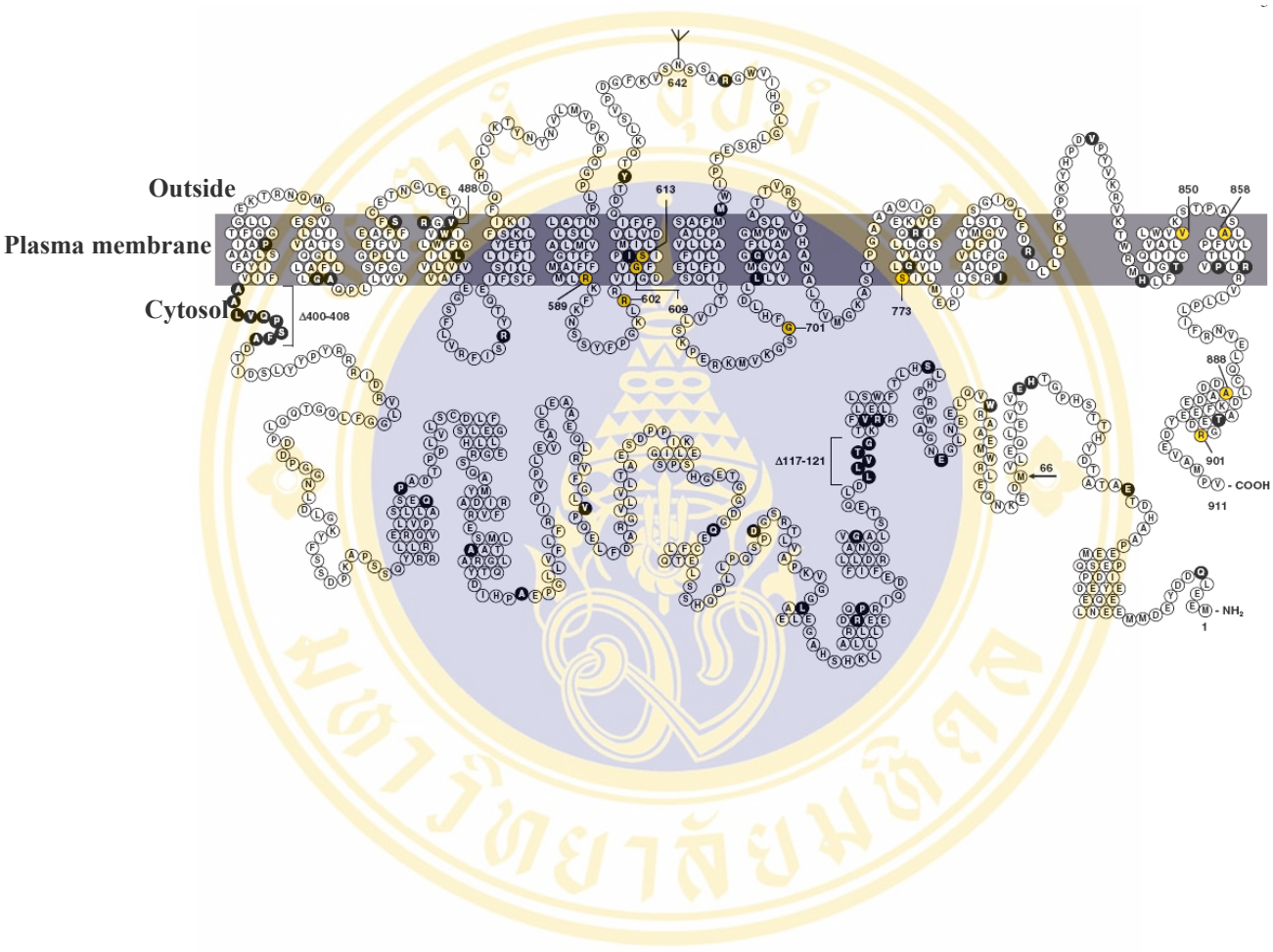


**Figure 2 Topological model of human AE1, taken from Shayakul C, *et al*. [63].**
Diagrammatic representation of AE1 topological model according to the traditional 13-span transmembrane (TM) model. Three structural parts in this model include cytoplasmic amino-terminal domain ($NH_2$), transmembrane domains, and carboxy terminal tail (COOH).

involved in number of functions unrelated to anion transport. The structure of the N-terminal cytoplasmic domain has been extensively studied. Biochemical, and crystallographic studies [4, 10, 64] reveal that the most peculiar structural feature of the N-terminal cytoplasmic domain of human eAE1 is its extraordinarily anionic N-terminus [57]. Among the first 33 residues of the polypeptide are 18 glutamic and aspartic acids. Furthermore, the above sequence contains no basic amino acids and the N-terminal methionine is N-acetylated [57, 65]. The negative charge of this region can be further augmented by tyrosine phosphorylation at position 8 [66]. Mild proteolysis of human eAE1 at the cytoplasmic surface causes the release of the entire N-terminal 372 or 373 residues [67]. A crystal structure of the cytoplasmic N-terminal of AE1 (cbd3, residues 1-379) has recently been reported at 0.26 nm (2.6 Å) resolution (Figure 3) [4]. It showed a globular structure, which is composed of 11 β-strands and 10 helical segments. Eight of the β-strands are assembled into a central β-sheet of mixed parallel and antiparallel strands. Two of the remaining strands (6 and 7, residues 176-185) form a β-hairpin. Along with the first 6 helices, these elements assemble into a globular domain spanning residues 55-290. However, the first 54 residues at N-terminus were not observed due to the flexibility of this part. The structure was also demonstrated in its dimer which is stabilized by interlocked dimerization arms contributed by both monomers. Analysis of the structure has provided insight into the architecture of cdb3 interactions with peripheral membrane proteins. This domain serves as a site for anchoring the protein to cytoskeleton via interaction with ankyrin, protein 4.2, protein 4.1, glyceradehyde-3-phosphate dehydrogenase (GAPDH), phosphofructokinase, aldolase, hemoglobin, hemichromes, and protein tyrosine kinase [5]. These interactions have significant consequences for the structure and function of the cell. Interactions with cytoskeletal elements influence cell shape, flexibility, and lifespan while interaction with glycolytic enzymes influence glucose metabolism [5].

### 3.2.2 Transmembrane domain

Approximately 55 kDa C-terminal domain (residues 404-882) constitutes a highly conserved hydrophobic domain is that predicted to transverse the lipid bilayer up to 12-14 times [7, 58]. It contains the post-translational modification site at the

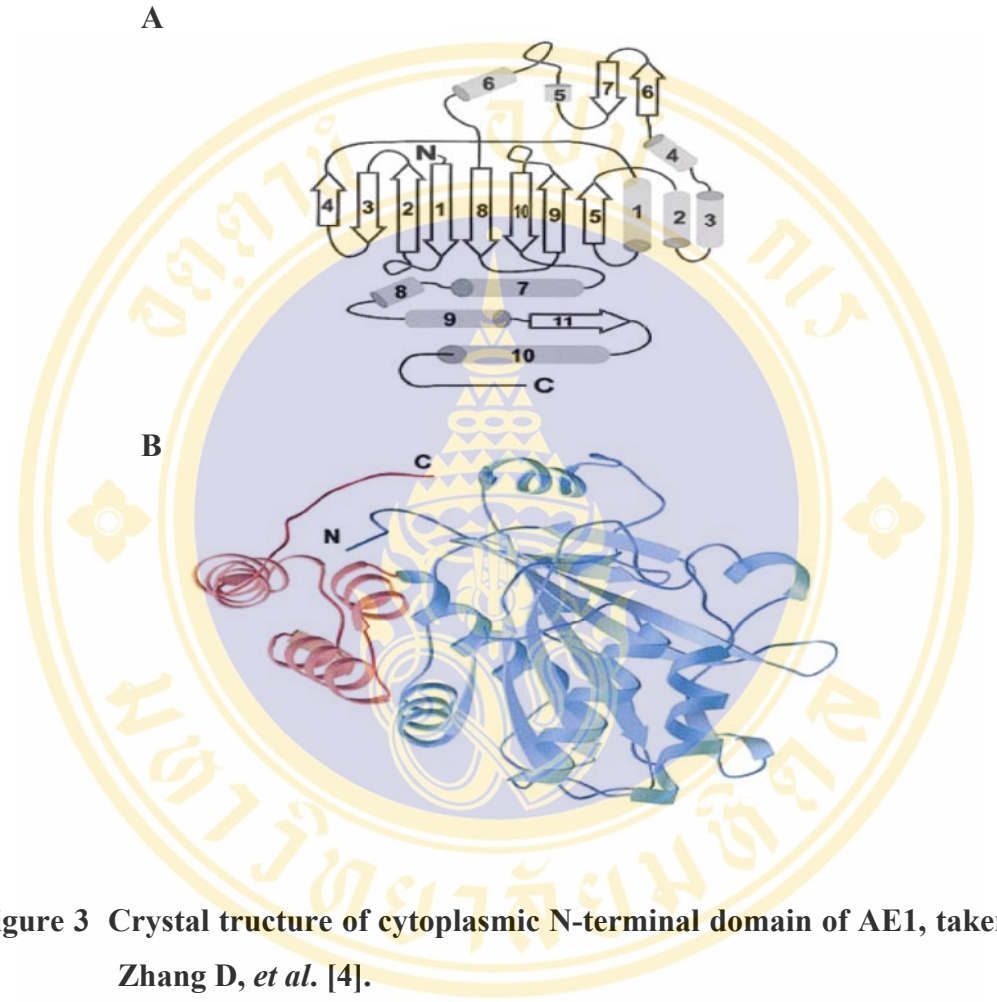


**Figure 3 Crystal tructure of cytoplasmic N-terminal domain of AE1, taken from Zhang D, *et al.* [4].**

A. Diagram of the cytoplasmic N-terminal domain of AE1 (cdb3) secondary structure with the following sequence assignments: $\beta_1$57-66, $\beta_2$73-82, $\beta_3$84-88, $\beta_4$92-96, $\alpha_1$104-116, $\beta_5$117-122, $\alpha_2$128-141, $\alpha_3$146-158, $\alpha_4$166-170, $\beta_6$176-180, $\beta_7$182-185, $\alpha_5$196-201, $\alpha_6$212-220, $\beta_8$224-234, $\beta_9$239-247, $\beta_{10}$263-271, $\alpha_7$278-290, $\alpha_8$292-300, $\alpha_9$304-316, $\beta_{11}$318-323, and $\alpha_{10}$328-347.

B. Monomer ribbon diagram of amino terminal domain AE1 with blue corresponding to the peripheral protein binding domain and red corresponding to the dimerization arm.

extracellular portion of the seventh transmembrane segment which is glycosylated with a single N-glycan chain at Asn642 [57, 58]. This domain facilitates the flux of ions from one side of a membrane to the other, down an electrochemical gradient (or a net gradient in the case of co-transporters and exchangers). It remains functional either when translated from cDNA clone encoding the isolated membrane domain or after proteolytic removal of a short C-terminal cytoplasmic tail [8]. The topography of AE1 transmembrane domain has been studied by using several techniques including chemical labeling [68, 69], scanning N-glycosylation mutagenesis [70, 71] and cysteine scanning mutagenesis [7, 72]. Circular dichroism measurements of transmembrane domain demonstrated that it contained 58% α-helix and was resistant to denaturation by guanidine hydrochloride [73]. The remaining 40% of the structure likely consists of small loops connecting the transmembrane segments and do not cross the lipid bilayer. Interestingly, the membrane segments digested with proteolytic enzymes and stripped of all extrinsic fragments revealed that the portions of red cell membrane proteins embedded in the lipid bilayer contain a very high (86-94%) content of α-helix. While the topology of the first 8 transmembrane segments is agreed to be the same, the last transmembrane segments is still controversial.

### 3.2.3 C-terminal cytoplasmic domain

The final short acidic C-terminal cytoplasmic tail (residues 883-911) is extensively functional characterized. This domain contains a highly conserved acidic LDADD sequence among anion exchangers (residues 886-890) which is a binding site for carbonic anhydrase II (CAII) [8, 74]. Several lines of evidence suggest that CAII interacting with AE1 provides the enhancement in anion transport [74, 75]. This domain also contains the phosphorylation site at Tyr904 which is phosphorylated in red blood cells [76]. In addition, removal of the last 35 amino acids including the CAII binding domain showed low level expression in HEK 293 cells [77]. This region would require for proper AE1 folding in the membrane of HEK 293 cells because the deleted protein exhibited poor binding to SITS affinity gel resin. Recently, the C-terminal 112-residues of AE1 were found to interact with p16, a key negative regulating protein for cell cycle [78].

### 3.3 Biosynthesis, post-translational modification and trafficking of AE1

#### 3.3.1 Biosynthesis of AE1

Many studies showed that eAE1 is synthesized only at the last stage of erythroid differentiation [79, 80]. It has been demonstrated that eAE1 is absent from rabbit nucleated bone marrow erythroid cells but the reticulocytes contain similar amount of proteins when compare to red blood cells [81]. Studies of membrane protein synthesis in reticulocytes from anemic rabbits showed that eAE1 was only incorporated into the membrane of the earliest stage of reticulocytes [81]. Moreover, another study has been shown that eAE1 presented in mature red blood cells is inserted into the membrane between the polychromatic normoblast and reticulocyte stage [82].

In humans, eAE1 is expressed in erythroid cells of first and second trimester human fetal liver [83]. Study of erythroid brust colonies in culture showed that small amount of eAE1 was expressed in human erythroblasts [84], however, the maturation stage of the human erythroid precursor that expresses eAE1 remains unclear.

#### 3.3.2 Post-translational modification

Once AE1 is synthesized, it undergoes several post-translational modifications including N-glycosylation, fatty acylation and phosphorylation [57, 58, 76, 85]. Expression study of endogenous erythrocyte proteins in a specific cell type revealed that newly synthesized AE1 moves from the ER to the Golgi network where it undergoes sugar modification and also associated with ER chaparone, calnexin [86]. Maturation of AE1 polypeptide was initiated when it was cotranslationally inserted into the ER membrane and glycosylated at a single Asn-linked site (Asn642) which resulted in susceptible to cleavage by endoglycosidase H (endo H) [87]. This N-glycan chain is heterogeneous in size on different AE1 molecules due to the variation in the number of repeating N-acetyllactosamine units present in each lactosaminoglycan chain [65]. Then, the polypeptide is processed to an endo H-resistant form, presumably in the Golgi complex, and subsequently becomes sensitive to extracellular protease 30-45 min after synthesis [88]. The C-terminal AE1 peptide containing palmitic acid had been isolated from human red cells [85]. The site for palmitoylation was identified to be Cys843 which located at residue position 69 from the C-terminal end [85]. Studies in *Xenopus* oocytes [89] and transfected HEK 293

cells [90] suggest that this palmitoylation site occurs near the cytosolic end of transmembrane segment and does not seem to be required for anion transport and cell surface expression of the protein.

Tyrosine phosphorylation has been reported to be involved in the modulation of a variety of erythrocyte functions, such as glycolysis, cell shape, cytoskeleton movements, and anion transport. It was found that Tyr8, Tyr20 and Tyr359 in the N-terminal domain and Tyr904 in the C-terminal domain of AE1 are phosphorylated in red blood cells [76]. AE1 is phosphorylated by $p72^{syk}$ protein tyrosine kinase (PTK) at Tyr8 and Tyr20. Increased phosphorylation at Tyr8 is involved in the inhibition of AE1 binding to glyceraldehyde-3-phosphate dehydrogenase, aldolase and phospho fructokinase. In addition, the phosphorylated Tyr359 and Tyr904 are necessary for correct localization and recycling of kAE1 to the basolateral membrane [24]. The steps underlying the mechanism of phosphorylation/dephosphorylation of AE1 was suggested and showed that many proteins involve in these steps [24].

### 3.3.3 Trafficking of AE1 to plasma membrane

Since AE1 is the most abundant protein of the human red blood cell membrane that presented at approximately $1 \times 10^6$ copies/cells, it requires an efficient mechanism to control the movement of the proteins from internal membrane to the cell surface. Many evidences have been shown that glycophorin A (GPA) has a role both in biosynthesis and facilitating of AE1 trafficking to the plasma membrane. The 36 kDa GPA protein represents the major glycoprotein of the red blood cell membrane displaying approximately one million copies per cells similar to AE1. Co-expression studies in *Xenopus* oocytes demonstrated that GPA can facilitate the movement of AE1 to the oocytes surface and induces an increased level of chloride transport in the oocytes [91, 92]. Although GPA can forms stable dimer, it was found that the effect of GPA on eAE1 trafficking is mediated by the GPA monomer [93].

Studies of AE1 null mice have shown the completely absence of GPA in red blood cells [94]. Furthermore, transgenic mice that express human GPA demonstrated that there is a tight coupling of GPA and AE1 expression in mouse red blood cells [95]. These studies support an important role of GPA in facilitating the trafficking of AE1 to the cell surface. Although how GPA supports the movement of eAE1 remains

unclear, it was suggested that GPA acts by modifying the folding pathway of AE1 so that it attains the fully active, native conformation in red blood cells [93]. The properly folded AE1 may be able to move rapidly to the cell surface, probably in concert with GPA.

In addition, the recycling of AE1 has been studied in chicken erythrocytes [25, 96, 97]. Chicken AE1 undergoes sugar modification in its initial transit through the secretory pathway and then delivery to the plasma membrane. Internalization and recycling of the protein to Golgi was occurred to acquire additional complex N-glycosyltion modifications [97]. During recycling to the Golgi, AE1 interacts with the cytoskeleton complex suggesting that the cytoskeleton may be involved in the post-Golgi trafficking of this membrane transporter [97]. Basolateral membrane sorting may require phosphorylation of Tyr44 and Try47 at the N-terminus because it matched to the YXXΦ (Y is tyrosine, X is any amino acid, and Φ is an amino acid with a bulky hydrophobic side chain) motif which function in endocytosis and TGN recycling signal for other membrane proteins [25]. It has been also postulated that actin cytoskeleton might play a role in regulating AE1 localization and stability in epithelial cells [96].

### 3.4 Function of AE1 in red blood cells

The known function of eAE1 in red blood cells can be divided into 2 categories which are anion transport proteins of red blood cells and an anchoring component to connect cytoplasmic proteins and cytoskeleton elements to the membrane.

#### 3.4.1 Anion transport and its role in respiration

In red blood cells, anion transport function of AE1 plays an important role in $CO_2$ carriage from the systemic tissue to the lung. Carbon dioxide generated by metabolism moves to the blood and diffuses into the red blood cells. As shown in Figure 4, the cytosolic CAII converts $CO_2 + H_2O$ into $HCO_3^-$ and $H^+$. At this step, eAE1 disposes of the newly generated $HCO_3^-$ in exchange for $Cl^-$ while de-oxygenated hemoglobin buffers the $H^+$. These two steps permit the red blood cells to take up additional $CO_2$. In the lung, this cycle reverse itself, releasing $CO_2$ into the blood for diffusion into the alveoli and excretion from the body via ventilation.

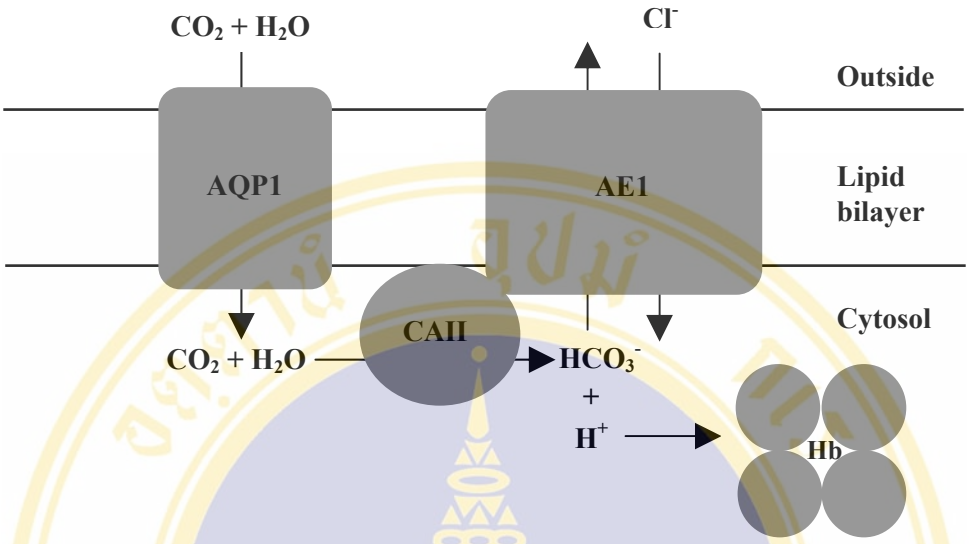


**Figure 4 A capnometabolon linking carbonic anhydrase II and AE1 in the red cells, taken from Reithmeir RA, *et al*. [98].**

In the tissues $CO_2$ diffuses into the red cell through the lipid bilayer. Inside the red cell it is hydrated by the action of carbonic anhydrase II (CAII) bound to the carboxyl-terminal tail of the anion exchanger 1 (AE1). The $HCO_3^-$ is delivered directly to AE1, which then exchanges $HCO_3^-$ for extracellular $Cl^-$. The $H^+$ is bound by hemoglobin (Hb) resulting in a lower affinity for $O_2$. $H_2O$ can enter the cell by diffusion and also via the water channel, aquaporin 1 (AQP1). If $CO_2$ can also permeate through AQP1 then the two substrates for CAII may originate from the cell exterior. The result of this integration of bicarbonate metabolism is that $CO_2$ from the cell exterior meets carbonic anhydrase bound to the inner membrane surface and is efficiently converted to bicarbonate, which is then channeled directly to the $HCO_3^-$ efflux pathway from the cell. In the lung the reverse happens. $HCO_3^-$ enters the cell via AE1 in exchange for intracellular $Cl^-$. The $HCO_3^-$ is channeled to CAII, dehydrated to $CO_2$, which then diffuses out of the red cell.

Both monomeric and dimeric AE1 possess anion transport activity. Low extracellular pH leads to increased AE1 transport activity [99]. Anion transport of AE1 can also be inhibited by negatively charged sulfonate compounds such as stilbene derivative-SITS and DIDS which react covalently with Lys542. The transport activity is inhibited by allosteric interaction of protein rather than blockage of the transport site [3, 94]. The Glu681 is believed to be located within the transport channel of AE1 where it acts as a proton donor for the anion/proton cotransport function. This glutamate is conserved in all anion exchangers and promotes ion selectivity and pH regulation [100]. It has been shown that CAII binds to the C-terminal cytoplasmic domain of AE1 [74]. This interaction has been reported to stimulate the enzyme activity suggesting a functionally significant enzyme-membrane interaction [101]. It was also suggested that this association are beneficial by that CAII can rapidly provide bicarbonate for AE1 [98]. There is a study demonstrated that treatment of AE1 transfected HEK 293 cells with CAII inhibitor resulted in nearly complete inhibition of anion transport activity [75]. Furthermore, a supportive evidence showed that HEK 293 cells transfected with AE1 mutant that cannot bind to CAII exhibited a reduced transport activity by 90% relative to wild type AE1 [102]. These results indicated that the interaction of AE1 with CAII facilitate AE1 activity by forming a bicarbonate transport metabolon.

### 3.4.2 Organization and regulation of red blood cell membrane

Human AE1 has shown that AE1 exists as stable dimers and tetramers in red cell membranes and detergent solutions [99]. High oligomeric form but not dimeric form of AE1 associated with cytoskeleton network [103]. AE1 was shown to bind spectrin via ankyrin, suggesting that AE1 acts in membrane cytoskeletal interaction to define erythrocyte shape and stability. *In vitro* studies indicate that spectrin and ankyrin, the major membrane skeleton components, are synthesized before AE1 during red blood cell development and only bind to the membrane and form a membrane skeleton after AE1 synthesis begins [104-106]. Mechanical properties of red blood cell membrane through its association with the membrane skeleton involve a multiprotein network lying just beneath and tethered to the plasma membrane [107]. Spectrin is the major component of the membrane skeleton. It was known that spectrin tetramers are

crosslinked by short actin filaments at junction complexes, which also include protein 4.1, myosin, tropomyosin, adducin, p55, and protein 4.9 [108]. The major binding site provided by ankyrin is required for the membrane skeleton attached to overlying the plasma membrane. Ankyrin possesses high affinity binding sites for the cytoplasmic domain of AE1 and the β-subunit of spectrin [109, 110]. Furthermore, interaction between protein 4.2 and ankyrin may help stabilization of the ankyrin–AE1 interaction [111, 112]. Organization of red blood cell membrane through association with cytoskeletal proteins is shown in Figure 5.

Studies of AE1 null mice, however, showed that a membrane skeleton with normal spectrin, actin, and protein 4.1 content can be assembled in the absence of AE1 [113]. It was suggested that cytoskeletal binding via glycophorin and band 4.1 is sufficient to maintain membrane integrity but cannot alone maintain the biconcave shape.

### 3.5 Proteins interacting with eAE1

#### 3.5.1 Ankyrin

Ankyrin is a 210 kDa protein that links the cytoplasmic domains of AE1 to the spectrin based subcortical membrane cytoskeleton [109]. One ankyrin molecule is bound to one β-subunit of the spectrin heterotetramer providing a major membrane attachment of cytoskeleton network. It was found that deletion of amino acids 1-79 of eAE1 eliminates high affinity ankyrin binding to AE1 [11]. However, another finding showed that ankyrin binding sites were suspected to be cysteine cluster (residues 201 and 317) and proline-rich hinge (residues 173-190) [66], implying that the amino terminus forms part of the ankyrin binding site. The binding of ankyrin to AE1 can protect AE1 from the trypsin digestion and decrease tyrosine phosphorylation in addition to decreasing in the interaction of AE1-ankyrin leads to instability of red cell shape [66].

#### 3.5.2 Protein 4.1

Protein 4.1 is a 78 kDa bipolar, monomeric protein which mediates the interaction between spectrin and actin. While protein 4.1 has shown a low affinity

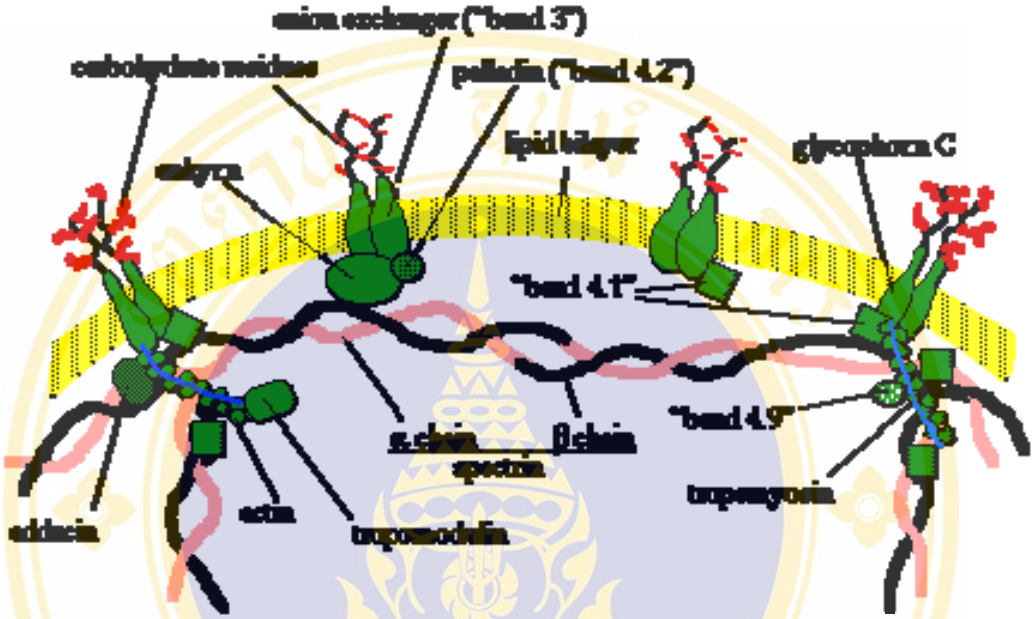


**Figure 5 The cartoon presenting organization of red blood cell membrane (Modified from Gilligan DM, *et al*. [108]).**

The protein components of the red cell membrane cytoskeleton; spectrin, ankyrin, band 4.2, glycophorin C, band 4.1, adducin, tropomyocin, band 4.9, are organized into a network that to stabilize anion exchanger 1 (band 3) to the plasma membrane.

binding to AE1, its major site of attachment to the membrane is at the cytoplasmic pole of glycophorin [114]. The binding of protein 4.1 to eAE1 is competed by ankyrin, suggesting that the overlapping of binding sites on the N-terminal AE1. The results from five independent experiments showed that residues at the acidic N-terminus are strongly involved in stabilizing the interaction between protein 4.1 and eAE1 [115]. However, the significance of the association between these two proteins is unclear.

### 3.5.3 Protein 4.2

Protein 4.2 is a 72 kDa cytoplasmic protein which presents at about 200,000 copies per erythrocyte cells [116]. The membrane binding of protein 4.2 can be abolished either by proteolytic removal of the cytoplasmic domain of eAE1 or by addition of the isolated cytoplasmic fragment to the membrane suspension, suggesting direct interaction between eAE1 and protein 4.2 but the site for this interaction has not yet been localized [117]. Protein 4.2 also binds to ankyrin and protein 4.1 but they have distinct binding sites on AE1. The recent evidences suggested that protein 4.2 play an important role in the interaction of eAE1 with protein in the Rh complex [118]. It is also able to bind several cytoskeletal proteins. Deficiency of protein 4.2 has been associated with spheroidal erythrocytes [119].

### 3.5.4 Glycolytic enzymes

Glyceraldehyde-3-phosphate dehydrogenase (GAPDH), aldolase, phosphofructo kinase and catalase are all reported to have high-affinity binding site at the extreme N-terminus of cytoplasmic domain of eAE1 [120-123]. Evidences supporting a physiologically relevant association between glycolytic enzymes and eAE1 have derived from three types of experiments. Firstly, a number of researchers have reported that GAPDH and aldolase are significantly inhibited upon association with the N-terminus of eAE1 and this inhibition can be modulated by changes in pH, ionic strength, and the concentrations of various metabolic intermediates. Secondly, rapid filtration experiments with saponin-lysed red blood cells have suggested that between one-third and two-thirds of the above enzymes are immobilized at the instant of cell lysis [124]. Finally, resealing of a mAb fragment ($F_{ab}$) specific for the glycolytic

enzyme binding site on eAE1 has been found to accelerate glycolysis, whereas introduction of the inhibitory eAE1 peptide into similar red blood cells causes a major reduction in glycolytic flux [125]. It was suggested that the interaction between glycolytic enzyme complex and eAE1 provided an increase efficiency of an enzymatic pathway with the channeling of substrates between sequential enzymes in a pathway [126].

### 3.5.5 Hemoglobin and hemichrome

The high affinity hemoglobin site on red blood cell ghosts has been shown in the cytoplasmic domain of eAE1 [127]. The region of the domain that involved in the interaction has been demonstrated to be the extreme N-terminal 23 residues [123, 128]. It is generally agreed that deoxyhemoglobin associates more strongly with eAE1 than oxyhemoglobin [127, 129].

Hemichrome is a product of oxidation and denaturation of hemoglobin. It also binds to the extreme N-terminus of eAE1 and induces extensive aggregation. In the intact red blood cells, hemichromes aggregation is associated with clustered eAE1 and the membrane [9]. It was also found that the hemichrome complexs isolated from sickle red blood cells contain eAE1 [130, 131].

### 3.5.6 Caspase 3

The caspases are a specialized family of cysteine-dependent aspartate-directed proteases. Caspase activation is a critical event in the onset of apoptosis. Human caspase 3 is perhaps the most universal apoptosis mediator. It is present in most mammalian cells predominantly in mature human red blood cells in which it is activated by oxidative stress [132]. It has shown that the cytoplasmic domain of eAE1 contains caspase 3 cleavage sites [133]. Proteolysis at these sites could potentially alter each of the characteristics of red cell structure and function regulated by the N-terminal cytoplasmic domain of eAE1.

### 3.5.7 Glucose transporter 1 (GLUT1)

The facilitative glucose transporter 1 (GLUT1) mediates the passive diffusion of D-glucose across the cell membrane of erythrocytes and the blood brain barrier [134].

GLUT1 consists of 12 hydrophobic transmembrane α-helices while the N-terminal region (residues 1-12), C-terminal region (residues 451-492), and a big central loop (residues 207-271), are all hydrophilic which are presumed to be important for the regulation of GLUT1 function [135]. The C-terminus of GLUT1 was shown to interact directly with the cytoplasmic domain of AE1. An impermeable cross-linker of AE1, bis (sulfosuccini-midyl) suberate, not only affected the anion exchanger rate but also declined both the glucose exit and entry rates across the membrane, implying that binding with AE1 can regulate GLUT1's activity [136].

### 3.5.8 Glycophorin A (GPA)

Glycophorin A is a bitopic integral membrane sialoglycoprotein that present in the red blood cell at a similar abundance to eAE1. There are many evidences for the interaction between glycophorin A and eAE1 in the red blood cell membrane. It was showed that anti-glycophorin A antibody decreases the rotational mobility of eAE1 in red blood cell membrane [137, 138]. Studies on transgenic mice to express human glycophorin A suggested that there is tight coupling of glycophorin A and eAE1 expression in mouse red blood cells [136] which is supported by the complete absence of glycophorin A from red blood cells of AE1-null mice [94]. The role of interaction between glycophorin A and eAE1 was demonstrated by many evidences showed that glycophorin A facilitates the movement of the human eAE1 to the cell surface [91-93].

### 3.5.9 Carbonic anhydrase II

Carbonic anhydrase II (CAII) is a 30 kDa monomeric protein with $Zn^{2+}$ ion located deep in the active site cavity. Binding of CAII to red blood cells membrane has been reported to stimulate the enzymatic activity. The residues 879-890 within the carboxyl-terminal sequence of AE1 are responsible for binding CAII [8]. The interaction of AE1 and CAII suggested an example of a metabolon which is a complex of enzyme involved in a metabolic pathway [98]. In this case, CAII would rapidly provide bicarbonate for AE1 and provide the enhancement in anion transport.

### 3.5.10 p16

Tumor suppressor p16 belongs to the CDKN2 cyclin-dependent kinase inhibitor

family that known to interact strongly with CDK4 and CDK6. It is known that p16 play a role in cell cycle regulation and maintaining homeostasis during erythroid differentiation [139]. Recently, it was found that the binding of cytosol p16 to the C-terminal domain of AE1 could accelerate AE1 move to plasma membrane with increased anion transport activity in HEK 293T cells. Transfection of AE1 induced endogenous expression of p16 in HEK 293T cells at 24 and 36 hr but decreased it at 48 and 72 hr, suggesting that the functional AE1 protein is a regulation factor for p16 protein. The interaction between p16 and AE1 seems to be related with regulation of cell proliferation, senescence and homeostasis [78].

### 3.6 The kidney isoform of anion exchanger 1 (kAE1)

Although transcription of eAE1 in erythroid precursors is under the control of an erythroid-specific promoter upstream of exon 1, the renal transcription arises from a distinct promoter within intron 3 of the AE1 gene [6]. Therefore, the codon Met1 and Met33 in eAE1 mRNA are missing in the kAE1 transcript but the ATG codon encoding for Met66 is present and used as the site of translation initiation of kAE1 isoform that lacks the first 65 amino acids at the N-terminus [140]. The kAE1 is a basolateral $Cl^-/HCO_3^-$ exchanger of the acid-secreting α-intercalated cell of the kidney. It plays an important role in urinary acidification process in the kidney. The kAE1 transcript lacks exon 1 through exon 3 of eAE1 transcript due to the use of the alternative promotor located within intron 3 [6].

#### 3.6.1 Role of kidney in regulation of acid-base homeostasis

Since acid-base equivalents are generated from cellular metabolism of dietary constituents and amino acid metabolism, the maintenance of acid-base balance is crucial for normal function of the organs and cells in human body. In addition to the lung, kidney plays a major role in the regulation of acid-base homeostasis. Kidney regulates the body's acid-base balance by three mechanisms: a) avid reabsorption of most of the filtered bicarbonate; b) excretion of titratable acid; and c) generation and excretion of ammonium. Bicarbonate reabsorption and acid excretion has to be regulated according to the production of acid equivalents by metabolism, and respiration via the exhalation of $CO_2$. These processes occur along the nephron and

are highly coordinated and tightly regulated to avoid acid-base disturbances, and to maintain ionic homeostasis.

The proximal tubule is the main site of reabsorption of bicarbonate [141, 142], but tubule segments beyond the proximal tubules play a significant role in the regulation of acid-base balance and bicarbonate transport [143, 144]. About 4500 mEq of $HCO_3^-$ are freely filtered in the glomerulum with the majority being recovered in the early segments of the proximal tubule through $Na^+$-dependent and -independent processes [34, 145]. This reclamation process in the proximal tubule minimally requires the following: $H^+$ secretion of an equivalent amount via the lumenal $Na^+/H^+$ exchanger (NHE3), $H^+$-ATPase; lumenal CAIV, CAII; and the electrogenic Na-dependent bicarbonate cotransporter (NBC1). A smaller fraction (only 5-10%) is subsequently reabsorbed in the loop of Henle and collecting duct. The collecting duct serves as the final regulatory pathway to fine-tune the levels of $H^+$ -secretion, $HCO_3^-$ generation and reabsorption resulting in urinary acidification [15, 144].

In addition to $HCO_3^-$ reabsorption, the kidney must regenerate new bicarbonate (approximately 50-100 mmol/day) in the process of acid-secretion (approximately 50-80 mEq $H^+$/day) to match the amount newly produced by systemic metabolism. This process requires activities of several transport proteins of the acid secreting α-intercalated cells located in the collecting duct, including vacuolar $H^+$-ATPase, cytosolic CAII, and the basolateral chloride-bicarbonate exchanger, kAE1. High amounts of acid production in this process results in the exposure of the collecting duct to extreme pH values if remaining unbuffered. The cellular mechanisms of $H^+$ secretion and $HCO_3^-$ reabsorption in the collecting duct is summarized in Figure 6.

### 3.6.2 Role of kAE1 in regulation of bicarbonate transport

A variety of $Cl^-/HCO_3^-$ -exchangers have been firstly described on a molecular level in the collecting duct [33-35]. They serve several functions such as: $HCO_3^-$ -reabsorption in the α-intercalated cells or $HCO_3^-$ -secretion in the β-intercalated cells, to modulate cell volume or cell pH regulation. The α-intercalated cells, which located in the collecting duct, have kAE1 to mediate the release of $HCO_3^-$ into the blood. kAE1 is found only at the basolateral pole of the α-intercalated cells and is often used as an immunohistochemical marker for these cells [146, 147].

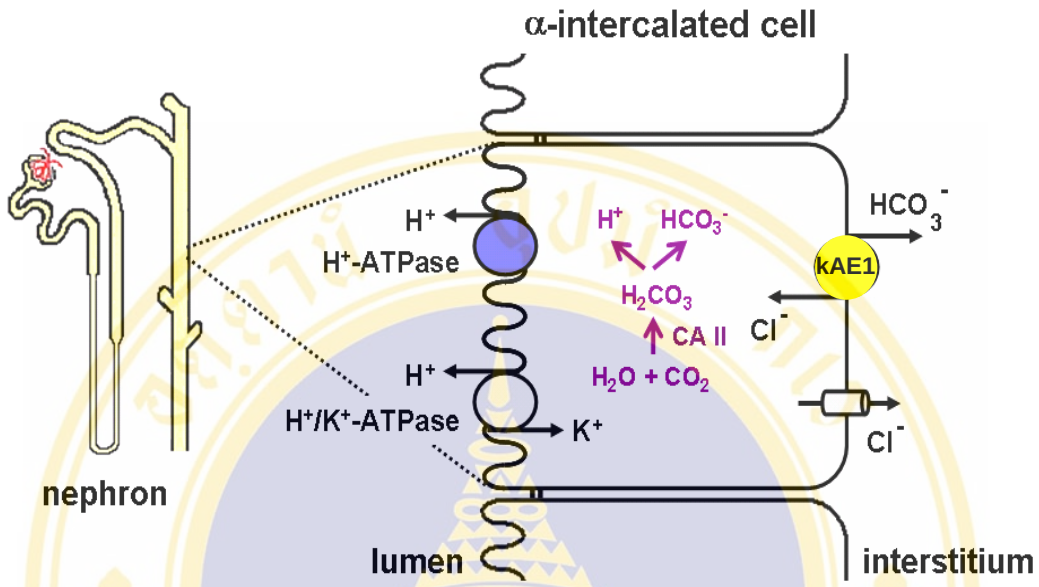


**Figure 6 Model of $HCO_3^-$ reabsorption/$H^+$ secretion in the distal tubules, taken from Yenchitsomanus PT, *et al.* [148].**

Type A intercalated cells produce the highest rate of $HCO_3^-$ reabsorption and $H^+$ secretion in the collecting duct. Several transporters; the vacuolar $H^+$-ATPase and a P-type gastric-like $H^+$-$K^+$-ATPase at the apical membrane and, an anion exchanger (kAE1) at the basolateral membrane, are present in these cells and potentially play a role in regulation of acid-base homeostasis.

In collecting duct, bicarbonate reabsorption is facilitated by $H^+$ secretion. The mechanism of bicarbonate reabsorption in the α-intercalated cells occurs through the enzymatic action of CAII that catalyzes the hydration of carbon dioxide to carbonic acid, which dissociates to form bicarbonate and hydrogen ions. The protons derived from this reaction are secreted into the tubule through the action of an $H^+$-ATPase or an $H^+/K^+$-ATPase in the apical membrane. The bicarbonate generated by this process leaves the tubular cell in exchange to chloride by kAE1 on the basolateral membrane and enters the blood stream.

kAE1 translocates monovalent anions by obligatory, electroneutral exchange independent of $Na^+$. The mechanism of AE1-mediated anion exchange is thought to be sequential (ping-pong). An anion is envisioned to bind to one surface of AE1, induce a conformational change that allows translocation of the anion across the plane of the lipid bilayer by traversal of the polypeptide's permeability barrier, and unbinding of anion from a distinct site on the other face of AE1. AE1 is then ready for a reversal of this transport process. The extracellular face also harbors covalent binding sites for the stilbene disulfonate inhibitor of anion transport and intramolecular cross-linker, $H_2$DIDS [149].

### 3.6.3 Distal renal tubular acidosis (dRTA)

Distal renal tubular acidosis (dRTA) is a clinical syndrome caused by impaired $H^+$ secretion in the distal and collecting tubules but retains normal bicarbonate reabsorption in the proximal tubule. The disease is characterized by systemic metabolic acidosis with inappropriately high urine pH (>5.5) and low ammonium excretion. Other clinical features include growth impairment, varying degrees of hypokalemia, muscle weakness, bone changes, nephrocalcinosis, nephrolithiasis, and renal failure secondary to chronic pyelonephritis and scarring. The syndrome of dRTA may be acquired in the context of systemic diseases, such as systemic lupus erythematosus (SLE), Sjögren's syndrome, and transplant rejection. Alternatively, dRTA may present as a familial disease transmitted in either autosomal dominant (AD) or recessive patterns (AR). It seems likely that the transporters involved in acid secretion and bicarbonate reabsorption in the kidney would be associated with dRTA. These transporters and enzymes include $H^+$-ATPase, $H^+/K^+$-ATPase, CAII and AE1.

Among these, mutations in the human AE1 gene are found to be associated worldwide with both forms of inherited dRTA [16, 150, 151]. The reported AE1 mutations associated with AD dRTA are R589H, G609R, S613F, A585D, A>L889X, R901X while those associated with AR dRTA are V488M, R602H, G701D, S773P and ΔV850 [63, 152, 153]. Functional studies of these AE1 mutations associated dRTA were conducted in many systems as described in the following section.

### 3.6.4 Functional studies of AE1 mutations associated wih dRTA

The molecular mechanisms of pathogenesis for specific AE1 mutations associated dRTA have been extensively studied which provide better understanding to how AE1 mutations cause the disease. Functional studies of AE1 mutations including their anion transport activity and protein trafficking have been studied in *Xenopus* oocytes and cultured mammalian cells. Expression of mutant R589H, R589C or S613F AE1 proteins in *Xenopus* oocytes exhibited slightly reduced anion exchange activity [154, 155]. However, when expressed AE1 R589H in HEK 293 cells, the mutant protein was severely reduced on cell surface as demonstrated by immunofluorescence and cell surface biotinylation techniques [156]. Reduced cell surface expression was accompanied by an absence of detectable anion transport activity. The stability of kAE1 R589H polypeptide in transfected HEK 293 cells was apparently unaltered, but ER exit was reduced and retarded. Most importantly, co-expression of kAE1 R589H with wild-type kAE1 resulted in heterodimer formation, accompanied by complete inhibition of wild-type kAE1 expression in the plasma membrane. This dominant negative trafficking defect could explain the pathogenesis of the dominant dRTA found in the patients [156]. The same phenomenon was observed when kAE1 R589H dRTA mutation stably expressed in nonpolarized and polarized MDCK cells [24]. Similarly, it was observed that the R901X or band 3 Walton retained normal $Cl^-$ transport activity in *Xenopus* oocytes but failed to express at the cell surface of HEK 293 cells, owing to intracellular retention with failure to reach the medial Golgi compartment [23]. Recently, a stably transfected cells model for expression of kAE1 and mutant proteins was developed in MDCK cells [24, 157]. In polarized cells, normal kAE1 was delivered to the basolateral membrane while the R589H and S613F could not reach the plasma membrane and R901X was mistargeted

to the apical membrane [24]. A more recently described AD dRTA mutant, kAE1 G609R (in TM7) exhibits normal anion transport in *Xenopus* oocytes and a depolarized trafficking phenotype in polarized epithelial cell monolayers similar to that of kAE1 901X [152]. This mutant protein appears to mistarget to the apical plasma membrane. These results demonstrated that AD dRTA can be occurred from intracellular retention or aberrant targeting of kAE1 in polarized kidney cells which would allow in alteration of electrochemical balance.

In addition, AE1 mutations associated with AR dRTA are found mostly in populations of Thailand [158-160], Malaysia, and Papua-New Guinea [161]. The first AR dRTA mutation found was AE1 G701D. Recessive dRTA patients with homozygous AE1 G701D have normal erythroid indices, eAE1 abundance, and sulfate transport activity. However, when expressed in the heterologous expression system of *Xenopus* oocytes, both kAE1 G701D and eAE1 G701D were functionally inactive owing to intracellular protein retention [162]. Co-expression of AE1 G701D with wild-type AE1 showed no dominant negative effect, consistent with the normal kidney phenotype in heterozygous individuals. Co-expression of red cell protein named glycophorin A (GPA) could completely rescue the anion transport activity of AE1 G701D-expressing oocytes, accompanied by transit of the mutant AE1 polypeptides to the plasma membrane [162]. The ability of glycophorin A to effect rescue of the AE1 G701D did not require normally homodimeric glycophorin A. Thus, the absence of the erythroid-specific GPA in the kidney strongly suggests that AE1 G701D polypeptide is also retained intracellularly in the α-intercalated cells, resulting in impaired urinary acidification in these patients [162]. A functional equivalent of glycophorin A in the α-intercalated cells has not been defined. Furthermore, this mechanism was supported by a parallel study of compound heterozygosity of G701D mutant with a recently described kAE1 S773P recessive mutant which showed that both mutants are impaired in trafficking to the plasma membrane in transfected HEK 293 cells [153]. The schematic models for dominant and recessive dRTA in polarized epithelial cells are shown in Figure 7.

### 3.7 kAE1 protein trafficking

All newly synthesized proteins require transportation mechanisms that regulate

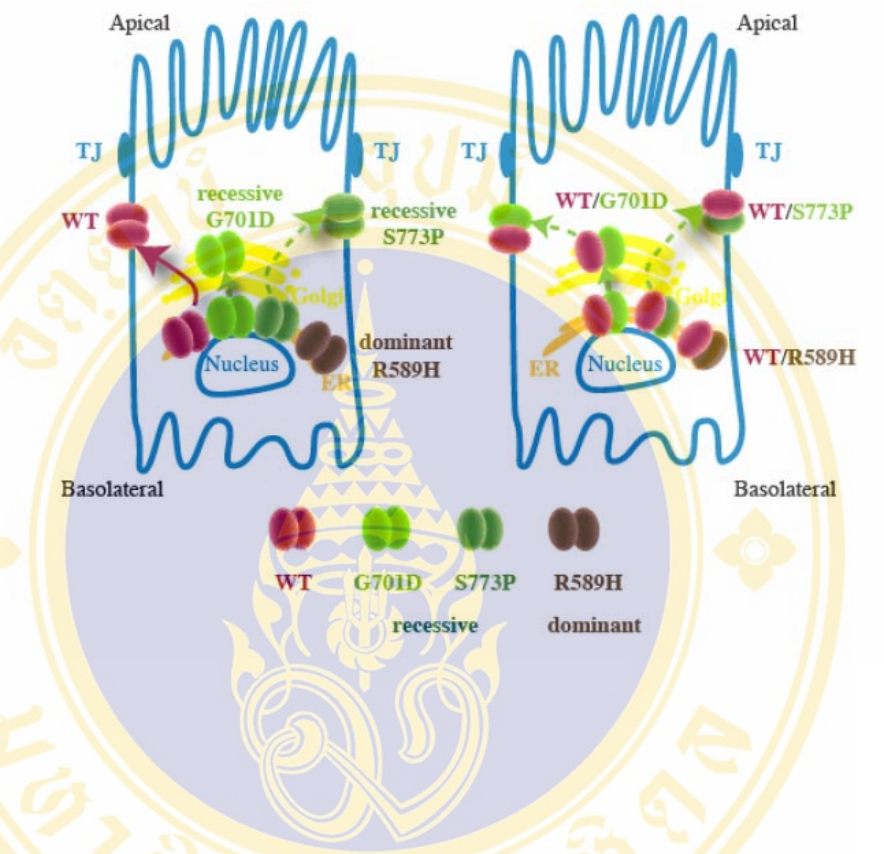


**Figure 7 The schematics illustrating the molecular mechanism for dominant and recessive dRTA in polarized epithelial cells, taken from Yenchitsomanus PT, *et al.* [148].**

Model of epithelial cells expressing wild-type kAE1, dominant or recessive mutants in homozygous (left) or heterozygous state (right). Dimers of wild-type kAE1 traffic to the basolateral membrane while dominant dRTA mutants (R585H) are retained in the ER. Recessive dRTA mutants are partially impaired (dotted lines) in their exit from the ER but can either traffic to the basolateral membrane (S773P) or are retained in the Golgi apparatus (G701D). Heterodimers of wild-type kAE1 and dominant kAE1 mutant are retained in the ER, while heterodimers of wild-type kAE1 and recessive kAE1 mutants can traffic to the basolateral membrane. TJ denotes tight junction.

the movement of proteins to a specific location within the cell where those proteins present their functions. Several mechanisms are required to ensure the directed movement of membrane components within cell and to control their delivery to the appropriate target membrane. There are two special mechanisms involved in this process which include “protein trafficking” and “protein targeting”. While protein trafficking focus on the translocation of protein from endoplasmic reticulum to Golgi and plasma membrane of nonpolarized cells, protein targeting focus on how protein target to the apical or basolateral membrane of polarized epithelial cells. The principle underlying the polarized distribution mechanisms is that sorting information that is often referred to sorting signal, sorting determinant or trafficking signal. To date, a few kinds of sorting signal have been identified. The sorting of type I membrane proteins to the basolateral membrane of kidney epithelial cells has been shown to be dependent upon dominant cytoplasmic sorting signals that direct the vectorial transport of newly synthesized proteins from the TGN to the basolateral membrane [163-165]. Many of these basolateral sorting signals are tyrosine-dependent [163, 164]. This motif is associated with localization to coated pits and clathrin-mediated endocytosis but they are also linked to basolateral sorting [166]. It has shown that these motifs are located on the cytoplasmic domain of the proteins where they can be accessible to interact with sorting machinery such as adaptor complex subunits. Tyrosine-based signal is mostly formed to the consensus motifs YXXΦ (Y is tyrosine, X is any amino acid, and Φ is an amino acid with a bulky hydrophobic side chain) [167] or NPXY (N is asparagines and P is proline) [167].

Many membrane transporters are known to sort to basolateral membrane through interaction of tyrosine-based signal motif in their cytoplasmic domains with adaptor protein complexes. Although the explanation for the movement of kAE1 to the basalateral membrane of the α-intercalated cells in the kidney remains unclear, it seems to be the motif YDEV (position 904-907) at the C-terminus of kAE1 conforms with the basolateral sorting motif, YXXΦ (Figure 8). It has been demonstrated that this motif play an important role in the polarized distribution of kAE1 at the cell surface of MDCK cells [77, 157]. AE1 with mutation of tyrosine to alanine at position 904 (Y904A) or deleted 11 amino acids (R901X) is mistargeted to apical and some at the basolateral membrane [157]. In general, a subset of YXXΦ is known to be

interacting with adaptor protein (AP) complexes, AP-1, AP-2, AP-3 and AP-4 [168]. Interaction of this motif with μ subunit of AP-1B is specific to polarized epithetial cells [169]. However, the AP-1B complex has not been involved in kAE1 targeting because the normal basolateral expression of wild type C-terminal tail kAE1 was observed in LLC-PK1 cell line which lacks μ1B subunit [157]. This suggested that other adaptor proteins are involved in basolateral sorting of kAE1.

Besides, the C-terminal domain of AE1 has been proposed to encode for PDZ (Post-Synaptic-Density-95/Discs-large/Zona-Occludence-1) interacting motif which can be recognized by class II PDZ domains, AMPV (Figure 8). This domain is known to be a modular protein interacting modules to provide a scaffold for the assembly of supramolecular complexes at the specific site. However, the protein that interacts with this domain has not been defined. The last four amino acids of AE1 are AMPV which may be responsible for the interaction of the AE1 and a PDZ-domain containing protein. Truncated C-terminal 4-5 residues AE1 protein demonstrated impaired trafficking of the protein in MDCK cells, suggesting that this PDZ-binding domain plays a crucial role in processing kAE1 to the plasma membrane [77]. More recently, Toye *et al* suggested that the C-terminus PDZ-binding motif is not necessary for basolateral targeting of kAE1. In addition, this motif may play some specific role in the efficient trafficking and/or retention at the basolateral membrane [170].

Interestingly, removal of the N-terminal kAE1 caused the protein localized to the apical membrane of stably transfected MDCK cells suggesting there is a determinant within the N-terminus sequences is required in addition to the YXXΦ motif in the C-terminus for basolateral kAE1 targeting [24]. It was proposed that tyrosine phosphorylation may play an important role in kAE1 trafficking [170]. There are two sites of tyrosine phosphorylation including Tyr359 in the N-terminus and Tyr904 in the C-terminus of AE1 which are phosphorylated in red blood cells. A potential role for phosphorylation in the basolateral localization of kAE1 was suggested by the observation that the substitution of phenylalanine for Tyr904 alters kAE1 targeting [24, 157]. It was suggested that the phosphorylation of Tyr904 in YDEV motif causes internalization of kAE1 from the basolateral membrane. Dephosphorylation of this motif by the phosphatase SHP2, which recruits by of Tyr359, allow the recycling of kAE1 back to the basolateral membrane.


**Figure 8 Carboxyl-terminal tail of human AE1.**

Amino acid sequences of the carboxy-terminal tail of human AE1 are shown from the position 872 to 911. The sequences in the boxes represent the known or putative CAII, AP and PDZ interacting sites.

### 3.7.1 The role of cytoskeleton in protein targeting

The cytoskeleton consists of many types of intracellular filamentous structures. Some are long polymers of smaller subunits, such as actin and microtubules, whereas others are composed of long chains of amino acids, such as intermediate filaments. These cytoskeletal elements participate in several important aspects including cell shape, cell motility, cell division, and signal transduction as well as their involvement in cell polarity. During the establishment of epithelial polarity, the actin cytoskeleton of MDCK cells undergoes a dramatic reorganization. Cells grown in subconfluent mono-layers possess discrete actin stress fibers in the basal membrane. During polarization, these stress fibers become much less prevalent as actin is redistributed for the most part to sites of cell–cell contact [96]. Actin cytoskeleton seems to be involved in maintenance of polarized cells.

The potential role of the actin cytoskeleton in directing the intracellular localization of AE1-4, major chicken-specific kidney AE1 isoform, was studied in MDCK cells [96]. They found that subconfluent monolayers of cells transfected with AE1-4 are associated with the actin cytoskeleton. Treatment with the actin-depolymerizing drug, latrunculin B, for 1 h before detergent lysis revealed that the detergent insoluble pool of AE1-4 was dramatically reduced in cells treated with this reagent. This result indicates that the maintenance of AE1-4 insolubility is almost entirely dependent upon an intact actin cytoskeleton in subconfluent cells. Although the exact role of the actin cytoskeleton in directing the intracellular trafficking of AE1 is unclear, the ability of mutant AE1 constructs to accumulate in the basolateral membrane of this cell type correlated with their ability to colocalize with phalloidin-stained stress fibers. However, there is no evidence reporting the involvement of actin cytoskeleton in targeting of membrane protiens to basolateral membrane of epithelial cells in human.

Apart from the actin cytoskeleton, microtubules also play an important role in maintaining the polarized distribution of some membrane proteins. Many evidences showed that transport of newly synthesized proteins to both apical and basalateral membrane depend on microtubule [171, 172]. Microtubules are dynamic structures that interact with intracellular organelles and vesicles by means of associated proteins, which include the so-called "microtubule motors" of the dynein and kinesin families

[173]. These motors take advantage of the intrinsic polarity of microtubules, and use energy derived from adenosine 5'-triphosphate (ATP) hydrolysis to cause vesicle/organelle movement in either the anterograde (kinesin - towards the "+" end) or retrograde (cytoplasmic dynein - towards the "-" end) direction along microtubules. It has been shown in many studies that microtubule disruption by colchicine or nocodazole perturbs the delivery of proteins to the cell surface, and causes a marked shift in the distribution of many membrane proteins from their usual surface location onto scattered intracellular vesicles [174].

Along with microtubules, the actin-based cytoskeleton is a dynamic and highly organized structure composed of filamentous (F) actin and associated proteins. Disruption of the actin cytoskeleton affects the polarized expression and function of cell surface proteins in a variety of ways. Like microtubules, actin filaments are also directional. They have a "+" and "-" end which can support vesicle movement via the myosin family of ATPases [175, 176]. Actin regulatory proteins have also been shown to directly bind to proteins involved in vesicular traficking [177]. Thus, actin filaments may, together with microtubules, serve as mechanical elements that drive and guide vesicle movement within cells [178].

### 3.8 Structural differences between kAE1 and eAE1

Previous research on the structure analysis of the N-terminal cytoplasmic domain of kAE1 showed both similarities and differences when compared to eAE1 [10]. Both isoforms exhibited only minor variation in α–helical and β–pleated sheet content. kAE1 was also observed to engage in the same conformational equilibrium characteristic of eAE1 whereas the tryptophan and cysteine clusters of kAE1 acted very differently from eAE1 in response to pH changes and oxidizing condition. In addition, the purified eAE1 and kAE1 cytoplasmic domains expressed in *E. coli* showed similar circular dichroism spectra, Stokes radius and the same pH-dependent conformational change, the cytoplasmic domain of eAE1 but not kAE1, appeared to be toxic to bacterial host [10]. Moreover, the intramolecular disulfide bond between Cys201 and Cys317 occurred in eAE1 is undetectable in the kAE1 cytoplasmic domain.

Interestingly, the three dimensional structure of the N-terminal cytoplasmic domain of eAE1 exhibited a globular structure which composed of a central β-strand containing amino acid residues 57-66 [4]. The lacking of the first 65 amino acids at the N-terminal domain of human kAE1 would cause the absence of a central β-strand seen in the eAE1 structure (Figure 9). The structural difference might alter function of the kAE1 cytoplasmic domain. Unlike eAE1, kAE1 does not bind to ankyrin, band 4.1, band 4.2, glyceraldehydes-3-phosphate dehydrogenase or aldolase [10]. It seems likely that the absence of the first 65 amino acids in kAE1 does change in the structure and protein-protein interactions. However, the proteins that interact with the N-terminus of kAE1 and play a role-like ankyrin, band 4.1, band 4.2 and glycolytic enzymes for anchorage kAE1 to cytoskeleton network in human kidney are still unknown.

### 3.9 Protein interacting with the cytoplasmic domain of kAE1

Up to date, a novel protein called kanadaptin (kidney anion exchanger adaptor protein) is the only one protein that has been reported to interact with the N-terminal of kAE1 [12]. The interaction of kanadaptin and kAE1 was identified by yeast two-hybrid screening of a mouse kidney cDNA library. Results from the interaction of GST-kanadaptin with kAE1 confirmed the yeast two-hybrid interaction and further suggest that the interaction is likely due to hydrophobic forces.

Northern blot analysis showed that kanadaptin was widely expressed at a low level in kidney, lung, liver, brain, testis, heart, and skeletal muscle, with the brain and testis having the highest expression, and there were at least two messages in the brain and kidney [12]. Furthermore, immunoblot analysis of supernatant from the cytosol fraction of rabbit kidney cortex, medulla, and papilla showed that kanadaptin is highly enriched in the papilla compared with the medulla, which is greater than the cortex.

Immunohistochemistry of rabbit kidney sections showed that kanadaptin was expressed in the kidney only in the collecting duct. It also showed a remarkable colocalization of kanadaptin and kAE1 when using simultaneous staining. Furthermore, kanadaptin was colocalized with kAE1 in the intracellular vesicles but

**Figure 9 Ribbon diagram of the monomer of cytoplasmic amino-terminal domain of eAE1, taken from Zhang D, *et al*. [4].**

The dark strand in the middle is the β-strand corresponding to the residues 1-65 which is absent in kAE1.

not when kAE1 was located in the basal and lateral plasma membranes. The result suggested that kanadaptin is part of a signal transduction machine that is important in targeting these kAE1 vesicles.

However, when the interaction of human kanadaptin with human kAE1 was studied in co-transfected HEK293 cells, the result from co-immunoprecipitation and histidine6-tagged co-purification showed that human kanadaptin does not bind to either human kAE1 and eAE1 [13]. Furthermore, co-expression of human kanadaptin with kAE1 has no effect on the trafficking of kAE1 from its site of synthesis in the endoplasmic reticulum to the plasma membrane. Taken together, these results reveal that while kanadaptin binds to kAE1 in mouse, the binding of kanadaptin and kAE1 is unlikely in human.

While the role of kanadaptin remains unclear, using immunofluorescence and subcellular fractionation approaches demonstrated that kanadaptin is localized within the nuclei of various epithelial and non-epithelial cultured cell types [179]. Furthermore, immunostaining revealed localization of kanadaptin in two subcellular locations, nuclei and mitochondria [180]. Whereas nuclear localization was demonstrated in virtually all cells, mitochondrial staining was restricted to certain cell types. By using an interspecies heterokaryon assay, it was demonstrated that kanadaptin has nuclear export activity. Thus, kanadaptin can be regarded to be a highly mobile nucleocytoplasmic shuttling and multilocalizing protein.

**4. Pantophysin**

Pantophysin (PPH) is a homologue of the neuroendocrine-specific protein synaptophysin which share a 43 percent overall amino acid sequence identity [181]. It contains four 23-29 amino acid long segments of significant hydrophobicity assumed to from transmembrane domains that are similar to synapthophysin. It also has many conserved features when compare to synapthophysin including, a potential N-glycosylation site in the first intravesicular loop domain (Asn72), paired cysteine residues in both intravesicular loops (Cysteine64, Cysteine 99, Cysteine 194, Cysteine 202) and charged residues within transmembrane domains (Lys37, Asp154). In contrast, the N- terminal amino acid sequences of pantophysin are different from

synapthophysin and the C-terminal of pantophysin has only a short 26 amino acid end domain which lacks the multiple tyrosine containing motif of synapthophysin.

Pantophysin mRNA is expressed in various murine cell lines including pluripotent embryonal stem cells, fibroblast derived 3T3-L1 cells and neuroendrocrine pituitary tumor derived AtT20 cells [181]. Immunofluorecence staining of bovine testis demonstrated that the cytoplasm of all cells showed strong multipunctate labeling with pantophysin antibodies whereas the surrounding extracellular matrix of lamina propria was negative [182]. Furthermore, strong pantophysin immunoreactivity was also seen in the duct epididymis, the exocrine gland (pancreas and parotid gland) and the gastrointestinal tract.

Studies of intracellular localization showed that pantophysin was predominantly localized in dot like structures in the cytoplasm and in a variable pattern around the nucleus [181]. It also colocalized with the transferin receptor, SCAMPs (secretory carrier associated membrane proteins) and cellubrevin which are marker for small vesicles that participate in shuttling, secretion, endocytosis and recycling. By using differential centrifugation, pantophysin positive vesicles could be enriched from A431 cells. These vesicles also contained synaptophysin, SCAMPs and cellubrevin which suggested that all these molecules perform similar basic function that are important for membrane domain biogenesis and maintenance including regulation of vesicle fusion and intravesicular milieu.

Although pantophysin is proposed to be associated with small cytoplasmic transport vesicle, its function in vesicle trafficking has been unclear. While pantophysin mRNA is expressed in 3T3-L1 cells and its level increased during differentiation of 3T3-L1 cells to adipocytes [183], study of pantophysin associated vesicle trafficking can be conducted in this system since this cell has a relatively large volume of vesicle trafficking. Immunoblot analysis indicates pantophysin is present exclusively in membrane fractions and relatively evenly distributed in the plasma membrane and internal membrane fractions [183]. Further analysis of pantophysin vesicles by sucrose gradient ultracentrifugation demonstrated that pantophysin and GLUT4 exhibited overlapping distribution profiles. Analysis of immunopurifed vesicles revealed that GLUT4 vesicles contain pantophysin. It also showed that

pantophysin was associated with VAMP2 which is involved in targeting intracellular transport vesicle.

The association of pantophysin with GLUT4 vesicles and its interaction with VAMP2 suggest a potential role for this protein in insulin-regulated translocation of GLUT4. To attempt to disrupt a potential function of pantophysin in GLUT4 vesicle trafficking, permeabilized adipocytes were incubated with the C-terminal cytosolic domain of pantophysin expressed as a GST fusion protein. It was found that GST-panto-CT had no effect on the ability of insulin to stimulate GLUT4 translocation [183]. However, microinjection of antibodies against pantophysin or microinjection of a C-terminal fragment of pantophysin inhibited insulin stimulated GLUT4 translocation [184]. Thus, the functional role of pantophysin in vesicle trafficking is unclear.

**5. Integrin-linked kinase**

Integrin-linked kinase (ILK) is a serine/threonine kinase which contains 452 amino acids with three structural domains. The N-terminus features four ankyrin repeats followed by a phosphoinositide-binding pleckstrin-homology-like domain [185]. The phosphoinositide binding motif partially overlaps with the kinase catalytic domain at the COOH-terminus. ILK was shown to have serine/threonine protein kinase activity which capable of both autophosphorylation and phosphorylation of exogenous substrates like myelin basic protein or phosphorylation of a peptide representing the β1-integrin domain and protein kinase B/Akt (PKB/Akt) [186].

ILK plays a key role in focal contact during ligand binding of integrin which resulted in cytoskeleton reorganization and intracellular signaling [187, 188]. Since ILK is capable of interacting with several intracellular protein, ligand binding of integrins induces clustering to form focal adhesions which followed by the recruitment of ILK and its intracellular interaction partners PINCH (particularly interesting new cysteine-histidine-rich protein-1), α-parvin, β-parvin and paxillin [189]. PINCH-1 is a LIM-only protein that co-localizes with integrins to focal adhesions and binds to the N-terminal ankyrin repeat domain of ILK [190]. The α and β-parvin are two highly related proteins composed of two tandemly arranged calponin homology (CH) domains, CH1 and CH2, involved in actin binding [191]. Both molecules associate

with residues in the catalytic domain of ILK and do not overlap with the binding site of PINCH-1 [192, 193].

ILK can mediate actin cytoskeleton dynamic by using many intracellular components. While ILK binds β-parvin via their CH2 domains [191], the phosphorylation of β-parvin at the CH2 domain by its binding partner ILK is required for the interaction of β-parvin with α-actinin which coupling the ILK, β-parvin and α-actinin complex to F-actin [194]. Further studies indicate that Rac and Rho are downstream targets of ILK, PINCH and parvin and that the ILK–PINCH–parvin complex is able to regulate actin cytoskeletal dynamics [195, 196]. The Cdc42/Rac1-specific guanine nucleotide exchange factor α-PIX (PAK-interactive exchange factor-α) [197-199] has been identified as an additional β-parvin binding partner. α-PIX is able to affect the regulation of Rac and Cdc42, key regulators of the actin cytoskeleton including filopodia and lamellipodia formation [199, 200]. Finally, ILK connects via PINCH to Nck-2 [201, 202], known to bind to DOCK180 (180 kDa protein downstream of CRK) [203], another guanine nucleotide exchange factor mediating actin cytoskeleton dynamics via Rac [204].

While linking of ILK to actin cytoskeleton can be demonstrated by many pathways, a complex formation of ILK, α-parvin and paxillin to actin cytoskeleton has been described in detail by Nikolopoulos and Turner [191]. It was showed that paxillin acts as a binding interface for both ILK and actopaxin (α-parvin) [205, 206]. Paxillin is a multidomain protein that localizes to focal adhesions and functions as a cytoskeletal scaffold protein for many proteins [207-209]. The amino terminus of paxillin contains five leucine-rich sequences (LDXLLXXL) named LD motifs which interact with their binding partners through conserved sequence know as PBSs (paxillin binding subdomain sequence). Actopaxin can bind directly to both F-actin and paxillin LD1 and LD4 motif via its PBSs which located within CH2 domain, suggesting a role for this complex in actin cytoskeleton [205]. Paxillin LD1 motif also binds to PBSs located within the carboxyl-terminal kinase domain of ILK [206]. Taken together, these results demonstrated the organization of ILK-paxillin-actopaxin complex into actin cytoskeleton (Figure 10).

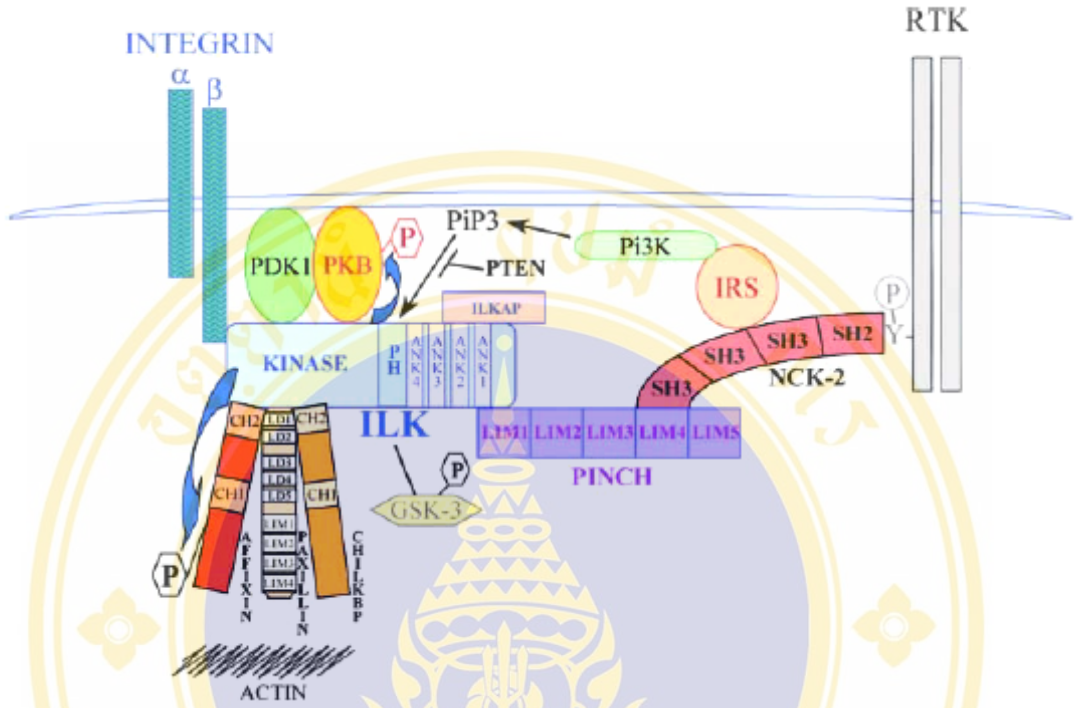


**Figure 10 Function of ILK to link integrins and receptor tyrosine kinase to the actin cytoskeleton and downstream signaling molecules, taken from Persad S, *et al*. [210].**

All of the indicated proteins have been shown to interact with ILK directly via a variety of biochemical and genetic techniques (207). PDK-1: phosphoinositide phospholipid-dependent kinase 1; PIP2: phosphoino sitide 4,5 bisphosphate; ANK: ankyrin; ILK-AP: ILK associated phosphatase; PH: pleckstrin homology; GSK-3: glycogen synthase kinase-3; PKB: protein kinase B/Akt; CH-ILKBP: calponin homology containing ILK binding protein.

Although ILK is linked to actopaxin via its interaction with paxillin, another study demonstrated a direct association between ILK and actopaxin [191]. In this study, it was demonstrated that the C-terminal domain of ILK contains the binding site for actopaxin while ILK binds to the CH2 domain of actopaxin. However, an actopaxin CH2 domain mutant defective for paxillin binding (PBSs) retains the capacity to bind ILK, indicating that paxillin and ILK binding sites on actopaxin are distinct. These data reinforce a primary role for paxillin in the recruitment of actopaxin and ILK which suggests that under certain physiologic conditions ILK binding alone may be sufficient for actopaxin recruitment. However, although actopaxin can bind directly to both the LD1 and LD4 motifs of paxillin, it may also interact indirectly with paxillin via ILK binding to LD1. Similarly, ILK can interact indirectly with the paxillin LD4 motif, possibly through association with actopaxin. How the cell utilizes the differential binding capacity of the paxillin LD motifs represents an important function to facilitate actin cytoskeleton dynamic.

**6. The outline of experimental studies in this thesis**

Structural difference between kAE1 and eAE1 has been raised to be a major cause that alters protein-protein interaction in kAE1 since it is unable to bind several proteins such as ankyrin, protein 4.1 as well as glycolytic enzymes. These proteins interact with the N-terminal cytoplasmic domain of eAE1 to provide the association of eAE1 with cytoskeleton network that required for red cells biconcave stability. In addition, glycophorin A (GPA), protein interacting with the extracellular side of putative transmembrane segment 8 of AE1, has been reported to be involved in biosynthesis and facilitates trafficking of AE1 to plasma membrane of red blood cells. Nevertheless, the protein interacting with the N-terminus of kAE1 has not been defined. Mutations in AE1 gene have been found to be associated with dRTA. The proposed molecular mechanism of the disease is involved in defect of the protein trafficking or mistargeting to an appropriate site of the α-intercalated cells. However, studies in red cells and *Xenopus* oocytes expressing the mutant AE1 revealed the mutant proteins were rescued by GPA and showed the normal transport activity. Naturally, GPA is not detectable in the α-intercalated cells of kidney. The protein that can play a role compensate GPA function in kidney has not been identified. Although

the recent protein named kanadaptin was identified to be associated with kAE1 in mouse kidney, it did not show interaction with kAE1 in human kidney.

The remarkable question need to be investigated is identification of the proteins that interact with the N-terminus of kAE1. The protein might involve in normal kAE1 trafficking and provide a clue for more understanding in pathogenesis of dRTA. Novel protein-protein interactions with the N-terminal kAE1 were identified in human kidney cDNA library by using GAL4 based yeast two-hybrid system. The cDNA clones isolated from the library were sequenced and submitted to search for the homologous sequences in the genome databases. The cDNA clones encoded for proteins of interest will be selected for further studies. The full-length of the selected cDNA clones can be obtained by PCR amplification using human kidney cDNA as template. The fragments encoded for selected proteins were expressed by cloning into eukaryotic expression vector. Interaction between kAE1 and interacting proteins was studied in human embryonic kidney (HEK 293) cells to imitate the physiological system. Co-expression studies including co-immunoprecipitation, affinity co-purification, subcellular localization, cell surface expression, mapping the region required for interaction and protein trafficking were investigated in condition of kAE1 express either alone or in combination with interacting proteins to observe the effect of interacting proteins on kAE1 expression. The data from these studies would provide insight into the detail of protein-protein interactions in kAE1 and mechanism of kAE1 trafficking in the kidney.

# CHAPTER IV
# MATERIALS AND METHODS

## 1. Experimental design

To identify proteins that interact with the N-terminus of kAE1, experimental strategies were divided into two parts. Part I consisted of experiments to identify proteins that interact with the N-terminus of kAE1 in yeast. Part II studied the interaction in mammalian cells following experiments to address the role of interacting protein in the physiological function of kAE1. Flow charts of experimental studies in each part are shown in Figures 11 and 12.

**Part I**, identification of candidate proteins that interact with the N-terminal kAE1 was conducted by using yeast two-hybrid system. The N-terminus of kAE1 (NkAE1, Met66-Pro403 of human AE1) was used as bait to screen its interactors in kidney cDNA library. Interaction of NkAE1 and interacting proteins was assayed by growth of yeast on synthetic dropout medium and screening of α-galactosidase activity. cDNA inserts of positive clones were sequenced. Genes with homology to the identified clone sequences were identified in databases, using BLAST software. Specificity tests were used to confirm the interaction between NkAE1 and interacting proteins in yeast.

**Part II**, interaction between kAE1 and interacting proteins (integrin-linked kinase (ILK), pantophysin (PPH), glycerealdehyde-3-phosphate dehydrogenase (GAPDH) and thymosin β4) from the two-hybrid screen was verified in human embryonic kidney (HEK 293) cells. Co-immunoprecipitation, affinity co-purification and immunofluorescence studies were carried out to demonstrate the specific interaction of kAE1 and interacting proteins. Cell surface biotinylation to address the role of interacting proteins on cell surface expression of kAE1 was also investigated. Detailed analysis of the interaction between kAE1 and ILK was studied by using FACS analysis, co-purification, Triton X-100 cytoskeleton extraction and $Cl^-/HCO_3^-$ exchange functional assays.

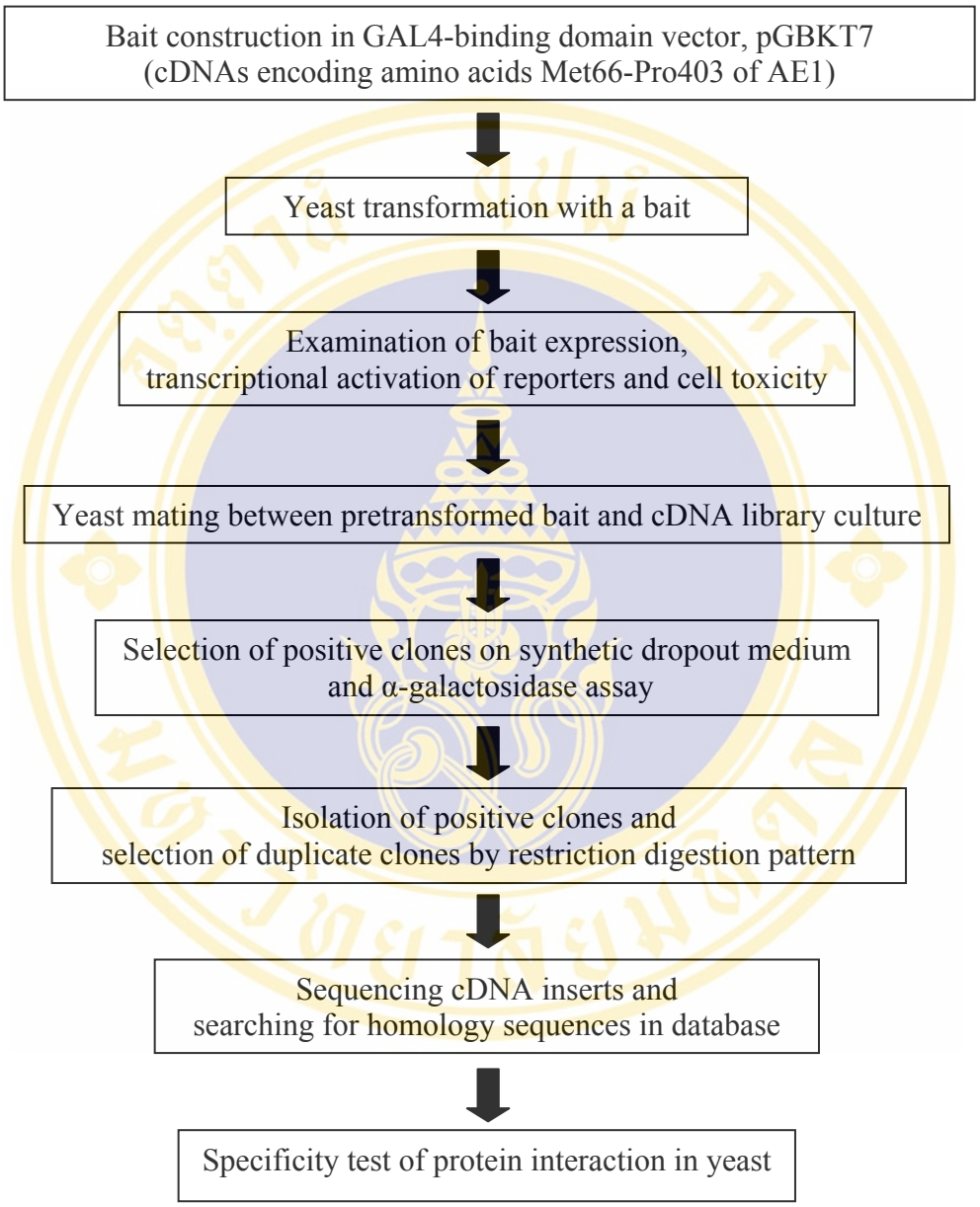


**Figure 11** Experimental strategy and steps in Part I: the identification of candidate proteins that interact with the N-terminal kAE1 by using yeast two-hybrid system.

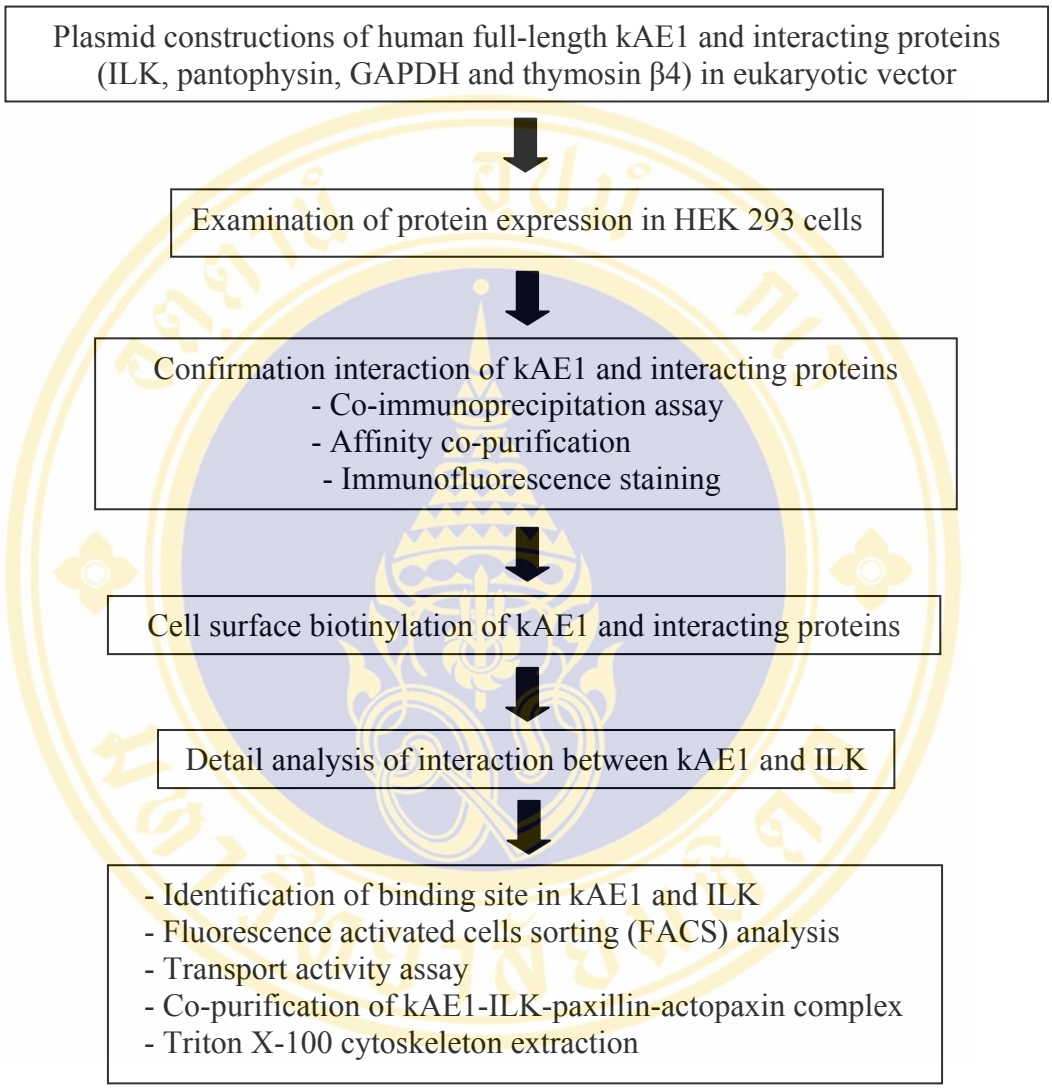


**Figure 12** Experimental strategy and steps in Part II: studies of the interaction between kAE1 and interacting proteins in human embryonic kidney (HEK 293) cells.

## 2. Materials

### For yeast two-hybrid screening

### 2.1 Pretransformed human kidney cDNA library

Human kidney cDNA library was cloned into GAL4-activation domain (GAL4-AD) vector, pACT2, using *Xho*I and *EcoR*I sites and transformed into *Saccharomyces cerevisiae* strain Y187 (*MATα*). This library was purchased from Clontech (see figure 13 A).

### 2.2 Plasmid Constructs

#### 1. GAL4-binding domain (GAL4-BD) vector, pGBKT7

The pGBKT7 vector expresses protein fused to amino acids 1-147 of the GAL4-binding domain. It replicates autonomously in both *E. coli* and *S. cerevisiae* thus it was used to construct the bait for library screening. This vector was purchased from Clontech (see Figure 13B ).

#### 2. pcDNA 3/kAE1

Human kAE1 cDNA, a generous gift of Prof. Dr. Reinhart Reithmeier's laboratory, University of Toronto, Canada, was inserted into the *Hind*III and *Bam*HI sites of pcDNA 3. The recombinant plasmid was used as template for PCR amplification of the N-terminal kAE1.

#### 3. pNkAE1 (bait)

The N-terminal kAE1 (residues Met66-Pro403 of AE1) cDNA was amplified from kAE1 construct using specific primers as followed. cDNA was insert to *Nco*I and *Sal*I sites of pGBKT7 to create bait (fusion GAL4-BA/NkAE1) for library screening. The construct was named pNkAE1 (Figure 39 in Appendix II).

#### 4. pGBKT7-53 in strain AH109

This plasmid encodes a DNA-BD/murine p53 fusion protein and pre-transformed into yeast strain AH109 served as a positive control plasmid.

#### 5. pGBKT7-Lamin C in strain AH109

This plasmid encodes a DNA-BD/human lamin C fusion protein and pre-transformed into yeast strain AH109 served as a negative control plasmid.

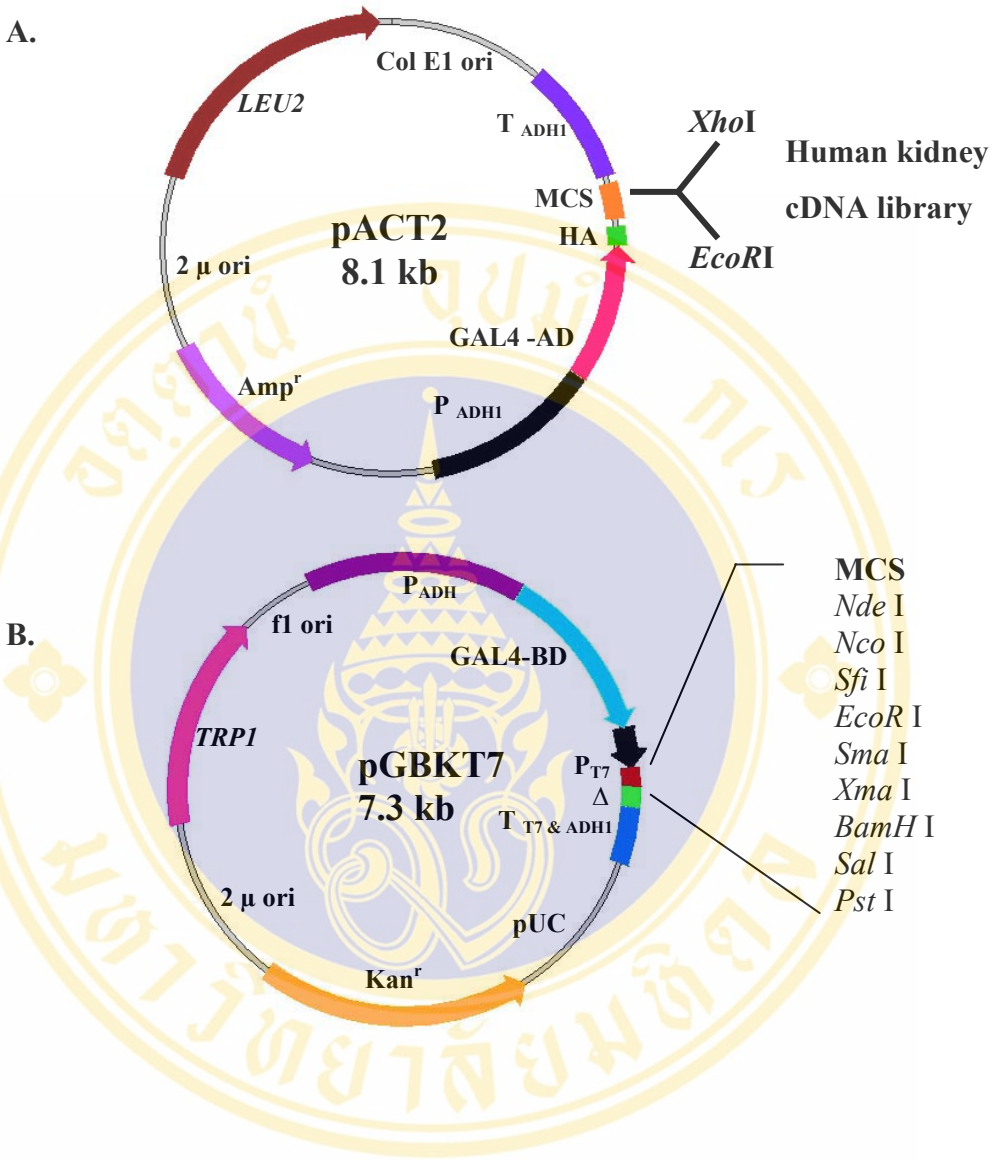


**Figure 13 Physical map of plasmid vectors for yeast two-hybrid system.**

**A.** pACT2 generates a fusion of GAL4-AD, an HA epitope tag, and cDNAs of human kidney library cloned into *Xho* I and *EcoR* I sites of this vector. It contains the constitutive *ADH1* promotor, transcription termination, ampicillin resistance gene and *LEU2* nutritional marker.

**B.** pGBKT7 generates a fusion of GAL4-BD and bait cDNAs. It contains *ADH1* promotor, T7 promotor, c-myc epitope tag, transcription termination, kanamycin resistance gene and *TRP1* nutritional marker. The N-terminal kAE1 was inserted into *Nco* I and *Sal* I sites of this vector.

**6. pTD1-1 in strain Y187**

This plasmid encodes an AD/SV40 large-T antigen fusion protein and pre-transformed into yeast strain Y187 served as a positive control plasmid. These control plasmids were purchased from Clontech.

### 2.3 Yeast strains (*S. cerevisiae*)

**1. AH109 (*MATa*) genotype**

The genotype of this yeast strain is *trp1-901, leu2-3,112, ura3-52, his3-200, gal4*Δ, *gal80*Δ,*LYS2::GAL1*$_{UAS}$-*GAL*$_{TATA}$-*HIS3*,*GAL2*$_{UAS}$-*GAL2*$_{TATA}$-*ADE2, URA3::MEL1*$_{UAS}$ -*MEL1*$_{TATA}$-*lacz MEL1*. It contains *HIS3, ADE2, MEL1* and *lacZ* reporters.

**2. Y187 (*MATα*) genotype**

The genotype of this yeast strain is *trp1-901, leu2-3,112, ura3-52, his3-200, gal4*Δ, *gal80*Δ, *ade2-101, met- URA3::GAL1*$_{UAS}$-*GAL1*$_{TATA}$-*laczMEL1*. It contains *MEL1* and *lacZ* reporters.

These yeast strains were purchased from Clontech.

### 2.4 Oligonucleotide primers

Primers used for DNA amplification and sequencing were designed by Primer Premier Program.

**1. Primers for amplification of the N-terminal kAE1 fragment**

Two primers named kAE001NcoI and kAE403SalI were designed to contain *Nco*I and *Sal*I restriction sites located at the 5’ and 3’ ends, respectively. These two restriction sites were used for cloning the enzyme-digested PCR into pGBKT7.

*Nco*I

**kAE001NcoI**: 5’- CAT G<u>CC **ATG** G</u>AC GAA AAG AAC CAG G –3’

**kAE403SalI**: 5’- CGC <u>GTC GAC</u> **TTA** GGG GCT GAA TGC A –3’

*Sal*I

**2. Primers for amplification of cDNA insert in library clones**

Two primers named LibADf and LibADr were designed for amplification of cDNA inserts of putative positive clones obtained from human kidney library screening.

**LibADf**: 5’- CTA TTC GAT GAT GAA GAT ACC CCA CCA AAC CC -3’

**LibADr**: 5’- GTG AAC TTG CGG GGT TTT TCA GTA TCT ACG AT -3’

**3. Primer for DNA sequencing of putative positive clones**

The primer named Libf was designed for sequencing of cDNAs insert in library clones obtained from the two-hybrid screening.

**LibInt-f**: 5'- CCA GAT TAC GCT AGC TTG GG -3

### 2.5 Antibodies

**1. GAL4 DNA-BD Monoclonal antibody**

This antibody was used to detect GAL4-binding domain fused to the bait protein. It was obtained from Clontech.

**2. Horseradish peroxidase conjugated rabbit anti-mouse antibody**

This antibody was obtained from Santa Cruz Biotechnology.

### 2.6 Yeast media

YPD medium for grown yeast stains and selective dropout medium for selection of protein interaction were made according to Appendix III.

**For studying in mammalian cells culture**

### 2.7 Cell lines

**1. Human embryonic kidney (HEK 293) cells**

Endothelial cell type human embryonic kidney (HEK 293) cells were grown in Dulbecco's modified Eagle's medium (DMEM) supplemented with 5% (v/v) fetal bovine serum, 5% (v/v) calf serum and 1% (v/v) penicillin/ streptomycin (Invitrogen) in 5% $CO_2$ at 37 $^{\circ}$C. These cells were maintained in Prof. Dr. Joseph Casey's laboratory, Department of Physiology, University of Alberta, Canada.

**2. Pig kidney epithelial cells (LLC-PK1)**

LLC-PK1 cells were grown in DMEM-F12 with 10% (v/v) calf serum and 0.5% (v/v) penicillin and streptomycin (Gibco Life Technologies) in 5% $CO_2$ at 37 $^{\circ}$C. These cells were maintained in Prof. Dr. Reinhart Reithmeier's Laboratory.

### 2.8 Plasmid vectors

**1. pcDNA 3.1**

This plasmid was purchased from Invitrogen, Carlsbad, CA, USA (see Figure 14 A).

**2. pcDNA 3.1/His B**

This plasmid was purchased from Invitrogen, Carlsbad, CA, USA (see Figure 14 B).

**3. pkAE1**

Human kAE1 full-length cDNA was cloned into *Hind*III and *Xho*I sites of pcDNA 3.1 (Invitrogen) by PCR-based amplification using specific primers. HA-tagged was introduced to the C-terminus. This wild-type kAE1 clone was named pkAE1 (Figure 40 in Appendix II).

**4. pkAE1CH-like**

cDNAs encoding calponin homology domain (CH) identified in the N-terminus of kAE1 with amino acids 27-189 was amplified using pkAE1 as template with specific primers. The PCR fragment with *Hind*III and *Xho*I sites at the ends was inserted to pcDNA 3.1 with HA-tagged at the C-terminus. This construct was named pkAE1CH-like (Figure 41 in Appendix II).

**5. pILK**

Human kidney cDNAs was used as template for amplification of full-length integrin-linked kinase (ILK). The PCR product was cloned into the *EcoR*I and *Xho*I sites of pcDNA 3.1/His B vector (Invitrogen), yielding the His-tagged construct pILK (Figure 42 in Appendix II).

**6. pS343A ILK and pE359K ILK**

The parental mutant clones (generous gift of Dr. Shoukat Dedhar, University of British Columbia) were used as template to make ILK mutants, S343A ILK and E359K ILK, expressed the kinase-dead domain (Figure 43 and 44 in Appendix II).

**7. pΔNtILK**

The plasmid pΔNtILK containing the coding sequence for ILK with a deletion of amino acid 1-192 at the N-terminus was constructed by PCR-based amplification using pILK as template (Figure 45 in Appendix II).

**8. pPanto**

Full-length pantophysin cDNA was cloned into the *EcoR*I and *Xba*I sites of pcDNA 3.1/His B vector (Invitrogen), yielding the His-tagged construct pPanto (Figure 46 in Appendix II).

**9. pGAPDH**

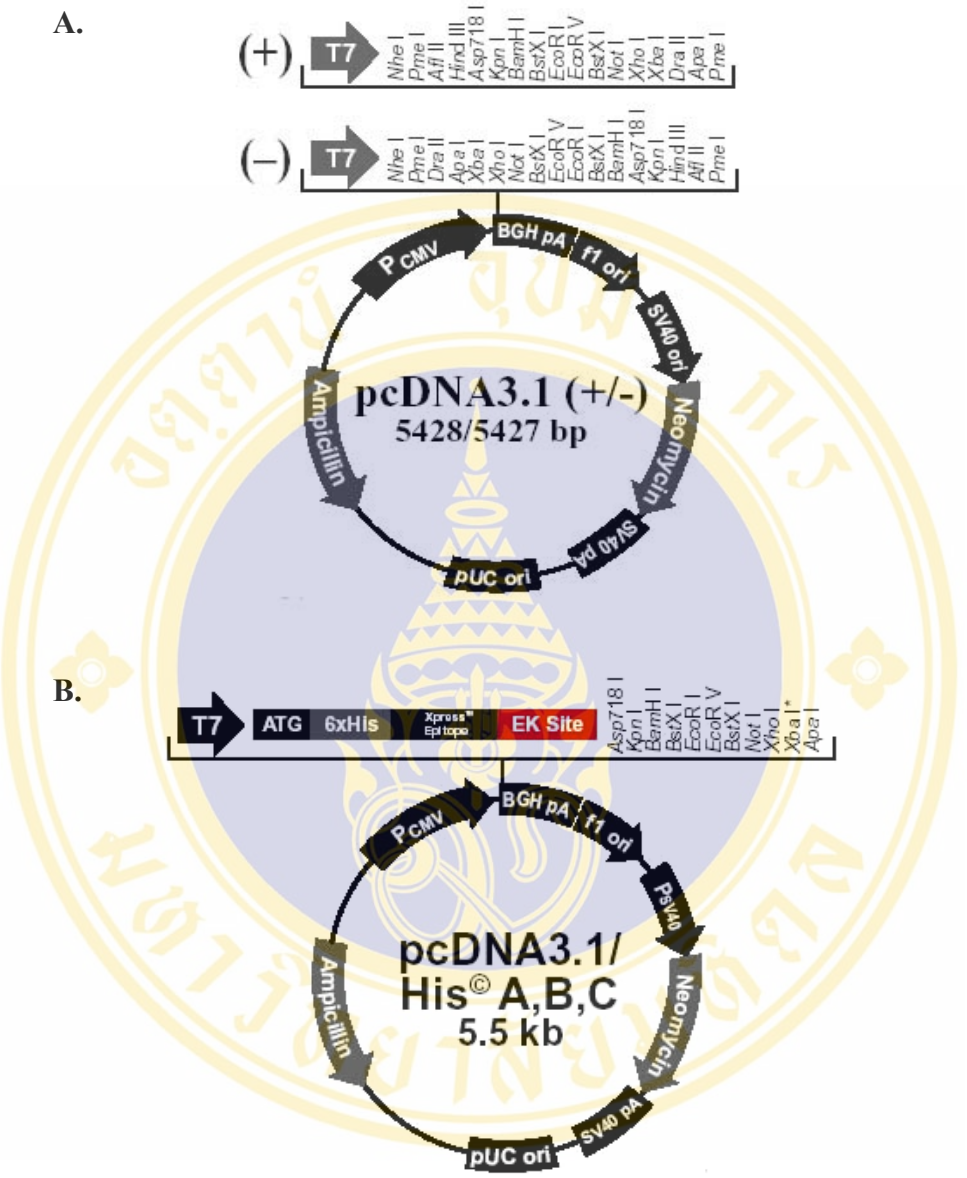


**Figure 14 Physical map of mammalian expression vectors.**

**A.** pcDNA 3.1 is untagged vector containing T7 and SV40 promotors. pkAE1 and pCHkAE1 were made by inserting full-length kAE1 and CH domain cDNAs into this vector (Invitrogen).

**B.** pcDNA 3.1/His B contains both poly-histidine tagged and Xpress epitopes with T7 and SV40 promotors. pILK, , pΔNtILK, S343A ILK, E559K ILK, pGAPDH, pPanto and pThymosin were made in this vector.

Full-length glyceraldehydes-3-phosphate dehydrogenase (GAPDH) cDNA was cloned into *EcoR*I and *Xho*I sites of pcDNA 3.1/His B vector (Invitrogen), yielding the His-tagged construct pGAPDH (Figure 47 in Appendix II).

**10. pThymosin**

Full-length thymosin cDNA was cloned into the *BamH*I and *EcoR*I sites of pcDNA 3.1/His B vector (Invitrogen), yielding the His-tagged construct pThymosin (Figure 48 in Appendix II).

**11. pJRC9**

Human AE1 cDNA was cloned into pRBG4, a generous gift of Prof. Dr. Joseph Casey, Department of Physiology, University of Alberta, Canada [90].

**12. kAE1 HA557 and eAE1 HA557**

AE1HA557 containing an extracellular hemagglutinin (HA) epitope inserted in position 557 was constructed by inserting the following condons; TAC CCA TAC GAT GTT CCA GAT TAC GCT between *Xba*I and *Hind*III restriction sites at position 781 and at the 3' end of cDNA, respectively [77]. The recombinant plasmids containing the kAE1 HA557 cDNA and eAE1 HA557 cDNA were named kAE1 HA557 and eAE1 HA557, respectively. kAE1 HA557, eAE1 HA557 and were a gift from Prof. Dr. Reinhart Reithmeier's laboratory.

## 2.9 Oligonucleotide primers

Primers for cloning the plasmids expressed in HEK 293 cells were shown in Table 2.

## 2.10 Antibodies

**Monoclonal antibodies**

1. **Mouse anti-His antibody** (Amersham Biosceinces)
2. **Mouse anti-actin antiboby** (Sigma)
3. **Mouse anti-paxillin antibody** (BD Transduction Laboratory)
4. **Mouse anti-green fluorescent protein (GFP) antibody**

This antibody was obtained from Prof. Dr. Joseph Casey, Department of Physiology, University of Alberta, Canada.

5. **Mouse anti-AE1 antibody (IVF12)**

This mouse monoclonal antibody against human AE1 carboxy-terminus was a

**Table 2 PCR primers for amplification of kAE1 and kAE1-interacting proteins.**

| cDNA | Primers | Primer sequences (5'>3') | Product size (kb) |
|---|---|---|---|
| kAE1 | kAE1HindIII-f<br>kAE1XhoI-r | CCCAAGCTT**ATG**GACGAAAAGAACCAGGAG<br>CCGCTCGAG**TTA**AGCGTAATCTGGAACATCG-TATGGGTACACAGGCATGGCCACTTC | 2.5 |
| kAE1CH-like domain | CHkAEHindIII-f<br>CHkAEXhoI-r | CCCAAGCTT**ATG**GGGGCCTGGGGCCGCC<br>CCGCTCGAG**TTA**AGCGTAATCTGGAACATCGT-ATGGGTACTCCAGCTCCGCTGCCTC | 0.16 |
| ILK | ILK-f<br>ILK-r<br>ILKEcoRI-f (nested)<br>ILKXhoI-r (nested) | GTCCTCAGGCTTCCCCAATCCAGG<br>AACCATGTCCCGACACCTCTGGAG<br>CCGGAATTCG**ATG**GACGACATTTTCACTC<br>CCGCTCGAG**CTA**CTTGTCCTGCATCTTC | 1.35 |
| GAPDH | GAPDH-f<br>GAPDH-r<br>GAPDHEcoRI-f (nested)<br>GAPDHXhoI-r (nested) | AGCCGAGCCACATCGCTCAGAC<br>CTCTTCCTCTTGTGCTCTTGCTGG<br>CCGGAATTCG**ATG**GGGAAGGTGAAGGTC<br>CCGCTCGAG**TTA**CTCCTTGGAGGCCATG | 1.0 |
| Thymosin β4 | Thym-f<br>Thym-r<br>ThymBamHI-f (nested)<br>ThymEcoRI-r (nested) | GACTTCGCTCGTACTCGTGCGCCT<br>AGGCAATGCTTGTGGAATGTACAGTG<br>CGCGGATCC**AATG**TCTGACAAACCCGATATGG<br>CCGGAATTC**TTA**CGATTCGCCTGCTTGC | 0.16 |
| Pantophysin | PantoEcoRI-f<br>PantoXbaI-r | CCGGAATTCG**ATG**TCCGGCTTCCAGATC<br>CTAGTCTAGA**TTA**TATTCCGGTAGGAGGTG | 0.72 |
| ΔNtILK | delILKEcoRI-f<br>delILKXhoI-r | CCGGAATTCG**ATG**CTTAACTTCCTGACG<br>CCGCTCGAG**TTA**CTTGTCCTGCATCTTC | 0.78 |
| S343A ILK | same as used for ILK | CCGGAATTCG**ATG**GACGACATTTTCACTC<br>CCGCTCGAG**CTA**CTTGTCCTGCATCTTC | 1.35 |
| E359K ILK | same as used for ILK | CCGGAATTCG**ATG**GACGACATTTTCACTC<br>CCGCTCGAG**CTA**CTTGTCCTGCATCTTC | 1.35 |

The sequences underlined are restriction sites. Initiation codon (ATG) and stop codons (TTA and CTA) are bolds.

generous gift of Dr. Michael Jennings, University of Arkansas, U.S.A.

**Polyclonal antibodies**

1. **Rabbit anti-HA antibody** (Santa Cruz Biotechnology)
2. **Rabbit anti-ILK antibody** (Sigma)
3. **Rabbit anti-actopaxin antibody** (Sigma)
4. **Rabbit anti-Ct AE1 antibody (1658)**

This polyclonal antibody detects human AE1 carboxy-terminus, a generous gift of Prof. Dr. Joseph Casey, Department of Physiology, University of Alberta, Canada.

**Secondary antibodies**

1. **Rabbit anti-mouse antibody coupled to FITC**
   (Molecular probes)
2. **Goat anti-rabbit antibody coupled to Cy3**
   (Jackson Immunoresearch Laboratories)
3. **Horseradish peroxidase conjugated donkey anti-rabbit antibody**
   (Santa Cruz Biotechnology)
4. **Horseradish peroxidase conjugated rabbit anti-mouse antibody**
   (Santa Cruz Biotechnology)

**3. Methods**

Since two parts of experimental studies were conducted in this thesis, the methodological details were divided into two parts. Part I consists of the methods used in identification of proteins interacting with the N-terminus of kAE1. Part II involves the methods used in the studies of physical and functional interaction between kAE1 and its interacting proteins in mammalian cells culture.

**Part I: Identification of candidate proteins interacting with the N-terminus of kAE1 using yeast two-hybrid screening**

Among techniques used for studying protein-protein interaction, yeast two-hybrid is known to be a powerful technique and widely used to identify novel protein-protein interaction. Therefore, yeast two-hybrid was carried out in the first step to identify the proteins that interact with kAE1. This part of experimental works includes cloning of the N-terminal kAE1 corresponding to amino acid Met66-Pro403 of human eAE1 in GAL4-BD expression vector which served as bait. Before using this bait for library screening, the construct was tested for toxicity effect, transcriptional activation of reporter genes, mating efficiency and the bait protein expression. Then, this construct was used for screening kAE1 interacting proteins in human kidney cDNA library by using yeast mating method. After elimination of the duplicate clones by PCR and restriction endonuclease analysis, independent positive clones were subjected to DNA sequencing and cDNAs obtained were submitted and searched for homologous sequences in databases. The putative positive clones of interest were selected, isolated from yeast cells and used for specificity test in yeast cells to confirm the interaction of kAE1 and its interacting proteins.

### 3.1 Construction of the bait plasmid

The first step in two-hybrid is to construct a plasmid that expressed GAL4-DNA binding domain fused to the N-terminus of kAE1 (NkAE1), corresponding to amino acids Met66-Pro403 of human eAE1.

#### 3.1.1 Preparation of N-terminal kAE1 cDNA

pcDNA 3/kAE1 was used as DNA template for PCR amplification using the specific primers named kAE001NcoI and kAE403SalI as shown in Materials. These primers generated the PCR product size corresponding to Met66-Pro403 of human eAE1. The PCR reaction was performed in a total volume of 50 µl containing 17 ng of plasmid DNA, 10 pmole of each primer, 2 mM dNTPs, 1x Pfu buffer (2 mM final concentration of $Mg^{2+}$). After mixing the reaction and denaturing at 95 °C for 2 min, the 0.9 unit *Pfu* DNA polymerase was added (Promega). The PCR cycles were performed on a thermal cycler GeneAmp®PCR system 2400 (Perkin Elmer Cetus, USA). After adding the enzyme, 40 PCR cycles were performed as follows: (i) denaturation at 94 °C for 20 sec, (ii) annealing at 55 °C for 20 sec, (iii) extension at 68

°C for 2 min 30 sec, followed by another 7 min of extension at 68°C in the final step. An aliquot of PCR product was resolved by 1% agarose gel electrophoresis and visualized by staining with ethidium bromide. The PCR product band was excised and DNA was extracted using QIAquick Gel Extraction Kit (Qiagen) according to the manufacturer's protocol.

### 3.1.2 Endonuclease digestion and ligation

GAL4-binding domain (GAL4-BD) vector, pGBKT7, and purified PCR product which contain *Nco*I and *Sal*I flanking at the end of the fragment were separately digested in 50 µl containing 2 µg of vector or PCR product, 1x buffer D, 1x BSA and 10 units of *Nco*I and *Sal*I each at 37 °C for 20 h. After incubation, the reaction mixture was examined for completely digestion using 1% agarose gel electrophoresis. The linearized pGBKT7 and PCR product of the N-terminal kAE1 were purified by QIAquick Gel Extraction Kit (Qiagen). The concentrations of the digested vector and PCR product were determined by comparing with known concentration of standard molecular weight DNA after running on agarose gel electrophoresis. The ligation reaction was performed according to the manufacturer's protocol in a total volume of 10 µl containing 50 ng of digested vector, 70 ng of insert (1:10 molar ratio), 10 mM ATP, 5 units of T4 DNA ligase and 1x ligation buffer (Invitrogen). The ligation mixture was incubated at 4 °C for 16 h.

### 3.1.3 Transformation, positive clones selection and DNA plasmid isolation

**1. Preparation of competent cells by SEM method of Inoue *et al.* [211]**

*E. coli* strain DH5α was streaked on LB agar plate and incubated at 37 °C for 16 h. A large colony was inoculated at 25 ml of SOB medium, pH 7.0 at 18 °C with vigorous shaking (~250 rpm) for 24 h. Then, the culture was transferred to 250 ml of the same medium and incubated at 18 °C with shaking until $A_{600}$ reached 0.4-0.6. The flask containing cell culture was removed from the incubator and placed on ice for 10 min. The culture was centrifuged at 2,500 x g for 10 min at 4 °C and discarded the supernatant. The cell pellet was resuspended in 80 ml of ice-cold TB solution (10 mM PIPES, 55 mM $MnCl_2$, 15 mM $CaCl_2$ and 250 mM KCl) and incubated on ice for 10

min. The cell pellet was collected by centrifugation at 2,500 x g for 10 min at 4 °C and discarded the supernatant. The pellet was gently resuspended in 20 ml of TB solution followed by adding DMSO to 7% final concentration, mixed well and the cell suspension was aliquot in the volume of 200 µl. The cells were immediately frozen in liquid nitrogen. These competent cells were used in transformation or kept at –80 °C.

**2. Transformation into *E. coli* strain DH5α**

Transformation of ligation mixture into *E. coli* strain DH5α was carried out by using the 5 µl of ligation mixture mixed with 200 µl of competent cells *E. coli* DH5α and incubated on ice for 30 min. Then, suddenly heat-shock at 42 °C for exactly 90 sec was performed and placed on ice for 2 min. The 800 µl of SOC medium was added and transformed reaction was incubated at 37 °C for 1 h in shaking incubator. The transformed cells were spread on LB plate containing 50 µg/ml kanamycin and incubated at 37 °C for 16 h.

**3. DNA plasmid isolation from *E. coli***

After obtaining the positive clones, these clones were selected for plasmid preparation by using cetyltrimethylammonium bromide (CTAB) method [212]. Briefly, the pellet of cultured bacterial transformants was resuspended in 200 µl of STET (8% (w/v) sucrose, 5% Triton X-100, 50 mM EDTA and 50 mM Tris-HCl, pH 8.0). The 25 µl of 10 mg/ml lysozyme solution was then added to the mixture and incubated at 37 °C for 10 min. The mixture was boiled at 100 °C for 45 sec and immediately centrifuged at 13,000 x g for 15 min at room temperature. The pellet (chromosomal DNA and cell debris) was removed by using sterile toothpick and 1/10 volume of 5% CTAB solution was added and mixed by inversion. The pellet was obtained by centrifugation of the mixture at 13,000 x g for 5 min and resuspended in 300 µl of 1.2 M NaCl by vigorously shaking. The 10 µl of 10 mg/ml RNaseA was added followed by incubation at 37 °C for 30 min. An equal volume of 1:1 phenol and chloroform mixture was added, then mixed and centrifuged at 13,000 x g for 10 min. The aqueous upper phase was transferred to a fresh microcentrifuge tube and 2 volumes of cooled absolute ethanol were added following incubation at -20 °C for 10 min. The DNA pellet was collected by centrifugation at 13,000 x g for 10 min, air-

dried and then resuspended in sterile water. The DNA solution was used for further analysis.

**4. Analysis of recombinant plasmids**

**4.1 Colony PCR**

Colony PCR was performed for screening putative positive clones. The transformed colonies were picked with sterile toothpicks and resuspended in 50 µl of sterile distilled water. The cell suspension was boiled at 100 °C for 15 min and then removed cells debris by centrifugation at 10,000 x g for 10 min. The 15 µl of the supernatant was used as template in PCR amplification. The PCR products were run on agarose gel electrophoresis to analyze whether recombinant clones contain the inserted fragment.

**4.2 Restriction enzyme digestion**

Restriction enzyme digestion was also performed to examine the presence of inserted fragment in recombinant plasmids with the same set of restriction enzymes used for the cloning step.

**5. Automated DNA sequencing**

The sequencing reaction was performed by using ABI PRISM™ Big Dye™ Terminator Cycle Sequencing Kit and analyzed by ABI PRISM™ 377 DNA sequencer. The reaction mixture was performed in a total volume of 20 µl by mixing 4 µl of premix (terminator ready mixed), 0.75 pmole of sequencing primer and 500 ng of pNkAE1. The sequencing reaction was performed for 25 cycles consisting of 96 °C for 10 sec, 50 °C for 5 sec and 60 °C for 4 min. The sequencing product was precipitated by adding 2 µl of 3 M sodium acetate (NaOAc) pH 4.8 and 50 µl of cooled absolute ethanol, and kept on ice for 10 min. The pellet was collected by centrifugation at 12,000 x g for 10 min and washed with 70% ethanol. The washed pellet was dried out at room temperature for 15 min. The pellet was resuspended in 25 µl of template suppression reagent (TSR) and heated at 95 °C for 2 min to denature the sequencing product followed by chilling on ice and analyzed by automated DNA sequencer ABI PRISM™ 377.

### 3.2 Transformation of the bait into yeast (*S. cerevisiae*) and verification of the bait properties

#### 3.2.1 Transformation of the bait into yeast

The bait plasmid was firstly transformed into *E. coli* DH5α to obtain the large amount of recombinant plasmids before introducing into the *MATa* yeast strain AH109 using the lithium acetate method [213]. The yeast strain AH109 was grown in 50 ml of YPDA media and incubated at 30 °C for 16-18 h with shaking at 250 rpm. The 30 ml of the yeast culture was transferred to a flask containing 300 ml of fresh YPDA media and further incubated at 30 °C until $OD_{600}$ reaches 0.4-0.6. The cells were collected by centrifugation at 1,000 x g for 5 min at room temperature. The pellet was washed in sterile distilled water and resuspended in 1.5 ml of freshly prepared sterile 1x TE/1x LiAc (Appendix III). The cell suspension served as yeast AH109 competent cells. The 0.1 µg of the bait plasmid and 0.1 mg of salmon sperm carrier DNA were added to the fresh microcentrifuge tube containing 0.1 ml of yeast competent cells and 0.6 ml of sterile PEG/LiAc, mixed well by vortexing and followed by incubating at 30 °C for 30 min. The 70 µl of DMSO was added and mixed by gentle inversion. After that, it was heat-shock in 42 °C water bath for 15 min, chilled on ice for 2 min and cells at 14,000 x g for 5 sec. at room temperature. The transformed cells were resuspened in sterile TE buffer and diluted at 1:10 or 1:100 dilutions before plating on synthetic dropout media lacking tryptophan (SD/-Trp). Plate was incubated at 30 °C until colonies appeared (2-4 days). Phenotype testing of constructs and yeast strains on SD media was shown in Table 3.

#### 3.2.2 Expression of fusion protein (GAL4-BD/NkAE1) in yeast

**1. Protein extraction from yeast transformed with pNkAE1**

The AH109 transformed with pNkAE1 or pGBKT7 (negative control) were grown in 5 ml of SD/-Trp liquid dropout medium and incubated at 30 °C for 16 h with shaking (~250 rpm). The 2 ml of pre-culture was added to new flasks containing 20 ml of YPDA medium and incubated at 30 °C with shaking until $A_{600}$ reaches 0.4-0.6. Number of cells (total $A_{600}$ unit) was calculated by multiplying $A_{600}$ with culture volume (20 ml). The cells were then collected by centrifugation at 1,000 x g for 5 min

**Table 3 Phenotype testing on various synthetic dropout media (SD).**

| Strain | SD/-Ade | SD/-His | SD/-Leu | SD/-Trp | SD/-Ura |
|---|---|---|---|---|---|
| AH109 | - | - | - | - | + |
| Y187 | - | - | - | - | + |
| AH109[NkAE1] | - | - | - | + | + |
| Y187[library] | - | - | + | - | + |
| AH109[p53] | - | - | - | + | + |
| AH109[laminC] | - | - | - | + | + |
| Y187[SV40] | - | - | + | - | + |

**- = no growth**

**+ = growth**

at 4 °C. After washing the pellet with 25 ml of ice-cold water and recovering cells by centrifugation, the pellet was immediately frozen in liquid nitrogen and thawed quickly. The cells were resuspended in pre-warmed complete cracking buffer (100 µl of complete cracking buffer per 7.5 $OD_{600}$ units of cells) (Appendix III). The cell suspension was transferred to a fresh microcentrifuge tube containing 80 µl of glass beads (Sigma) and heated the sample at 70 °C for 10 min. The sample was mixed vigorously for 1 min by vortexing. Cell debris and unbroken cells were removed by centrifugation at 14,000 x g for 5 min at 4 °C. The supernatant was transferred to the new tube. The cell debris was treated by placing at 100 °C for 5 min and then vortexing for 1 min. The pellet was removed by centrifugation at 14,000 x g for 5 min at 4 °C. The supernatant was combined with another part of supernatant as previously prepared and boiled it at 95 °C for 3 min before loading on SDS-PAGE.

**2. SDS-polyacrylamide gel electrophoresis (SDS-PAGE) and immunoblotting**

SDS-PAGE was performed as previously described [214]. The protein samples were loaded on 10% SDS-PAGE and run under constant 170 volts for 1 h. The broad-range standard protein marker (Promega) was also loaded on the same gel. After electrophoresis, the gel was soaked in the transfer buffer for 2 min. The nitrocellulose membrane and filter papers were soaked in transfer buffer as well. Transblotting was performed using a Trans-Blot® SD semi-dry electrophoretic transfer cell (Bio-Rad) under constant current of 3 $mA/cm^2$ for 1.5 h. The transferred protein bands on nitrocellulose membrane was incubated with blocking buffer containing 5% skim milk for 1 h and then added monoclonal mouse anti-GAL4 DNA-BD antibody at dilution 1:4,000 in 5% skim milk for 16 h at 4 °C with shaking to detect fusion protein of GAL4-BD/NkAE1. The blot was washed with 1x TBST for three times and then incubated with rabbit anti-mouse IgG conjugated with horseradish peroxidase (HRP) at dilution 1:1000 in 5% skim milk and placed on rocking platform at room temperature for 1 h. The blot was washed with 1x TBST three times and incubated with 1:1 of ECL plus Western Blotting Detection System (Amersham) for 5 min according to manufacturer's instruction. Protein bands were visualized by exposing the blot to the X-ray film.

### 3.2.3 Testing toxicity effect, transcriptional activation and mating efficiency of the bait protein

Toxicity of the GAL4-BD/NkAE1 fusion protein was tested by comparing growth rate of the AH109 transformed either with pNkAE1 (bait strain) or the empty pGBKT7 vector (vector strain) in SD/-Trp liquid dropout medium. The two cultures were incubated at 30 °C for 2 days with shaking. An aliquot of the cultures was taken and measured $OD_{600}$. The growth rate of the two cultures should be similar.

For transcriptional activation, the bait strain and vector strain cultures were plated on SD/-Trp or SD/-Trp/-His/-Ade dropout plates at $10^{-2}$ dilution and then incubated at 30 °C for 4 days. *LacZ* reporter gene encoding β-galactosidase enzyme was examined by using colony lift assay. Briftly, the sterile Whatman 3MM filter paper was presoaked by placing in 5 ml of Z buffer/X-Gal solution (Appendix III) in a clean 100-mm plate. Then, another dry filter paper was placed on the surface of the plate of colonies and then rubbed gently with the side of forceps to help colonies cling to the filter. Holes were poked through the filter into the agar to orient the filter. When the filter had been evenly wetted, it was lifted off from the agar plate with forceps, then transferred colonies facing up to the pool of liquid nitrogen and submerged the filter for 10 sec. The filter was removed from liquid nitrogen and allowed it to thaw at room temperature and then placed colonies side up on the presoaked filter. The filter was incubated at room temperature and checked for the appearance of blue colonies. The colonies should be white on SD/-Trp and do not grow on SD/-Trp/-His/-Ade plates to ensure that the bait is unable to autonomous activate transcription of *LacZ, HIS3* and *ADE2* reporter genes.

In addition, mating efficiency of the bait strain was examined by comparing with mating efficiency of pGBKT7-53 and pTD1-1 (positive controls). The large colony of bait strain and pTD1-1 (GAL4-AD control plasmid) transformed in Y187 was picked and transferred to a microcentrifuge tube containing 0.5 ml of 2x YPDA then mixed vigorously by vortexing. Mating of positive controls was performed the same way in another microcentrifuge tube. The mating cultures were incubated at 30 °C for 20 h. Mating mixtures were diluted with sterile water at $10^{-2}$ dilutions before plating on SD/-Trp, SD/-Leu and SD/-Trp/-Leu then incubated at 30 °C until colonies appear. Mating efficiency was calculated as followed:

Mating efficiency = # cfu/ml of diploid x 100/ # cfu/ml of limiting partner

(# viable cfu/ml = cfu x 1000 µl x ml/ volume plated (µl) x dilution factor)

The SD/-Trp or SD/-Leu containing less number of colonies is served as limiting partner.

### 3.3 Yeast two-hybrid screening of human kidney cDNA library

The two-hybrid library screening was performed by using yeast mating. The bait strain was grown in 50 ml of SD/-Trp liquid dropout medium at 30 °C for 16-24 h with shaking (~250 rpm). The $OD_{600}$ should be more than 0.8. The cells were collected by centrifugation at 1,000 x g for 5 min and resuspended in the residual liquid. The one aliquot (~1.0 ml) frozen kidney library was thawed out in a room temperature water bath with gently vortex and combined with the bait strain in 2-L sterile flask containing 45 ml of 2x YPDA/kanamycin, then incubated at 30 °C for 20-24 h with gentle swirling (30-50 rpm) to allow mating. The mating mixture was transferred to a sterile centrifuge bottle and spun down by centrifugation at 1,000 x g for 10 min. The cell pellet was resuspended with 0.5x YPDA/kanamycin and spread the mating mixture on large (150-mm) plates containing SD/-Ade/-His/-Leu/-Trp dropout media. Plates were incubated at 30 °C until colonies appeared. The positive clones were further screened for α-galactosidase activity (MEL1) by growing the colonies on SD/-Ade/-His/-Leu/-Trp dropout medium containing X-α-Gal (Clontech) indicator plate. The positive controls were performed accompanying the experimental included pGBKT7-53 (murine p53) and pTD1-1 (SV40 large T-antigen).

### 3.4 Isolation of cDNA positive clones from yeast and analysis of redundant clones

The plasmid DNA of positive two-hybrid colonies was isolated from yeast by standard lyticase method [215]. Briefly, the positive colonies were grown in 5 ml of SD/-Leu to select the library plasmids. The cells were collected by centrifugation at 14,000 x g for 5 min and resuspended in lysis solution (5 units/µl of lyticase enzyme (Sigma) in TE buffer). The cell suspension was incubated at 37 °C for 1 h with shaking and then the 20% of SDS was added to the reaction and mixed vigorously. The tube containing cell suspension was placed in liquid nitrogen and performed

freeze-thaw cycles for 3 times and then mixed with vortex. The volume of cell suspension was brought up to 200 µl with sterile water and added with an equal volume of 1:1 of phenol and chloroform mixture solution, then centrifuged at 14,000 x g for 10 min. The aqueous upper phase was transferred to a fresh microcentrifuge tube. Ammonium acetate (10 M) was added to the aqueous solution followed by adding 2 volumes of absolute ethanol to precipitate DNA. The DNA pellet was collected by centrifugation at 14,000 x g for 10 min, then air-dried and resuspended in sterile distilled water.

To eliminate the redundant clones, the DNA obtained from the previous step was used as templates for PCR amplification and restriction enzyme digestion. cDNA inserts were amplified by PCR using primers, designed flanking multiple cloning site of library plasmid, named LibADf and LibADr (shown in Materials). The PCR reaction was performed in a total volume of 25 µl containing 0.3 µg of plasmid DNA, 10 pmole of each primer, 2 mM dNTPs, 1x Pfu buffer (2 mM final concentration of $Mg^{2+}$) and the 0.9 unit *Pfu* DNA polymerase (Promega). The 40 PCR cycles were performed as follows: (i) denaturation at 95 °C for 2 min (ii) denaturation at 94 °C for 20 sec, (iii) annealing and extension steps were various depending on the size of inserts, followed by another 7 min of extension at 68 °C in the final step. An aliquot of PCR product was resolved by 1% agarose gel electrophoresis and visualized by staining with ethidium bromide. The PCR products were purified by using QIAGEN PCR Purification Kit (Qiagen) according to the manufacturer's instruction followed by digesting of PCR products with *Hae*III restriction enzymes to eliminate the library duplicate clones. The digested products were resolved on 1.5% agarose gel electrophoresis and then compared the digestion pattern among the positive clones. One of duplicate clones was used as a representative of the groups and subjected to DNA sequencing.

### 3.5 Sequencing of cDNA inserts and searching for homology sequences

Partial cDNA sequencing of the purified PCR product of independent clones were performed by Macrogen company, Korea, using a primer named LibInt-f designed from the sequences which located upstream of cDNA insertion sites. The inserted cDNA sequences of positive clones obtained from DNA sequencing were

verified the presence of an open reading frame (ORF) and searched for homology sequences in GenBank and the protein databases by BLAST search. The putative proteins that gave a high homology were further analyzed and classified into groups.

### 3.6 Specificity test of protein interaction in yeast

The isolated candidate plasmids from yeast might be mixed by bait and library cDNA plasmids which carrying ampicillin resistant gene. Thus, transformation of isolated yeast plasmids into *E. coli* DH5α was performed to obtain one type of plasmid. Briefly, the plasmids were transformed as previously described in section 3.1.3. The transformed cells were spread on LB plate containing 50 mg/ml ampicillin and incubated at 37 °C for 16 h. The plasmids were then isolated from bacterial colonies by using QIAGEN Plasmid Mini columns (Qiagen) and re-transformed to yeast strain AH109 as previously described. The Y187 pre-transformed with each candidate plasmids were mated with strain AH109 transformed with either original bait (pNkAE1), pGBKT7 vector, pGBKT7-53 or pGBKT7-Lamin C. The mating mixture was grown on the SD/-Ade/-His/-Lue/-Trp containing X-α-Gal.

In the meantime, positive colonies on SD/-Ade/-His/-Lue/-Trp dropout medium were further screened for β-galactosidase (LacZ reporter) activity using colony filter lift assay as described above in section 3.2.3. The $Ade^+$, $His^+$, $MEL^+$ and $LacZ^+$ positive colonies were selected and proposed to be proteins interacting with kAE1.

## Part II: Studies of interaction between kAE1 and interacting proteins in transfected human embryonic kidney (HEK 293) cells

The proteins that proposed to be kAE1 interacting proteins identified in yeast two-hybrid system are integrin-linked kinase (ILK), pantophysin, glyceraldehydes-3-phosphate dehydrogenase (GAPDH) and thymosin β4. Therefore, the experimental works in this part focuses on studies of physical and functional interaction of kAE1 and interacting proteins in mammalian cells culture. The first step of this part is to construct human full-length kAE1 and kAE1 interacting proteins in eukaryotic vector. However, no full-length cDNA clones of kAE1 interacting proteins were obtained from yeast two-hybrid screening. To obtain kidney specific transcripts of the interacting proteins, human kidney tissue was used as a source for RNA isolation and

full-length cDNAs synthesis. Human kidney cDNA was then used as template for PCR-based amplification cloning of cDNAs encoding kAE1 interacting proteins into eukaryotic vector. Expression of full-length kAE1 and its interacting proteins were carried out in human embryonic kidney (HEK 293) cells. The techniques used here were co-immunoprecipitation, affinity co-purification and immunofluorescence to demonstrate the specific interaction between kAE1 and interacting proteins. Cell surface biotinylation, Fluorescence activated cell sorting (FACS) analysis, Triton X-100 cytoskeleton extraction and transport activity assay were performed to examine the role of the interacting proteins effect on the physiological function of kAE1.

### 3.7 Plasmid construction of kAE1 and interacting proteins

#### 3.7.1 Plasmid construction of kAE1

A plasmid named pcDNA 3/kAE1 containing human kAE1 cDNA was used as template for amplification a full-length kAE1 with two primers named kAE1HindIII and kAE1XhoI (Table 2). kAE1XhoI primer was designed to introduce hemagglutinin (HA) epitope tag downstream of the last codon of the gene. These primers generated the PCR product size of 2.5 kb containing *Hind*III and *Xho*I restriction sites flanking at the 5' and 3' ends, respectively. The PCR reaction was performed in a total volume of 50 µl containing 17 ng of plasmid DNA, 10 pmole of each primers, 2 mM dNTPs, 1x Pfu buffer (2 mM final concentration of $Mg^{2+}$). After mixing the reaction and denaturing at 95 °C for 2 min, the 0.9 unit *Pfu* DNA polymerase was added (Promega). The PCR cycles were performed on a thermal cycler GeneAmp®PCR system 2400 (Perkin Elmer Cetus, USA). After adding the enzyme, 40 PCR cycles were performed as follows: (i) denaturation at 94 °C for 20 sec, (ii) annealing at 58 °C for 20 sec, (iii) extension at 68 °C for 3 min 30 sec, followed by another 7 min of extension at 68 °C in the final step. An aliquot of PCR products were analyzed on 1% agarose gel electrophoresis and visualized by staining in ethidium bromide. PCR product was excised and purified by using QIAGEN Gel Extraction Kit (Qiagen). The purified PCR fragment was digested with *Hind*III and *Xho*I, and then ligated into *Hind*III/*Xho*I cut pcDNA 3.1 vector (Invitrogen). The ligation mixture was transformed into *E. coli* DH5α and screened for positive clones as previously described. The construct was

verified by DNA sequencing. This wild type kAE1 with HA-tagged at the C-terminus construct was named pkAE1.

cDNA encoding calponin homology domain (CH) identified in the N-terminus of kAE1 with amino acids 27-189 was amplified using pkAE1 as template with specific primers namely CHkAEHindIII and CHkAEXhoI (Table 2). The PCR reaction was performed by the same condition as full-length kAE1 amplification except extension step at 68 °C for 2 min was used. PCR fragment with *Hind*III and *Xho*I sites at the ends was inserted to pcDNA 3.1 with HA-tagged at the C-terminus. This construct was verified by DNA sequencing. This construct was named pCHkAE1.

### 3.7.2 Plasmid construction of kAE1 interacting proteins

#### 1. RNA extraction of kidney tissue

Total RNA was prepared from homogenate kidney tissue by using TRIzol® reagent (Life Technologies, USA) with careful and gentle handling to preserve the required longest mRNA. Firstly, 100 µl of TRIzol® reagent was added to lyse homogenate kidney tissue between homogenized tissues. Then it was added again with 400 µl of TRIzol reagent and incubated for 5 min at room temperature. The 200 µl of chloroform was added and incubated for 3 min and the mixture was centrifuged at 12,000 x g for 15 min at 4 °C. The aqueous upper phase was transferred to a new tube and total RNA was precipitated by using 500 µl of isopropanol, incubated at room temperature and centrifuged at 12,000 x g for 10 min at 4 °C. RNA pellet was washed by adding 75% ethanol. It was then resuspended in DEPC-$H_2O$ and kept at –70 °C. RNA solution was diluted and the RNA concentration was calculated as followed the equation: RNA concentration = ($A_{260}$ x dilution factor x 40 µg/ml)/ 1000.

#### 2. Full-length cDNA synthesis

The isolated RNA from kidney tissue was used template for cDNA synthesis by using RNase H-free reverse transcriptase (Superscript ™ II RT) with oligo (dT) 12-18 primer in the SUPERSCRIPT™ Pre-amplification System for First Strand cDNA Synthesis (Life Technologies). The mixture was prepared by mixing the total RNA about 5 µg with 0.5 µl of oligo (dT) primer. The 30 units of Rnasin® Ribonuclease

inhibitor (Promega) was then added to the mixture, incubated at 70 °C for 10 min and immediately chilled on ice for at least 1 min. The solution containing 50 mM KCl, 2.5 $MgCl_2$, 500 µl dNTPs, 10 mM dithiothreitol (DTT), 20 mM Tris-HCl, pH 8.4 was added into the mixture and incubated at 42 °C for 5 min. The 200 units of RNase H-free Superscript™ II RT were added. cDNA synthesis was performed at 42 °C for 90 min and terminated by incubation at 70 °C for 15 min. The reaction mixture was added with 2 units of RNase H (Life Technologies) and incubated at 37 °C for 20 min. An aliquot of the first strand cDNA was used as template for kAE1 interacting proteins amplification in PCR reaction.

### 3. DNA cloning of kAE1 interacting proteins

cDNAs encoding full-length ILK, PPH, GAPDH and thymosin β4 were amplified by PCR using human kidney cDNA as template. The first round PCR was performed in 25 µl reaction volume containing 1x Pfu buffer, 2 mM dNTPs, 10 pmole of each primer (Table 2), and 2 µl of human kidney cDNA. The PCR was started by prewarming cDNA at 95 °C for 5 min before adding 1 unit of *Pfu* DNA polymerase. The 35 cycles were performed with PCR profiles at 94 °C for 20 sec, 58 °C for 20 sec and 68 °C for 3 min 30 sec. The final extension step was carried out at 68 °C for 7 min. The PCR products of ILK, GAPDH and thymosin β4 from the first round were used as the templates for nested PCR by the same condition as the first round PCR amplification. The primers used for nested PCR are shown in Table 2. An aliquot of PCR products were analyzed on 1% agarose gel electrophoresis and visualized by staining in ethidium bromide. PCR products of ILK and GAPDH contain *EcoR*I/*Xho*I, pantophysin contains *EcoR*I/*Xba*I sites, and thymosin β4 contains *BamH*I/*EcoR*I at the ends of fragments were inserted to pcDNA 3.1/His B. These constructs were named pILK, pGAPDH, pPanto and pThymosin with poly-histidine tag at the N-terminus (Appendix I). The sequences of inserted fragments were verified by automated sequenceing.

The plasmid pΔNtILK containing the coding sequence for ILK with a deletion of amino acids 1-192 at the N-terminus was constructed by PCR-based amplification with specific primers (Table 2) using pILK as template. In addition, the parental mutant clones were used as template to make ILK mutants, S343A ILK and E359K

ILK, expressed the kinase-dead domain. The PCR reaction was carried out by the same condition as described above. The primers used for amplification of ILK mutants were shown in Table 2. The PCR fragments of ILK mutants were digested with *EcoR*I and *Xho*I and inserted to *EcoR*I and *Xho*I sites of pcDNA 3.1/His B. The DNA sequences of inserted fragment were confirmed by automated DNA sequencing.

### 3.8 Cell culture of human embryonic kidney (HEK 293) cells

HEK 293 cells stock was obtained from Prof. Dr. Joseph Casey. The stock was maintained in his laboratory, University of Alberta, Canada. The cells were grown in complete medium consisted of Dulbecco's modified Eagle's medium (DMEM) supplemented with 5% (v/v) fetal bovine serum, 5% (v/v) calf serum and 1% (v/v) penicillin/streptomycin (Invitrogen). The cells culture was maintained in 75-$cm^2$ flask in 5% $CO_2$ at 37 $^{\circ}$C. Cells were sub-cultured twice a week following the standard protocol of Dr. Casey's laboratory. Briefly, the 100% confluent cells in flask was washed three times with 10 ml of pre-warmed 1x PBS and then incubated cells with 4 ml of 1x PBS to allow cells detach at room temperature for 10 min. The flask was whacked by hand to lift the cells. Pre-warmed complete medium at the volume of 4 ml was added into the flask. The whole mixture of cells was suck up and down with pipetter for 10 times. An aliquot of cells at 0.5 ml was transferred into the new 75-$cm^2$ and then the complete medium was added to 25 ml. The flask of cells was incubated at 37 $^{\circ}$C in 5% $CO_2$.

For long term storage of cell lines, they must be kept frozen in liquid nitrogen. Cells were sub-cultured as usual and transferred to the cryo vial tube containing 10% DMSO. The mixture of cells and DMSO was mixed well before placed in liquid nitrogen tank. Once the stock of cells was needed, it can be recovered by removing the vial from the liquid nitrogen tank and placing immediately in 37 $^{\circ}$C water bath. After thawing the cells, outside of the vial was wiped off with 70% ethanol and then the cells were transferred into a fresh 15-ml tube containing 9 ml of complete medium. The cells were mixed up and down by pipetter and collected by centrifugation at 2,000 x g for 5 min. The cells were resuspended in 5 ml of complete medium and then mixed them. After that, the cells were transferred into a new 75- $cm^2$ flask and 20 ml of complete medium was added to make the final of 25 ml. The flask of cells was

placed in 37 °C with 5% $CO_2$ until confluent and sub-culturing process were carried out again.

### 3.9 Transient transfection of HEK 293 cells

Plasmid DNA for transfection was purified with the EndoFree™ plasmid maxi kit (Qiagen). The transient transfection using the calcium phosphate precipitation was performed in this study [216]. The culture of HEK 293 cells was split as previously described and plated 4-8 h before transfection at a density of $10^6$ per 60 mm-dish or approximately 25% confluency (12.5% confluency for anion exchange and cytoskeleton assays). At the time of transfection, the 590 µl of 2x HEPES solution was added to a microcentrifuge tube. In another microcentrifuge tube was added with 507 µl of sterile water, 72 µl of $CaCl_2$ and then plasmid construct (1.6 µg of pkAE1 (or pCHkAE1) and 2 µg of ILK (or GAPDH, pantophysin, thymosin β4 and ILK mutants) in combination with empty vector to total of 3.8 µg of cDNAs. Cells for anion exchange and cytoskeleton assays were transfected with 0.4 µg kAE1 cDNA and 2 µg ILK cDNA. The $CaCl_2$/water/DNA mixture was drop-wised to the 2xHEPES solution and incubated at room temperature for 15 min. After that, the transfection mixture was mixed up and down by pipetter and then added 316 µl of transfection mixture drop-wise to the plated cells evenly. The transfected cells were incubated at 37 °C with 5% $CO_2$ for 48 h before performing further studies.

### 3.10 Protein expression in HEK 293 cells

#### 3.10.1 Protein sample preparation

Two days post-transfection, the transfected HEK 293 cells were washed once with 1x PBS and incubated in 250 µl of 2x SDS sample loading buffer at room temperature for 10 min to lyse the cells. The cells were recovered by scraping with the rubber stick and transferred to a fresh microcentrifuge tube. The solution was mixed by using the needle sucking up and down for several times and then heated it at 65 °C for 5 min. The protein sample was set aside for loading to SDS-PAGE and immunoblotting to examine protein expression in HEK 239 cells. The sample can be kept at -20 °C up to one month.

### 3.10.2 SDS-PAGE and immunoblotting

Proteins were electrophoresed on 10% SDS-PAGE and run under 120 constant volts for 2 h. After electrophoresis, the gel, polyvinylidene difluoride membrane (PVDF) and filter papers were soaked in the transfer buffer for 2 min. Transblotting was performed by using a Trans-Blot® SD semi-dry electrophoretic transfer cell (Bio-Rad) under 100 constant volts for 1 h. Blot was blocked in 10 ml of TBSTM (Tris-buffered saline with Tween 20 containing 5% (w/v) non-fat dry milk powder (Carnation) for 1 h at room temperature and then incubated in TBSTM containing 1:1,000 diluted anti-HA or 1:3,000 diluted anti-AE1 polyclonal antibodies (Santa Cruz Biotechnology) for kAE1 detection for 12–16 h at 4 °C. The blot was washed three times with TBST and then probed with 10 ml of 1:1,000 diluted donkey anti-rabbit antibody conjugated-horseradish peroxidase (HRP) in TBSTM for 1 h at room temperature. The non-specific binding was removed from the blot by washing three times with TBST. The protein bands were detected by incubating blots with 1:1 Enhanced Chemiluminescence Luminol reagent, ECL, (Perkin Elmer Life Sciences) and visualized using a Kodak Image Station 440CF.

ILK and ILK mutants were detected using anti-ILK polyclonal antibody (Sigma) at dilution of 1:4,000 or anti-His monoclonal antibody at the dilution of 1:3,000. GAPDH and pantophysin were also detected by anti-His antibody followed by incubating with 1:1000 of rabbit anti-mouse antibody conjugated-HPR and detection process was performed as previously described.

The same blot can be probed with another antibody after stripping with 10 ml of 100 mM 2-mercaptoethanol, 62.5 mM Tris-HCl, pH 6.8 at 50 °C for 10 min. Blots were then washed with TBST and incubated in 10 ml of TBSTM containing either mouse anti β-actin monoclonal antibody at dilution 1:2,000 (Sigma), anti paxillin monoclonal antibody at dilution 1:10,000 (BD Transduction Labs) or anti actopaxin antibody at dilution 1:3,000 (Sigma) to detect endogenous actin, paxillin and actopaxin expression in HEK 293 cells.

## 3.11 Co-immunoprecipitation assay

To demonstrate whether ILK, GAPDH, pantophysin and thymosin β4 identified in yeast two-hybrid screen could interact with full-length kAE1 by using another

technique, co-immunoprecipitation assay was performed. Before performing the experiment, Protein A-Sepharose resin mixture was firstly prepared according to the protocol of Prof. Dr. Joseph Casey's laboratory. The 20 ml of 75% slurry Sepharose CL-4B resin (Sigma) was taken from stock bottle and transferred into 50-ml tube to obtain 15 ml bed volume. The resin was collected by centrifugation at 1,000 x g for 5 min and then washed twice with 10 volumes of sterile water. Resin was centrifuged at 1,000 x g for 5 min. To make 35% slurry, 15 ml of resin was mixed with 42.85 ml of IPB buffer (1 mM EDTA, 0.5% (v/v) Igepal (Nonidet P-40 detergent), 150 mM NaCl, 2% (w/v) BSA, 10 mM Tris-HCl pH 7.5) and incubated at room temperature of 2 h. The Sepharose CL-4B resin was served as a cross linker. In the meantime, 10 ml of IPB buffer was added to 0.5 g of Protein A-Sepharose (Amersham) and then incubated at room temperature for 2 h. Resin was collected by centrifugation at 1,000 x g for 5 min and added to 10 ml of IPB buffer to obtain 25% slurry resin. An equal volume of 35% slurry Sepharose CL-4B and 25% Protein A-Sepharose resin was mixed and $NaN_3$ was added to the resin mixture to 0.02% (v/v) final concentration. The Protein A-Sepharose resin mixture can be kept at 4 $^{\circ}$C for few months.

To carry out co-immunoprecipitation assay, HEK 293 cells were either co-transfected with HA-tagged kAE1 and His-tagged ILK (GAPDH, pantophysin or thymosin β4) or kAE1 alone. Two days post-transfection, the transfected cells were washed twice with 5 ml of phosphate buffer saline (PBS) (150 mM NaCl, 3 mM KCl, 6.5 mM $Na_2HPO_4$, 1.5 mM $KH_2PO_4$, pH 7.4) and allowed to detach in 2 ml of PBS for 10 min at room temperature. Cells were collected by centrifugation at 3,000 x g for 5 min and lysed with 500 µl of $IPB^+$ buffer (1 mM EDTA, 0.5% (v/v), Igepal (Nonidet P-40 detergent), 150 mM NaCl, 2% (w/v) bovine serum albumin, 10 mM Tris-HCl pH 7.5 and protease inhibitors) on ice for 15 min. The insoluble fraction was removed by centrifugation at 13,000 x g for 10 min at 4 $^{\circ}$C. The supernatants were transferred to a fresh microcentrifuge tubes containing 2 µl of pre-immune rabbit serum and 50 µl of Protein A-Sepharose resin mixture to pre-clear the cell lysates. Tubes were incubated for 2 h at room temperature, with constant rotation. Resin was then removed by centrifugation at 7,500 x g for 5 min. The procedure was repeated using monoclonal anti-His antibody (Amersham Bioscience) in place of pre-immune serum, and the mixture was incubated at 4 $^{\circ}$C for 12–16 h. After incubation, resin was collected by

centrifugation and washed thoroughly with wash buffer 1 (0.1 mM EDTA, 0.1% Igepal, 150m M NaCl, 10 mM Tris-HCl, pH 7.5) and wash buffer 2 (0.1 mM EDTA, 10 mM Tris-HCl, pH 7.5). Proteins were eluted with 2x SDS-PAGE sample loading buffer containing 2% (v/v) 2-mercaptoethanol and heated at 65 °C for 5 min. The immunoprecipitates were analyzed by SDS-PAGE and immunoblotting.

### 3.12 Affinity co-purification

To confirm the results of co-immunoprecipitation, affinity co-purification was further performed by using the advantage of poly-histidine tagged on the N-terminus of ILK or other kAE1 interacting proteins. HEK 293 cells co-expressing kAE1 and His-tagged ILK (pantophysin and GAPDH) or expressing kAE1 alone were collected and lysed in 1 ml of $IPB^{+}$ buffer as previously described. In addition, $Co^{2+}$ chelate resin (BD Bioscience) was taken from 4 °C of the stock bottle and transferred to a new microcentrifuge tube. The resin was washed twice with sterile water to remove ethanol which used for resin preservation. After that, resin was collected by centrifugation at 900 x g for 5 min, incubated for 10 min in 1x equilibration buffer (150 mM NaCl, l50 mM sodium phosphate buffer, pH 7.0) and then collected resin by centrifugation. The cell lysates were then incubated with 200 µl of $Co^{2+}$ resin for 16 h at 4 °C with rotation. Resin was collected by centrifugation at 900 x g for 5 min and washed three times with 1x equilibration buffer. Bound proteins were eluted with the 1x equilibration buffer containing 1.5 M imidazole. Eluates were collected and mixed with sample loading buffer then heated at 65 °C for 5 min. The samples were subjected to SDS-PAGE and immunoblotting. The presence of kAE1 in the eluates was detected by anti-HA antibody.

### 3.13 Immunofluorescence staining

HEK 293 cells grown on coverslips in 6 well-plate were co-transfected with kAE1 and ILK (GAPDH or pantophysin) while LLC-PK1 cells grown on coverslips in 6 well-plate were transfected with kAE1. Two days post-transfection, cells were washed once with warmed 1x PBS and fixed with 4% paraformaldehyde in 1x PBS at room temperature for 1 h. After rinsing twice with 1x PBS containing 1 mM $MgCl_2$ and 1 mM $CaCl_2$ ($PBS^{++}$), coverslips were incubated in quenching buffer (100 mM

glycine in 1x PBS) for 5 min. Cells were permeabilized in 0.2% Triton X-100 at room temperature for 15 min followed by washing twice with 1x $PBS^{++}$. The coverslips were blocked with 1% BSA in 1x $PBS^{++}$ for 30 min and then incubated with primary antibodies (1:500 dilution of rabbit anti-HA polyclonal antibody and 1:500 dilution of mouse anti-His monoclonal antibody to detect kAE1 and ILK, GAPDH or pantophysin, respectively) for 60 min at room temperature while endogenous ILK in LLC-PK1 cells were stained with 1:1000 diluted monoclonal mouse anti-ILK antibody and kAE1 was stained with 1:1000 of anti-AE1 antibody for 60 min at room temperature. After washing three times with 1x $PBS^{++}$, the coverslips were incubated with a mixture of 1:8000 dilution Cy3-conjugated goat anti-rabbit and FITC-conjugated rabbit anti-mouse antibodies to visualize kAE1 and ILK (GAPDH or pantophysin) , respectively. The coverslips were washed three times with 1x $PBS^{++}$ and then mounted with Prolong Anti-fade reagent (Molecular Probes, Inc. Canada). Fluorescence images were captured by LSM510 confocal microscopy. Fluorescein was visualized by excitation at 488 nm and emission was monitored at 520 showing ILK while kAE1 was visualized by excitation at 568 nm and emission was monitored at 590 nm.

### 3.14 Cell surface biotinylation

Transfected HEK cells with kAE1 and ILK (pantophysin and GAPDH) or kAE1 alone were washed with 5 ml of ice-cold PBS and borate buffer (10 mM boric acid, 154 mM NaCl, 7.2 mM KCl, 1.8 mM $CaCl_2$, pH 9.0). Cells were treated with 4 ml of 0.5 mg/ml Sulfo-NHS-SS-Biotin (Pierce) in cold borate buffer and incubated on ice for 30 min. Unreacted reagent was then quenched by rinsing the cells three times with quenching buffer (192 mM glycine, 25 mM Tris, pH 8.3). Cells were collected and lysed with 500 µl of $IPB^{+}$, on ice for 15 min. The insoluble material was removed by centrifugation. Half of the lysate was taken for immunoblotting (Total fraction, T). The rest was incubated with ImmunoPure (Pierce) immobilized streptavidin (100 µl) for 12-16 h at 4 $^{\circ}$C with rotation to bind the biotinylated proteins. The resin was collected by centrifugation at 7,500 x g, 5 min. The supernatant (unbound fraction, U) was taken for immunoblotting. The streptavidin resin was washed three times with washing buffer as described above. 2x SDS sample loading buffer containing 2% 2-

mercaptoethanol was added to the resin (bound fraction), and heated at 65 °C for 10 min. Samples were analyzed by SDS-PAGE and immunoblotting using anti-HA antibody for kAE1 detection. The blot was stripped and incubated with mouse anti-actin antibody to normalize the protein expression in each fraction. As a control, cell surface biotinylation assays were also done in HEK 293 cells transfected with the cytosolic marker protein, Yellow fluorescent protein (YFP), to confirm that biotinylation was solely restricted to the cell surface.

### 3.15 Fluorescence activated cell sorting (FACS) analysis

The kAE1HA557 and eAE1HA557 plasmids were constructed by insertion of hemaglutinin epitope (HA) at the third extracellular loop of the kAE1 and eAE1 plasmids. Therefore, when kAE1HA557 and eAE1HA557 were expressed, the HA epitope will expose to extracellular and it can be used to determine the amount of cell surface expression by staining with fluorescent antibody that recognize the HA epitope of kAE1 and eAE1 at the third loop. The fluorescence signal can be measured by flow cytometry. HEK 293 cells co-expressed kAE1 or eAE1 plus ILK or expressed kAE1 or eAE1 alone were trypsinized at 4 °C for 5 min, centrifuged to collect the cells and resuspended in Hank's balance salt solution (HBSS) with 1% BSA. The living transfected HEK 293 cells were incubated with 1:1000 dilution of mouse anti-HA antibody in Hank's solution with 1% BSA for 15 min, then the cells were stained by goat anti-mouse Alexa 488 (1:1000) for 15 min on ice. The samples were washed and analyzed using Beckman-Coulter EPICS Elite flow cytometer (Becton Dickinson, Mountain View, CA). The intensity of the fluorescent signal was determined by quantification of the level of the cell surface expression of kAE1.

### 3.16 Transport activity assay

The transport activity of kAE1 was monitored using a fluorescence assay, as previously described [75]. Non-charged, non-fluorescent ester form of the BCECF-AM (2', 7'-bis-(2-carboxyethyl)-5-(and-6)-carboxyfluorescein-acetoxymethyl ester was used to load HEK 293 cells. Because BCECF-AM is non-charged, it rapidly diffuses across the cell's membranes and enters HEK 293 cells. When the dye goes

inside, the intracellular esterases will cleave the ester bond and then release charged BCECF, which fluorescences according to the intracellular pH.

Briefly, HEK 293 cells were grown on poly-L-lysine-coated glass coverslips in 60-mm tissue culture dishes, and transiently co-transfected as described above with the cDNA for kAE1 alone, kAE1 + ILK, or pcDNA 3.1 (+) empty vector. Two days post-transfection, cells were washed with serum-free DMEM (Invitrogen) and incubated with 2 µM BCECF-AM in 4 ml serum-free DMEM (37 °C, 15 min). Coverslips were mounted into a fluorescence cuvette, inside a fluorimeter, and perfused at 3.5 ml/min alternately with Ringer's buffer (5 mM glucose, 5 mM potassium gluconate, 1 mM calcium gluconate, 1 mM $MgSO_4$, 2.5 mM $NaH_2PO_4$, 25 mM $NaHCO_3$, and 10 mM HEPES, pH 7.4), containing either 140 mM NaCl or 140 mM Na gluconate. Both buffers were bubbled continuously with air containing 5% $CO_2$. Fluorescence changes were monitored by a Photon Technologies International (London, Ontario, Canada) RCR fluorimeter at excitation wavelengths of 440 and 502.5 nm and emission wavelength of 528.7 nm. Calibration with the nigericin/high potassium method [217] was used to convert fluorescence measurements to intracellular pH (pHi) with pH values of 6.5, 7.0, and 7.5. Transport activity was calculated as change in pHi/min, and expressed as a percentage of kAE1 transport activity. The transport activity of sham-transfected cells was subtracted from the rate of change to correct for background activity. Statistical analysis was performed using Kaleidagraph software (Synergy Software, Reading, PA, USA).

### 3.17 Triton X-100 cytoskeleton extraction

HEK 293 cells co-transfected with kAE1 plus ILK or kAE1 alone were washed three times with ice-cold PBS and incubated with 400 µl of Triton X-100 extraction buffer (0.5% Triton X-100, 100 mM NaCl, 3 mM $MgCl_2$, 0.1 mM DTT, 25 mM KCl, 1.8 mM $CaCl_2$, 10 mM Tris-HCl pH 7.5 and protease inhibitors) on ice for 15 min. Cells were collected and using ultracentrifugation at 30,000 x g for 10 min at 4 °C. The supernatant (detergent-soluble fraction, So.) was taken for immunoblotting. The pellet (detergent-insoluble fraction, Ins.) was dissolved in 40 µl of SDS buffer (1% (w/v) SDS, 2 mM EDTA, 10 mM Tris-HCl pH 7.5 and protease inhibitors) by sucking it up and down with a pipetter. $IPB^+$ (360 µl) buffer was then added to the suspension,

and samples were incubated on ice for 15 min. Particulate material was separated by centrifugation at 30,000 x g for 10 min to obtain the supernatant, which now contained insoluble proteins. Soluble and insoluble fractions were resolved on SDS-PAGE and immunoblotting, using anti-HA antibody for kAE1 detection.

# CHAPTER V
# RESULTS

## Part I: Identification of proteins interacting with the N-terminal domain of kAE1 (NkAE1) by using yeast two-hybrid system

### 1. Construction of the bait plasmid

The DNA fragment corresponding to Met66-Pro403 of human eAE1 (NkAE1) was amplified by PCR using pcDNA3/kAE1 plasmid as DNA template and kAE001NcoI and kAE403SalI as primers. The PCR product containing *Nco*I and *Sal*I restriction sites flanking at the 5' and 3' end was digested with a combination of *Nco*I and *Sal*I, and then the digested fragment was purified by QIAGEN Gel Extraction Kit. The purified fragment was subsequently ligated to *Nco*I/*Sal*I-digested pGBKT7 vector. An aliquot of ligation mixture was transformed into *E.coli* DH5α competent cells. The transformants were selected on LB plate containing 100 μg/ml of ampicillin.

To identify the putative positive clones, colony PCR screening using kAE001NcoI and kAE403SalI primers and restriction enzymes analysis using *Nco*I and *Sal*I were performed. The expected size of PCR products were obtained from 10 recombinant clones screening (Figure 15A) and the plasmids of these clones were isolated by CTAB method and then used for restriction enzymes analysis to confirm the presence of inserted fragments. The results showed that all 10 clones gave two DNA digested fragments corresponding to the *Nco*I/*Sal*I-digested pGBKT7 and *Nco*I/*Sal*I-digested the NkAE1 (Figure 15B). Three of these positive clones (clones no. 7, 8 and 9) were subjected to automated DNA sequencing to verify the inserted sequences. It was found that all three clones contained the correct cDNA fragments corresponding to Met66-Pro403 of human AE1. The recombinant plasmid was named pNkAE1 and subsequently used as bait for screening human kidney cDNA library.

### 2. Analysis of fusion protein (GAL4-BD/NkAE1) expressed from pNkAE1

To test the expression of fusion protein GAL4-BD/NkAE1 from pNkAE1, the

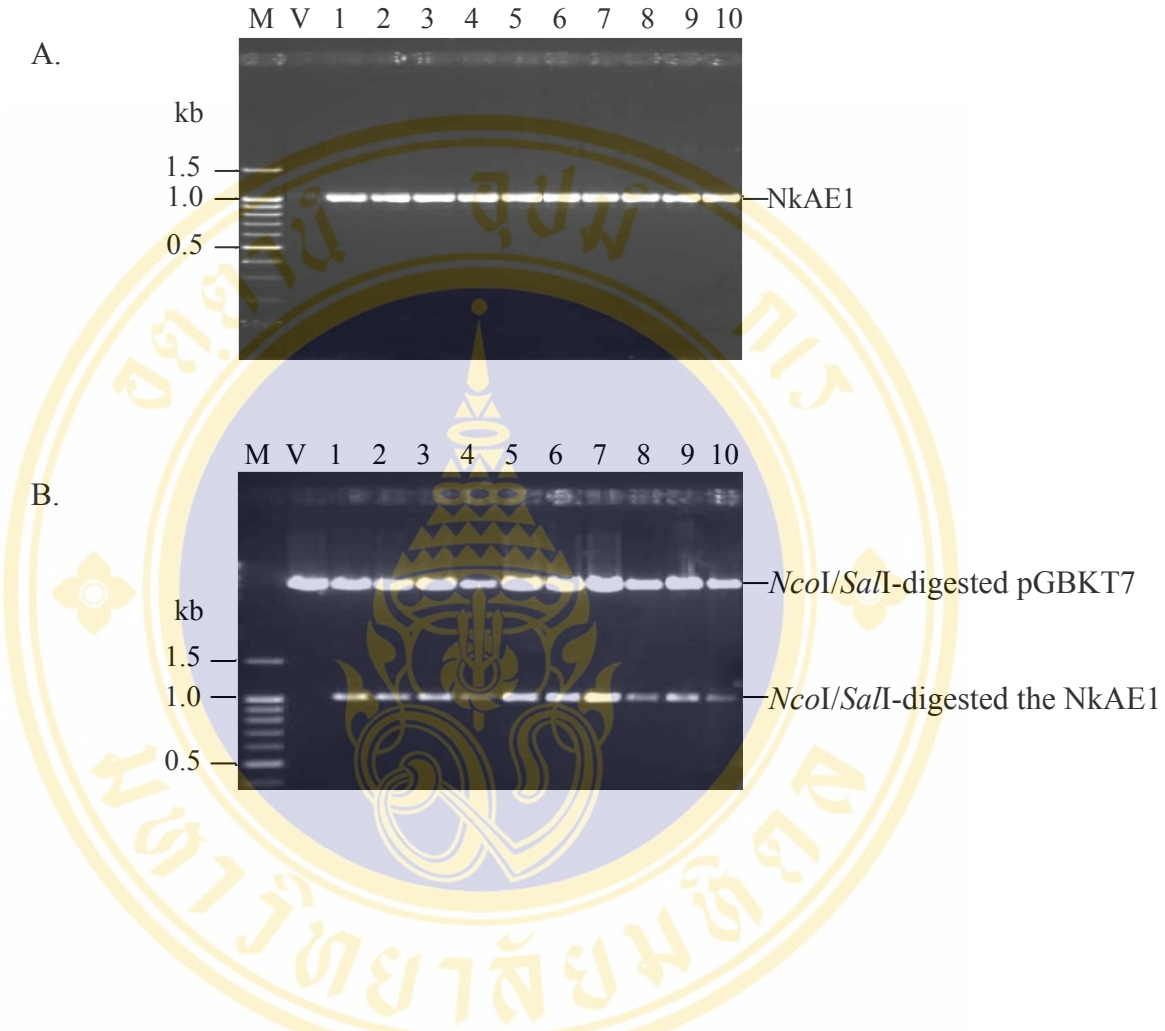


**Figure 15 Analysis of pNkAE1 by PCR and restriction endonucleases.**

A. PCR amplification of pNkAE1 was performed and the amplified products were analyzed on 1% agarose gel electrophoresis.

B. The recombinant clones were digested with *Nco*I and *Sal*I and digested reactions were analyzed on 1% agarose gel electrophoresis.

Lane M is λ-*Hind*III digested DNA marker.

Lane V is pGBKT7 vector.

Lanes 1-10 are recombinant clones from clone numbers 1-10.

purified plasmid was transformed in the MATα AH109 yeast strain as described in method section 3.2.1. The clone grown on SD/-Trp plate was selected and the expressed protein was extracted and analyzed. The protein samples were resolved on SDS-PAGE and were detected by immunoblotting using mouse anti-GAL4 DNA-BD antibody as a primary antibody and followed by HRP-conjugated anti-mouse IgG antibody (method section 4.3.2.3). The result showed that GAL4 DNA-BD antibody could detect expression of GAL4-BD at molecular weight of 22 kDa (Figure 16, lane 1) while the fusion protein GAL4-BD/NkAE1 was detected as a protein with molecular weight of 60 kDa as expected (Figure 16, lane 2).

**3. Analysis of bait (pNkAE1) properties**

Prior to use pNkAE1 as a bait to screen NkAE1 interacting partners in the cDNA library by yeast two-hybrid assay, toxicity effect, transcriptional activation and mating efficiency properties of pNkAE1 were tested. pNkAE1 was transformed into the *MATα* AH109 yeast strain. Toxicity test was used to verify the bait whether affect the yeast growth by comparing growth rate of the strain AH109 transformed with pNkAE1 plasmid to the AH109 transformed with empty pGBKT7 vector. It was found that $A_{600}$ of the bait strain and the vector strain were 0.35 and 0.40, respectively, which suggested that the bait did not show toxicity to the yeast host cells.

Apart from toxicity test, auto-transcriptional activation of pNkAE1 for *HIS3*, *ADE2* reporter genes was tested by plating the yeast transformed with pNkAE1 on SD/-Trp/-His/-Ade plate. The result showed that the yeast transformants did not grow on SD/-Trp/-His/-Ade plate, suggesting that pNkAE1 is unable to activate transcription of *HIS3*, *ADE2* reporter genes. In addition, the transcription of *LacZ* reporter gene was examined by monitoring β-galactosidase activity using colony lift assay of yeast transformants from SD/-Trp plate. It was found that the yeast transformed with pNkAE1 appeared slightly blue colonies on the lifted filter but it is not seeming significantly different from yeast transformed with pGBKT7 (negative control) (Figure 17). The background might be generated from the plasmid backbone. Therefore, this bait did not activate transcription of *LacZ* reporter genes by itself.

Since yeast mating was performed to screen interacting proteins in this study, mating efficiency of the pNkAE1 comparing with the mating control (pGBKT7-53 x

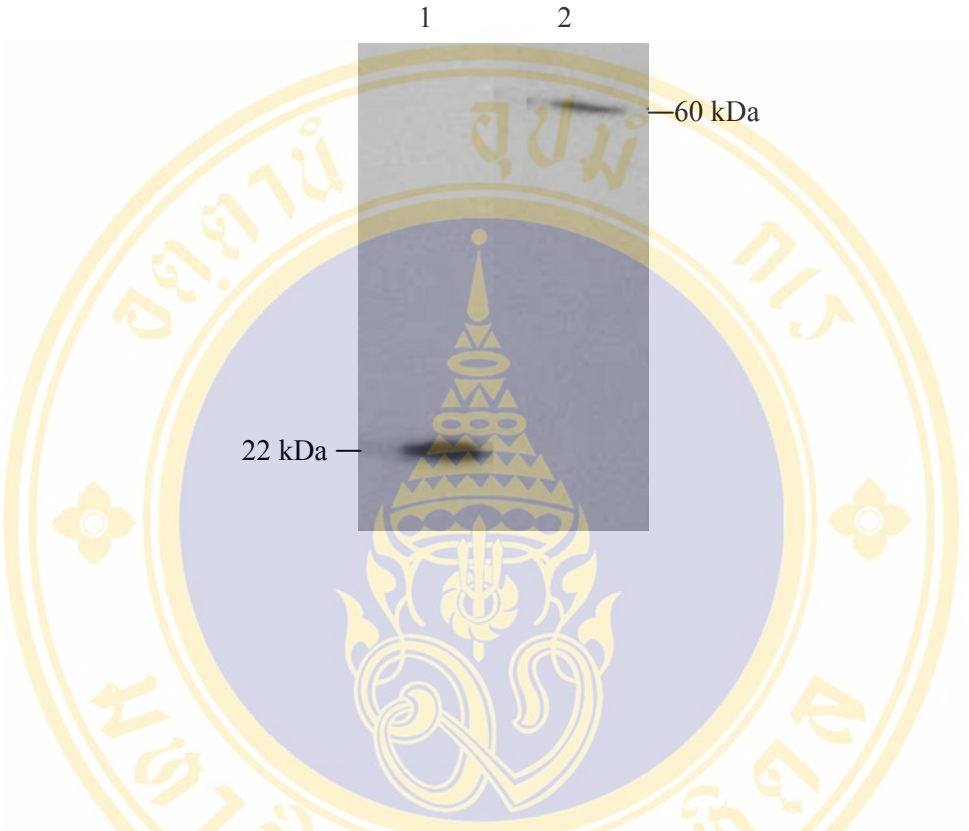


**Figure 16 Expression of GAL4-BD/NkAE1 fusion protein.**

Immunoblot analysis of the fusion protein, GAL4-BD/NkAE1, expressed from pNkAE1 clone number 9 was detected by mouse monoclonal antibody against GAL4-DNA binding protein at 1:3000 dilution.

Lane 1 is the protein extracts from yeast strain AH109 transformed with pGBKT7 vector, served as a negative control.

Lane 2 is the protein extract from yeast strain AH109 transformed with pNkAE1.

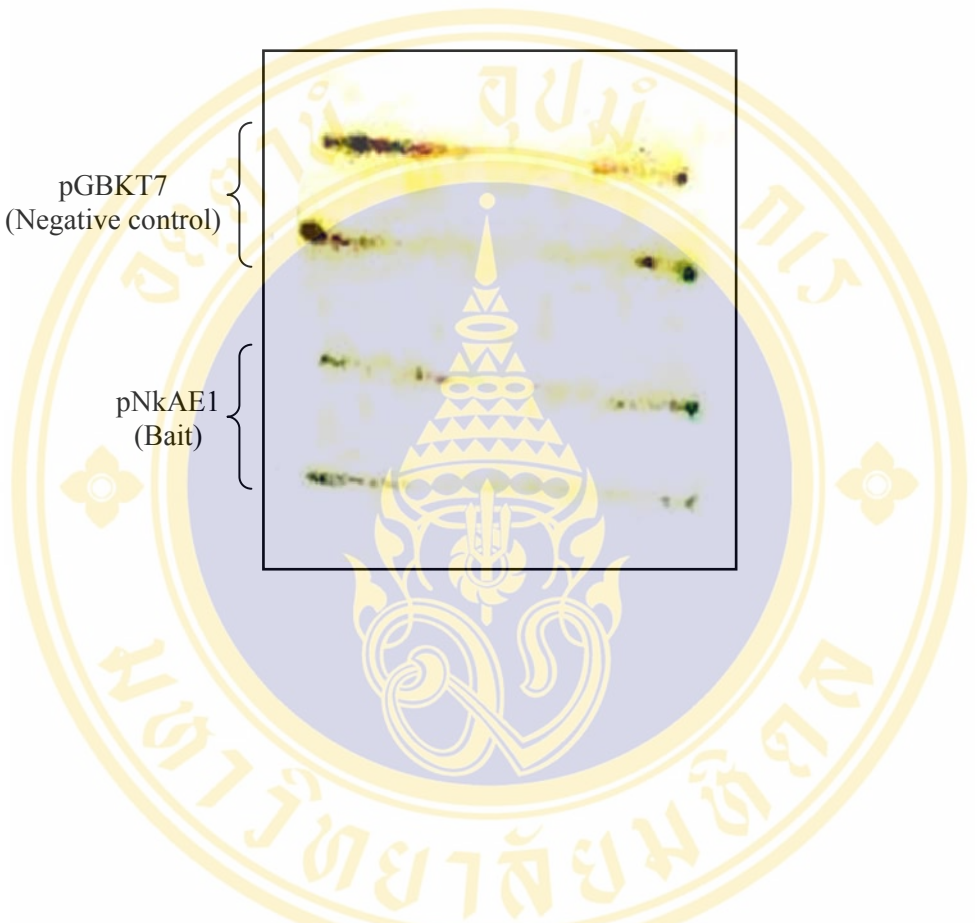


**Figure 17 Analysis of transcriptional activation of pNkAE1 (Bait).**

The transformed yeast strain AH109 with either pNkAE1 (Bait) or pGBKT7 (Negative control) was grown on SD/-Trp plate. The yeast colonies were lifted on the filter paper and monitored β-galactosidase activity by appearance of blue color of colonies on the lifted filter.

pTD1-1) was examined. Number of diploid colonies on SD/-Trp/-Leu plates of mating control and pNkAE1 mating with pTD1-1 revealed 600 and 500 colonies, respectively. Fewer colonies on SD/-Trp for both reactions indicated a limiting partner of mating. This was used for calculation of mating efficiency as shown in method section 3.2.2. It was found that mating efficiency of mating control and pNkAE1 mating with pTD1-1 were 6% and 7.1%, respectively, suggesting that pNkAE1 can mate with its partner efficiently. According to the appropriate bait properties, the pNkAE1 could be used as bait to screen the proteins that interact with the N-terminal kAE1 in human kidney cDNA library by yeast two-hybrid system.

**4. Yeast two-hybrid screening of proteins interacting with the N-terminal kAE1**

Yeast two hybrid screening was carried out to identify the proteins that interact with the kAE1 N-terminal domain in human kidney cDNA library as described in method section 3.3. The transformant yeast AH109 with pNkAE1 was mated with pre-transformed kidney cDNA library in Y187 strain. The cDNA was constructed in pACT2 to express the fusion protein containing GAL4-AD. The yeast mating of pGBKT-53 and pTD1-1 was served as positive interaction control. Approximately $1x10^6$ independent clones in cDNA library were screened and interaction between the N-terminal kAE1 and interacting proteins was examined by growth of diploid yeast cells on SD/-Trp/-Leu/-His/-Ade to verify the expression of HIS3, ADE2 reporters. The results from this step showed 151 diploid yeast colonies could grow on SD/-Ade/-Leu/-Trp/-His after incubating at 30 $^{\circ}$C for 2 weeks. All of 151 positive colonies were later selected and re-streaked on SD/-Trp/-Leu/-His/-Ade containing X-α-Gal for further screening α-galactosidase activity (MEL1 reporter) (Figure 18). On the basis of intensity blue colony determined the affinity binding between two proteins, total 133 positive colonies including robust and moderate blue colonies that might carry interaction between kAE1 and interacting proteins were selected for further analysis.

**5. Identification of duplicate clones from library screening**

To reduce the redundant clones from library screening, the plasmid DNA of selected 133 positive two-hybrid colonies was isolated from yeast by standard lyticase

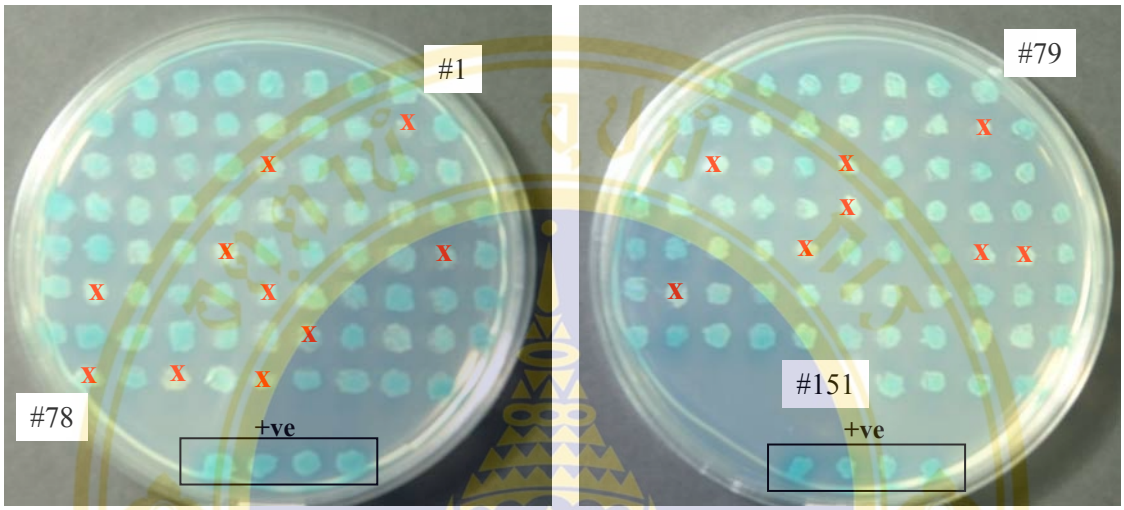


**Figure 18 Yeast two-hybrid screening of human kidney cDNA library by yeast mating.**

Interaction between the NkAE1 and interacting proteins was examined by growth of diploid yeast on SD/-Trp/-Leu/-His/-Ade containing X-α-Gal. According to intensity of blue colonies, the 107 robust and 26 moderate blue colonies were selected while 18 faint blue colonies (**X**) were omitted. The "+ve" is yeast mating between pGBKT-53 and pTD1-1 served as positive interaction control.

method as described in method section 4.3.4. These plasmids were used as DNA templates for PCR amplification of the inserted cDNAs in the library clones. PCR reaction was performed by using the primers flanking multiple cloning site of library plasmid named LibADf and LibADr. Since the size of cDNAs inserted in the library was varied from 0.5 kb to 4.0 kb, PCR amplification condition was optimized to amplify the cDNAs inserts of all 133 positive clones. cDNA inserts of all 133 positive clones could be amplified and shown in Figure 19. After that, the PCR products were purified by using QIAGEN PCR Purification Kit. The purified PCR products were subsequently digested with *Hae*III to eliminate the library duplicate clones. The digested products were analyzed on 1.5% agarose gel electrophoresis and visualized by staining with ethidium bromide. The digested fragment pattern results of PCR products were analyzed and compared among the positive clones (Figure 20). The result showed that restriction enzyme analysis can get rid of 12 repetative clones out of 133. Therefore, total 121 independent clones were obtained and further subjected to partial DNA sequencing.

**6. Sequencing of cDNA inserts and searching for homology sequences**

To verify inserted cDNAs of 121 independent clones, partial DNA sequencing of the purified PCR products of all 121 clones were performed by using a primer named LibInt-f with an annealing site upstream of the cDNA inserted fragment. The sequencing results showed 109 independent clones could be analyzed while that of the others 12 clones were not obtained since the numerous repeat nucleotide sequences (Poly T tracks) reading trough the inserted fragments. The obtained sequences were searched for homology sequences in GenBank and protein databases by BLAST. The putative proteins that gave a high homology were shown in Table 4. Seventy-three clones were identified as known proteins while 36 clones were hypothetical proteins.

As mentioned, the trafficking mechanism of kAE1 to express on the cell membrane has been poorly understood. The criteria for selection of the independent clones for further study was therefore involved in the possibility of the proteins would be participating in kAE1 trafficking. Thus, 21 independent clones encoding known proteins and randomly selection of 14 clones encoding hypothetical proteins as

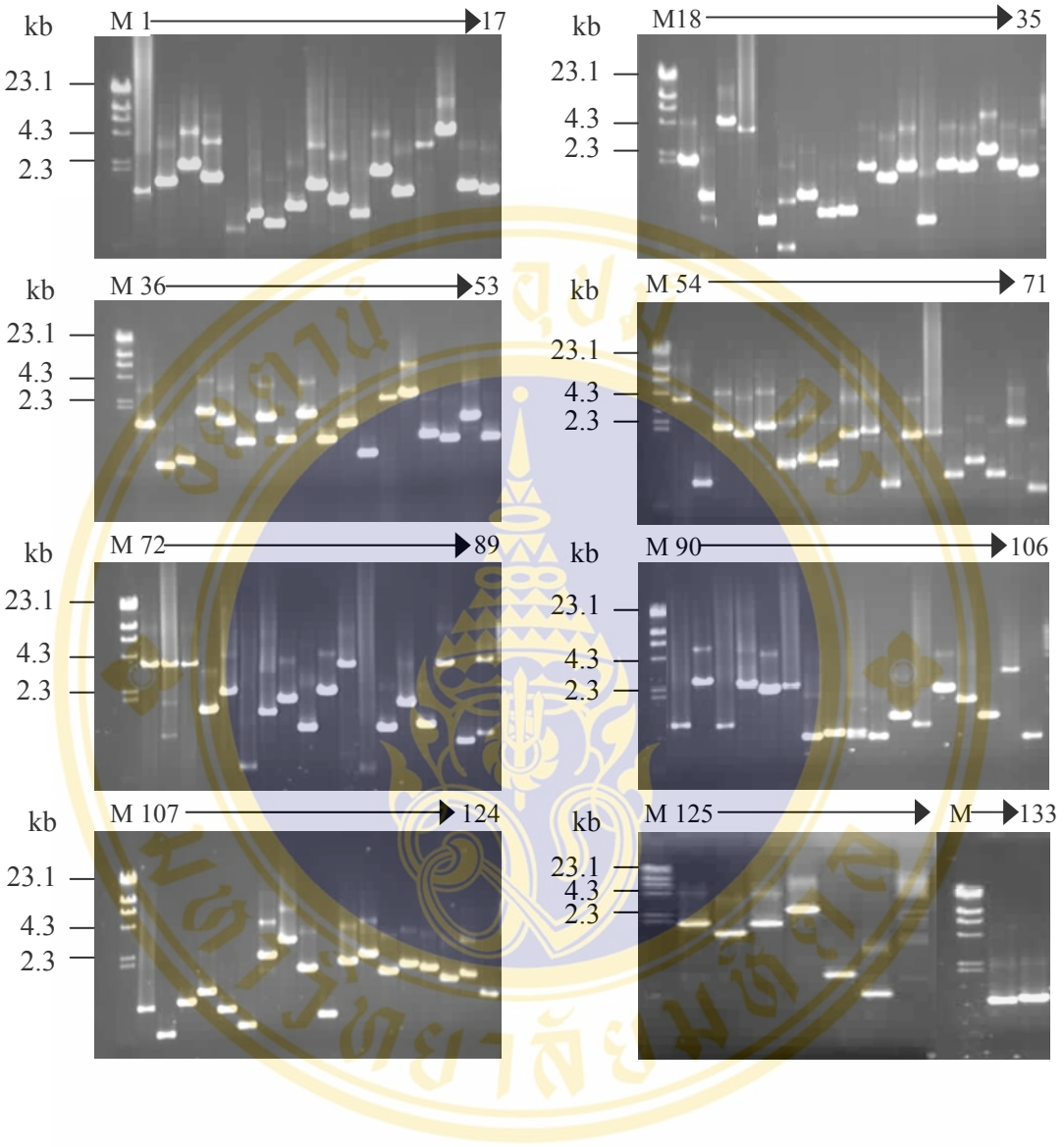


**Figure 19 PCR amplification of isolated positive clones from library screening.**

PCR amplification of cDNAs in positive clones isolated from initial library screening. Amplified PCR products were analyzed on 1% agarose gel electrophoresis.

Lane M is λ-*Hind*III digested DNA marker.

Lanes 1-133 are amplified cDNA inserts of all 133 positive clones corresponding size of PCR products varied from 0.5 kb to 4.0 kb.

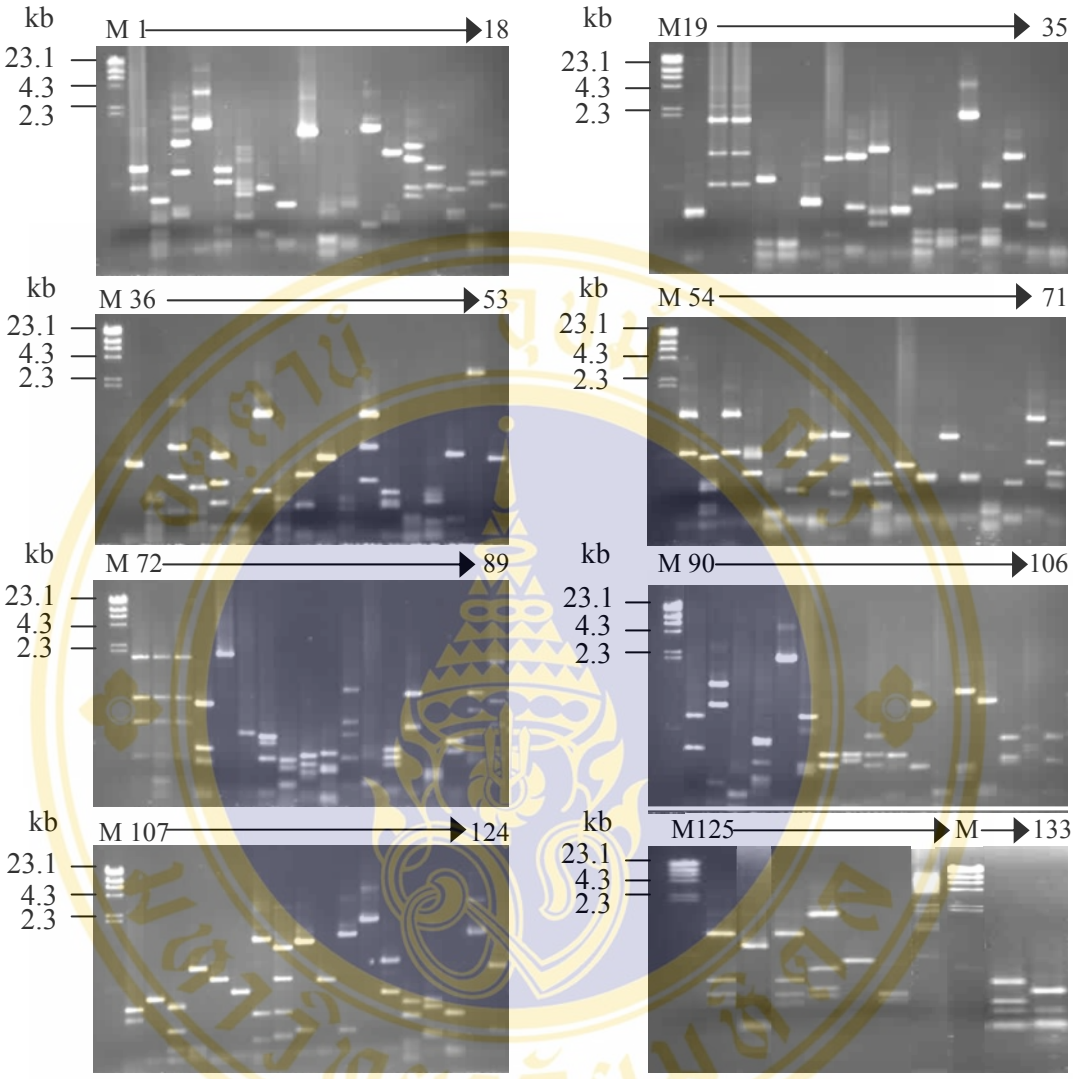


**Figure 20 Restriction endonuclease analysis of putative positive clones.**

PCR products of all 133 putative positive clones from library screening were digested with *Hae*III and the digested fragments were analyzed on 1.5% agarose gel electrophoresis. Duplicate clones were grouped by similar restriction pattern.

Lane M is λ-*Hind*III digested DNA marker.

Lanes 1-133 are *Hae*III-digested fragments of PCR products from positive clone numbers 1-133.

**Table 4 BLAST searches of nucleotide sequences from yeast two- hybrid screen of a human kidney cDNA library with the N-terminal kAE1.**

| Accession number | BLAST description | Proposed function | E-value |
|---|---|---|---|
| **Protein involved in metabolism** | | | |
| NM000282.1 | Propionyl CoA carboxylase | Enzyme in catabolic pathway of amino acids | 0.00 |
| NM000035.1 | Aldolase B* | Fructose metabolism | 0.00 |
| NM033055.1 | Ortholog of mouse hippocampus | Carbohydrate transport and metabolism | 0.00 |
| BC014085.1 | GAPDH* | Carbohydrate metabolism& membrane fusion | 0.00 |
| NM015423.2 | Aminoadipate-semialdehyde dehydrogenase | Biosynthetic pathway of lysine | e -169 |
| BC000306.1 | L-3-hydroxyacyl CoA dehydrogenase | Mitochondrial beta-oxidation of fatty acids | 0.00 |
| AJ003100.1 | Glycogen synthase 2 | Glycogen biosynthesis | 8e -42 |
| AF069984.1 | Nitrilase homolog 1 | Nitrogen metabolism | 6e -77 |
| BT007538.1 | Prosaposin | Lysosomal degradation of sphingolipid | 1e -20 |
| NM000016.2 | Acyl CoA dehydrogenase | Mitochondrial beta-oxidation of fatty acids | 0.00 |
| AY195792.1 | Mitochondrial protein (7 clones) | Electron-Transfer Proteins | 0.00 |
| **Transport and binding proteins** | | | 0.00 |
| AF030356.1 | Peroxisome, pex1 | Protein import into peroxisome matrix | 0.00 |
| AJ535113.1 | MHC class I | Antigen presenting cells | 3e -144 |
| NM003361.1 | Uromodulin | May regulate the circulating of cytokines | 0.00 |
| NM006288.2 | Thy-1 cell surface antigen | Cell-ligand interaction | 0.00 |
| NM003107.2 | Sex determining region Y box 4 | Regulation of embryonic development | e-113 |
| BC007034.1 | Metallothioneine 2A (2 clones) | Bind to metal ions | 0.00 |
| BC007900.1 | DAZ associated protein 2 | Germ-cell specific binding protein | 0.00 |
| NM004048 | β- 2 microglobulin | Immunoglobulin | 0.00 |
| NM015423.2 | Zn finger | Nucleic acid binding protein region | e-145 |
| **Protein trafficking** | | | |
| NM004487.1 | Giantin* | Cross-bridges of Golgi complex | 0.00 |
| BC020938 | Pantophysin* | Vesicle trafficking | 0.00 |
| NM003574.2 | Vesicle-associated membrane protein* | Associated with SNARE proteins | e-118 |
| NM178814.2 | Adaptor-related protein complex 1, σ 3* | Role in protein sorting in trans-Golgi network | 0.00 |
| NM003145.2 | ER translocon, TRAP β subunit* | Regulate the retention of ER resident proteins | 0.00 |
| NM001679.1 | Na+/K+ ATPaseβ subunit* | Non catalytic domain, unknown function | 0.00 |
| NM001677.1 | Na+/K+ ATPase β1 subunit* (2 clones) | Regulate assembly of α/β hetero domain | 0.00 |
| **Protein involved in apoptosis** | | | |
| NM014246.1 | Cadherin EGF LAG G-type receptor 1* | Receptor in cell/cell signaling | e-135 |
| NM030782.2 | Cisplatin resistance related protein | Associated with apoptosis | 2.7 |

**Table 4 BLAST searches of nucleotide sequences from yeast two-hybrid screen of a human kidney cDNA library with the N-terminal kAE1 (Cont.).**

| Accession number | BLAST description | Proposed function | E-value |
|---|---|---|---|
| **Protein degradation** | | | |
| XM841900 | Ubiquitin protein ligase | Protein degradation | 0.00 |
| BC020807 | Proteosome | Protein degradation | 0.00 |
| **Membrane associated proteins** | | | |
| NM001081.2 | Cubilin (2 clones) | Receptor for intrinsic factor B12 complexes | 0.00 |
| XM016625.5 | Voltage anion channel (2 clones) | Channel through mitochondrial membrane | 0.00 |
| NM016121.2 | K channel tetramerization domain | Protein forms a potassium-selective channel | 0.00 |
| NM0014002 | Endothelial G-protein receptor 1* | Regulate differentiation of endothelial cells | 0.00 |
| NM0176575.2 | Protocadherin LKC* | Cell-cell adhesion molecules | 0.00 |
| **Cytoskeleton associated proteins** | | | |
| BC000909.2 | Laminin A* | Mediate attachment and organization of cells | 0.00 |
| BC053572.1 | Actin gamma 1* | Cytoskeleton | 0.00 |
| NM021109.1 | Thymosin β 4* | Organization of the cytoskeleton | 0.00 |
| NM005112.3 | WD repeat Domain 1* | Induced disassembly of actin filaments | e-79 |
| NM0149921 | Dishevelle activator of morphogenesis 1* | Actin binding protein, cytokinesis | 2e -84 |
| BC001554.1 | Integrin-linked kinase* | Mediating focal adhesion targeting | 0.00 |
| AF328728.1 | Vimentin | Regulate intermediate filament protein | 0.00 |
| NM000146.2 | Ferritin (4 clones) | Iron-storage Protein | 0.00 |
| NM001846.1 | Collagen type IV | Constituent of the basement membranes | 0.00 |
| NM001101.2 | β-actin | Cytoskeleton component | 0.00 |
| NM014991.3 | WD repeat and FYVE domain 3* | Target cytosolic protein for degradation | 0.00 |
| **Transcription and translation factors** | | | |
| NM001030055 | RhoGTPase activating protein | Termination step of protein translation | 0.00 |
| AF202445 | dsRNA binding protein | Facilitating interaction with dsRNA | 0.00 |
| BC001633.1 | TU translation elongation factor | Deliver aminoacylated tRNA to the ribosome | 0.00 |
| BC010046.1 | Nuclear factor* | Signal transduction and cell communication | 0.00 |
| NM003110 | Transcription factor SP1 | Constitutive and induced expression of gene | 0.00 |
| NM001402.4 | Translation EF1 α 1 | Required for protein translation | 0.00 |
| AC009321.18 | Poly T | Nuclear pore translocation | 0.00 |
| **Protein involved in carcinoma and undefined function** | | | |
| Z61349.1 | CpG island | Located around the promoters of genes | 0.00 |
| BC004262.1 | Similar to cactin | Interacts with the Drosophila IkappaB protein | 0.00 |
| BC040004.1 | Similar to myeloid/lymphoid | Adenocarcinoma | 0.00 |
| BC040004.1 | Similar to myeloid-linage | Carcinoma | 0.00 |
| BC002989.1 | Human glutamine rich | ND | 0.00 |
| BC035531.6 | Cas-Br-M retroviral transformed sequence | Lineage lymphoma b | 0.00 |

**Table 4 BLAST searches of nucleotide sequences from yeast two-hybrid screen of a human kidney cDNA library with the N-terminal kAE1 (Cont.).**

| Accession number | BLAST description | Proposed function | E-value |
|---|---|---|---|
| **Hypothetical proteins** | | | |
| NM014749.1 | KIAA0586* | Proline rich region | 0.00 |
| BC035980.1 | Clone: 4133024* | Regulation of cytoskeleton | 0.00 |
| AC092038.3 | Chromosome 3 clone RP11-89F18* | ND | 0.00 |
| AC112673.7 | Chromosome 8 clone RP11-212F11* | ND | 0.00 |
| BC012018.1 | Clone IMAGE: 4477559 | ND | 0.00 |
| AC127515.9 | Chromosome 17 clone RP13-6309 | ND | 0.00 |
| AL136093.8 | Chromosome 6 clone RP3-472A9* | ND | 0.00 |
| AL607077.4 | Clone RP11-474I15 | Reverse transcriptase | 0.00 |
| AE003589.3 | Drosophila chromosome 26 | ND | 0.00 |
| NM015936.1 | Similar to tyrosyl-tRNA synthase | ND | 0.00 |
| NM025112.1 | Similar to limonene synthase | Chloroplast precursor | 0.00 |
| NM015328.1 | KIAA0828 | Hydrolyse S-adenosyl-homocystein | e-160 |
| NM004554.2 | Similar to Nuclear factor activated T-cell | Signal transduction in atrial fibrillation | 0.00 |
| AC092755.4 | Conserve TIG domain | Regulation of transcription | 0.00 |
| AP002961.2 | Chromosome 11 clone RP11-2I22 | ND | 0.015 |
| AC021744.14 | Chromosome 8 clone RP11-284H18* | ND | 0.00 |
| NM032889.2 | Clone MGC11308* | ND | 0.00 |
| AC005531.2 | Chromosome 7 clone RP4-701016 | ND | 0.00 |
| AC073578.17 | Chromosome 12 RP11-897M7* | ND | 0.00 |
| AL022345.2 | Chromosome 10 clone XX-Y738F9 | ND | 0.00 |
| AL583783.6 | Alu family | Polymorphisms in the human genome | 0.00 |
| XM037809.3 | KIAA1671 | Similar to tankyrase 1 binding protein | 0.00 |
| BC021670.1 | Clone MGC: 22710 | ND | 0.00 |
| AY274808.1 | KIAA1749 (tropomyosin)* | Muscle protein inhibits contraction of actin | 0.00 |
| AP000769.5 | Chromosome 11 CMB9-22P13 | ND | 0.00 |
| BC010868.1 | FLJ14600 * | Role in membrane sorting in mitochondria | 0.00 |
| XM037797.4 | Clone MGC1842 | ND | 0.00 |
| AC090868.4 | Chromosome 15 clone RP11-795G3 | ND | 0.00 |
| XM086408.4 | KIAA1228 (conserve C2 domain)* | $Ca_2^+$-dependent membrane-targeting module | 0.00 |
| BC039469.1 | Clone IMAGE: 4513453 | ND | e-167 |
| AC073848.4 | Chromosome 4, clone RP11-669M16* | ND | 0.00 |
| AK122583.1 | FLJ00294 | Cytoskeleton associated protein | 4e -94 |
| AC005089.3 | Chromosome 7 clone CTA-315H11 | ND | 0.00 |
| AC139677.4 | Chromosome 7 clone RP11-1070B7* | ND | 0.00 |
| NM033212.1 | Clone LOC92922 | ND | e-110 |
| AK056173.1 | FLJ31611* | ND | 0.00 |

E-value = Expectation value; a low E-value score is a good hit to a model. Asterisks represent proteins selected for specificity test. ND = not determined.

indicated by asterisks in Table 4 were selected for specificity test of protein-protein interaction in yeast.

**7. Specificity test of interaction between the N-terminal kAE1 and putative positive clones in yeast**

To verify interaction between the N-terminal kAE1 and interacting proteins identified from initial yeast two-hybrid screen, the second specificity test was performed by using pair-wise mating method. The plasmids of 35 candidate clones were isolated from yeast and then transformed into *E.coli* DH5α and selected on medium containing ampicillin. All 35 clones carrying the recombinant plasmids pACT2 with cDNA inserted fragments are grown on the selective medium. The isolated plasmids from *E.coli* were re-transformed into yeast strain Y187. In addition, pNkAE1, pGBKT7 vector, pGBKT7-53 and pGBKT7-Lamin C plasmids were transformed into the strain AH109. After that, the Y187 transformed with each candidate clones were mated with either bait (pNkAE1), pGBKT7 vector, pGBKT7-53 or pGBKT7-Lamin C, pre-transformed in the AH109. The true interaction between the N-terminal kAE1 and interacting proteins were analyzed by growth of diploid yeast cells on SD/-Ade/-His/-Leu/-Trp dropout plates containing X-α-Gal and colony filter lift assay used for assay β-galactosidase activity (LacZ reporter). It was found that only 9 clones from 35 independent clones (Table 4) namely giantin (accession number NM004487.1), GAPDH (accession number BC014085.1), laminin A (accession number BC000909.2), pantophysin (accession number BC020938), ILK (accession number BC001554.1), thymosin β4 (accession number NM021109.1) and three unknown functional hypothetical proteins named A24, B61 and C57 (accession numbers: AC139677.4, AC073848.4 and AC073578.17, respectively) showed very strong blue colonies on SD/-Ade/-His/-Leu/-Trp containing X-α-Gal when mating with pNkAE1. However, some of them also showed faint blue colonies when mating with pGBKT7, or pGBKT7-Lamin C (Figure 21). In addition, Figure 22 showing the results from colony lift assay were more reliable because they showed strong blue colonies when mating GAPDH, pantophysin, ILK and thymosin β4 with pNkAE1 while no background when mating with pGBKT7, pGBKT7-53 or pGBKT7-Lamin C.

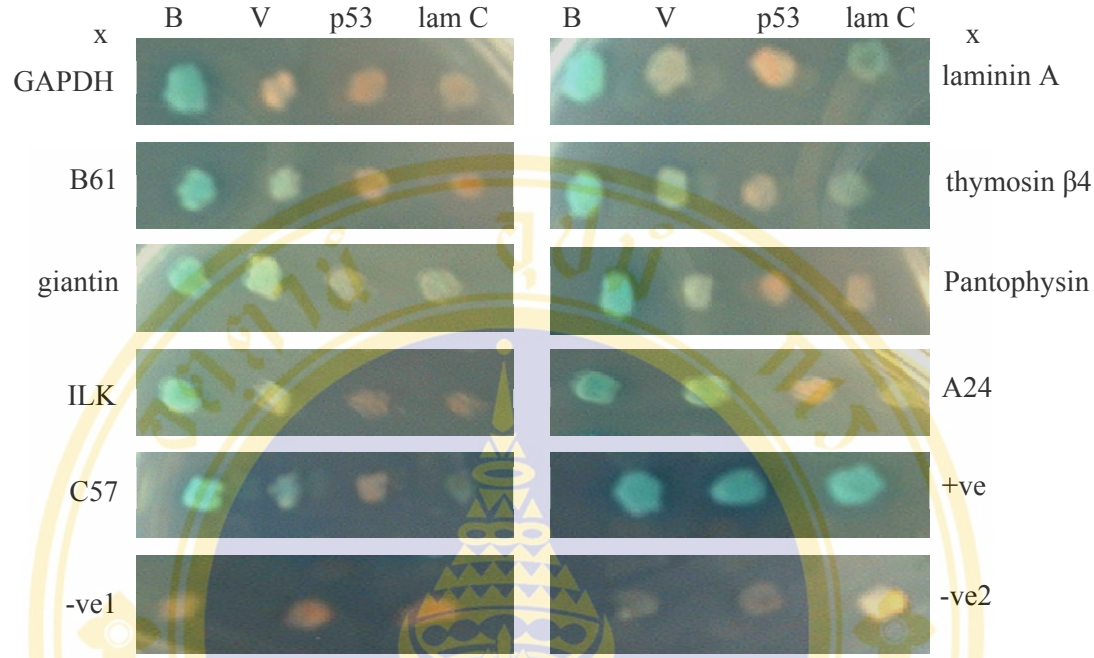


**Figure 21 Specificity test of interaction between the N-terminal kAE1 and putative positive clones in yeast on SD/-Ade/-His/-Lue/-Trp/ X-α-Gal.** Growth of diploid yeast cells on SD/-Ade/-His/-Lue/-Trp/ X-α-Gal when yeast Y187 transformed with positive clones named GAPDH, giantin, ILK, laminin A, pantophysin, thymosin β4, hypothetical proteins (A24, B61 and C57) were mated with either pNkAE1 (B), pGBKT7 (V), pGBKT7-53 (p53) or pGBKT7-Lamin C (lam C), retransformed in the AH109.

"+ve" is yeast mating between pGBKT-53 and pTD1-1 (positive control).

"-ve1" is yeast mating between pNkAE1 and pTD1-1 (negative control).

"-ve2" is yeast mating between pGBKT7 and pTD1-1 (negative control).

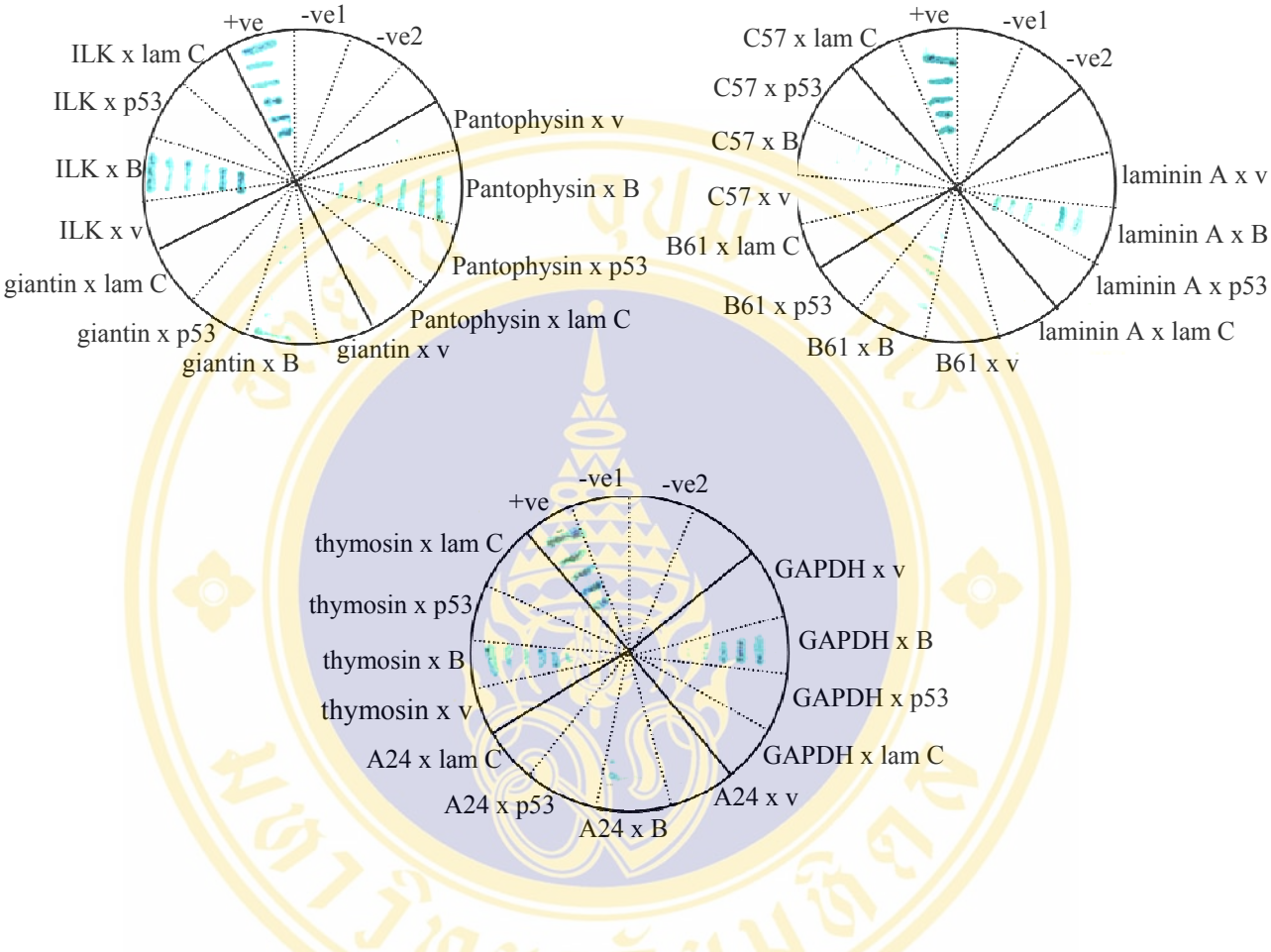


**Figure 22 Interaction of N-terminal kAE1/ positive clones by colony lift assay.**

Diploid yeast colonies of positive clones named GAPDH, giantin, ILK, laminin A, pantophysin, thymosin β4, hypothetical proteins (A24, B61 and C57) mating with pNkAE1 (B), pGBKT7 (V), pGBKT7-53 (p53) or pGBKT7-Lamin C (lam C) were lifted from SD/-Ade/-His/-Lue/-Trp plates by using filter papers and presoaked in Z buffer/ X-Gal solution and then checked for the appearance of blue colonies by expression of LacZ reporter.

"+ve" is yeast mating between pGBKT-53 and pTD1-1 (positive control).

"-ve1" is yeast mating between pNkAE1 and pTD1-1 (negative control).

"-ve2" is yeast mating between pGBKT7 and pTD1-1 (negative control).

Sequencing results also showed these positive clones revealed the sequences encoding in frame fusion protein of GAPDH, pantophysin, ILK and thymosin β4 with GAL4-activation domain presented in pACT2 vector. Therefore, GAPDH, pantophysin, ILK and thymosin β4 were proposed to be proteins interacting with the N-terminal kAE1.

**Part II: Interactions between kAE1 and interacting proteins in transfected human embryonic kidney (HEK 293) cells**

**8. Construction of recombinant plasmids encoding full-length human kAE1 and interacting proteins**

To construct the recombinant plasmid encoding human full-length kAE1 with hemagglutinin (HA) epitope tag at the C-terminus, pcDNA 3/kAE1 plasmid was used as template in PCR reaction using specific primers named kAE1HindIII and kAE1XhoI (Table 2). The sequences encoding for HA tag were used for introducing at the 3' end of the inserted fragment. The agarose gel electrophoresis showed an amplified fragment of 2.5 kb as expected. The amplified products digested with *Hind*III and *Xho*I were inserted to *Hind*III/*Xho*I digested pcDNA 3.1 (+) vector. The ligation mixture was transformed into *E.coli* DH5α and transformants were selected on LB plate containing 100 μg/ml of ampicillin. Restriction endonuclease analysis of recombinant clones with *Hind*III and *Xho*I was performed to screen for the presence of cDNA insert in these recombinant plasmids. As expected, the result showed two fragments of digested DNA corresponding to 5.4 kb of pcDNA 3.1 and 2.5 kb of full-length kAE1 (Figure 23A). Insert sequences of three recombinant clones were verified by automated sequencing and the results showed that all of them did not carry any mutation. This recombinant plasmid served as wild type kAE1 with HA-tagged at the C-terminus. It was named pkAE1.

In the meantime, kidney specific isoform of kAE1 interacting proteins, GAPDH, ILK, pantophysin and thymosin β4 were designed to test interaction with kAE1 in this study. At the beginning, full-length cDNAs coding sequences of GAPDH (accession number BC014085.1), ILK (accession number BC001554.1), pantophysin (accession number BC020938) and thymosin β4 (accession number NM021109.1) were searched from NCBI database and the coding sequences were used for primers design to amplify GAPDH, ILK, pantophysin and thymosin β4. The result from BLAST search

indicated that the positive clones obtained carrying full-length of pantophysin cDNA. Therefore, the primers were designed to amplify the full-length fragment (Table 2). The other three positive clones carrying only partially sequences of cDNA fragment. To clone the full-length of the three cDNAs from human kidney, cDNA derived from human kidney was initially generated using oligo dT primer. The cDNA was then used as templates to generate the fragments corresponding to GAPDH, ILK, and thymosin β4 by using nested PCR. The amplified fragments of GAPDH and ILK with *EcoR*I and *Xho*I, pantophysin with *EcoR*I and *Xba*I and thymosin β4 with *BamH*I and *EcoR*I, sites were digested with respect restriction enzymes and inserted into corresponding sites of pcDNA 3.1/His B vector to generate poly-histidine tag (His-tag) at the N-terminus of the proteins. Restriction enzyme analysis was used to screen the recombinant plasmid by using the same restriction enzymes used for DNA cloning. The results showed two fragments of DNA corresponding to 5.5 kb of pcDNA 3.1/His B and the inserts at 1.35 kb of ILK (Figure 23B, lanes 1-4), 1 kb of GAPDH (lanes 5-9), 0.72 of pantophysin (lanes 10-14) and 0.16 of thymosin β4 (lanes 15-19). The inserted cDNAs were verified by automated sequencing and the recombinant plasmids were named pGAPDH, pILK, pPanto and pThymosin. These plasmids were used to verify protein expression in HEK 293 cells.

**9. Human kAE1 and interacting proteins expressed in transfected HEK 293 cells**

To examine the expression of kAE1 and interacting proteins (GAPDH, ILK, pantophysin and thymosin β4), pkAE1, pGAPDH, pILK, pPanto and pThymosin were transfected in HEK 293 cells using standard calcium phosphate method as described in Materials and Methods. Cell lysates of HEK 293 cells transfected with either kAE1, GAPDH, ILK, pantophsin or thymosin β4 were prepared. Immunoblots of cell lysate from kAE1 showed robust protein expression at molecular weight 96 kDa as expected using anti-HA antibody against HA-tagged at the C-terminus of the protein (Figure 24, lane 2). In addition, highly expression of GAPDH (lane 4), ILK (lane 5), pantophysin (lane 6) and thymosin β4 (lane 7) were appeared at molecular weight 33 kDa, 51 kDa, 28 kDa and 15 kDa, respectively, detected by using anti-His antibody against His-tagged at the N-terminus of these proteins. The faint upper bands of the proteins came from nonspecific binding of anti-His antibody which also could be detected in cell

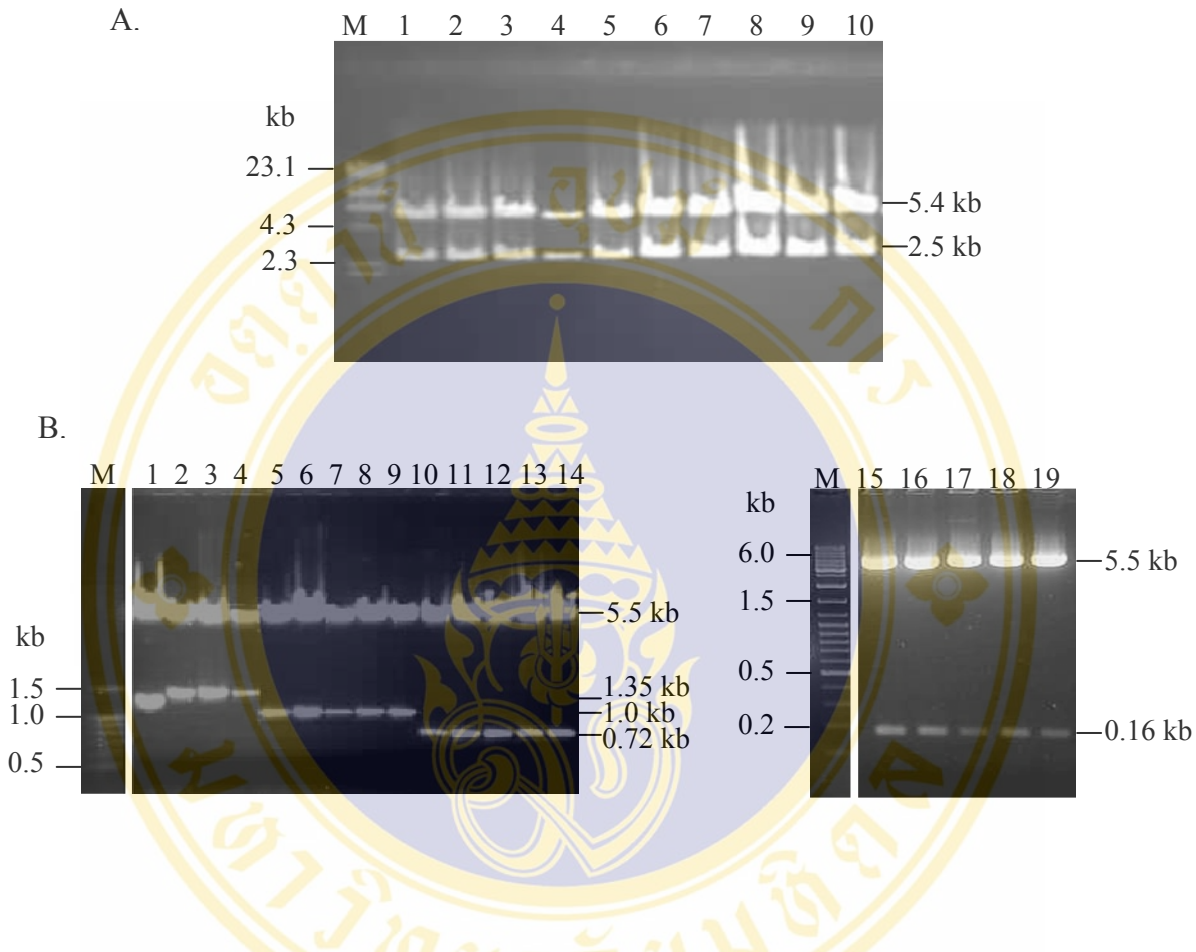


**Figure 23 Restriction endonuclease analysis of full-length kAE1 and interacting proteins.**

Restriction endonuclease digestions of recombinant plasmids containing kAE1 and interacting proteins (ILK, GAPDH, pantophysin and thymosin β4) were analyzed by agarose gel electrophoresis.

A. Lanes 1-10 were pkAE1 containing full-length kAE1 digested with *Hind*III and *Xho*I.

B. Lanes 1-4 were *EcoR*I/*Xho*I-digested pILK (integrin-linked kinase), lanes 5-9 were *EcoR*I/*Xho*I-digested pGAPDH (glyceraldehyde -3-phosphate dehydrogenase), lanes 10-14 were *EcoR*I/*Xba*I-digested pPanto (pantophysin) and lanes 15-19 were *BamH*I/*EcoR*I-digested pThymosin (thymosin β4). Lane M is λ-*Hind*III digested DNA marker.

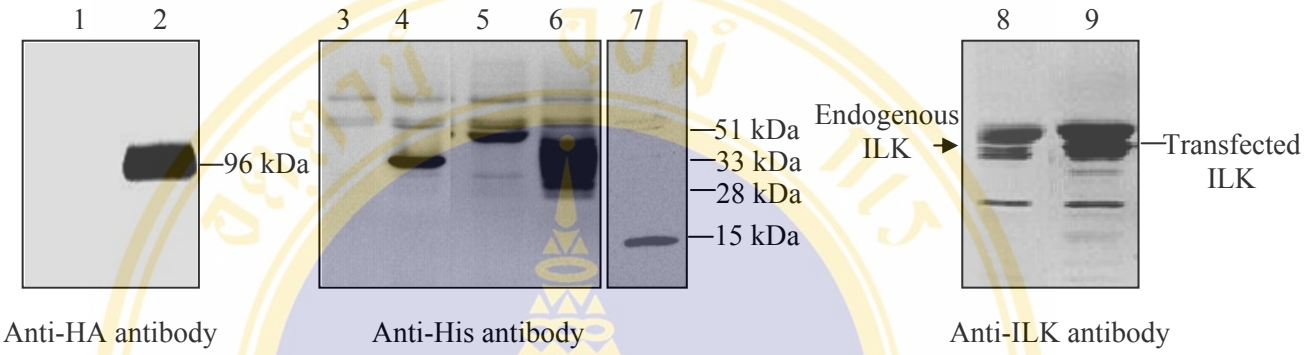


**Figure 24 Human kAE1 and interacting proteins expressed in transfected HEK 293 cells.**

HEK 293 cells transfected with either 1.6 µg of HA-tagged kAE1 (lane 2) or 2.0 µg of His-tagged interacting proteins (GAPDH (lane 4), ILK (lanes 5 and 9), pantophysin (lane 6) and thymosin β4 (lane 7)) were lysed with 2x SDS-PAGE sample loading buffer and subjected to 10% SDS-PAGE and immunoblotting. Blots were probed with anti-HA, anti-His and anti-ILK antibodies for kAE1, interacting proteins and ILK detection, respectively. Lanes 1, 3 and 8 are untransfected cells probed with anti-HA and anti-His and anti-ILK antibodies, respectively.

lysate of untransfected HEK 293 cells (lane 3). Pantophysin is highly glycosylated membrane protein; thus, it showed the broad band of protein expression [183] while thymosin β4 expression was detected at molecular weight larger than the previously report (5.4 kDa) [218] because of His-tagged. Using anti-ILK antibody, the transfected ILK was expressed 4-fold higher than endogenous ILK (lane 9).The upper and lower bands of 51 kDa appeared as nonspecific binding of antibody. These results suggested that pkAE1, pGAPDH, pILK, pPanto and pThymosin constructs expressed the proteins of interest efficiently in transfected HEK 293 cells.

**10. Physical interaction between kAE1 and interacting proteins**

In order to verify the interaction between kAE1 and its interacting proteins identified in yeast two-hybrid screen, co-immunoprecipitation experiments were performed using HEK 293 cells either co-transfected with kAE1 and ILK (or GAPDH, pantophysin, thymosin β4) or transfected with kAE1 alone. The mild lysis solution containing 0.5% Nonidet P-40 and 0.15 M NaCl was used to solubilize the HEK 293 cells for preserving interaction of kAE1 and its interacting proteins. Anti-His monoclonal antibody was used to precipitate His-tagged ILK (or GAPDH, pantophysin, thymosin β4) from the cell lysate of transfected HEK 293 cells. The presence of kAE1 in the immunoprecipitates was determined by immunoblotting using anti-HA antibody (Figure 25). The results showed that kAE1 precipitation was dependent on the expression of either ILK (Figure 25A), pantophysin (Figure 25B) GAPDH (Figure 25C). kAE1 was not detected in immunoprecipitate when co-expressing with thymosin β4 depite this interaction was detected in yeast (Figure 25D). The possibility is that the differences of protein biosynthesis in yeast and human cells might slightly change the structure of thymosin β4 in different species which would alter protein-protein interaction. Thus, co-immunoprecipitation results indicated that ILK, GAPDH and pantophysin associated with kAE1 in transfected HEK 293 cells.

**11. Affinity co-purification of kAE1 and interacting proteins**

To further verify the specificity of interaction between kAE1 and its interacting proteins, affinity co-purification using $Co^{2+}$ resin was also carried out. N-terminal

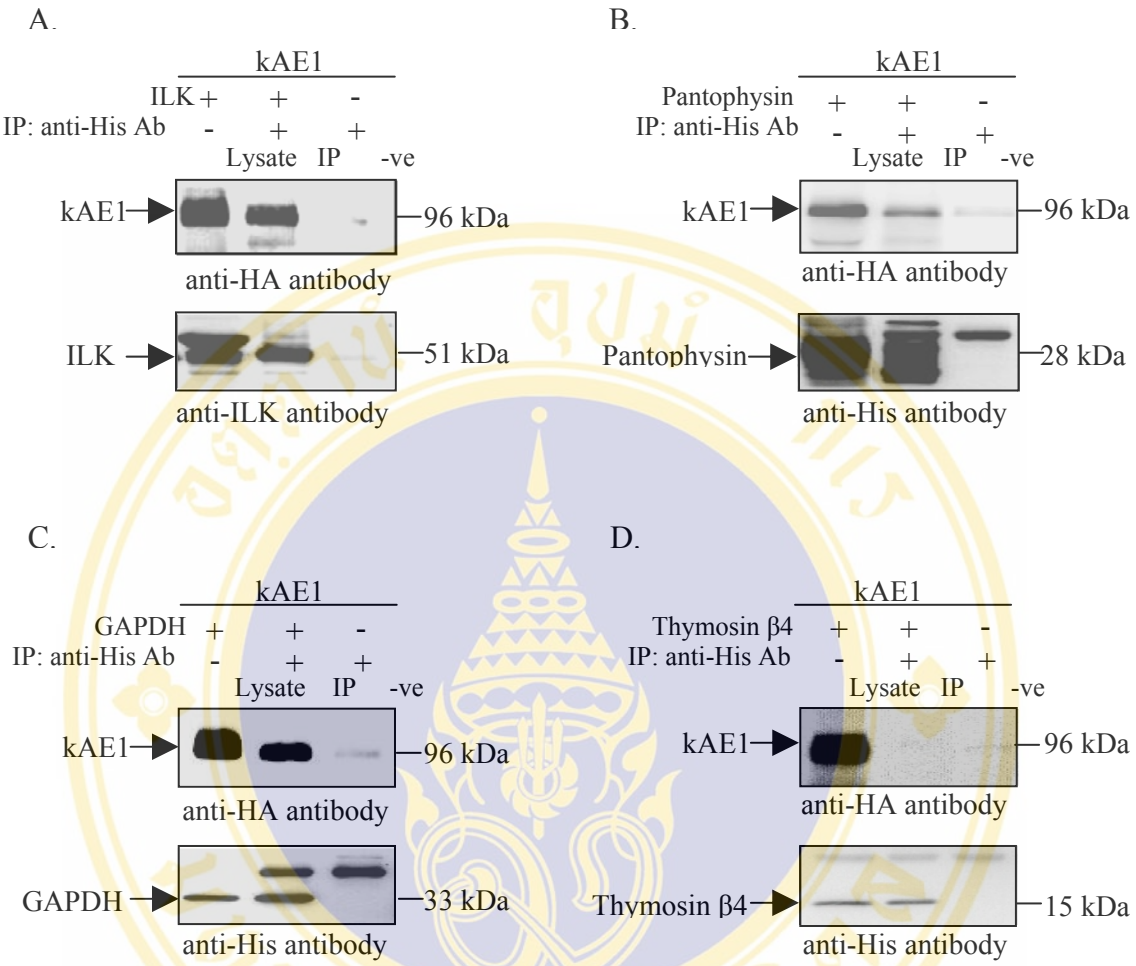


**Figure 25 Co-immunoprecipitation of kAE1 with interacting proteins in HEK 293 cells.**

HEK 293 cells were transfected with kAE1 alone or co-transfected with kAE1 interacting proteins (ILK (A), pantophysin (B), GAPDH (C) and thymosin β4 (D)) as indicated. Cell lysates were either set aside for later analysis (Lysates), or immunoprecipitated with anti-His antibody (IP). Cell lysates expressing kAE1 were also subjected to immunoprecipitation with anti-His antibody (-ve). Samples were subjected to SDS-PAGE and immuno blotting. Blots were probed for kAE1, using anti-HA antibody and for ILK with anti-ILK antibody while pantophysin, GAPDH and thymosin β4 were detected by anti-His antibody.

poly-histidine-tagged ILK (or GAPDH, pantophysin) was co-expressed with kAE1 or kAE1 expressed alone in HEK 293 cells. The complex of His-tagged ILK, GAPDH and pantophysin with kAE1 was purified by using $Co^{2+}$ resin, which binds proteins containing poly-histidine. The protein complex was then eluted from resin with high concentrations of imidazole containing buffer. As expected, kAE1 could be detected in the eluent using anti-HA antibody when co-expressed with ILK, GAPDH or pantophysin (Figure 26). ILK, GAPDH and pantophysin were also detected in the bound fractions using anti-His antibody. HA-tagged kAE1 did not bind to $Co^{2+}$ resin. Thus, no band was detected by anti-HA antibody (Figure 26, lane 3). These results demonstrated that ILK, GAPDH and pantophysin interacted specifically with kAE1, as supported by co-immunoprecipitation and His tagged co-purification assays.

**12. Localization of kAE1 and interacting proteins**

Localization of kAE1 and its interacting proteins were investigated by using immunofluorescence studies. HEK 293 cells were co-transfected with kAE1 plus either ILK, GAPDH or pantophysin while LLC-PK1 cells were transfected with kAE1 alone. Antibody against HA-tagged was used to detect kAE1 whereas anti-His antibody was used to detect His-tagged ILK, GAPDH and pantophysin in transfected HEK 293 cells. Cross-reaction of anti-HA and anti-His antibodies with untransfected HEK 293 cells was not detected. Expression of kAE1 and endogenous ILK in LLC-PK cells was labeled with anti-AE1 and anti-ILK antibodies, respectively. The confocal images showing pantophysin as fluorescent green-colored was located largely in cytoplasm particularly endoplamic reticulum and near the plasma membrane (Figure 27A). Co-localization of kAE1 and pantophysin was predominantly in intracellular compartments but small proportion kAE1 was co-localized with pantophysin observed at plasma membrane (Figure 27A). GAPDH co-localized with kAE1 was also observed in intracellular region (Figure 27B). Pantophysin and GAPDH interact with kAE1 might be involved in the regulation of kAE1 translocation between compartments in transfected HEK 293 cells. Although, ILK was stained in cytoplasm, co-localization of ILK and kAE1 was detected mainly at the plasma membrane of transfected HEK 293 cells (Figure 27C), implying ILK involved in kAE1 trafficking. This hypothesis was supported when endogenous ILK in LLC-PK1

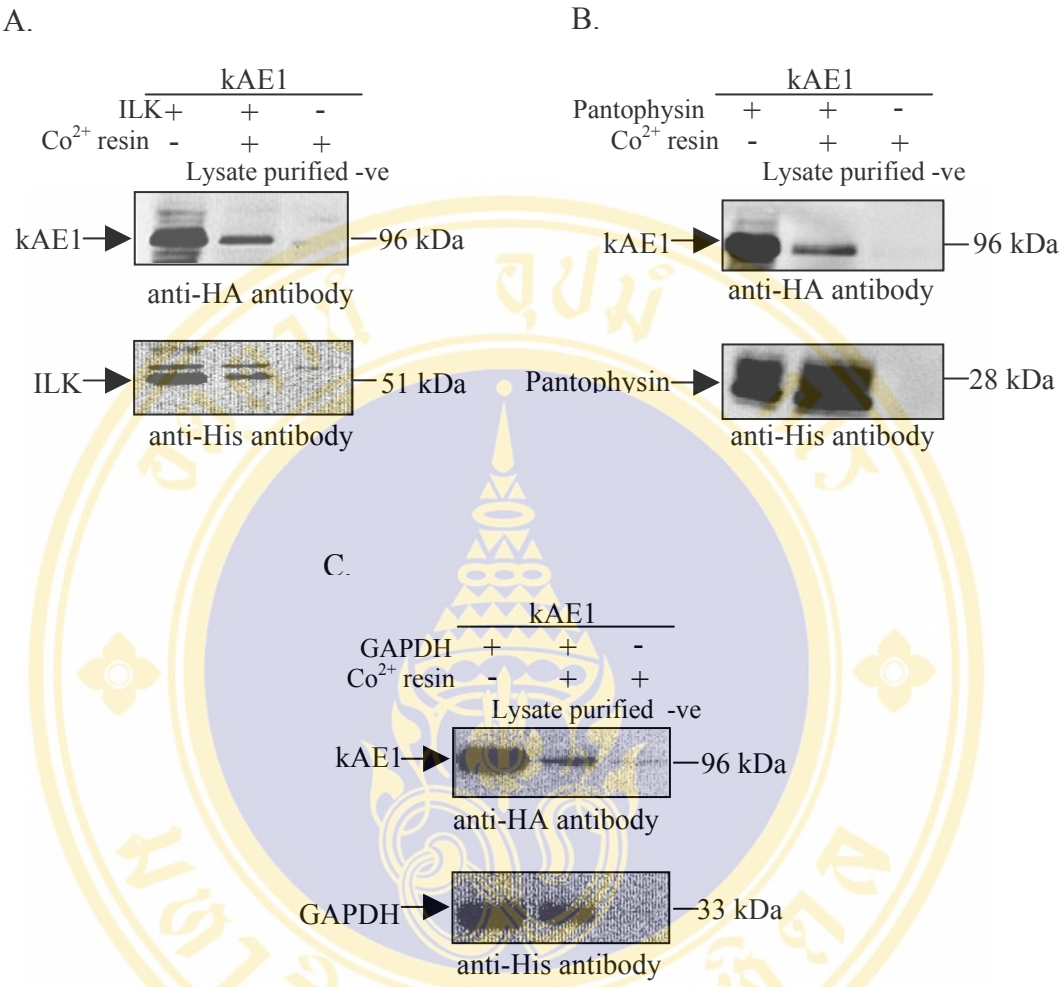


**Figure 26 Affinity co-purification of kAE1 and interacting proteins.**

HEK 293 cells were transiently transfected with HA-tagged kAE1 alone or co-transfected with His-tagged ILK (A), Pantophysin (B), or GAPDH (C) as indicated. Cell lysates were either set aside for later analysis (lysates), or incubated with $Co^{2+}$ affinity resin at 4 $^{\circ}$C (purified). Cell lysates from cells expressing kAE1 alone was also purified by $Co^{2+}$ affinity resin (-ve). Samples were subjected to SDS-PAGE and immunoblotting. Blots were probed with anti-HA and anti-His antibodies to detect kAE1 and ILK (pantophysin or GAPDH), respectively.

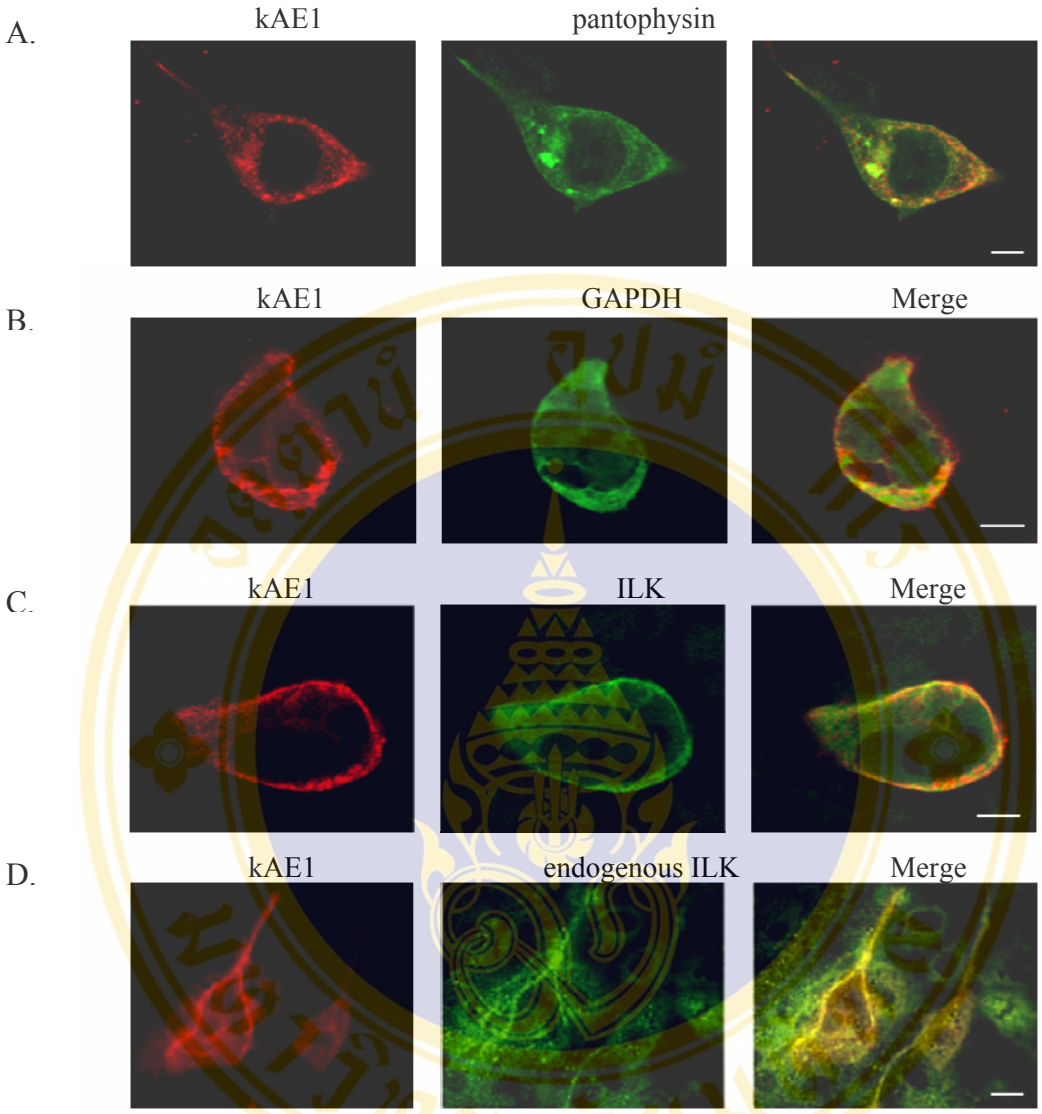


**Figure 27 Co-localization of kAE1 with pantophysin, GAPDH and ILK.**

Confocal images of HEK 293 cells co-expressing kAE1 with pantophysin (A), GAPDH (B) or ILK (C) and LLC-PK1 cells expressing kAE1 and endogenous ILK (D) as indicated. HEK 293 cells co-transfected with pantophysin, GAPDH or ILK and kAE1 were stained with anti-His and anti-HA antibodies. LLC-PK1 cells were stained with the mixture of anti-ILK antibody and anti-AE1 antibody for endogenous ILK and kAE1 detection. Cy3-conjugated goat anti-rabbit and FITC-conjugated rabbit anti-mouse antibodies were used to visualize kAE1 and pantophysin or GAPDH or ILK, respectively. Zeiss LSM 510 confocal microscopy was used to capture the images. Bar = 10 μm.

cells was stained mainly in intracellular and peri-nuclear regions, but it could be detected at cell surface of kAE1 transfected LLC-PK1 cells. Moreover, ILK co-localized with kAE1 particularly at the plasma membrane as shown in yellow fluorescent (Figure 27D), suggested that ILK was possibly coincident directed and trafficked to the cell surface via interacting with kAE1.

**13. Effect of interacting proteins on cell surface expression of kAE1**

To examine whether the over-expression of ILK, GAPDH or pantophysin (PPH) affect the cell surface expression of kAE1 in HEK 293 cells, cell surface biotinylation was performed as described in the Materials and Methods. HEK 293 cells transfected with kAE1 alone or kAE1 plus interacting proteins (ILK, GAPDH or pantophysin) were treated with a membrane impermeable biotinylating reagent. The biotinylated kAE1 proteins were bound to streptavidin resin and eluted from the resin by sample loading buffer containing 2% 2-mercaptoethanol to break disulfide bond. Unfortunately, the amount of kAE1 in the biotinylated fraction could not be detected by anti-HA antibody because the biotinylated kAE1 is eluted very poorly from streptavidin resin as noted previously [75, 88, 219]. The result showed that a reduction in the amount of protein in the unbound fraction relative to the total fraction of kAE1 in the presence of ILK was clearly evident compared with kAE1 while GAPDH and pantophysin were not (Figure 28A). By using the difference in the amount of kAE1 in the supernatant (lanes U) and total (lanes T) fractions, percentage of biotinylated kAE1 located on cell surface was calculated with respect to comparable band densities by using (T-U/ T) x 100%. The remainder was unlabeled and is interpreted as located within the cells. Data was corrected for differences in loading by probing blots for actin. HEK 293 cells expressing kAE1 alone was represented as 100% and compared to kAE1 co-expressed with interacting proteins. Thus, the percentage of cell surface expression was calculated to be 32 ± 7% kAE1, 31± 7% kAE1 plus pantophysin, 50 ± 7% kAE1 plus ILK and 33 ± 3% kAE1 plus GAPDH (mean ± S.D, n = 4). Figure 28B shows cell surface expression of kAE1 was increased by 56% in the presence of ILK transfected in HEK 293 cells. Cytosolic yellow fluorescent protein (YFP) in transfected cells was used as a control for the

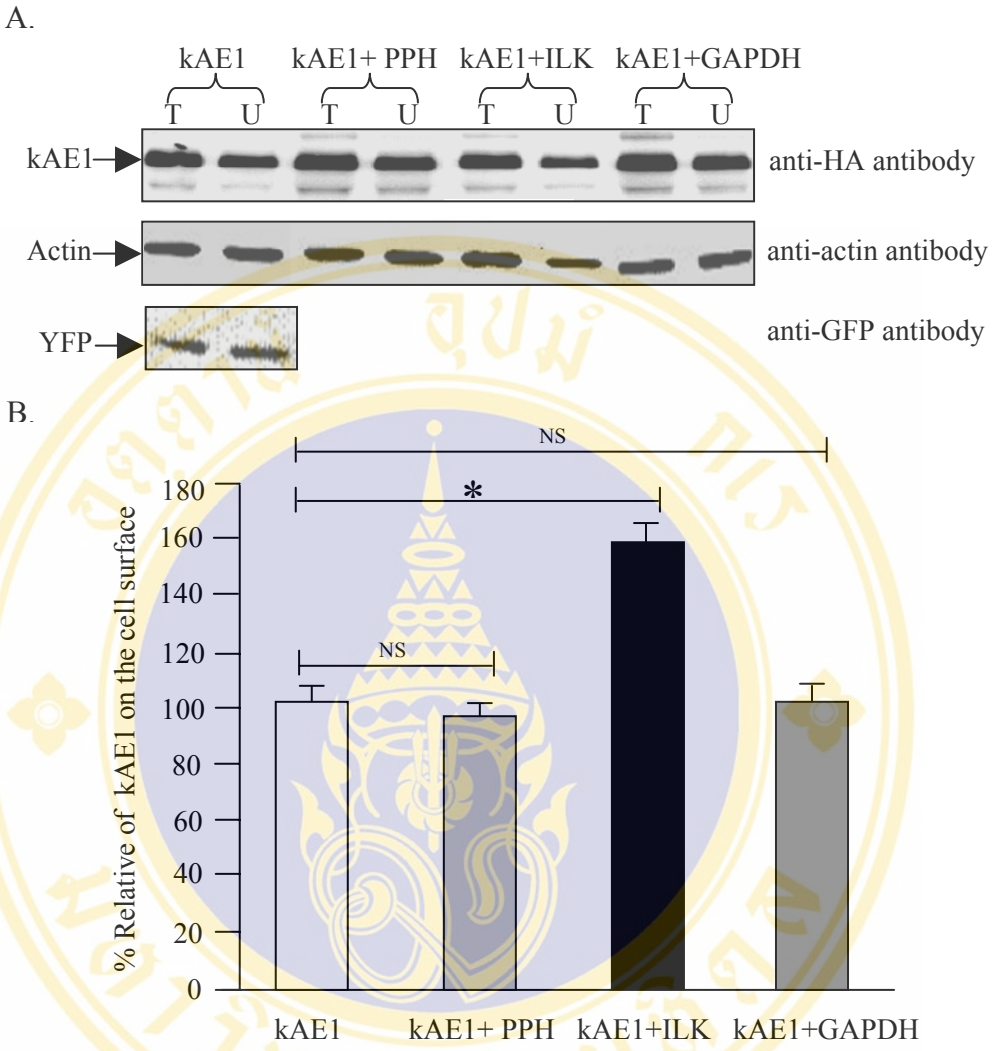


**Figure 28 Effect of interacting proteins on processing of kAE1 to the cell surface of HEK 293 cells.**

A. Immunoblotting using anti-HA antibody for kAE1 detection shows the amount of protein expression in total kAE1 fraction (T), kAE1 not bound to streptavidin beads (U). Actin was used as an internal control to verify protein expression while YFP used as a negative control to assess the degree of access of the biotinylation reagent to the cytosol. PPH is pantophysin.

B. Quantification of kAE1 expressed on the cell surface, normalized to the fraction of kAE1 expressed alone. The error bar shows mean ± S.D. with n = 4. Asterisk indicates significant difference ($p<0.05$), unpaired t-test. NS indicates no significantly difference between partners tested.

spurious biotinylation of cytosolic protein. YFP was biotinylated to an extremely low (0.009 ± 2%, mean ± S.D, n = 4), indicating that the cell surface biotinylation protocol indentified cell surface protein only. Actin was used as an internal control to monitor protein expression. Expression of actin in each lane should be the same according to equal amount of protein loading. However, a reduction of actin was observed in unbound fraction of kAE1 when co-expressed with ILK while it did not change when co-expressed with GAPDH, pantophysin or expressed kAE1 alone (lanes U), implying that actin might be recruited to associate with kAE1 via interacting with ILK. These results indicated that the cell surface expression of kAE1 was increased in the presence of ILK, but GAPDH and pantophysin did not affect kAE1 cell surface expression.

As mentioned previously, the mechanism by which kAE1 traffics to the cell membrane has not been identified. Interestingly, ILK was shown in this study to specifically interact with kAE1 and played a role in facilitating kAE1 movement to the cell surface in HEK 293 cells. Although GAPDH and pantophysin did associate with kAE1, both proteins had no effect on the cell surface expression of kAE1 (Figures 25, 26, 27 and 28). This raises the possibility that ILK might be a key protein involved in the enhancement of kAE1 transport to the plasma membrane in human kidney cells. Therefore, the detailed analysis of interaction between kAE1 and ILK was performed as shown below.

**Detail analysis of interaction between kAE1 and ILK**

**14. Identification of kAE1 binding site in ILK**

To determine the ILK region interacting with kAE1, co-immunoprecipitation was performed by using ILK mutants (Figure 29A). ΔNtILK is deletion mutant lacking amino acids 1-192 including ankyrin repeats and PH domain at the N-terminus, necessary for localization of ILK to focal adhesion [220]. HEK 293 cells were co-transfected with kAE1 and ΔNtILK or tranfected with kAE1 alone. The lysate was then incubated with anti-His antibody to precipitate His-tagged ΔNtILK. ΔNtILK bound to kAE1 efficiently (Figure 29B), indicating that the C-terminal catalytic domain of ILK is sufficient for kAE1 binding. The upper band (lane 1) was

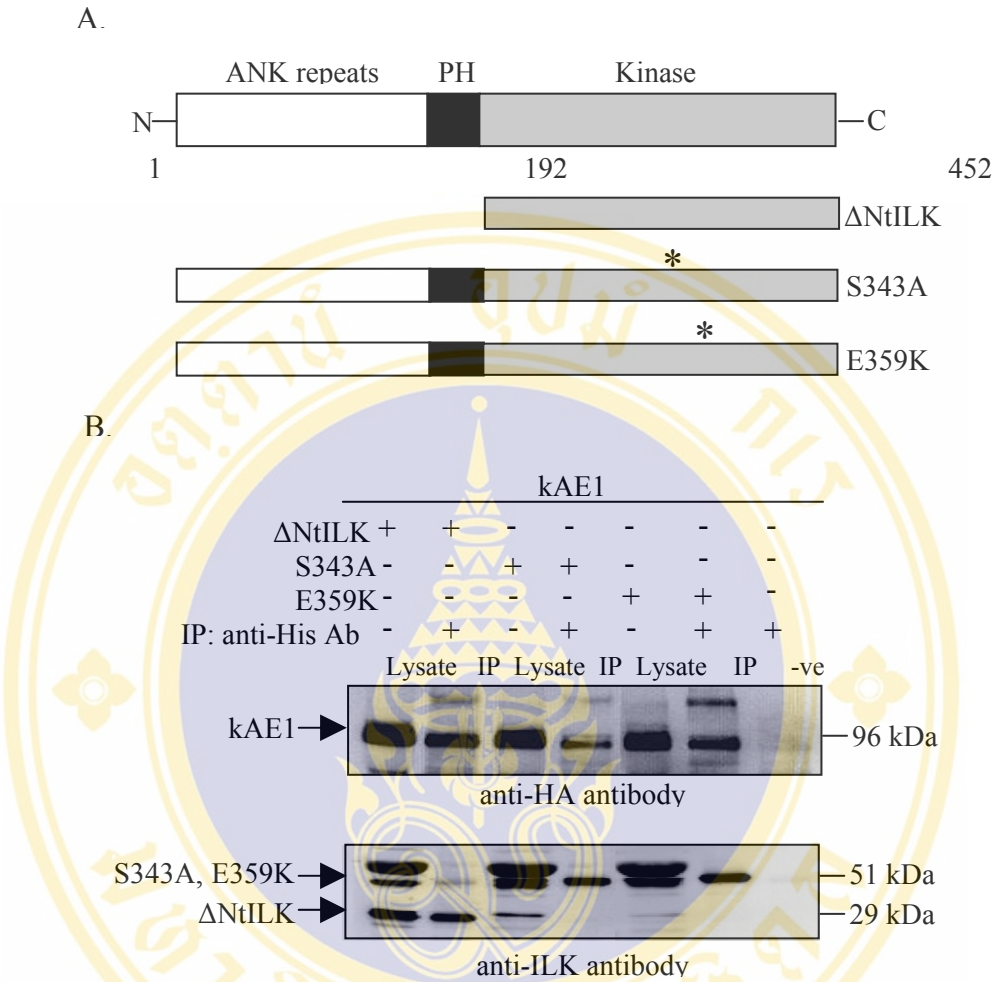


**Figure 29 Identification of the kAE1 binding domain in ILK.**

A. The structure of human ILK includes ankyrin repeats and plecktrin homology domain (PH) at the N-terminus (residues 1-192) and the C-terminal kinase activity domain (residues 193-452). ΔNtILK is a construct deleted of amino acids 1-192. S343A and E559K are kinase-dead point mutants of ILK. Asterisks represent the mutated ILK positions.

B. The interaction of HA-tagged kAE1 with His-tagged ILK mutants was examined by co-immunoprecipitation assay in HEK 293 cells. Cell lysates were prepared and directly analysed (lysate) or subjected to immuno precipitation with anti-His antibody (IP). Samples were immunoblotted and probed with anti-HA antibody (to detect HA-kAE1) or anti-ILK antibody, as indicated.

non-specific binding of protein to anti-ILK antibody in cell lysate but this band was not shown in immunoprecipitate (lane 2). The role of ILK kinase activity in biological function is unclear. In at least two cases catalysis by ILK is needed for ILK interaction with antoher protein; S343A ILK lacks kinase activity and is unable to mediate interaction with 3-phosphoinositide-dependent kinase (PDK) [185, 221]. Similary, the E359K mutation of ILK yields a kinase-dead mutant with impaired binding to paxillin and focal adhesion targets [191]. To examine the role of ILK's kinase activity in kAE1 binding, co-immunoprecipitation was carried out by using cells co-expressing kAE1 with S343A or E359K ILK, or expressing kAE1 alone. Both catalytically-dead ILK mutants retained ability to bind kAE1 (Figure 29B). The bands at position corresponding to molecular weight smaller than 51 kDa and higher than 29 kDa at the bottom are non-specific (lanes 3 and 5). However, these bands disappeared in immunoprecipitate (lanes 4 and 6). The results showed that the C-terminus of ILK is sufficient to bind kAE1, yet kinase activity of ILK is not necessary for the interaction.

However, the effect of the N-terminal ILK and kinase activity were also investigated whether they play a role in cell surface processing of kAE1. Cell surface biotinyation of kAE1 when co-expressed with ILK wild-type or ΔNtILK or S343A ILK mutants was determined as previously described in result section 13 (Figure 30A). The percentage of cell surface expression was calculated to be 33 ± 5% kAE1, 49 ± 6% kAE1 plus ILK, 48 ± 5% kAE1 plus ΔNtILK and 46 ± 3% kAE1 plus S343A ILK (mean ± S.D, n = 6). Figure 30B shows co-expression of either ΔNtILK or S343A ILK could increase cell surface expression of kAE1 as well as wild type ILK. Reduction of actin was also observed in unbound fraction of kAE1 when co-expressed with ΔNtILK or S343A ILK (lanes U). These results indicated that the ankyrin repeats and PH domain at the N-terminus and kinase activity at the C-terminus of ILK are not required for processing of kAE1 to the cell surface.

**15. Calponin homology (CH)-like domain found in the N-terminal kAE1 is a binding domain for ILK**

The C-terminal domain of ILK contains the binding sites for β-integrins, and cytoplasmic adaptor proteins named actopaxin (α-parvin), affixin (β-parvin) and

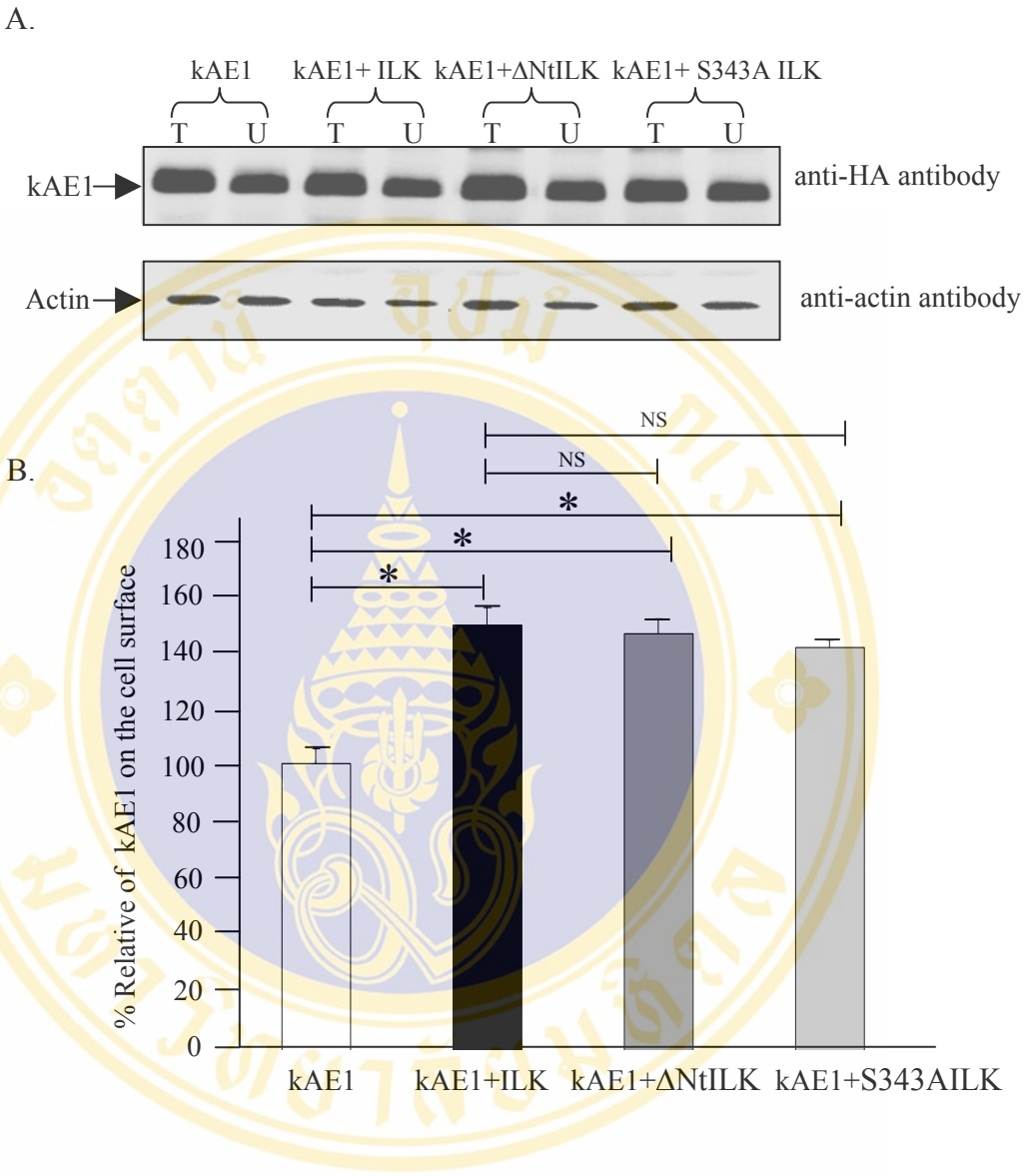


**Figure 30 Effect of ankyrin repeats, PH domain and kinase activity of ILK on cell surface processing of kAE1.**

A. Immunoblotting using anti-HA antibody for kAE1 detection shows the amount of protein expression in total kAE1 fraction (T), unbound kAE1 (U) when co-expressed with ILK, ΔNtILK or S343A ILK. Actin was used as an internal control to verify protein expression.

B. Quantification of kAE1 expressed on the cell surface, normalized to the fraction of kAE1 expressed alone. The error bar shows mean ± S.D. with n = 6, unpaired t-test. Asterisk indicates significant difference ($p<0.05$). NS indicates no significantly difference between partners tested.

paxillin [189, 222]. Actopaxin and affixin interact with ILK via their calponin homology (CH) domains. These CH domains mediate the connection of ILK to the actin cytoskeleton [191, 223]. Since kAE1 interacts with the C-terminus of ILK, it led to the question whether kAE1 similarly contains a CH domain. Sequence alignment of the N-terminal region of kAE1 (NM_000342) and proteins containing CH domains, calponin (AK223234.1), β-spectrin (NP_842565), was performed by multiple sequence alignment, using ClustalW software. Because sequences encoding CH domain are variable among proteins and species, it is not surprised that the result of alignment showed low similarity among proteins. However, a portion of the N-terminal region of kAE1 (residues 27-189) did align convincingly with other CH domains (Figure 31A). Whether the homology is reflected at the three-dimensional level was also examined. The crystal structure of the CH domain from spectrin was compared to the crystal structure for amino acids 27-189 of kAE1 (Figure 31B and 31C). The kAE1 structure is derived from the structure for eAE1 [4]. The predicted CH domain in the N-terminal domain of kAE1 looked similar to CH domain in spectrin, particularly at the N-terminus of the domain that known to be necessary for binding ability [224-226]. To test whether the putative CH domain identified in kAE1 forms the binding site for ILK, cDNA encoding amino acids 27-189 of kAE1CH-like domain was cloned into pcDNA 3.1 (+) vector. The kAE1 CH-like domain was expressed with a C-terminal HA-epitope tag. Co-immunoprecipitation experiment was carried out using the lysate from HEK 293 cells co-expressing the kAE1 CH-like domain, with ILK or alone. The result showed anti His-antibody could bring down CH domain when co- expressed with His-tagged ILK (Figure 32), but not when the kAE1 CH-like domain was expressed alone (Figure 32). This suggests that a previously unidentified CH domain (residues 27-189) in the N-terminal domain of kAE1 mediated the interaction with ILK.

**16. Interaction between erythrocyte anion exchanger 1 (eAE1) and ILK**

kAE1 is identical to eAE1 except it lacks the first 65 amino acids at the N-terminus. kAE1 does not interact with the proteins that interact with the N-terminal domain of eAE1 [10, 11], which might be caused by alteration of protein structure. However, results above demonstrated that the CH domain (residues 27-189) found in

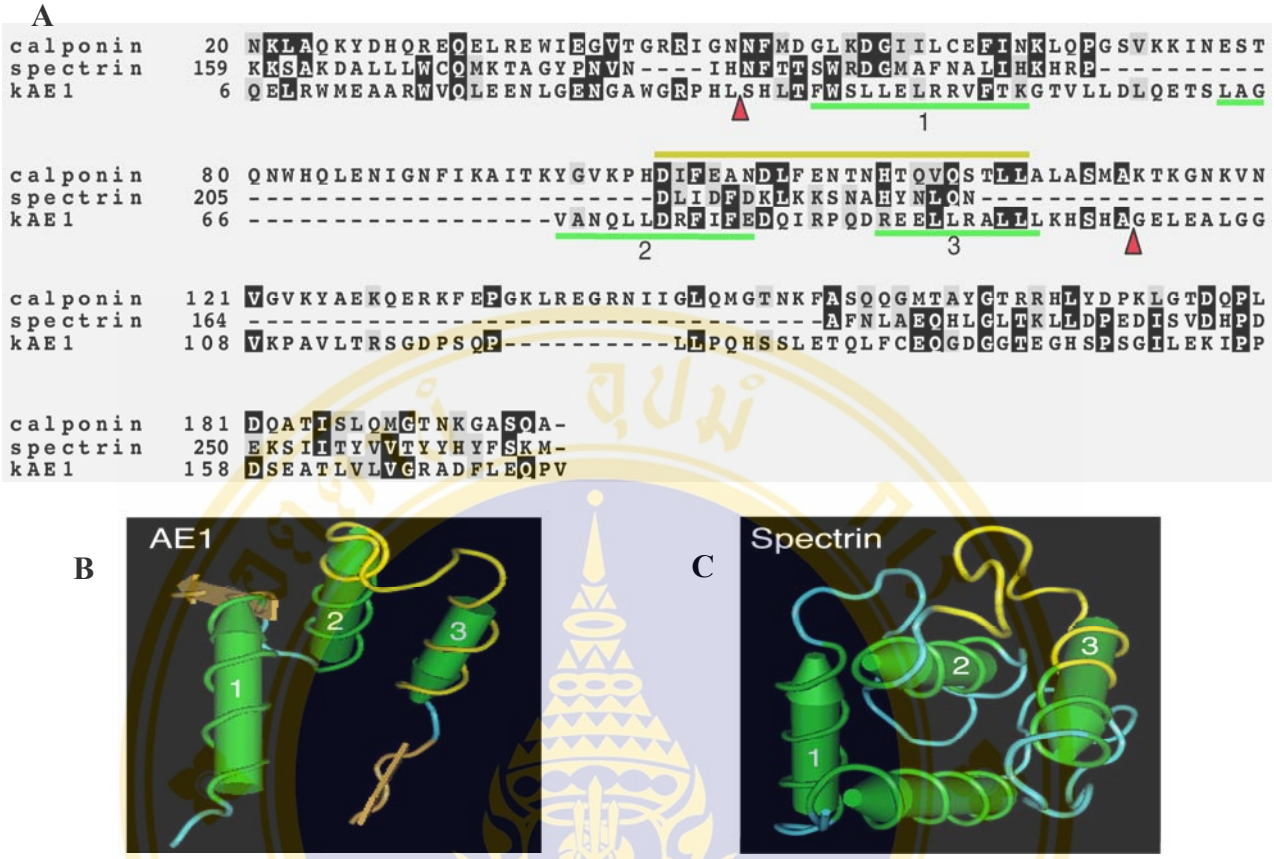





**Figure 31 Sequence and structural homology between kAE1 and calponin homology domain proteins**.

A. Amino acid sequence alignments of human calponin, β-spectrin and kAE1. Residues in black boxes indicate identical residues while grey represent conservative changes. The yellow underline indicates that most highly conserved amino acid sequences, whose location is shown in yellow in panels B and C. Helical regions of the kAE1 sequence are underlined in green and numbered 1-3.

B. Crystal structure of eAE1, representing residues 36-98 (red triangles in panel A mark the region of the crystal structure) of kAE1 [4].

C. Crystal structure of the calponin homology domain of β-spectrin (residues 159-268) [227]. B and C, green rods represent α-helical regions. The helices are numbered 1-3, corresponding to the numbering in panel A. Orange ribbons represent β-sheet regions. Yellow regions represent the segments with the most-highly conserved amino acid sequence. Images were rendered with Cn3D software.

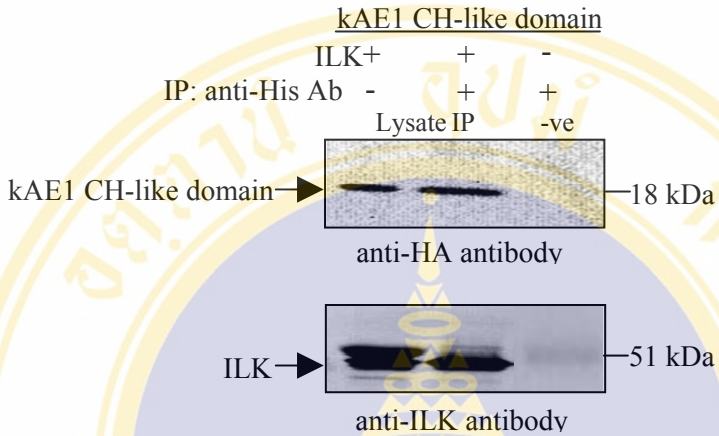


**Figure 32 Identification of the ILK binding domain in kAE1.**

HEK 293 cells were transiently transfected with HA-tagged kAE1 CH-like domain (residues 27-189 of kAE1) alone or co-transfected with His-tagged ILK. Cell lysates were either directly analysed (lysate) or immunoprecipitated with anti His-antibody (IP). Cell lysates expressing kAE1 CH-like domain alone were also subjected to immunoprecipitation with anti-His antibody (-ve). Samples were subjected to SDS-PAGE and immuno blotting. Blots were probed with anti-HA to detect the kAE1 CH-like domain or with anti-ILK antibody as indicated.

the N-terminus of kAE1 was ILK binding site. As shown in Figure 31B, this region is also present in the N-terminal region of eAE1. Thus, it is possible that eAE1 may also interact with ILK. Co-immunoprecipitation of HEK 293 cells co-expressed eAE1 and ILK was carried out to determine whether eAE1 interacts with ILK by using the cells expressed eAE1 alone as a negative control. eAE1 was able to bind ILK when using anti-His antibody for precipitation (Figure 33, lane 2). This suggests that the absence of the first 65 amino acids in the N-terminal kAE1 does not affect the structural alteration of ILK binding site in both proteins. Therefore, the structural feature required for ILK interaction is retained in both kAE1 and eAE1.

**17. Analysis of kAE1 and eAE1 cell surface expression by fluorescence activated cell sorting (FACS)**

Since eAE1 was also found to interact with ILK (Figure 33), the question arose whether ILK increase cell surface expression of eAE1. Fluorescence activated cell sorting (FACS) analysis was used to determine cell surface expression of kAE1 and cells expressing protein at the cell surface. In the presence of ILK, cell surface expression of kAE1 HA557 was increased to be 31.90 ± 5% when compared to kAE1 HA557 alone (19.88 ± 4% in addition to cell surface expressions of eAE1 with or without ILK were 25.40 ± 3% and 21.60 ± 5% (mean ± SD, n = 5), respectively. ILK increased cell surface expression of kAE1 HA557 by 160% while eAE1 HA557 was increased by 117% when kAE1 or eAE1 alone was represented as 100% (Figure 34). Transfected cells with empty vector (pcDNA 3.1) and staining cells with secondary antibodies were used as negative controls. Although ILK interacted with eAE1, it seems likely that eAE1 trafficking to the cell surface was slightly affected by the interaction with ILK. In contrast, ILK interacted with kAE1 and facilitated kAE1 trafficking to the cell surface in a higher level when compared to eAE1. It has known that glycophorin A (GPA) facilitates the movement of eAE1 to the cell surface of red blood cells membrane [91, 92]. Therefore, this result suggests that ILK might play a role in an isoform-specific manner.

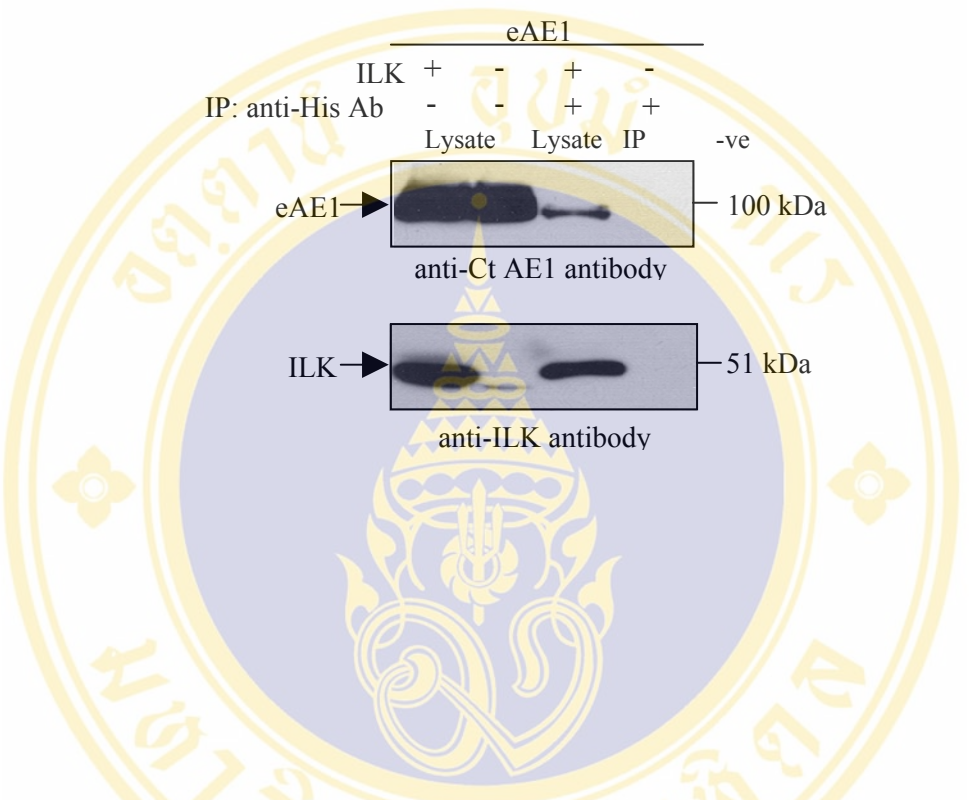


**Figure 33 Interaction between eAE1 and ILK.**

HEK 293 cells were transiently transfected with eAE1 alone or co-transfected with His-tagged ILK, as indicated. Cell lysates were either set aside for later analysis (lysates), or immunoprecipitated with anti-His antibody (IP). Cell lysates expressing eAE1 alone were also subjected to immunoprecipitation with anti-His antibody (-ve). Samples were subjected to SDS-PAGE and immunoblotting. Blots were probed for eAE1, using anti-AE1 antibody or for ILK using anti-ILK antibody, as indicated.

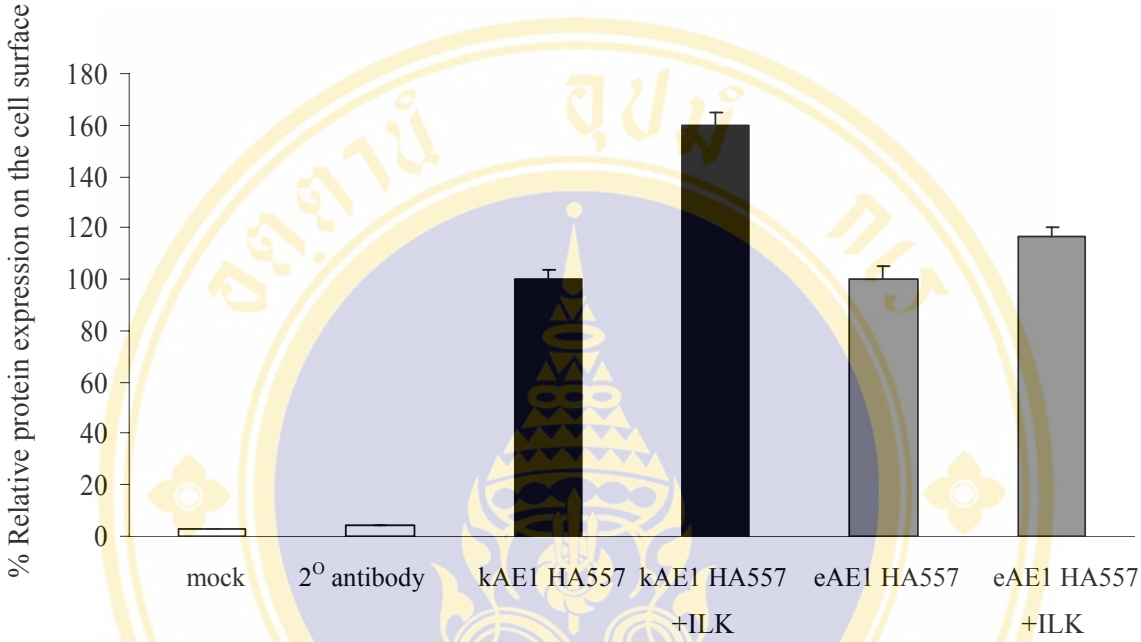


**Figure 34 FACS analysis revealing cell surface expression of kAE1 and eAE1.**
The bar graph showed the percentage of cell surface expression of kAE1 HA557 or eAE1 HA557 co-expressed with ILK in transfected HEK 293 cells as indicated. The cells were stained with anti-HA antibody for kAE1 or eAE1 detection. Goat anti-mouse Alexa 488 was used to visualize kAE1 or eAE1. The signal was analyzed by using Beckman-Coulter EPICS Elite flow cytometer. The error bar shows the standard deviation (SD) of the results from five independent experiments.

**18. kAE1 anion exchange transport activity**

The increase of kAE1 cell surface expression induced by ILK suggested that ILK could alter the level of $Cl^-/HCO_3^-$ exchange activity of ILK/kAE1 expressing cells. The transport activity of kAE1 in the presence of ILK was assessed using a whole cell $Cl^-/HCO_3^-$ exchange assay [75]. Transfected cells were grown on glass coverslips and loaded with the pH-sensitive dye BCECF-AM. Cells were perfused in a fluorescence cuvette alternately with $Cl^-$ containing and Cl- free buffer, to establish transmembrane [$Cl^-$] gradient, facilitating kAE1-mediated $Cl^-/HCO_3^-$ exchange [228]. Transport rates were determined by linear regression of the rate of pHi change in the first 30 seconds of alkalinization following removal of extracellular chloride (Figure 35A). Cell transfected with vector-alone displayed a low level of apparent transport activity (Figure 35A, panel beneath), which is substracted from the rate of kAE1-transfected cells during analysis (Figure 36B). Initial resting pH values of the cell samples were sufficiently similar (7.23±0.01 for kAE1 alone, and 7.12±0.06 for kAE1 plus ILK) that pH-dependent changes buffer capacity did not influence the measured rates of transport. From the raw data (Figure 35A), it is evident that ILK increased the rate of pH change following change of [$Cl^-$] in the medium, consistent with dramatic effect on $Cl^-/HCO_3^-$ exchange rate. Indeed, analysis revealed that ILK increased kAE1 transport activity by 84 ± 28% (n=3) (Figure 35B).

To determine the source of the increase in transport rate, the possibility that ILK increased the expression level of ILK. Immunoblot data showed that ILK did not increase to the total expression level of kAE1 in transfected cells (relative to kAE1 alone, kAE1 level was 101±6% when expressed with ILK (Figure 35C). The increase in transport activity of kAE1 was upon ILK expression, is numerically in line with the observed increase in cell surface expression.

**19. Association of kAE1 with actin complex via interacting with ILK**

kAE1 was found to interact with ILK through the CH domain of kAE1 (Figure 32). Since CH domains act as binding sites in intermediaries in complexes with the actin cytoskeleton [189, 223], led the hypothesis that ILK promotes interaction of kAE1 with cytoskeleton. In addition, kAE1 is unable to bind to ankyrin, protein that connects eAE1 to actin cytoskeleton in red blood cells [229]. To examine this

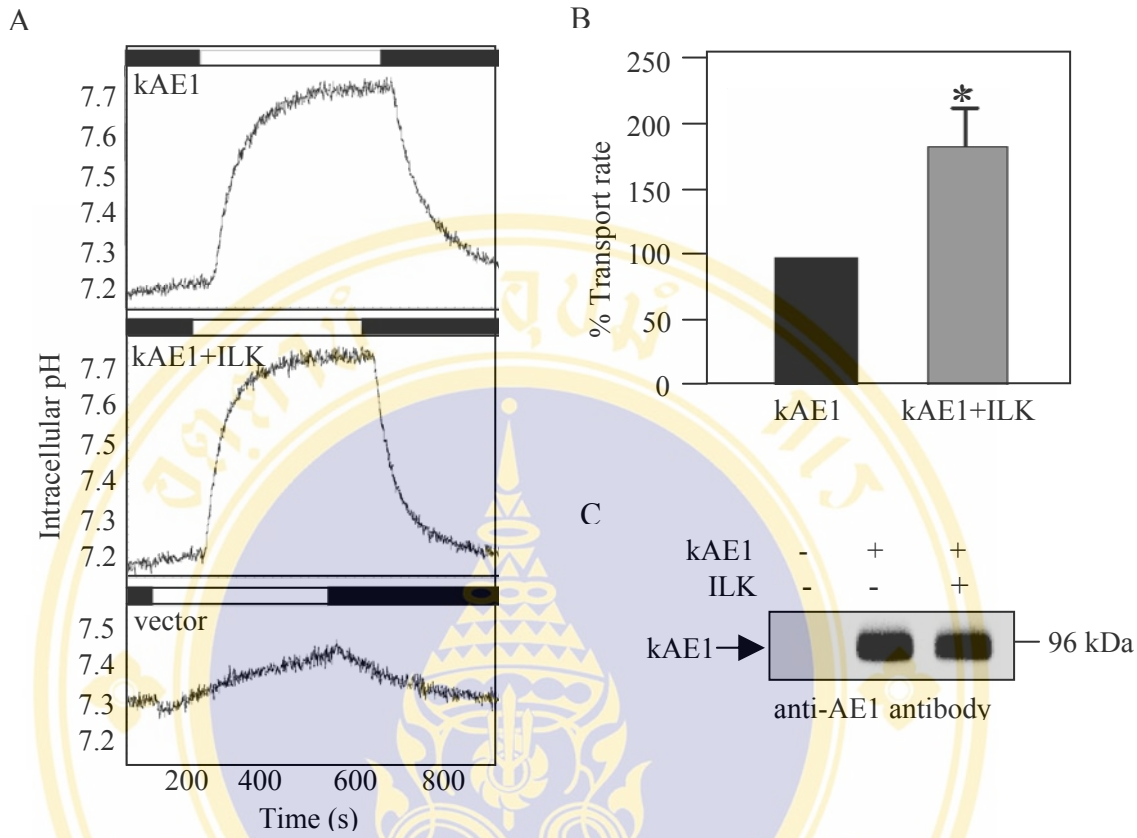


**Figure 35 Anion exchange activity of kAE1 in the presence or absence of ILK.**

A. Intracellular pH of HEK 293 cells transfected with kAE1, kAE1 + ILK, or vector alone. The transfected cells were loaded with BCECF-AM dye and perfused in a fluorescence cuvette alternately with Ringer's buffer containing 140 mM NaCl (black bar) or 140 mM Na gluconate (white bar) as indicated above each panel.

B. Transport anion exchange rate of kAE1. Mean values are expressed relative to transport rate of cells transiently transfected with kAE1 cDNA alone. Transport rates (n = 3) were corrected for the background of HEK 293 cells. Asterisk represents $P<0.05$, unpaired t-test.

C. Expression of kAE1 was monitored from 60 mm dishes that contained the coverslips used for anion exchange assays. Cell lysates were subjected to SDS-PAGE, and immunoblotting. kAE1 was detected with monoclonal anti-AE1 antibody (IVF12).

possibility, the lysates from HEK 293 cells transfected with kAE1 plus His tagged ILK or kAE1 alone were prepared and incubated with $Co^{2+}$ affinity resin. Endogenous paxillin and actopaxin were detected in the lysate of HEK 293 cells using anti-paxillin monoclonal antibody and anti-actopaxin polyclonal antibody, respectively. Proteins were eluted from the resin with 1.5 M imidazole containing buffer. As expected, on immunoblots kAE1 was co-purified with His-tagged ILK. The blot was then stripped and re-probed with anti-paxillin and anti-actopaxin antibodies. These immunoblots revealed that endogenous paxillin and actopaxin associated with the complex of ILK/kAE1 (Figure 36 lane 2). Paxillin or actopaxin were not detected when kAE1 was expressed without ILK (Figure 36, lane 3). This suggests that kAE1 interacted with the actin cytoskeleton through a complex containing ILK, paxillin and actopaxin.

**20. Triton X-100 insoluble cytoskeleton extraction**

To explore the role of ILK in connecting kAE1 to actin cytoskeleton, the effect of non-ionic detergent extraction on solubility of kAE1 was assessed. Treatment of cells with non-ionic detergents such as Triton X-100 will solubilize typical cytoplasmic and membrane proteins while leaving intact the F-actin cytoskeleton and its associated proteins relatively intact. Therefore, HEK 293 cells transfected with kAE1 plus ILK or kAE1 alone were extracted with extraction buffer containing 0.5% (v/v) Triton-X-100 as described in Materials and Methods. The distribution of kAE1 in insoluble fraction and soluble fraction was examined on immunoblots probed with anti-HA antibody to detect kAE1. The amount of kAE1 in Triton X-100 insoluble fraction significantly increased in the presence of ILK (Figure 37A). kAE1 localization in soluble and insoluble fractions was quantified by densitometry. The percentage of kAE1 in insoluble fraction was calculated to be $14 \pm 6\%$ kAE1, and $20 \pm 5\%$ kAE1 plus ILK (mean ± S.D., n = 4). The bar graph shows the quantification of kAE1 accumulated more in insoluble fractions when expressed kAE1 with ILK compared with kAE1 alone (Figure 37B). This indicates that ILK may mediate kAE1 interaction with the actin cytoskeleton in HEK 293 cells.

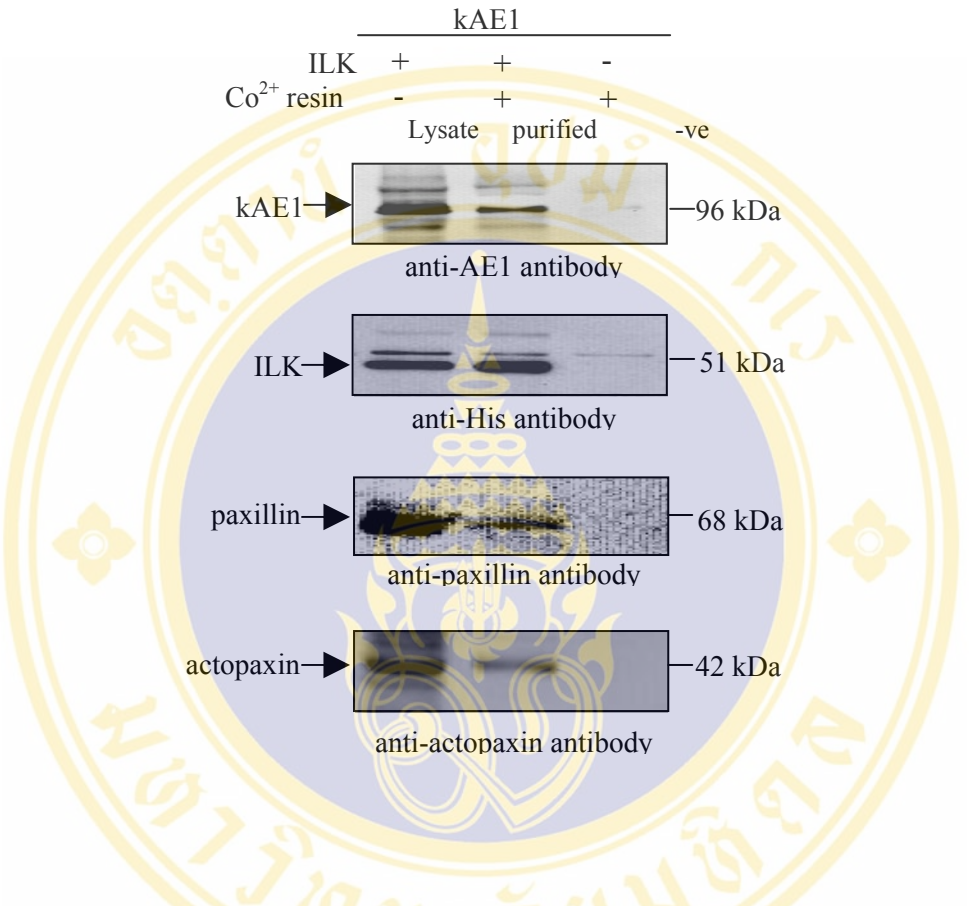


**Figure 36 Co-association of kAE1 with actin complex via interacting with ILK.** HEK 293 cells were transiently transfected with HA-tagged kAE1 alone or co-transfected with His-tagged ILK, as indicated. Cell lysates were either set aside for later analysis (lysates), or incubated with $Co^{2+}$ affinity resin at 4 °C. Cell lysates expressing kAE1 was also purified by $Co^{2+}$ affinity resin (-ve). Resin was washed and subsequently eluted with buffer containing 1.5 M imidazole. Samples were subjected to SDS-PAGE and immunoblotting. Blots were probed with anti-HA and anti-His antibodies for kAE1 and ILK detection, respectively and with anti-paxillin and anti-actopaxin antibodies, as indicated.

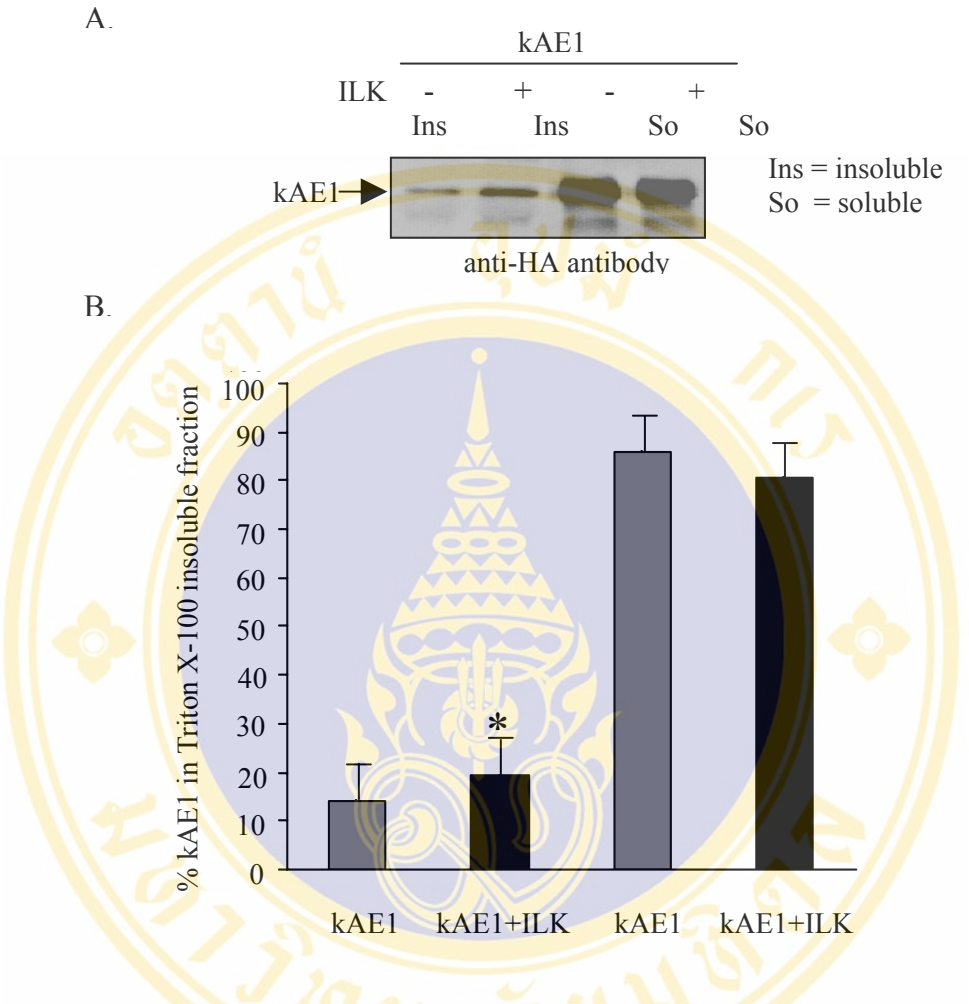


**Figure 37 Association of kAE1 with the insoluble cytoskeleton.**

A. HEK 293 cells co-expressing kAE1 and ILK or kAE1 alone were incubated with Triton X-100 extraction buffer. Cells were collected and spun down. The pellet (detergent-insoluble fraction, Ins) was resuspended in SDS buffer. Detergent-soluble fraction (supernatant, So) and -insoluble fraction (Ins) were resolved by SDS-PAGE. Immunoblots were probed with anti-HA antibody to detect kAE1.

B. Quantification of the percentage of kAE1 in cytoskeleton extraction fraction calculated by insoluble or soluble kAE1/ total kAE1 x 100%; total kAE1 = insoluble + soluble. The error bar shows mean ± S.D. with n = 4. Asterisk indicates significant difference ($p<0.05$), unpaired t-test, between presence and absence of ILK.

# CHAPTER VI
# DISCUSSION

Although the only difference of amino acid sequence between the kidney isoform (kAE1) and the erythroid isoform (eAE1) is the absence of 65 amino acid residues at the N-terminus of kAE1, the functional differences between eAE1 and kAE1 are considerable because kAE1 no longer binds ankyrin, protein 4.1, protein 4.2 as well as glycolytic enzymes [10, 11]. This implies that the alteration of protein-protein interactions of kAE1 would be caused by some structural changes of the protein into different protein folding. Mutations in kAE1 gene have been discovered to be associated with distal renal tubular acidosis (dRTA) [15, 230]. The proposed mechanism of the disease involves the defect in protein trafficking or targeting to an appropriate site of α-intercalated cells in kidney, which results in impairing bicarbonate movement across the basolateral membrane [23]. Possible additional pathogenic mechanisms include the impairment of interaction between kAE1 and chaperone proteins. Glycophorin A (GPA) has been postulated to have a chaperone-like role in enhancing trafficking through internal compartments during eAE1 biosynthesis but unfortunately, it is not present in the kidney [91, 162]. Kanadaptin was identified to interact with kAE1 and suggested to be involved in protein trafficking in mouse kidney [12]. More recently, it was found that there is no interaction between kAE1 and kanadaptin in human kidney [13, 14]. The unidentified proteins that play a role in regulation of kAE1 expressed at the cell surface have, however, not been defined. Recently, it has shown that both N-terminal and C-terminal domains of kAE1 are required for basolatera localization in polarized cells. While the C-terminus of kAE1 interacts with carbonic anhydrase II, the large N-terminal cytoplasmic domain has not been well characterized and the mechanism by which the kAE1 N-terminal domain facilitates protein to express at the cell surface is still unknown. To understand the role of the N-terminal domain of kAE1, we explored which proteins interact with kAE1.

The experiments carried out in this thesis thus attempt to answer the question by identifying the proteins that interact with the N-terminal domain of kAE1. The experimental studies were divided into two steps. The initial screening to identify the proteins interact with the N-terminal domain of kAE1 in human kidney cDNA library was performed by using yeast two-hybrid system. Then, interaction between kAE1 and interacting proteins identified in the two-hybrid system was verified in human kidney cell culture. The effect of interacting protein on physiological function of kAE1 was further investigated. The results from this study are discussed below.

**1. Yeast two-hybrid screening of proteins interacting with the N-terminal kAE1**

The crucial step essential for the feasibility of yeast two-hybrid is a bait construction. The recombinant plasmid named pNkAE1 constructed to express a fusion protein of GAL4-binding domain and the N-terminal kAE1 (residues Met66-Pro403 of human eAE1) was used as a bait for screening interacting partners. Since the system is based on reconstitution of a transcription factor, brought together by the interacting fusion proteins, examining the bait properties such as auto-transcriptional activation capacity, mating efficiency and western blot analysis are important for overall success of the experiments. In the present study, yeast strain AH109 containing either pNkAE1 or pGBKT7 vector were used to test transcriptional activation. The result showed that this bait had no activation of LacZ, HIS3 and ADE2 reporters as it did not give any blue colony on the lifted filter by colony lift assay and did not grow on SD/-Trp/-His and SD/-Trp/-Ade plates. Although co-transformation method has been extensively used for yeast two-hybrid screening, yeast mating assay was chosen to screen protein-protein interaction in this study since the assay has several advantages [231]. For example, the assay can screen the whole cDNA library to find the novel interactions, it is also useful for the proteins which their constitutive expression interfere yeast viability and auto transcriptional activation of reporters in haploid cell are less sensitive in diploid cell. In addition, western blot analysis was performed to examine the expression of GAL4-BD/NkAE1 fusion protein in yeast. The expected protein band at molecular weight about 60 kDa was detected by using anti-GAL4 DNA-binding domain antibody. According to the bait

properties, pNkAE1 was suitable bait for the screening of interacting partners in a human kidney cDNA library by yeast two-hybrid system.

Approximately $1x10^6$ independent clones in human kidney cDNA library were screened on high stringency selective medium lacking adenine, leucine, tryptophan, and histidine (SD/-Ade/-Leu/-Trp/-His). This initial two-hybrid screening conferred 151 yeast colonies of $HIS^+$ and $ADE^+$. These colonies were then picked up to confirm $MEL^+$ phenotype by testing α-galactosidase activity on dropout medium containing X-α-Gal. The correlation between the strength of interaction and the reporter activity has been established [232]. In weak interactions, the protein complex will easily dissociate, leading to small amount of the interaction complexes binding to the reporter gene promoter. Conversely in strong interactions large amounts of protein complexes will activate transcription of reporter genes more than that of weak interaction. The results of this study showed that 133 colonies gave strong and moderate blue colonies while other 18 faint blue colonies were not included in this study as they may be false positive clones. After that, a number of redundant cDNA positive clones were removed by restriction digestion pattern. PCR products of cDNA inserts were amplified by using isolated yeast plasmid from the library as templates. *Hae*III, a four cutter, was used to digest the amplified products to generate the restriction digestion pattern and then the positive clones were grouped on the basis of its restriction digestion pattern. The total 121 clones revealed a unique restriction pattern were subjected to automated DNA sequencing to determine the inserted sequences of these putative positive clones. Only 109 clones were analyzed as shown in Table 4 whereas that of the others 12 clones were not obtained due to the numerous repeat nucleotide sequences (Poly T tracks) reading through the inserted fragments. The clones were identified in sequence databases as involved in many cellular processes, including metabolism, transport and binding, trafficking, apoptosis, transcription and translation. Some clones were identified as encoding membrane or cytoskeletal-associated proteins while others are not defined for their function yet. All of the matches from the BLAST search had very low E-values indicating statistical significance. To confirm whether the positive interactions from initial screening were valid, the 21 clones encoding the known proteins that might be involved in kAE1 trafficking and randomly selected of 14 clones encoding for hypothetical proteins as

indicated by asterisks in Table 4 were tested for the specificity of interaction with the NkAE1 in yeast. The results showed that only 9 putative clones were proposed to be true positives on the basis of interaction between the NkAE1 and the proteins (integrin-linked kinase (ILK), pantophysin, glyceraldehyde-3-phosphate dehydrogenase (GAPDH), giantin, thymosin β4, laminin A and other three hypothetical proteins (A24, B61 and C51)) allowed growth of diploid yeast on synthetic dropout medium. These suggested that even yeast two-hybrid screening is a powerful tool for a large-scale screening to identify novel protein-protein interactions; there are some limitations inherent to the method. The major disadvantage of yeast two-hybrid screening is false positives emerging from auto-activating transcription of reporter genes and non-specific binding to GAL4-binding domain in the vector [233]. The false-positive clones may be explained by cDNAs that encode proteins able to bind the promoter used to drive expression of reporter genes. Alternatively, these proteins were not hybrid with the GAL4 activation domain, but were active following over-expression of the genes being carried on a multiple copy plasmid. There are collections showing that some proteins obtained from the two-hybrid screening using many diverse baits, which include ribosomal subunit, heat shock proteins, proteasome subunits and cytoskeleton components, were classified as common false positive because their biological function involves binding a large number of different proteins or nonspecific charge and coiled-coil interaction [231]. Thus, using the two-hybrid system, it is critical to test each initial positive against unrelated proteins fused to the DNA-binding domain and to eliminate those that do not show specificity for the target protein as done in our experiment. Therefore, the specificity test for the 74 out of 109 positive clones is required prior to selection for further study.

Although the fusion 9 proteins were proposed as psossible kAE1-interacting proteins, the threshold of the positive read-out according to the α-galactosidase activity (MEL1 reporter) demonstrated that some proteins slightly activated reporters when it interacted with either GAL4-binding domain or p53 protein (Figure 21); results of β-galactosidase activity (LacZ reporter) assay were more reliable without background (Figure 22). Thus, four cDNA fragments encoding ILK, pantophysin, GAPDH and thymosin β4 were selected for further studies based on the strength of interaction and reporter activity.

**2. Interaction between kAE1 and interacting proteins**

Protein-protein interaction identified in yeast two-hybrid should be validated by independent approaches such as co-immunoprecipitation, co-purification, immunofluorescence and etc. Since glycosylation processes in protein biosynthesis would be different in yeast and humans [234], the nature of protein structures might be also changed by this process, potentially causing proteins to interact falsely with target proteins. In this study, co-immunoprecipitation, affinity co-purification and immunofluorescence methods were accessed in human embryonic kidney (HEK 293) to confirm the association between kAE1 and interacting proteins (GAPDH, pantophysin and ILK) (Figure 25 and 26). In addition, cell surface biotinylation studies were performed to demonstrate the effect of interacting proteins on cell surface expression of kAE1. Results showed that only ILK promoted kAE1 cell surface expression, whereas GAPDH and pantophysin did not (Figure 27). However, it was still not clear whether GAPDH and pantophysin are also involved in kAE1 trafficking. These proteins may participate in the translocation process between membrane compartments during kAE1 transport inside the cells and then kAE1 was eventually facilitated to the cell surface of the α-intercalated cells via interacting with ILK.

Apart from its glycolytic function, GAPDH is also required for cycling of transport vesicles [235, 236]. GAPDH catalyzed membrane fusion in systems that use microtubule-directed vesicular trafficking (e.g., GLUT4 vesicle trafficking, endoplasmic reticulum to Golgi vesicular tubular cluster membrane trafficking). GAPDH was proposed to be recruited to tubulin-associated vesicles in a Rab- and GTP-dependent manner. Subsequent protein kinase C (PKC) phosphorylation changes GAPDH conformation, altering its interactions with tubulin and facilitating membrane fusion by de-inhibition of GAPDH. Consequently, GAPDH can be released from the target membrane in an ATP-dependent fashion (which may require additional ATP dependent chaperones). Since both kAE1 and GLUT4 are similar in term of they are integral membrane transporters, it is possible that GAPDH might play a role in the process that facilitates and regulates appropriate membrane fusion during kAE1 trafficking.

Although the lack of highly acidic N-terminal domain of AE1 has been proposed to explain the absence of GAPDH association with kAE1, GAPDH was

immunolocalized to kAE1 concentrated in the basolateral membrane of the α-intercalated cells in rat kidney medulla. Interestingly, immunoreactivity was not detected in the plasma membrane of any other cell types in the kidney, indicating its predominant association with kAE1-rich membranes [237]. Therefore, it is likely that GAPDH may have binding sites in addition to previously described for such binding to AE1.

Pantophysin is another intriguing molecule that may play a multifunctional role in vesicle biogenesis and transport. Recently, pantophysin has been reported to co-localize with the ubiquitous vesicle protein, vesicle-associated membrane protein 2 (VAMP2)/ cellubrevin and secretory carrier-associated membrane proteins (SCAMPs) [181, 182]. Although the role of pantophysin in vesicle trafficking is unclear, this protein is present in GLUT4-containing vesicles in adipocytes [183]. Pantophysin was proposed to be involved in GLUT4 vesicle translocation in adipocytes. It is possible that kAE1 might have the protein biosynthesis including protein translocation pathway between membrane compartments inside the cells prior to express on the cell surface. kAE1 interacts with pantophysin which then associate with the ubiquitous vesicle protein such as VAMP2 and SCAMPs forming the vesicle to traffic within the cells.

**3. Detailed analysis of interaction between kAE1 and ILK**

The finding that ILK co-localized with kAE1 at the cell surface despite it is an intracellular protein (Figure 28) and ILK could promote processing of kAE1 to the cell surface of HEK 293 cells suggests a possible role of ILK in facilitating kAE1 cell surface expression. Integrin-linked kinase (ILK), a serine/threonine kinase, was originally discovered as a $\beta_1$ integrin cytoplasmic tail-binding protein [186]. Ankyrin repeats at the N-terminus of ILK interact with the LIM-only adaptor protein PINCH [190], while the C-terminus of ILK interacts with $\beta_1$ integrin, paxillin and actopaxin. ILK is a central protein in control of several signaling pathways through interacting with many proteins. Therefore, it is also important to know which ILK region is required for mediating kAE1-ILK interaction. We found that ILK uses its C-terminal catalytic subunit to interact with kAE1, whereas the N-terminus of ILK is not required for kAE1 binding (Figure 29B). To determine whether the catalytic activity of ILK is required for the interaction with kAE1, the kinase-dead domain mutants (S343A and

E359K ILKs) were used to assess their interaction with kAE1. Results showed that both kinase-dead ILK mutants were able to interact with kAE1 (Figure 29B). This observation suggested that although the C-terminal catalytic domain of ILK was required for its interaction with kAE1, the kinase activity of ILK is not necessary for ILK to interact with kAE1.

Previous studies showed that the C-terminus of ILK interacts with both paxillin via its LD1 motif and actopaxin via its calponin homology (CH) domain [191, 206]. While ILK interacts with paxillin through its conserved sequences known as paxillin binding sub-domain (PBS, residues 384-390), the actopaxin binding site cover almost residues of the C-terminus of ILK (residues 136-452). It is likely that paxillin and actopaxin binding sites on ILK are distinct [192]. Moreover, paxillin binds both actopaxin and ILK; the associations between actopaxin-ILK-paxillin constitute an evolutionarily conserved integrin-dependent remodeling of the actin cytoskeleton [205]. kAE1 may interact with ILK at the site different from paxillin and actopaxin. The interaction of kAE1 and ILK would thus not disturb the regulation of other signaling pathways.

It has been known that ankyrin domain mediates the association of ILK with the LIM-only adaptor protein PINCH, a component of growth factor receptor signaling and actin reorganization pathways, to regulate focal adhesion localization and that serine 343 is invoved in stimulation of PKB/AKt phosphorylation in COS cells to regulate cell survival and apoptosis [190]. In this study, the role of ankyrin repeats at the N-terminal and kinase activity at the C-terminal ILK on cell surface expression of kAE1 was also examined. However, the result showed ankyrin repeats, PH domain and kinase activity of ILK were not required for processing of kAE1 to the cell surface (Figure 30). This might suggest that cell surface expression of kAE1 increased by ILK is not involved in the downstream action of growth factor receptor signaling and phosphorylation of PKB/AKt.

In the meantime, the region in kAE1 that mediates ILK interaction was also identified. Sequence alignment of the N-terminus of kAE1 and proteins containing calponin homology (CH) domain showed that amino acid residues 27-189 of the N-terminal kAE1 did align convincingly with other CH domains. The CH domain is a protein module of about 100 amino acid residues, first identified at the N-terminus of

muscle regulatory protein called calponin, an actin binding protein [238]. The striking feature shared among CH domains in their tertiary structure in addition to the primary sequence identity between CH domains of different proteins ranges from 5-20% [227]. In this regard the kAE1 CH domain is not exceptional as it displayed 12 and 13% sequence identity with spectrin and calponin CH domains, respectively, over the 152 residues identified as the CH domain of kAE1. Molecular modeling also assessed structural similarities between the N-terminus of kAE1 and CH domain from human β-spectrin [227]. The globular fold of the CH domain is built of four core helices, three forming a loose triple helix bundle, and one to three short helices present in the loops between the core helices [239]. The crystal structure for human eAE1 cytoplasmic domain shows that the region corresponding to residues 27-189 of kAE1 has overall similarity the secondary structure to CH domain of spectrin (Figure 31B and C). The role of these kAE1 residues in mediating interaction with ILK was confirmed by co-immunoprecipitation. The result shows that these residues of kAE1 specifically interact with ILK (Figure 32). Taken together, we propose that ILK interacts with kAE1 via the predicted CH-like domain in the N-terminus of kAE1. ILK also interacts with eAE1 (Figure 33), which suggests that the removal of the first 65 amino acids at the N-terminus of kAE1 does not alter the folded structure of CH domain in eAE1. However, FACS analysis results revealed that co-expression of ILK had slightly increased cell surface expression of eAE1 (Figure 34) when compared with that of kAE1, suggestin ILK might play a role in an isoform specific manner. It implies that another protein has ILK-like function espressed in red cell membrane. Evidence shows that glycophorin A (GPA) facilitates the movement of eAE1 to the cell surface and has a chaperone-like role, enhancing trafficking during eAE1 biosynthesis [91, 92]; interaction between ankyrin and eAE1 also provides predominant connection between membrane and underlying spectrin/actin cytoskeleton network [229]. Nevertheless, GPA is not found in α-intercalated cells of kidney [162], where kAE1 is unable to bind ankyrin [10].

$Cl^-/HCO_3^-$ exchange assays assessed whether ILK affects the physiological function of kAE1. Results revealed that ILK has an impact on the transport activity of kAE1 since the presence of ILK markedly increased transport activity of kAE1 (Figure 35B). Accordingly, the increment of kAE1 transport activity showed a correlation to

the result of cell surface biotinylation. Since ILK is a linker protein, connecting extracellular matrix and actin cytoskeleton, ILK may promote cell surface expression of kAE1 by connection of kAE1 to the actin cytoskeleton. Interestingly, the cell surface biotinylation experiment demonstrated that actin is possibly involved in cell surface processing of kAE1 as the amount of actin was reduced in unbound fraction of kAE1 when co-expressed with ILK (Figure 27). Expression of actin which used as an internal control was supposed to be the same in each lane according to equal amount of protein loading. Many lines of evidence have shown that the association between ILK, paxillin and actopaxin facilitated the complex to the actin cytoskeleton via CH domain of actopaxin [191]. Similarly, ILK may also link kAE1 to actin cytoskeleton via the ILK-paxillin-actopaxin complex as kAE1-ILK complex could recruit endogenous paxillin and actopaxin in HEK 293 cells (Figure 36). This finding was confirmed by the observation that ILK increased the association of kAE1 with Triton shells, indicative of increased association with the actin cytoskeleton (Figure 37). Taken together, the results suggested that kAE1 was attached to the actin cytoskeleton complex via its interaction with ILK-paxillin-actopaxin complex. Since both kAE1 and actopaxin use their CH domain to interact with ILK, this leads to the speculation that ILK regulates the interaction of kAE1 to actin cytoskeleton via interacting with actopaxin. It might be explained by two possibilities. Firstly, actopaxin is able to interact with ILK at a site distinct from kAE1 so that actopaxin binds to actin filaments without interference from kAE1. Secondly, ILK binds paxillin, which in turn binds actopaxin [205]; thus, the CH domain of actopaxin does not compete with kAE1 for interaction with ILK and allows actopaxin interacting directly with actin filament.

As shown in this study, the association of the N-terminal region of kAE1 with the actin cytoskeleton has a significant impact on the increase of kAE1 cell surface expression. Expression studies in polarized MDCK cells revealed that kAE1 has two basolateral targeting determinants, one in the N-terminus and another in the C-terminus. Deletion at either the N- or C-termini resulted in apical localization of the protein, suggesting that the presence of both determinants is essential for correct basolateral localization of kAE1 [24]. Thus, the N-terminal domain of kAE1 may have a role in the polarized targeting pathway via associating with actin cytoskeleton

before/after the C-terminus becomes involved. Although it remains unclear what mechanism contributes to kAE1 trafficking or targeting to basolateral membrane, the mechanisms to ensure the direct movement of kAE1 within the cell and control their delivery to the destination would be required for understanding. The proposed mechanism is involved when kAE1 reaches the trans-Golgi network; it is loaded into transport vesicle using the N-terminus of kAE1 exposed to cytosolic environment. At this step, the N-terminus of kAE1 interacts with the ILK-paxillin-actopaxin complex, and then links the transport vesicle to actin cytoskeleton via this complex. The interaction of transport vesicle-contained kAE1-ILK-paxillin-actopaxin complex to actin cytoskeleton can support vesicle movement via the molecular motors by taking advantage of the intrinsic polarity of actin filament that have "+" and "-" ends, and use energy derived from adenosine 5'-triphosphate (ATP) hydrolysis by the myosin family of ATPases [175].

Data from previous studies has shown that the sequences at the N-terminus of major chicken-specific kidney AE1 isoform (AE1-4) were required for the association of this variant transporter with the actin-based cytoskeleton, basolateral sorting as well as recycling from the plasma membrane to the Golgi [96]. It was found that cells transfected with AE1-4 are associated with the actin cytoskeleton and the detergent insolubility pool of AE1-4 was dramatically reduced in cells treated with the actin-depolymerizing drug, latrunculin B, which indicates that the maintenance of AE1-4 insolubility is almost entirely dependent upon an intact actin cytoskeleton in sub-confluent cells. Furthermore, it has been proposed that AE1-4 accumulate in the basolateral membrane of this cell type correlated with their ability to co-localize with phalloidin stained stress fibers.

More experiment has done by Dr. Gonzalo L. Vilas to determine whether kAE1 and ILK form complex in kidney using sucrose gradient ultracentrifugation. Although, most of ILK migrated to the bottom of sucrose gradients consistent with interaction with a large cytoskeleton complex, ILK was also found in the sucrose gradient fraction containing kAE1. However, little kAE1 was found associated with the cytoskeletal fraction of kidney detergent lysates. This data suggested that either kAE1/ILK interaction was disturbed by the membrane solubility of sucrose gradient condition or kAE1 interacted with ILK that is not cytoskeleton-associated. This

previous finding suggested that localization of ILK to cytoskeletal fraction contrasts with this study in the experiment using kidney cell line (HEK 293) where kAE1 and ILK associated in a soluble complex as demomstrated by co-immunoprecipitation. The difference results might be from several variations for example the kidney tissue was heterogenous containing cell types that expressed ILK, not only the α-intercalated cells that express kAE1. Therefore, the ratio of kAE1: ILK seems likely much higher in HEK 293 cells than in the whole kidney. However, the similar findings were obtained when using both polarized MDCK cells and human kidney sections which demonstrated that the subcellular location of kAE1 and ILK in both polarized MDCK cells and human kidney sections showed that some fraction of ILK co-localized with kAE1 at the basolateral membrane (performed by Dr. Saranya Kittanakom). It suggested that ILK may act to link kAE1 to underlying cytoskeleton, thereby stabilizing kAE1 at the cell surface to increase steady-state level of this kAE1 on the plasma membrane.

Although there is no direct evidence for the involvement of actin cytoskeleton in cell polarity or targeting of membrane protiens to basolateral membrane of epithelail cells in human, another study proposed that microtubule based motors are involved in the transport of proteins from trans-Golgi network to the apical or basolateral membrane [171, 172]. Possible cytoskeleton complex including kAE1/ILK is shown in Figure 38.

Alternatively, protein phosphorylation may also be used to regulate kAE1 trafficking. Tyrosine phosphorylation influences the localization of proteins by regulating their interactions with cellular targeting and/or internalization machinery [2, 240, 241]. Similar to eAE1, both Tyr359 in the N-terminal domain and Tyr904 in the C-terminus are also present in kAE1 and supposed to be phophorylated as in red blood cells [76]. The recent observation suggests that the substitution of phenylalanine for Tyr904 can alter kAE1 targeting [24] while the potential role of Tyr359 is poorly understood. Phosphorylation of Tyr904 in YDEV motif was suggested to cause internalization of kAE1 from the basolateral membrane to the endosomes [170]. Dephosphorylation of this motif by the phosphatase SHP2, which recruits by the phosphorylation of Tyr359. It is possible that once ILK interacts with kAE1, the C-terminal kinase domain of ILK would phosphorylate Tyr359 at the N-terminus of

kAE1 which is required for the action of the phosphatase to dephosphorylate Tyr904 in YDEV-basolateral sorting to allow the recycling of kAE1 back to the basolateral membrane. Studies to address the role of ILK in this hypothesis remain to be evaluated.

**4. Future studies**

The data presented in this thesis serves as a model to describe the mechanism of normal kAE1 trafficking to the plasma membrane of HEK 293 cells is dependent upon the interaction between kAE1 and ILK-paxillin-actopaxin-actin cytoskeleton complex. The cell lines used in this study are, however, limited. In addition, expression studies in stable polarized cells line such as MDCK cells will help to define more conclusively the role of ILK in the basolateral targeting of kAE1. Besides actin cytoskeleton, protein phosphorylation may be necessary for correct localization and recycling of kAE1 to the basolateral membrane. The result would provide more details for normal kAE1 trafficking to the α-intercalated cells of the kidney nephron. Mutations in kAE1 gene are associated with dRTA. Defects in protein trafficking and loss of interaction with an adaptor protein of kAE1 (like ILK) likely underlay dRTA. Therefore, studies of interaction between kAE1 mutants and ILK may lead to greater understanding of the molecular pathogenesis of dRTA.

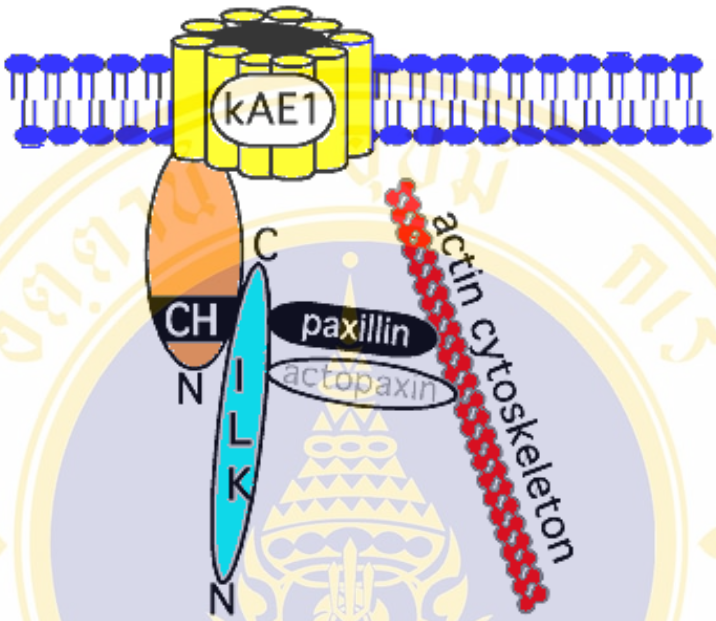


**Figure 38 Possible cytoskeleton complex including kAE1/ILK.**

kAE1 is comprised of two major domains: an N-terminal cytoplasmic domain (N-terminus marked N) and a C-terminal integral membrane domain responsible for anion transport. Near the N-terminus of kAE1 is a newly-identified calponin homology domain (CH), which forms the binding site for integrin-linked kinase (ILK). The CH binding region of ILK is near the C-terminus (C) of ILK. In turn ILK binds the two actin-binding proteins, paxillin and actopaxin to form a complex of ILK and kAE1 with the actin cytoskeleton. Cytoskeletal binding may stabilize kAE1 at the cell surface, maximizing cell surface kAE1 levels, and possibly aiding in basolateral targeting in epithelial cells.

# CHAPTER VII
# CONCLUSION

The study in this thesis is proposed to identify the candidate proteins that interact with the N-terminal domain of kAE1 (NkAE1). Yeast two-hybrid system was conducted to identify the interacting proteins by using GAL4-BD/NkAE1 (Met66-Pro403 of eAE1) fusion protein as a bait to screen cDNA library derived from the human kidney. Interacting proteins were identified and chosen for further study on the basis that interaction between NkAE1 and interacting proteins allowed growth of yeast on medium lacking adenine, leucine, tryptophan, and histidine containing X-α-Gal. Four proteins namely integrin-linked kinase (ILK), glyceraldehydes-3-phosphate dehydrogenase (GAPDH), pantophysin and thymosin β4 were proposed to be the NkAE1 interacting proteins.

Interaction between kAE1 and interacting proteins was further verified in the co-expression experiments in human embryonic kidney (HEK 293) cells. The results of co-immunoprecipitation and affinity co-purification revealed kAE1 associated with ILK, GAPDH or pantophysin but not thymosin β4. Interestingly, the result from cell surface biotinylation demonstrated ILK promoted cell surface expression of kAE1 while GAPDH and pantophysin did not. Accordingly, ILK also increased the $Cl^-/HCO_3^-$ transport activity of kAE1 suggesting the role of ILK increases in the cell surface expression of kAE1. Detail analysis to identify the regions required for the kAE1-ILK interaction revealed kAE1 interacted with the C-terminus of ILK though the previously undetected kAE1 CH domain in the N-terminus. The ankyrin repeats, PH domain and kinase activity of ILK were not required for facilitating of kAE1 to express at the cell surface. Also, ILK was found to interact with eAE1. It means that the absence of the 65 amino acids at the N-terminus of kAE1 does not alter the folded structural of CH domain binding site in eAE1. In contrast, ILK did not significantly increase cell surface expression of eAE1 when compared with that of kAE1, implying

that ILK plays a role in isoform specific manner as a key protein involved in kAE1 transport to express at the cell surface in the kidney.

Furthermore, the study to examine the role of ILK in kAE1 trafficking revealed that the kAE1-ILK complex can recruit endogenous paxillin and actopaxin from HEK 293 cells, suggesting that kAE1-ILK-paxillin-actopaxin complex links kAE1 to the actin cytoskeleton. In the same way, another finding confirmed that ILK induced increased association of kAE1 with Triton shells, indicative of increased kAE1 association with the actin. It seems likely that actin cytoskeleton involved in kAE1 transport to express at the cell surface via a complex containing ILK, paxillin and actopaxin. Taken together, these present data demonstrated for the first time that ILK is a protein that promotes cell surface expression of kAE1 in transfected HEK 293 cells by mediating interactions with the actin cytoskeleton.

# REFERENCES


1. Godinich MJ, Jennings ML. Renal chloride-bicarbonate exchangers. Curr Opin Nephrol Hypertens. 1995 Sep;4(5):398-401.
2. Sterling D, Casey JR. Bicarbonate transport proteins. Biochem Cell Biol. 2002;80(5):483-97.
3. Brosius FC, 3rd, Alper SL, Garcia AM, Lodish HF. The major kidney band 3 gene transcript predicts an amino-terminal truncated band 3 polypeptide. J Biol Chem. 1989 May 15;264(14):7784-7.
4. Zhang D, Kiyatkin A, Bolin JT, Low PS. Crystallographic structure and functional interpretation of the cytoplasmic domain of erythrocyte membrane band 3. Blood. 2000 Nov 1;96(9):2925-33.
5. Tanner MJ. The structure and function of band 3 (AE1): recent developments (review). Mol Membr Biol. 1997 Oct-Dec;14(4):155-65.
6. Schofield AE, Martin PG, Spillett D, Tanner MJ. The structure of the human red blood cell anion exchanger (EPB3, AE1, band 3) gene. Blood. 1994 Sep 15;84(6):2000-12.
7. Fujinaga J, Tang XB, Casey JR. Topology of the membrane domain of human erythrocyte anion exchange protein, AE1. J Biol Chem. 1999 Mar 5;274(10):6626-33.
8. Vince JW, Reithmeier RA. Identification of the carbonic anhydrase II binding site in the $Cl^-/HCO_3^-$ anion exchanger AE1. Biochemistry. 2000 May 9;39(18):5527-33.
9. Low PS. Structure and function of the cytoplasmic domain of band 3: center of erythrocyte membrane-peripheral protein interactions. Biochim Biophys Acta. 1986 Sep 22;864(2):145-67.
10. Wang CC, Moriyama R, Lombardo CR, Low PS. Partial characterization of the cytoplasmic domain of human kidney band 3. J Biol Chem. 1995 Jul 28;270(30):17892-7.

11. Ding Y, Casey JR, Kopito RR. The major kidney AE1 isoform does not bind ankyrin (Ank1) in vitro. An essential role for the 79 $NH_2$-terminal amino acid residues of band 3. J Biol Chem. 1994 Dec 23;269(51):32201-8.
12. Chen J, Vijayakumar S, Li X, Al-Awqati Q. Kanadaptin is a protein that interacts with the kidney but not the erythroid form of band 3. J Biol Chem. 1998 Jan 9;273(2):1038-43.
13. Kittanakom S, Keskanokwong T, Akkarapatumwong V, Yenchitsomanus PT, Reithmeier RA. Human kanadaptin and kidney anion exchanger 1 (kAE1) do not interact in transfected HEK 293 cells. Mol Membr Biol. 2004 Nov-Dec;21(6):395-402.
14. Wongthida P, Akkarapatumwong V, Limjindaporn T, Kittanakom S, Keskanokwong T, Eurwilaichitr L, et al. Analysis of the interaction between human kidney anion exchanger 1 and kanadaptin using yeast two-hybrid systems. Gen Mol Biol. 2006;29(1):14-22.
15. Rodriguez-Soriano J. New insights into the pathogenesis of renal tubular acidosis--from functional to molecular studies. Pediatr Nephrol. 2000 Oct;14(12):1121-36.
16. Alper SL. Genetic diseases of acid-base transporters. Annu Rev Physiol. 2002;64:899-923.
17. Sly WS, Hewett-Emmett D, Whyte MP, Yu YS, Tashian RE. Carbonic anhydrase II deficiency identified as the primary defect in the autosomal recessive syndrome of osteopetrosis with renal tubular acidosis and cerebral calcification. Proc Natl Acad Sci U S A. 1983 May;80(9):2752-6.
18. Kraut JA, Hiura J, Besancon M, Smolka A, Sachs G, Scott D. Effect of hypokalemia on the abundance of HK alpha 1 and HK alpha 2 protein in the rat kidney. Am J Physiol. 1997 Jun;272(6 Pt 2):F744-50.
19. Karet FE. Inherited renal tubular acidosis. Adv Nephrol Necker Hosp. 2000;30:147-62.

20. Bruce LJ, Unwin RJ, Wrong O, Tanner MJ. The association between familial distal renal tubular acidosis and mutations in the red cell anion exchanger (band 3, AE1) gene. Biochem Cell Biol. 1998;76(5):723-8.

21. Sawasdee N, Udomchaiprasertkul W, Noisakran S, Rungroj N, Akkarapatumwong V, Yenchitsomanus PT. Trafficking defect of mutant kidney anion exchanger 1 (kAE1) proteins associated with distal renal tubular acidosis and Southeast Asian ovalocytosis. Biochem Biophys Res Commun. 2006 Nov 24;350(3):723-30.

22. Vasuvattakul S, Yenchitsomanus PT, Vachuanichsanong P, Thuwajit P, Kaitwatcharachai C, Laosombat V, et al. Autosomal recessive distal renal tubular acidosis associated with Southeast Asian ovalocytosis. Kidney Int. 1999 Nov;56(5):1674-82.

23. Quilty JA, Cordat E, Reithmeier RA. Impaired trafficking of human kidney anion exchanger (kAE1) caused by hetero-oligomer formation with a truncated mutant associated with distal renal tubular acidosis. Biochem J. 2002 Dec 15;368(Pt 3):895-903.

24. Toye AM, Banting G, Tanner MJ. Regions of human kidney anion exchanger 1 (kAE1) required for basolateral targeting of kAE1 in polarised kidney cells: mis-targeting explains dominant renal tubular acidosis (dRTA). J Cell Sci. 2004 Mar 15;117(Pt 8):1399-410.

25. Adair-Kirk TL, Dorsey FC, Cox JV. Multiple cytoplasmic signals direct the intracellular trafficking of chicken kidney AE1 anion exchangers in MDCK cells. J Cell Sci. 2003 Feb 15;116(Pt 4):655-63.

26. Busa WB, Nuccitelli R. Metabolic regulation via intracellular pH. Am J Physiol. 1984 Apr;246(4 Pt 2):R409-38.

27. Edmonds BT, Murray J, Condeelis J. pH regulation of the F-actin binding properties of Dictyostelium elongation factor 1 alpha. J Biol Chem. 1995 Jun 23;270(25):15222-30.

28. Ritter M, Woll E, Haussinger D, Lang F. Effects of bradykinin on cell volume and intracellular pH in NIH 3T3 fibroblasts expressing the ras oncogene. FEBS Lett. 1992 Aug 3;307(3):367-70.

29. Joseph D, Tirmizi O, Zhang XL, Crandall ED, Lubman RL. Polarity of alveolar epithelial cell acid-base permeability. Am J Physiol Lung Cell Mol Physiol. 2002 Apr;282(4):L675-83.

30. Nosek TM, Fender KY, Godt RE. It is diprotonated inorganic phosphate that depresses force in skinned skeletal muscle fibers. Science. 1987 Apr 10;236(4798):191-3.

31. Gross E, Abuladze N, Pushkin A, Kurtz I, Cotton CU. The stoichiometry of the electrogenic sodium bicarbonate cotransporter pNBC1 in mouse pancreatic duct cells is 2 $HCO_3^-$:1 $Na^+$. J Physiol. 2001 Mar 1;531(Pt 2):375-82.

32. Adrogue HE, Adrogue HJ. Acid-base physiology. Respir Care. 2001 Apr;46(4):328-41.

33. Mount DB, Romero MF. The SLC26 gene family of multifunctional anion exchangers. Pflugers Arch. 2004 Feb;447(5):710-21.

34. Romero MF, Fulton CM, Boron WF. The SLC4 family of $HCO_3^-$ transporters. Pflugers Arch. 2004 Feb;447(5):495-509.

35. Romero MF. Molecular pathophysiology of SLC4 bicarbonate transporters. Curr Opin Nephrol Hypertens. 2005 Sep;14(5):495-501.

36. Kopito RR, Lodish HF. Primary structure and transmembrane orientation of the murine anion exchange protein. Nature. 1985 Jul 18-24;316(6025):234-8.

37. Alper SL, Kopito RR, Libresco SM, Lodish HF. Cloning and characterization of a murine band 3-related cDNA from kidney and from a lymphoid cell line. J Biol Chem. 1988 Nov 15;263(32):17092-9.

38. Kudrycki KE, Newman PR, Shull GE. cDNA cloning and tissue distribution of mRNAs for two proteins that are related to the band 3 $Cl^-/HCO_3^-$ exchanger. J Biol Chem. 1990 Jan 5;265(1):462-71.

39. Burnham CE, Amlal H, Wang Z, Shull GE, Soleimani M. Cloning and functional expression of a human kidney $Na^+$:$HCO_3^-$ cotransporter. J Biol Chem. 1997 Aug 1;272(31):19111-4.

40. Abuladze N, Lee I, Newman D, Hwang J, Boorer K, Pushkin A, et al. Molecular cloning, chromosomal localization, tissue distribution, and functional

expression of the human pancreatic sodium bicarbonate cotransporter. J Biol Chem. 1998 Jul 10;273(28):17689-95.

41. Bevensee MO, Schmitt BM, Choi I, Romero MF, Boron WF. An electrogenic $Na^+$-$HCO^-_3$ cotransporter (NBC) with a novel COOH-terminus, cloned from rat brain. Am J Physiol Cell Physiol. 2000 Jun;278(6):C1200-11.
42. Choi I, Romero MF, Khandoudi N, Bril A, Boron WF. Cloning and characterization of a human electrogenic $Na^+$-$HCO^-_3$ cotransporter isoform (hhNBC). Am J Physiol. 1999 Mar;276(3 Pt 1):C576-84.
43. Choi I, Aalkjaer C, Boulpaep EL, Boron WF. An electroneutral sodium/bicarbonate cotransporter NBCn1 and associated sodium channel. Nature. 2000 Jun 1;405(6786):571-5.
44. Pushkin A, Abuladze N, Newman D, Lee I, Xu G, Kurtz I. Cloning, characterization and chromosomal assignment of NBC4, a new member of the sodium bicarbonate cotransporter family. Biochim Biophys Acta. 2000 Sep 7;1493(1-2):215-8.
45. Parker MD, Ourmozdi EP, Tanner MJ. Human BTR1, a new bicarbonate transporter superfamily member and human AE4 from kidney. Biochem Biophys Res Commun. 2001 Apr 20;282(5):1103-9.
46. Grichtchenko, II, Romero MF, Boron WF. Extracellular $HCO_3^-$ dependence of electrogenic Na/$HCO_3$ cotransporters cloned from salamander and rat kidney. J Gen Physiol. 2000 May;115(5):533-46.
47. Melvin JE, Park K, Richardson L, Schultheis PJ, Shull GE. Mouse down-regulated in adenoma (DRA) is an intestinal $Cl^-/HCO_3^-$ exchanger and is up-regulated in colon of mice lacking the NHE3 $Na^+/H^+$ exchanger. J Biol Chem. 1999 Aug 6;274(32):22855-61.
48. Soleimani M, Greeley T, Petrovic S, Wang Z, Amlal H, Kopp P, et al. Pendrin: an apical $Cl^-/OH^-/HCO_3^-$ exchanger in the kidney cortex. Am J Physiol Renal Physiol. 2001 Feb;280(2):F356-64.
49. Xie Q, Welch R, Mercado A, Romero MF, Mount DB. Molecular characterization of the murine Slc26a6 anion exchanger: functional comparison with Slc26a1. Am J Physiol Renal Physiol. 2002 Oct;283(4):F826-38.

50. Lohi H, Kujala M, Makela S, Lehtonen E, Kestila M, Saarialho-Kere U, et al. Functional characterization of three novel tissue-specific anion exchangers SLC26A7, -A8, and -A9. J Biol Chem. 2002 Apr 19;277(16):14246-54.

51. Demuth DR, Showe LC, Ballantine M, Palumbo A, Fraser PJ, Cioe L, et al. Cloning and structural characterization of a human non-erythroid band 3-like protein. Embo J. 1986 Jun;5(6):1205-14.

52. Stuart-Tilley A, Sardet C, Pouyssegur J, Schwartz MA, Brown D, Alper SL. Immunolocalization of anion exchanger AE2 and cation exchanger NHE-1 in distinct adjacent cells of gastric mucosa. Am J Physiol. 1994 Feb;266(2 Pt 1):C559-68.

53. Brosius FC, 3rd, Pisoni RL, Cao X, Deshmukh G, Yannoukakos D, Stuart-Tilley AK, et al. AE anion exchanger mRNA and protein expression in vascular smooth muscle cells, aorta, and renal microvessels. Am J Physiol. 1997 Dec;273(6 Pt 2):F1039-47.

54. Sander T, Toliat MR, Heils A, Leschik G, Becker C, Ruschendorf F, et al. Association of the 867Asp variant of the human anion exchanger 3 gene with common subtypes of idiopathic generalized epilepsy. Epilepsy Res. 2002 Oct;51(3):249-55.

55. Tsuganezawa H, Kobayashi K, Iyori M, Araki T, Koizumi A, Watanabe S, et al. A new member of the $HCO_3^-$ transporter superfamily is an apical anion exchanger of beta-intercalated cells in the kidney. J Biol Chem. 2001 Mar 16;276(11):8180-9.

56. Parker MD, Boron WF, Tanner MJ. Characterization of human AE4 as an electroneutral, sodium-dependent bicarbonate transporter. FASEB J. 2002;16:A796.

57. Tanner MJ, Martin PG, High S. The complete amino acid sequence of the human erythrocyte membrane anion-transport protein deduced from the cDNA sequence. Biochem J. 1988 Dec 15;256(3):703-12.

58. Lux SE, John KM, Kopito RR, Lodish HF. Cloning and characterization of band 3, the human erythrocyte anion-exchange protein (AE1). Proc Natl Acad Sci U S A. 1989 Dec;86(23):9089-93.

59. Hubner S, Michel F, Rudloff V, Appelhans H. Amino acid sequence of band-3 protein from rainbow trout erythrocytes derived from cDNA. Biochem J. 1992 Jul 1;285 ( Pt 1):17-23.

60. Kim HR, Yew NS, Ansorge W, Voss H, Schwager C, Vennstrom B, et al. Two different mRNAs are transcribed from a single genomic locus encoding the chicken erythrocyte anion transport proteins (band 3). Mol Cell Biol. 1988 Oct;8(10):4416-24.

61. Showe LC, Ballantine M, Huebner K. Localization of the gene for the erythroid anion exchange protein, band 3 (EMPB3), to human chromosome 17. Genomics. 1987 Sep;1(1):71-6.

62. Sahr KE, Taylor WM, Daniels BP, Rubin HL, Jarolim P. The structure and organization of the human erythroid anion exchanger (AE1) gene. Genomics. 1994 Dec;24(3):491-501.

63. Shayakul C, Alper SL. Defects in processing and trafficking of the AE1 $Cl^-$ /$HCO_3^-$ exchanger associated with inherited distal renal tubular acidosis. Clin Exp Nephrol. 2004 Mar;8(1):1-11.

64. Chang SH, Low PS. Identification of a critical ankyrin-binding loop on the cytoplasmic domain of erythrocyte membrane band 3 by crystal structure analysis and site-directed mutagenesis. J Biol Chem. 2003 Feb 28;278(9):6879-84.

65. Fukuda M, Dell A, Oates JE, Fukuda MN. Structure of branched lactosaminoglycan, the carbohydrate moiety of band 3 isolated from adult human erythrocytes. J Biol Chem. 1984 Jul 10;259(13):8260-73.

66. Willardson BM, Thevenin BJ, Harrison ML, Kuster WM, Benson MD, Low PS. Localization of the ankyrin-binding site on erythrocyte membrane protein, band 3. J Biol Chem. 1989 Sep 25;264(27):15893-9.

67. Mawby WJ, Findlay JB. Characterization and partial sequence of di-iodosulphophenyl isothiocyanate-binding peptide from human erythrocyte anion-transport protein. Biochem J. 1982 Sep 1;205(3):465-75.

68. Jennings ML, Anderson MP, Monaghan R. Monoclonal antibodies against human erythrocyte band 3 protein. Localization of proteolytic cleavage

sites and stilbenedisulfonate-binding lysine residues. J Biol Chem. 1986 Jul 5;261(19):9002-10.

69. Erickson HK. Cytoplasmic disposition of aspartate 821 in anion exchanger from human erythrocytes. Biochemistry. 1997 Aug 19;36(33):9958-67.

70. Popov M, Tam LY, Li J, Reithmeier RA. Mapping the ends of transmembrane segments in a polytopic membrane protein. Scanning N-glycosylation mutagenesis of extracytosolic loops in the anion exchanger, band 3. J Biol Chem. 1997 Jul 18;272(29):18325-32.

71. Popov M, Li J, Reithmeier RA. Transmembrane folding of the human erythrocyte anion exchanger (AE1, Band 3) determined by scanning and insertional N-glycosylation mutagenesis. Biochem J. 1999 Apr 15;339 ( Pt 2):269-79.

72. Tang XB, Fujinaga J, Kopito R, Casey JR. Topology of the region surrounding Glu681 of human AE1 protein, the erythrocyte anion exchanger. J Biol Chem. 1998 Aug 28;273(35):22545-53.

73. Oikawa K, Lieberman DM, Reithmeier RA. Conformation and stability of the anion transport protein of human erythrocyte membranes. Biochemistry. 1985 Jun 4;24(12):2843-8.

74. Vince JW, Reithmeier RA. Carbonic anhydrase II binds to the carboxyl terminus of human band 3, the erythrocyte $C1^-/HCO_3^-$ exchanger. J Biol Chem. 1998 Oct 23;273(43):28430-7.

75. Sterling D, Casey JR. Transport activity of AE3 chloride/bicarbonate anion-exchange proteins and their regulation by intracellular pH. Biochem J. 1999 Nov 15;344 Pt 1:221-9.

76. Yannoukakos D, Meyer HE, Vasseur C, Driancourt C, Wajcman H, Bursaux E. Three regions of erythrocyte band 3 protein are phosphorylated on tyrosines: characterization of the phosphorylation sites by solid phase sequencing combined with capillary electrophoresis. Biochim Biophys Acta. 1991 Jul 1;1066(1):70-6.

77. Cordat E, Li J, Reithmeier RA. Carboxyl-terminal truncations of human anion exchanger impair its trafficking to the plasma membrane. Traffic. 2003 Sep;4(9):642-51.

78. Fu GH, Wang Y, Xi YH, Shen WW, Pan XY, Shen WZ, et al. Direct interaction and cooperative role of tumor suppressor p16 with band 3 (AE1). FEBS Lett. 2005 Apr 11;579(10):2105-10.

79. Chang H, Langer PJ, Lodish HF. Asynchronous synthesis of erythrocyte membrane proteins. Proc Natl Acad Sci U S A. 1976 Sep;73(9):3206-10.

80. Lehnert ME, Lodish HF. Unequal synthesis and differential degradation of alpha and β-spectrin during murine erythroid differentiation. J Cell Biol. 1988 Aug;107(2):413-26.

81. Light ND, Tanner MJ. Erythrocyte membrane proteins. Sequential accumulation in the membrane during reticulocyte maturation. Biochim Biophys Acta. 1978 Apr 20;508(3):571-6.

82. Foxwell BM, Tanner MJ. Synthesis of the erythrocyte anion-transport protein. Immunochemical study of its incorporation into the plasma membrane of erythroid cells. Biochem J. 1981 Apr 1;195(1):129-37.

83. Wainwright SD, Tanner MJ, Martin GE, Yendle JE, Holmes C. Monoclonal antibodies to the membrane domain of the human erythrocyte anion transport protein. Localization of the C-terminus of the protein to the cytoplasmic side of the red cell membrane and distribution of the protein in some human tissues. Biochem J. 1989 Feb 15;258(1):211-20.

84. Fukuda M, Fukuda MN, Papayannopoulou T, Hakomori S. Membrane differentiation in human erythroid cells: unique profiles of cell surface glycoproteins expressed in erythroblasts *in vitro* from three ontogenic stages. Proc Natl Acad Sci U S A. 1980 Jun;77(6):3474-8.

85. Okubo K, Hamasaki N, Hara K, Kageura M. Palmitoylation of cysteine 69 from the COOH-terminal of band 3 protein in the human erythrocyte membrane. Acylation occurs in the middle of the consensus sequence of F--I-IICLAVL found in band 3 protein and G2 protein of Rift Valley fever virus. J Biol Chem. 1991 Sep 5;266(25):16420-4.

86. Popov M, Reithmeier RA. Calnexin interaction with N-glycosylation mutants of a polytopic membrane glycoprotein, the human erythrocyte anion exchanger 1 (band 3). J Biol Chem. 1999 Jun 18;274(25):17635-42.

87. Braell WA, Lodish HF. Biosynthesis of the erythrocyte anion transport protein. J Biol Chem. 1981 Nov 10;256(21):11337-44.

88. Li J, Quilty J, Popov M, Reithmeier RA. Processing of N-linked oligosaccharide depends on its location in the anion exchanger, AE1, membrane glycoprotein. Biochem J. 2000 Jul 1;349(Pt 1):51-7.

89. Kang D, Karbach D, Passow H. Anion transport function of mouse erythroid band 3 protein (AE1) does not require acylation of cysteine residue 861. Biochim Biophys Acta. 1994 Sep 14;1194(2):341-4.

90. Casey JR, Ding Y, Kopito RR. The role of cysteine residues in the erythrocyte plasma membrane anion exchange protein, AE1. J Biol Chem. 1995 Apr 14;270(15):8521-7.

91. Groves JD, Tanner MJ. Glycophorin A facilitates the expression of human band 3-mediated anion transport in *Xenopus* oocytes. J Biol Chem. 1992 Nov 5;267(31):22163-70.

92. Groves JD, Tanner MJ. The effects of glycophorin A on the expression of the human red cell anion transporter (band 3) in *Xenopus* oocytes. J Membr Biol. 1994 May;140(1):81-8.

93. Young MT, Beckmann R, Toye AM, Tanner MJ. Red-cell glycophorin A-band 3 interactions associated with the movement of band 3 to the cell surface. Biochem J. 2000 Aug 15;350 Pt 1:53-60.

94. Hassoun H, Hanada T, Lutchman M, Sahr KE, Palek J, Hanspal M, et al. Complete deficiency of glycophorin A in red blood cells from mice with targeted inactivation of the band 3 (AE1) gene. Blood. 1998 Mar 15;91(6):2146-51.

95. Auffray I, Marfatia S, de Jong K, Lee G, Huang CH, Paszty C, et al. Glycophorin A dimerization and band 3 interaction during erythroid membrane biogenesis: *in vivo* studies in human glycophorin A transgenic mice. Blood. 2001 May 1;97(9):2872-8.

96. Adair-Kirk TL, Cox KH, Cox JV. Intracellular trafficking of variant chicken kidney AE1 anion exchangers: role of alternative $NH_2$ termini in polarized sorting and Golgi recycling. J Cell Biol. 1999 Dec 13;147(6):1237-48.

97. Ghosh S, Cox KH, Cox JV. Chicken erythroid AE1 anion exchangers associate with the cytoskeleton during recycling to the Golgi. Mol Biol Cell. 1999 Feb;10(2):455-69.

98. Reithmeier RA. A membrane metabolon linking carbonic anhydrase with chloride/bicarbonate anion exchangers. Blood Cells Mol Dis. 2001 Jan-Feb;27(1):85-9.

99. Jennings ML. Oligomeric structure and the anion transport function of human erythrocyte band 3 protein. J Membr Biol. 1984;80(2):105-17.

100. Sekler I, Lo RS, Kopito RR. A conserved glutamate is responsible for ion selectivity and pH dependence of the mammalian anion exchangers AE1 and AE2. J Biol Chem. 1995 Dec 1;270(48):28751-8.

101. Parkes JL, Coleman PS. Enhancement of carbonic anhydrase activity by erythrocyte membranes. Arch Biochem Biophys. 1989 Dec;275(2):459-68.

102. Sterling D, Reithmeier RA, Casey JR. Carbonic anhydrase: in the driver's seat for bicarbonate transport. Jop. 2001 Jul;2(4 Suppl):165-70.

103. Casey JR, Reithmeier RA. Analysis of the oligomeric state of Band 3, the anion transport protein of the human erythrocyte membrane, by size exclusion high performance liquid chromatography. Oligomeric stability and origin of heterogeneity. J Biol Chem. 1991 Aug 25;266(24):15726-37.

104. Cox JV, Stack JH, Lazarides E. Erythroid anion transporter assembly is mediated by a developmentally regulated recruitment onto a preassembled membrane cytoskeleton. J Cell Biol. 1987 Sep;105(3):1405-16.

105. Hanspal M, Hanspal JS, Kalraiya R, Palek J. The expression and synthesis of the band 3 protein initiates the formation of a stable membrane skeleton in murine Rauscher-transformed erythroid cells. Eur J Cell Biol. 1992 Aug;58(2):313-8.

106. Hanspal M, Palek J. Biogenesis of normal and abnormal red blood cell membrane skeleton. Semin Hematol. 1992 Oct;29(4):305-19.

107. Liu SC, Palek J, Yi SJ, Nichols PE, Derick LH, Chiou SS, et al. Molecular basis of altered red blood cell membrane properties in Southeast Asian

ovalocytosis: role of the mutant band 3 protein in band 3 oligomerization and retention by the membrane skeleton. Blood. 1995 Jul 1;86(1):349-58.

108. Gilligan DM, Bennett V. The junctional complex of the membrane skeleton. Semin Hematol. 1993 Jan;30(1):74-83.
109. Bennett V, Stenbuck PJ. The membrane attachment protein for spectrin is associated with band 3 in human erythrocyte membranes. Nature. 1979 Aug 9;280(5722):468-73.
110. Bennett V, Stenbuck PJ. Association between ankyrin and the cytoplasmic domain of band 3 isolated from the human erythrocyte membrane. J Biol Chem. 1980 Jul 10;255(13):6424-32.
111. Korsgren C, Cohen CM. Associations of human erythrocyte band 4.2. Binding to ankyrin and to the cytoplasmic domain of band 3. J Biol Chem. 1988 Jul 25;263(21):10212-8.
112. Rybicki AC, Heath R, Wolf JL, Lubin B, Schwartz RS. Deficiency of protein 4.2 in erythrocytes from a patient with a Coombs negative hemolytic anemia. Evidence for a role of protein 4.2 in stabilizing ankyrin on the membrane. J Clin Invest. 1988 Mar;81(3):893-901.
113. Peters LL, Shivdasani RA, Liu SC, Hanspal M, John KM, Gonzalez JM, et al. Anion exchanger 1 (band 3) is required to prevent erythrocyte membrane surface loss but not to form the membrane skeleton. Cell. 1996 Sep 20;86(6):917-27.
114. Anderson RA, Marchesi VT. Regulation of the association of membrane skeletal protein 4.1 with glycophorin by a polyphosphoinositide. Nature. 1985 Nov 21-27;318(6043):295-8.
115. Lombardo CR, Willardson BM, Low PS. Localization of the protein 4.1-binding site on the cytoplasmic domain of erythrocyte membrane band 3. J Biol Chem. 1992 May 15;267(14):9540-6.
116. Bennett V. The membrane skeleton of human erythrocytes and its implications for more complex cells. Annu Rev Biochem. 1985;54:273-304.

117. Korsgren C, Cohen CM. Purification and properties of human erythrocyte band 4.2. Association with the cytoplasmic domain of band 3. J Biol Chem. 1986 Apr 25;261(12):5536-43.

118. Tanner MJ. Band 3 anion exchanger and its involvement in erythrocyte and kidney disorders. Curr Opin Hematol. 2002 Mar;9(2):133-9.

119. Bracher NA, Lyons CA, Wessels G, Mansvelt E, Coetzer TL. Band 3 Cape Town (E90K) causes severe hereditary spherocytosis in combination with band 3 Prague III. Br J Haematol. 2001 Jun;113(3):689-93.

120. Yu J, Steck TL. Isolation and characterization of band 3, the predominant polypeptide of the human erythrocyte membrane. J Biol Chem. 1975 Dec 10;250(23):9170-5.

121. Murthy SN, Liu T, Kaul RK, Kohler H, Steck TL. The aldolase-binding site of the human erythrocyte membrane is at the $NH_2$ terminus of band 3. J Biol Chem. 1981 Nov 10;256(21):11203-8.

122. Higashi T, Richards CS, Uyeda K. The interaction of phosphofructokinase with erythrocyte membranes. J Biol Chem. 1979 Oct 10;254(19):9542-50.

123. Salhany JM. Binding of cytosolic proteins to the erythrocyte membrane. J Cell Biochem. 1983;23(1-4):211-22.

124. Jenkins JD, Madden DP, Steck TL. Association of phosphofructokinase and aldolase with the membrane of the intact erythrocyte. J Biol Chem. 1984 Aug 10;259(15):9374-8.

125. Low PS, Rathinavelu P, Harrison ML. Regulation of glycolysis via reversible enzyme binding to the membrane protein, band 3. J Biol Chem. 1993 Jul 15;268(20):14627-31.

126. Green DE, Murer E, Hultin HO, Richardson SH, Salmon B, Brierley GP, et al. Association of integrated metabolic pathways with membranes. I. Glycolytic enzymes of the red blood corpuscle and yeast. Arch Biochem Biophys. 1965 Dec;112(3):635-47.

127. Walder JA, Chatterjee R, Steck TL, Low PS, Musso GF, Kaiser ET, et al. The interaction of hemoglobin with the cytoplasmic domain of band 3 of the human erythrocyte membrane. J Biol Chem. 1984 Aug 25;259(16):10238-46.

128. Murthy SN, Kaul RK, Kohler H. Hemoglobin binds to the amino-terminal 23-residue fragment of human erythrocyte band 3 protein. Hoppe Seylers Z Physiol Chem. 1984 Jan;365(1):9-17.

129. Chetrite G, Cassoly R. Affinity of hemoglobin for the cytoplasmic fragment of human erythrocyte membrane band 3. Equilibrium measurements at physiological pH using matrix-bound proteins: the effects of ionic strength, deoxygenation and of 2,3-diphosphoglycerate. J Mol Biol. 1985 Oct 5;185(3):639-44.

130. Kannan R, Labotka R, Low PS. Isolation and characterization of the hemichrome-stabilized membrane protein aggregates from sickle erythrocytes. Major site of autologous antibody binding. J Biol Chem. 1988 Sep 25;263(27):13766-73.

131. Kannan R, Yuan J, Low PS. Isolation and partial characterization of antibody- and globin-enriched complexes from membranes of dense human erythrocytes. Biochem J. 1991 Aug 15;278 ( Pt 1):57-62.

132. Mandal D, Moitra PK, Saha S, Basu J. Caspase 3 regulates phosphatidylserine externalization and phagocytosis of oxidatively stressed erythrocytes. FEBS Lett. 2002 Feb 27;513(2-3):184-8.

133. Schulze-Osthoff K, Walczak H, Droge W, Krammer PH. Cell nucleus and DNA fragmentation are not required for apoptosis. J Cell Biol. 1994 Oct;127(1):15-20.

134. Kasahara M, Hinkle PC. Reconstitution and purification of the D-glucose transporter from human erythrocytes. J Biol Chem. 1977 Oct 25;252(20):7384-90.

135. Cairns MT, Alvarez J, Panico M, Gibbs AF, Morris HR, Chapman D, et al. Investigation of the structure and function of the human erythrocyte glucose transporter by proteolytic dissection. Biochim Biophys Acta. 1987 Dec 11;905(2):295-310.

136. Jiang W, Ding Y, Su Y, Jiang M, Hu X, Zhang Z. Interaction of glucose transporter 1 with anion exchanger 1 in vitro. Biochem Biophys Res Commun. 2006 Jan 27;339(4):1255-61.

137. Nigg EA, Bron C, Girardet M, Cherry RJ. Band 3-glycophorin A association in erythrocyte membrane demonstrated by combining protein diffusion measurements with antibody-induced cross-linking. Biochemistry. 1980 Apr 29;19(9):1887-93.

138. Che A, Cherry RJ. Loss of rotational mobility of band 3 proteins in human erythrocyte membranes induced by antibodies to glycophorin A. Biophys J. 1995 May;68(5):1881-7.

139. Minami R, Muta K, Umemura T, Motomura S, Abe Y, Nishimura J, et al. p16(INK4a) induces differentiation and apoptosis in erythroid lineage cells. Exp Hematol. 2003 May;31(5):355-62.

140. Kollert-Jons A, Wagner S, Hubner S, Appelhans H, Drenckhahn D. Anion exchanger 1 in human kidney and oncocytoma differs from erythroid AE1 in its $NH_2$ terminus. Am J Physiol. 1993 Dec;265(6 Pt 2):F813-21.

141. Igarashi T, Sekine T, Watanabe H. Molecular basis of proximal renal tubular acidosis. J Nephrol. 2002 Mar-Apr;15 Suppl 5:S135-41.

142. Igarashi T, Sekine T, Inatomi J, Seki G. Unraveling the molecular pathogenesis of isolated proximal renal tubular acidosis. J Am Soc Nephrol. 2002 Aug;13(8):2171-7.

143. Capasso G, Unwin R, Rizzo M, Pica A, Giebisch G. Bicarbonate transport along the loop of Henle: molecular mechanisms and regulation. J Nephrol. 2002 Mar-Apr;15 Suppl 5:S88-96.

144. Unwin RJ, Shirley DG, Capasso G. Urinary acidification and distal renal tubular acidosis. J Nephrol. 2002 Mar-Apr;15 Suppl 5:S142-50.

145. Boron WF. Sodium-coupled bicarbonate transporters. Jop. 2001 Jul;2(4 Suppl):176-81.

146. Verlander JW, Madsen KM, Low PS, Allen DP, Tisher CC. Immunocytochemical localization of band 3 protein in the rat collecting duct. Am J Physiol. 1988 Jul;255(1 Pt 2):F115-25.

147. Wagner S, Vogel R, Lietzke R, Koob R, Drenckhahn D. Immunochemical characterization of a band 3-like anion exchanger in collecting duct of human kidney. Am J Physiol. 1987 Aug;253(2 Pt 2):F213-21.

148. Yenchitsomanus P, Kittanakom S, Rungroj N, Cordat E, Reithmeier RA. Molecular mechanisms of autosomal dominant and recessive distal renal tubular acidosis caused by SLC4A1 (AE1) mutations. Journal of Molecular and Genetic Medicine. 2005;1(2):49-62.

149. Passow H. Molecular aspects of band 3 protein-mediated anion transport across the red blood cell membrane. Rev Physiol Biochem Pharmacol. 1986;103:61-203.

150. Wrong O, Bruce LJ, Unwin RJ, Toye AM, Tanner MJ. Band 3 mutations, distal renal tubular acidosis, and Southeast Asian ovalocytosis. Kidney Int. 2002 Jul;62(1):10-9.

151. Yenchitsomanus PT. Human anion exchanger1 mutations and distal renal tubular acidosis. Southeast Asian J Trop Med Public Health. 2003 Sep;34(3):651-8.

152. Rungroj N, Devonald MA, Cuthbert AW, Reimann F, Akkarapatumwong V, Yenchitsomanus PT, et al. A novel missense mutation in AE1 causing autosomal dominant distal renal tubular acidosis retains normal transport function but is mistargeted in polarized epithelial cells. J Biol Chem. 2004 Apr 2;279(14):13833-8.

153. Kittanakom S, Cordat E, Akkarapatumwong V, Yenchitsomanus PT, Reithmeier RA. Trafficking defects of a novel autosomal recessive distal renal tubular acidosis mutant (S773P) of the human kidney anion exchanger (kAE1). J Biol Chem. 2004 Sep 24;279(39):40960-71.

154. Bruce LJ, Cope DL, Jones GK, Schofield AE, Burley M, Povey S, et al. Familial distal renal tubular acidosis is associated with mutations in the red cell anion exchanger (Band 3, AE1) gene. J Clin Invest. 1997 Oct 1;100(7):1693-707.

155. Jarolim P, Shayakul C, Prabakaran D, Jiang L, Stuart-Tilley A, Rubin HL, et al. Autosomal dominant distal renal tubular acidosis is associated in three families with heterozygosity for the R589H mutation in the AE1 (band 3) $Cl^-/HCO_3^-$ exchanger. J Biol Chem. 1998 Mar 13;273(11):6380-8.

156. Quilty JA, Li J, Reithmeier RA. Impaired trafficking of distal renal tubular acidosis mutants of the human kidney anion exchanger kAE1. Am J Physiol Renal Physiol. 2002 May;282(5):F810-20.

157. Devonald MA, Smith AN, Poon JP, Ihrke G, Karet FE. Non-polarized targeting of AE1 causes autosomal dominant distal renal tubular acidosis. Nat Genet. 2003 Feb;33(2):125-7.

158. Yenchitsomanus PT, Vasuvattakul S, Kirdpon S, Wasanawatana S, Susaengrat W, Sreethiphayawan S, et al. Autosomal recessive distal renal tubular acidosis caused by G701D mutation of anion exchanger 1 gene. Am J Kidney Dis. 2002 Jul;40(1):21-9.

159. Yenchitsomanus PT, Sawasdee N, Paemanee A, Keskanokwong T, Vasuvattakul S, Bejrachandra S, et al. Anion exchanger 1 mutations associated with distal renal tubular acidosis in the Thai population. J Hum Genet. 2003;48(9):451-6.

160. Sritippayawan S, Sumboonnanonda A, Vasuvattakul S, Keskanokwong T, Sawasdee N, Paemanee A, et al. Novel compound heterozygous SLC4A1 mutations in Thai patients with autosomal recessive distal renal tubular acidosis. Am J Kidney Dis. 2004 Jul;44(1):64-70.

161. Bruce LJ, Wrong O, Toye AM, Young MT, Ogle G, Ismail Z, et al. Band 3 mutations, renal tubular acidosis and South-East Asian ovalocytosis in Malaysia and Papua New Guinea: loss of up to 95% band 3 transport in red cells. Biochem J. 2000 Aug 15;350 Pt 1:41-51.

162. Tanphaichitr VS, Sumboonnanonda A, Ideguchi H, Shayakul C, Brugnara C, Takao M, et al. Novel AE1 mutations in recessive distal renal tubular acidosis. Loss-of-function is rescued by glycophorin A. J Clin Invest. 1998 Dec 15;102(12):2173-9.

163. Matter K, Hunziker W, Mellman I. Basolateral sorting of LDL receptor in MDCK cells: the cytoplasmic domain contains two tyrosine-dependent targeting determinants. Cell. 1992 Nov 27;71(5):741-53.

164. Honing S, Hunziker W. Cytoplasmic determinants involved in direct lysosomal sorting, endocytosis, and basolateral targeting of rat lgp120 (lamp-I) in MDCK cells. J Cell Biol. 1995 Feb;128(3):321-32.

165. Hunziker W, Fumey C. A di-leucine motif mediates endocytosis and basolateral sorting of macrophage IgG Fc receptors in MDCK cells. Embo J. 1994 Jul 1;13(13):2963-9.

166. Lin SH, Cheema-Dhadli S, Gowrishankar M, Marliss EB, Kamel KS, Halperin ML. Control of excretion of potassium: lessons from studies during prolonged total fasting in human subjects. Am J Physiol. 1997 Nov;273(5 Pt 2):F796-800.

167. Canfield WM, Johnson KF, Ye RD, Gregory W, Kornfeld S. Localization of the signal for rapid internalization of the bovine cation-independent mannose 6-phosphate/insulin-like growth factor-II receptor to amino acids 24-29 of the cytoplasmic tail. J Biol Chem. 1991 Mar 25;266(9):5682-8.

168. Bonifacino JS, Traub LM. Signals for sorting of transmembrane proteins to endosomes and lysosomes. Annu Rev Biochem. 2003;72:395-447.

169. Ohno H, Tomemori T, Nakatsu F, Okazaki Y, Aguilar RC, Foelsch H, et al. Mu1B, a novel adaptor medium chain expressed in polarized epithelial cells. FEBS Lett. 1999 Apr 23;449(2-3):215-20.

170. Toye AM. Defective kidney anion-exchanger 1 (AE1, Band 3) trafficking in dominant distal renal tubular acidosis (dRTA). Biochem Soc Symp. 2005(72):47-63.

171. Brown D, Sabolic I, Gluck S. Colchicine-induced redistribution of proton pumps in kidney epithelial cells. Kidney Int Suppl. 1991 Jul;33:S79-83.

172. Lafont F, Burkhardt JK, Simons K. Involvement of microtubule motors in basolateral and apical transport in kidney cells. Nature. 1994 Dec 22-29;372(6508):801-3.

173. Schroer TA, Sheetz MP. Functions of microtubule-based motors. Annu Rev Physiol. 1991;53:629-52.

174. Brown D, Stow JL. Protein trafficking and polarity in kidney epithelium: from cell biology to physiology. Physiol Rev. 1996 Jan;76(1):245-97.

175. Cheney RE, Mooseker MS. Unconventional myosins. Curr Opin Cell Biol. 1992 Feb;4(1):27-35.

176. Fath KR, Mamajiwalla SN, Burgess DR. The cytoskeleton in development of epithelial cell polarity. J Cell Sci Suppl. 1993;17:65-73.
177. Fausser JL, Ungewickell E, Ruch JV, Lesot H. Interaction of vinculin with the clathrin heavy chain. J Biochem (Tokyo). 1993 Oct;114(4):498-503.
178. Rogers SL, Gelfand VI. Myosin cooperates with microtubule motors during organelle transport in melanophores. Curr Biol. 1998 Jan 29;8(3):161-4.
179. Hubner S, Jans DA, Xiao CY, John AP, Drenckhahn D. Signal- and importin-dependent nuclear targeting of the kidney anion exchanger 1-binding protein kanadaptin. Biochem J. 2002 Jan 15;361(Pt 2):287-96.
180. Hubner S, Bahr C, Gossmann H, Efthymiadis A, Drenckhahn D. Mitochondrial and nuclear localization of kanadaptin. Eur J Cell Biol. 2003 May;82(5):240-52.
181. Haass NK, Kartenbeck MA, Leube RE. Pantophysin is a ubiquitously expressed synaptophysin homologue and defines constitutive transport vesicles. J Cell Biol. 1996 Aug;134(3):731-46.
182. Windoffer R, Borchert-Stuhltrager M, Haass NK, Thomas S, Hergt M, Bulitta CJ, et al. Tissue expression of the vesicle protein pantophysin. Cell Tissue Res. 1999 Jun;296(3):499-510.
183. Brooks CC, Scherer PE, Cleveland K, Whittemore JL, Lodish HF, Cheatham B. Pantophysin is a phosphoprotein component of adipocyte transport vesicles and associates with GLUT4-containing vesicles. J Biol Chem. 2000 Jan 21;275(3):2029-36.
184. Bradley RL, Cleveland KA, Cheatham B. The adipocyte as a secretory organ: mechanisms of vesicle transport and secretory pathways. Recent Prog Horm Res. 2001;56:329-58.
185. Delcommenne M, Tan C, Gray V, Rue L, Woodgett J, Dedhar S. Phosphoinositide-3-OH kinase-dependent regulation of glycogen synthase kinase 3 and protein kinase B/AKT by the integrin-linked kinase. Proc Natl Acad Sci U S A. 1998 Sep 15;95(19):11211-6.
186. Hannigan GE, Leung-Hagesteijn C, Fitz-Gibbon L, Coppolino MG, Radeva G, Filmus J, et al. Regulation of cell adhesion and anchorage-dependent

growth by a new β 1-integrin-linked protein kinase. Nature. 1996 Jan 4;379(6560):91-6.

187. Brakebusch C, Bouvard D, Stanchi F, Sakai T, Fassler R. Integrins in invasive growth. J Clin Invest. 2002 Apr;109(8):999-1006.

188. Giancotti FG, Ruoslahti E. Integrin signaling. Science. 1999 Aug 13;285(5430):1028-32.

189. Wu C, Dedhar S. Integrin-linked kinase (ILK) and its interactors: a new paradigm for the coupling of extracellular matrix to actin cytoskeleton and signaling complexes. J Cell Biol. 2001 Nov 12;155(4):505-10.

190. Tu Y, Li F, Goicoechea S, Wu C. The LIM-only protein PINCH directly interacts with integrin-linked kinase and is recruited to integrin-rich sites in spreading cells. Mol Cell Biol. 1999 Mar;19(3):2425-34.

191. Nikolopoulos SN, Turner CE. Molecular dissection of actopaxin-integrin-linked kinase-Paxillin interactions and their role in subcellular localization. J Biol Chem. 2002 Jan 11;277(2):1568-75.

192. Tu Y, Huang Y, Zhang Y, Hua Y, Wu C. A new focal adhesion protein that interacts with integrin-linked kinase and regulates cell adhesion and spreading. J Cell Biol. 2001 Apr 30;153(3):585-98.

193. Mongroo PS, Johnstone CN, Naruszewicz I, Leung-Hagesteijn C, Sung RK, Carnio L, et al. β-parvin inhibits integrin-linked kinase signaling and is downregulated in breast cancer. Oncogene. 2004 Nov 25;23(55):8959-70.

194. Yamaji S, Suzuki A, Kanamori H, Mishima W, Yoshimi R, Takasaki H, et al. Affixin interacts with α-actinin and mediates integrin signaling for reorganization of F-actin induced by initial cell-substrate interaction. J Cell Biol. 2004 May 24;165(4):539-51.

195. Zhang Y, Chen K, Tu Y, Wu C. Distinct roles of two structurally closely related focal adhesion proteins, α-parvins and β-parvins, in regulation of cell morphology and survival. J Biol Chem. 2004 Oct 1;279(40):41695-705.

196. Khyrul WA, LaLonde DP, Brown MC, Levinson H, Turner CE. The integrin-linked kinase regulates cell morphology and motility in a rho-associated kinase-dependent manner. J Biol Chem. 2004 Dec 24;279(52):54131-9.

197. Rosenberger G, Jantke I, Gal A, Kutsche K. Interaction of αPIX (ARHGEF6) with β-parvin (PARVB) suggests an involvement of αPIX in integrin-mediated signaling. Hum Mol Genet. 2003 Jan 15;12(2):155-67.
198. Brakebusch C, Fassler R. The integrin-actin connection, an eternal love affair. Embo J. 2003 May 15;22(10):2324-33.
199. Mishima W, Suzuki A, Yamaji S, Yoshimi R, Ueda A, Kaneko T, et al. The first CH domain of affixin activates Cdc42 and Rac1 through αPIX, a Cdc42/Rac1-specific guanine nucleotide exchanging factor. Genes Cells. 2004 Mar;9(3):193-204.
200. Etienne-Manneville S, Hall A. Rho GTPases in cell biology. Nature. 2002 Dec 12;420(6916):629-35.
201. Tu Y, Li F, Wu C. Nck-2, a novel Src homology2/3-containing adaptor protein that interacts with the LIM-only protein PINCH and components of growth factor receptor kinase-signaling pathways. Mol Biol Cell. 1998 Dec;9(12):3367-82.
202. Wu C. Integrin-linked kinase and PINCH: partners in regulation of cell-extracellular matrix interaction and signal transduction. J Cell Sci. 1999 Dec;112 ( Pt 24):4485-9.
203. Tu Y, Kucik DF, Wu C. Identification and kinetic analysis of the interaction between Nck-2 and DOCK180. FEBS Lett. 2001 Mar 2;491(3):193-9.
204. Brugnera E, Haney L, Grimsley C, Lu M, Walk SF, Tosello-Trampont AC, et al. Unconventional Rac-GEF activity is mediated through the Dock180-ELMO complex. Nat Cell Biol. 2002 Aug;4(8):574-82.
205. Nikolopoulos SN, Turner CE. Actopaxin, a new focal adhesion protein that binds paxillin LD motifs and actin and regulates cell adhesion. J Cell Biol. 2000 Dec 25;151(7):1435-48.
206. Nikolopoulos SN, Turner CE. Integrin-linked kinase (ILK) binding to paxillin LD1 motif regulates ILK localization to focal adhesions. J Biol Chem. 2001 Jun 29;276(26):23499-505.
207. Turner CE. Paxillin. Int J Biochem Cell Biol. 1998 Sep;30(9):955-9.
208. Turner CE, Glenney JR, Jr., Burridge K. Paxillin: a new vinculin-binding protein present in focal adhesions. J Cell Biol. 1990 Sep;111(3):1059-68.

209. Turner CE. Paxillin and focal adhesion signalling. Nat Cell Biol. 2000 Dec;2(12):E231-6.

210. Persad S, Dedhar S. The role of integrin-linked kinase (ILK) in cancer progression. Cancer Metastasis Rev. 2003 Dec;22(4):375-84.

211. Inoue H, Nojima H, Okayama H. High efficiency transformation of Escherichia coli with plasmids. Gene. 1990 Nov 30;96(1):23-8.

212. Del Sal G, Manfioletti G, Schneider C. The CTAB-DNA precipitation method: a common mini-scale preparation of template DNA from phagemids, phages or plasmids suitable for sequencing. Biotechniques. 1989 May;7(5):514-20.

213. Gietz D, St Jean A, Woods RA, Schiestl RH. Improved method for high efficiency transformation of intact yeast cells. Nucleic Acids Res. 1992 Mar 25;20(6):1425.

214. Laemmli UK. Cleavage of structural proteins during the assembly of the head of bacteriophage T4. Nature. 1970 Aug 15;227(5259):680-5.

215. Ling M, Merante F, Robinson BH. A rapid and reliable DNA preparation method for screening a large number of yeast clones by polymerase chain reaction. Nucleic Acids Res. 1995 Dec 11;23(23):4924-5.

216. Ruetz S, Lindsey AE, Ward CL, Kopito RR. Functional activation of plasma membrane anion exchangers occurs in a pre-Golgi compartment. J Cell Biol. 1993 Apr;121(1):37-48.

217. Thomas JA, Buchsbaum RN, Zimniak A, Racker E. Intracellular pH measurements in Ehrlich ascites tumor cells utilizing spectroscopic probes generated in situ. Biochemistry. 1979 May 29;18(11):2210-8.

218. Ballweber E, Hannappel E, Huff T, Stephan H, Haener M, Taschner N, et al. Polymerisation of chemically cross-linked actin:thymosin β(4) complex to filamentous actin: alteration in helical parameters and visualisation of thymosin β (4) binding on F-actin. J Mol Biol. 2002 Jan 25;315(4):613-25.

219. Quilty JA, Reithmeier RA. Trafficking and folding defects in hereditary spherocytosis mutants of the human red cell anion exchanger. Traffic. 2000 Dec;1(12):987-98.

220. Oloumi A, McPhee T, Dedhar S. Regulation of E-cadherin expression and β -catenin/Tcf transcriptional activity by the integrin-linked kinase. Biochim Biophys Acta. 2004 Apr 1;1691(1):1-15.

221. Persad S, Attwell S, Gray V, Mawji N, Deng JT, Leung D, et al. Regulation of protein kinase B/Akt-serine 473 phosphorylation by integrin-linked kinase: critical roles for kinase activity and amino acids arginine 211 and serine 343. J Biol Chem. 2001 Jul 20;276(29):27462-9.

222. Wu C. The PINCH-ILK-parvin complexes: assembly, functions and regulation. Biochim Biophys Acta. 2004 Jul 5;1692(2-3):55-62.

223. Yamaji S, Suzuki A, Sugiyama Y, Koide Y, Yoshida M, Kanamori H, et al. A novel integrin-linked kinase-binding protein, affixin, is involved in the early stage of cell-substrate interaction. J Cell Biol. 2001 Jun 11;153(6):1251-64.

224. Matsuda C, Kameyama K, Tagawa K, Ogawa M, Suzuki A, Yamaji S, et al. Dysferlin interacts with affixin (beta-parvin) at the sarcolemma. J Neuropathol Exp Neurol. 2005 Apr;64(4):334-40.

225. Corrado K, Mills PL, Chamberlain JS. Deletion analysis of the dystrophin-actin binding domain. FEBS Lett. 1994 May 16;344(2-3):255-60.

226. Kuhlman PA, Hemmings L, Critchley DR. The identification and characterisation of an actin-binding site in α-actinin by mutagenesis. FEBS Lett. 1992 Jun 15;304(2-3):201-6.

227. Carugo KD, Banuelos S, Saraste M. Crystal structure of a calponin homology domain. Nat Struct Biol. 1997 Mar;4(3):175-9.

228. Lindsey AE, Schneider K, Simmons DM, Baron R, Lee BS, Kopito RR. Functional expression and subcellular localization of an anion exchanger cloned from choroid plexus. Proc Natl Acad Sci U S A. 1990 Jul;87(14):5278-82.

229. Benting JH, Rietveld AG, Simons K. N-Glycans mediate the apical sorting of a GPI-anchored, raft-associated protein in Madin-Darby canine kidney cells. J Cell Biol. 1999 Jul 26;146(2):313-20.

230. Bastani B, Gluck SL. New insights into the pathogenesis of distal renal tubular acidosis. Miner Electrolyte Metab. 1996;22(5-6):396-409.

231. Golemis EA, Serebriiskii I, Law SF. The yeast two-hybrid system: criteria for detecting physiologically significant protein-protein interactions. Curr Issues Mol Biol. 1999;1(1-2):31-45.

232. Estojak J, Brent R, Golemis EA. Correlation of two-hybrid affinity data with in vitro measurements. Mol Cell Biol. 1995 Oct;15(10):5820-9.

233. Bartel P, Chien CT, Sternglanz R, Fields S. Elimination of false positives that arise in using the two-hybrid system. Biotechniques. 1993 Jun;14(6):920-4.

234. Kelleher DJ, Karaoglu D, Mandon EC, Gilmore R. Oligosaccharyltransferase isoforms that contain different catalytic STT3 subunits have distinct enzymatic properties. Mol Cell. 2003 Jul;12(1):101-11.

235. Tisdale EJ. Glyceraldehyde-3-phosphate dehydrogenase is required for vesicular transport in the early secretory pathway. J Biol Chem. 2001 Jan 26;276(4):2480-6.

236. Tisdale EJ. Glyceraldehyde-3-phosphate dehydrogenase is phosphorylated by protein kinase Ciota /lambda and plays a role in microtubule dynamics in the early secretory pathway. J Biol Chem. 2002 Feb 1;277(5):3334-41.

237. Ercolani L, Brown D, Stuart-Tilley A, Alper SL. Colocalization of GAPDH and band 3 (AE1) proteins in rat erythrocytes and kidney intercalated cell membranes. Am J Physiol. 1992 May;262(5 Pt 2):F892-6.

238. Stradal T, Kranewitter W, Winder SJ, Gimona M. CH domains revisited. FEBS Lett. 1998 Jul 17;431(2):134-7.

239. Bramham J, Hodgkinson JL, Smith BO, Uhrin D, Barlow PN, Winder SJ. Solution structure of the calponin CH domain and fitting to the 3D-helical reconstruction of F-actin:calponin. Structure (Camb). 2002 Feb;10(2):249-58.

240. Sundberg U, Beauchemin N, Obrink B. The cytoplasmic domain of CEACAM1-L controls its lateral localization and the organization of desmosomes in polarized epithelial cells. J Cell Sci. 2004 Mar 1;117(Pt 7):1091-104.

241. Quick MW, Hu J, Wang D, Zhang HY. Regulation of a gamma-aminobutyric acid transporter by reciprocal tyrosine and serine phosphorylation. J Biol Chem. 2004 Apr 16;279(16):15961-7.

# APPENDIX

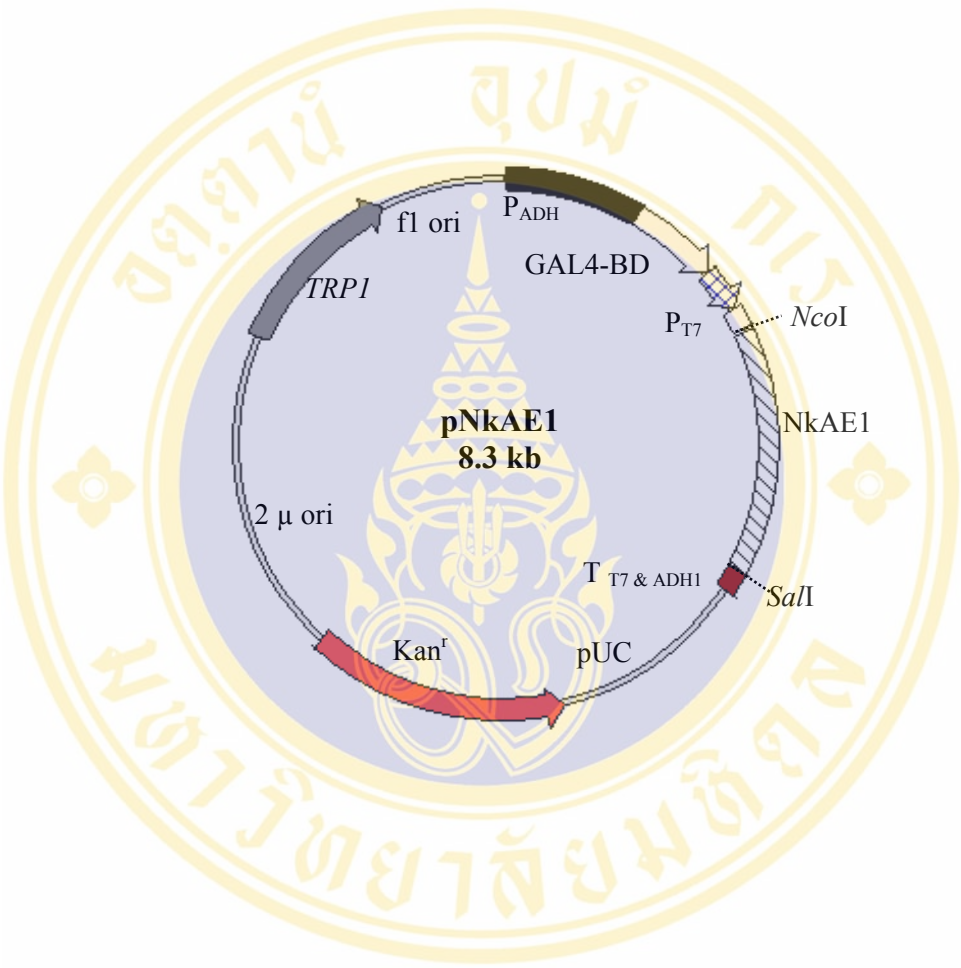


**Figure 39 Physical map of recombinant plasmid pNkAE1.**

The figure represents the recombinant plasmid pNkAE1 containing cDNA encoding NkAE1, the N-terminus of kidney anion exchanger 1 (Met66-Pro403 of human eAE1). The other regions illustrate the pGBKT7 vector backbone.

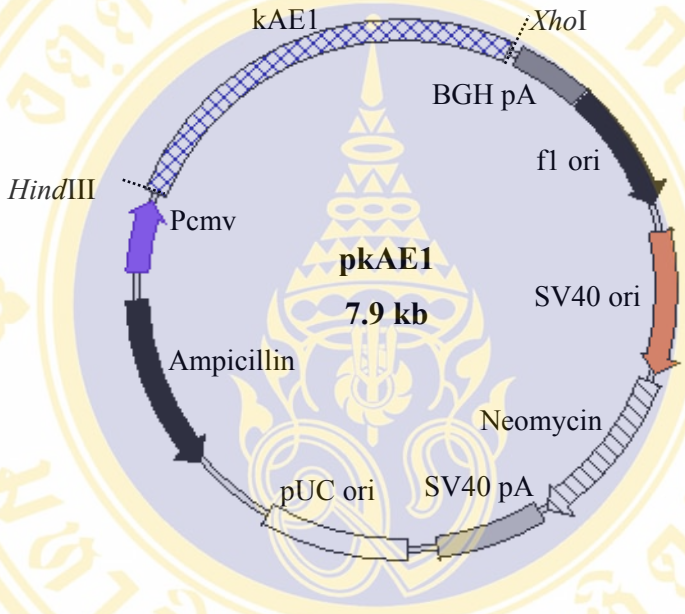


**Figure 40 Physical map of recombinant plasmid pkAE1.**

The figure represents the recombinant plasmid pkAE1 containing cDNA encoding full length human kidney anion exchanger 1 (kAE1). The other regions illustrate the pcDNA 3.1 (+) vector backbone.

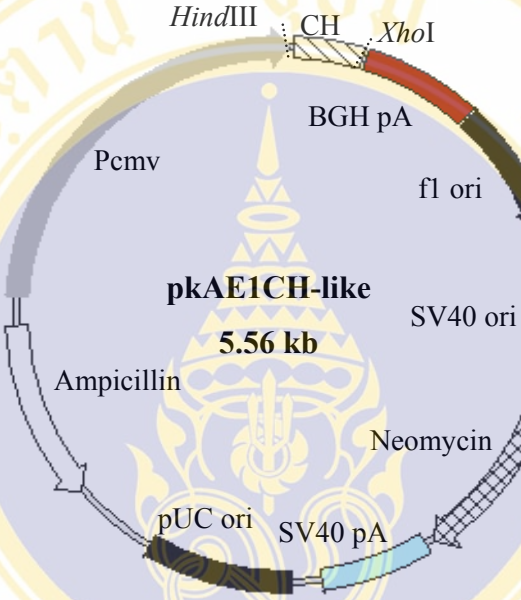


**Figure 41 Physical map of recombinant plasmid pkAE1CH-like.**

The figure represents the recombinant plasmid pkAE1CH-like containing cDNA encoding calponin homology domain (CH) identified in the N-terminus of kAE1 with amino acids 27-189. The other regions illustrate the pcDNA 3.1 (+) vector backbone.

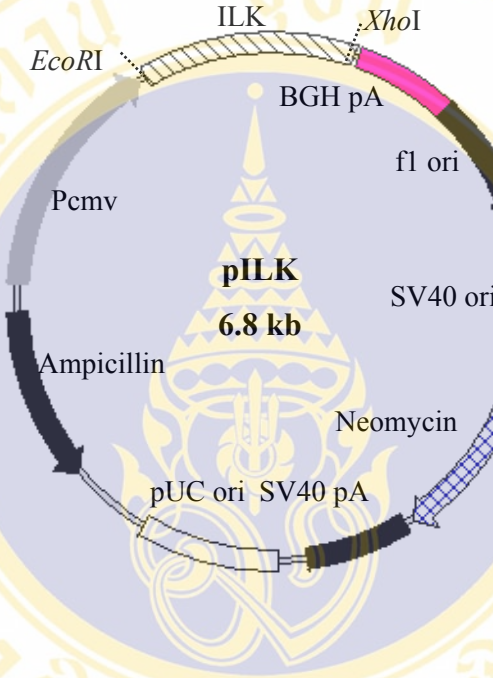


**Figure 42 Physical map of recombinant plasmid pILK.**

The figure represents the recombinant plasmid pILK containing cDNA encoding full length human integrin-linked kinase (ILK). The other regions illustrate the pcDNA 3.1/His B vector backbone.

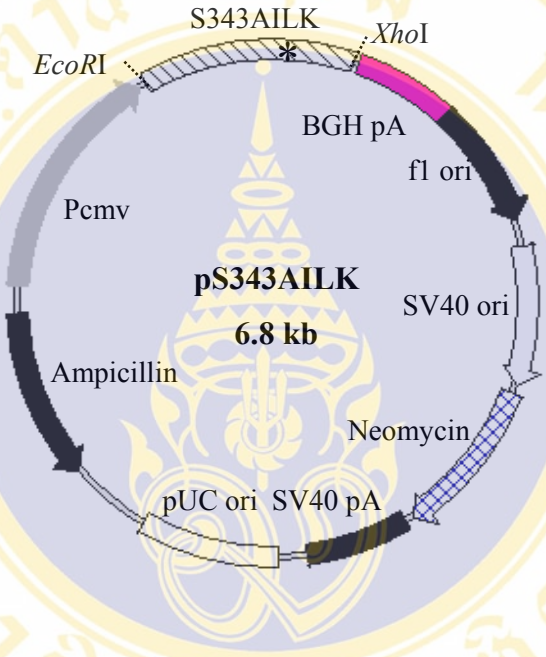


**Figure 43 Physical map of recombinant plasmid pS343AILK.**

The figure represents the recombinant plasmid pS343AILK containing the coding sequence for ILK mutant (S343A) to express kinase-dead domain (S343AILK). The other regions illustrate the pcDNA 3.1/His B vector backbone.

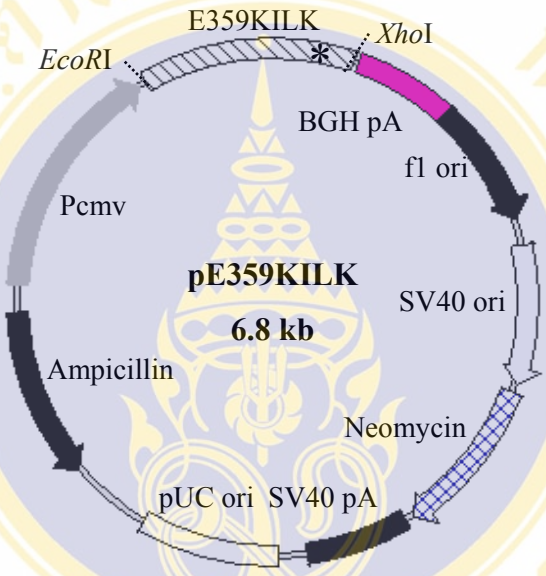


**Figure 44 Physical map of recombinant plasmid pE359KILK.**

The figure represents the recombinant plasmid pE359KILK containing the coding sequence for ILK mutant (E359K) to express kinase-dead domain (E359KILK). The other regions illustrate the pcDNA 3.1/His B vector backbone.

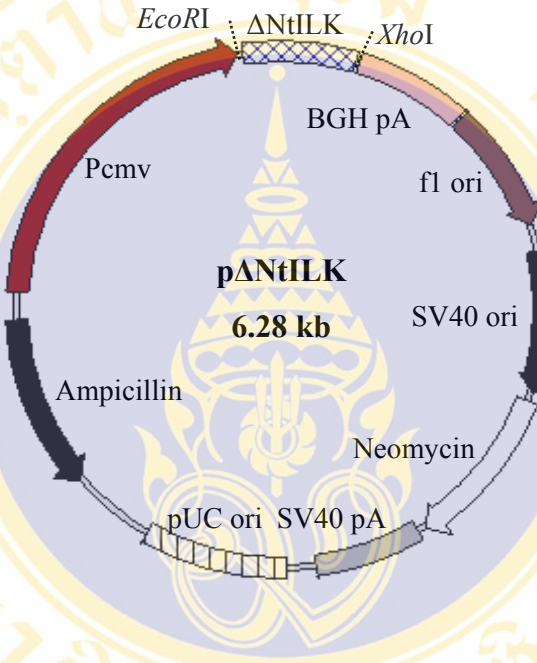


**Figure 45 Physical map of recombinant plasmid pΔNtILK.**

The figure represents the recombinant plasmid pΔNtILK containing the coding sequence for ILK with a deletion of amino acid 1-192 at the N-terminus (pΔNtILK). The other regions illustrate the pcDNA 3.1/His B vector backbone.

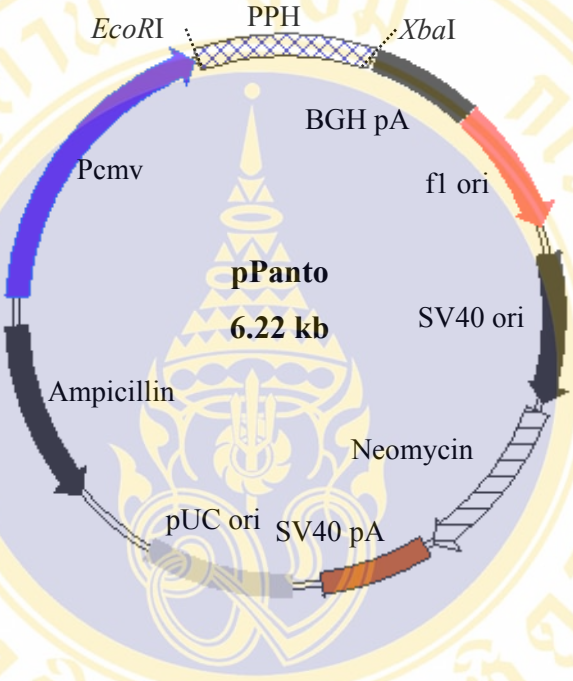


**Figure 46 Physical map of recombinant plasmid pPanto.**

The figure represents the recombinant plasmid pPanto containing cDNA encoding full length human pantophysin (PPH). The other regions illustrate the pcDNA 3.1/His B vector backbone.

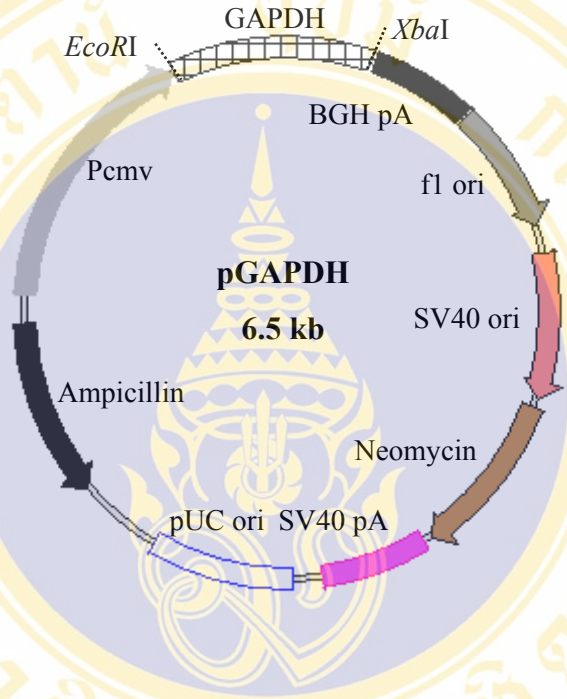


**Figure 47 Physical map of recombinant plasmid GAPDH.**

The figure represents the recombinant plasmid pGAPDH containing cDNA encoding full length glyceraldehydes-3-phosphate dehydrogenase (GAPDH). The other regions illustrate the pcDNA 3.1/His B vector backbone.

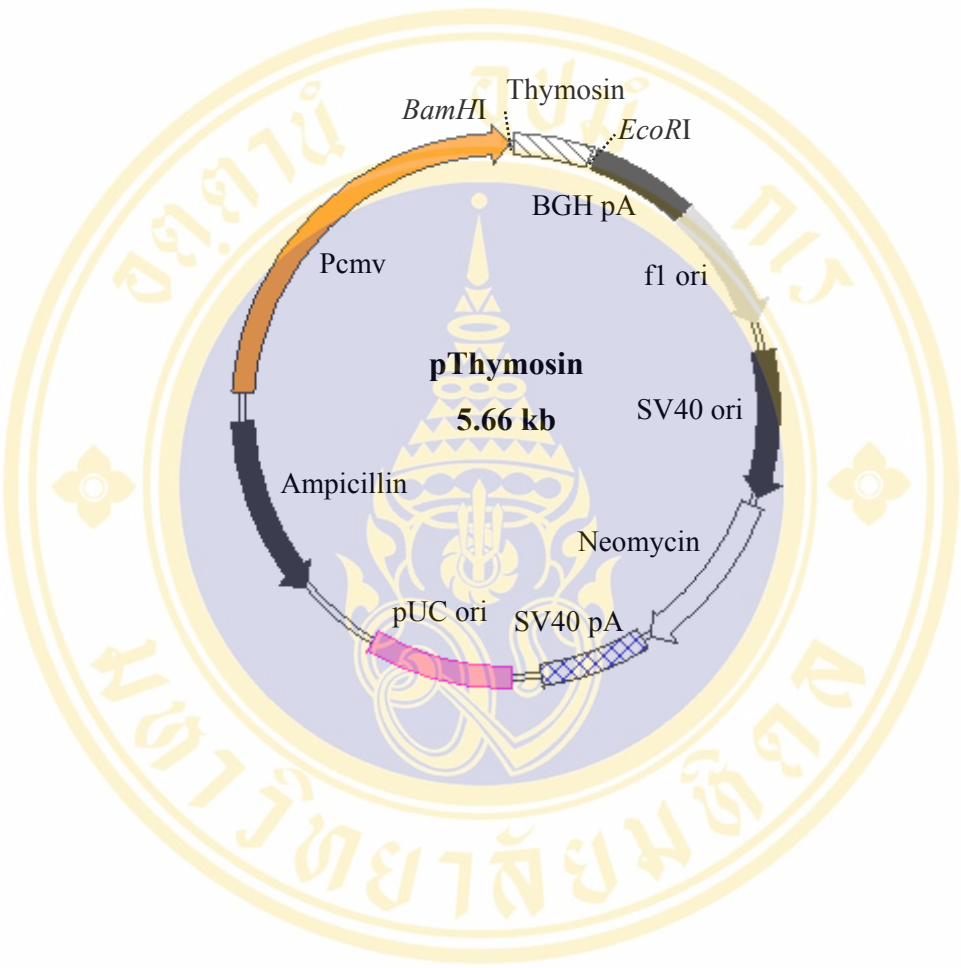


**Figure 48 Physical map of recombinant plasmid pThymosin.**

The figure represents the recombinant plasmid pThymosine containing cDNA encoding full length human thymosin β4. The other regions illustrate the pcDNA 3.1/His B vector backbone.

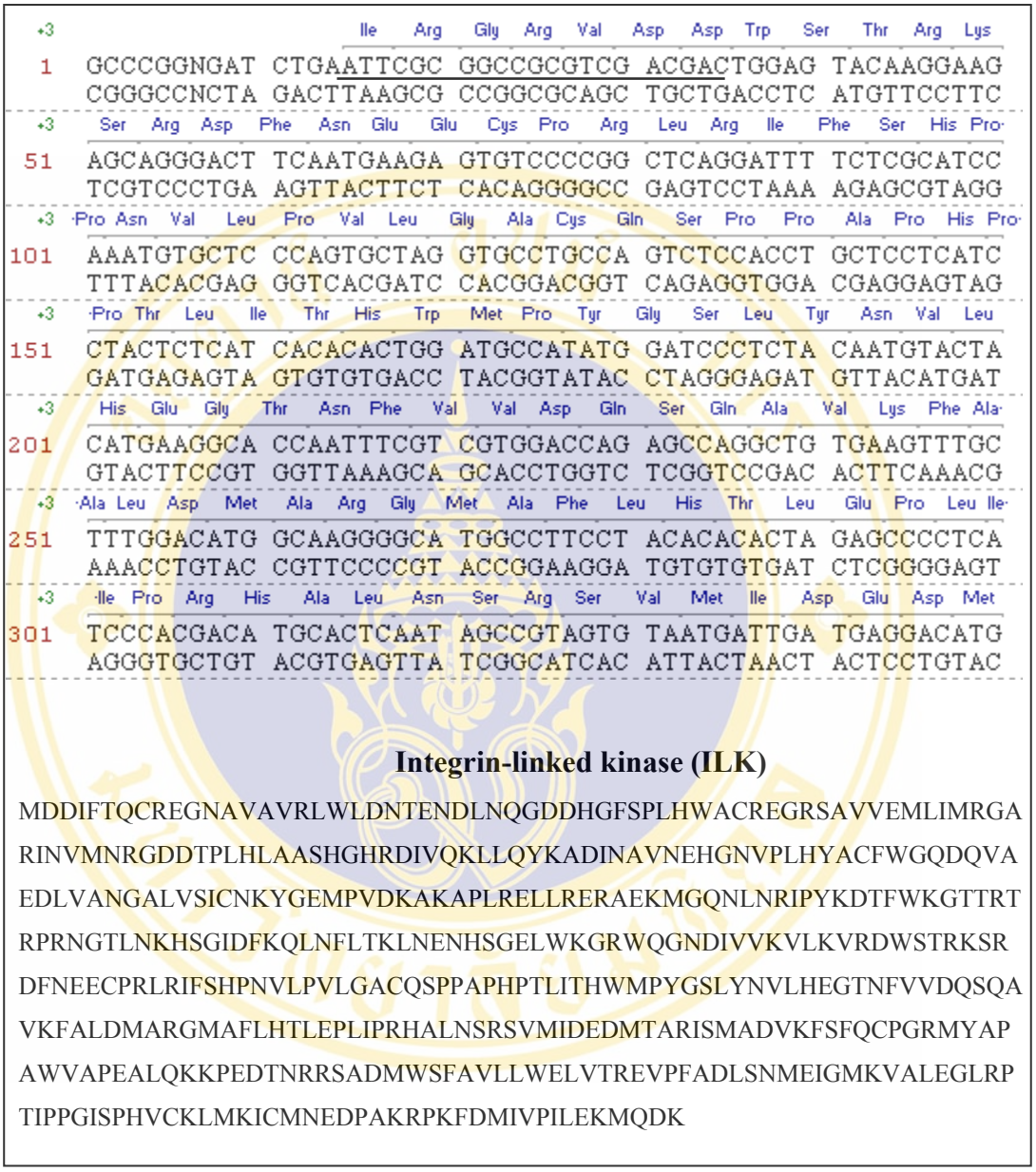


**Integrin-linked kinase (ILK)**

MDDIFTQCREGNAVAVRLWLDNTENDLNQGDDHGFSPLHWACREGRSAVVEMLIMRGA
RINVMNRGDDTPLHLAASHGHRDIVQKLLQYKADINAVNEHGNVPLHYACFWGQDQVA
EDLVANGALVSICNKYGEMPVDKAKAPLRELLRERAEKMGQNLNRIPYKDTFWKGTTRT
RPRNGTLNKHSGIDFKQLNFLTKLNENHSGELWKGRWQGNDIVVKVLKVRDWSTRKSR
DFNEECPRLRIFSHPNVLPVLGACQSPPAPHPTLITHWMPYGSLYNVLHEGTNFVVDQSQA
VKFALDMARGMAFLHTLEPLIPRHALNSRSVMIDEDMTARISMADVKFSFQCPGRMYAP
AWVAPEALQKKPEDTNRRSADMWSFAVLLWELVTREVPFADLSNMEIGMKVALEGLRP
TIPPGISPHVCKLMKICMNEDPAKRPKFDMIVPILEKMQDK

**Figure 49 cDNA insert encoding ILK screened by yeast two-hybrid system.**

The figure illustrates cDNA insert sequences of positive clone encoding in-frame ILK obtained from yeast two-hybrid screening (upper). The underlined represent adaptor linker for cloning purpose. Human ILK composes of 452 amino acids (lower).

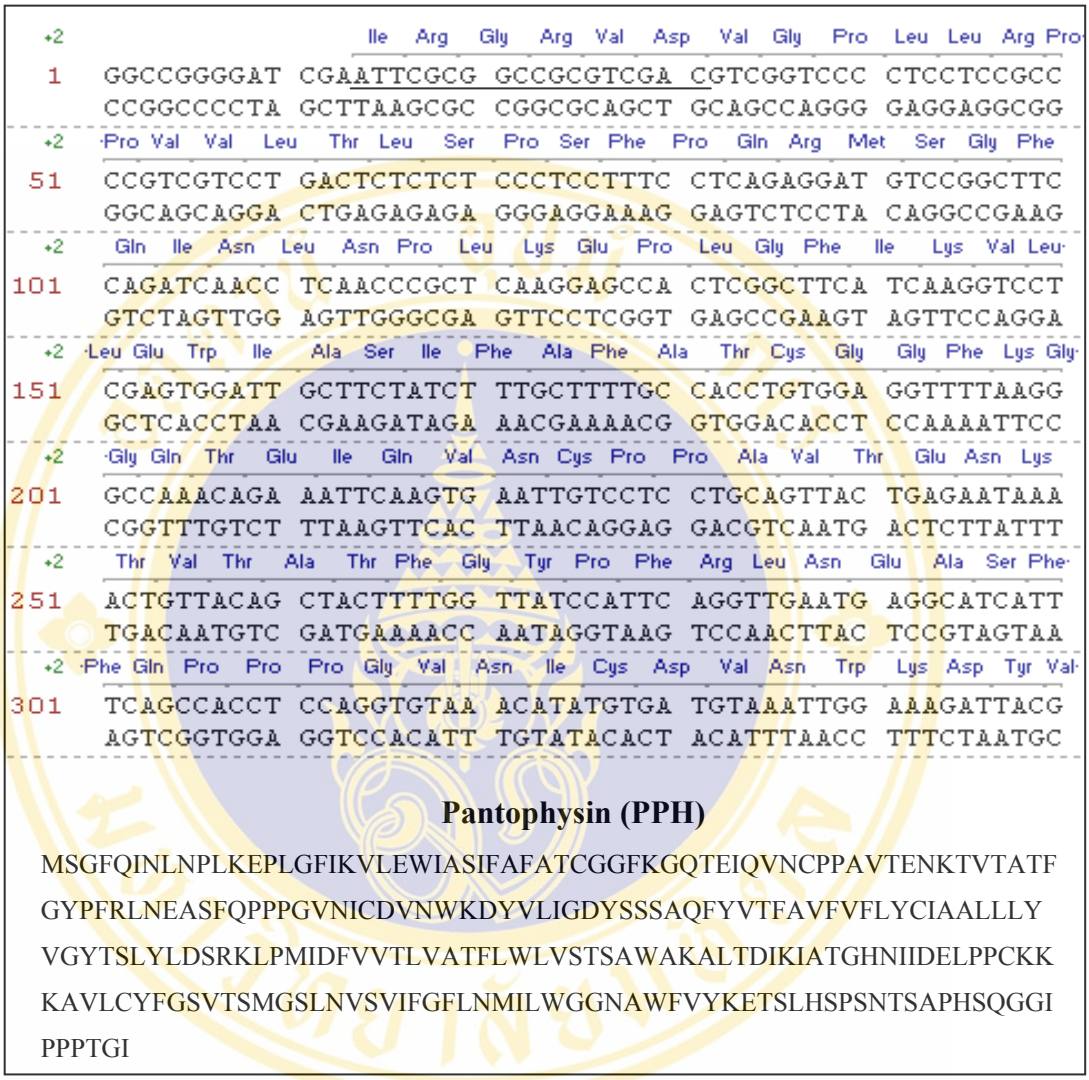


**Figure 50 cDNA insert encoding pantophysin screened by yeast two-hybrid system.**

The figure illustrates cDNA insert sequences of positive clone obtained from yeast two-hybrid screening (upper). These sequences are homologous to synaptophysin-like protein (pantophysin). The underlined represent adaptor linker for cloning purpose. Human pantophysin composes of 241 amino acids (lower).

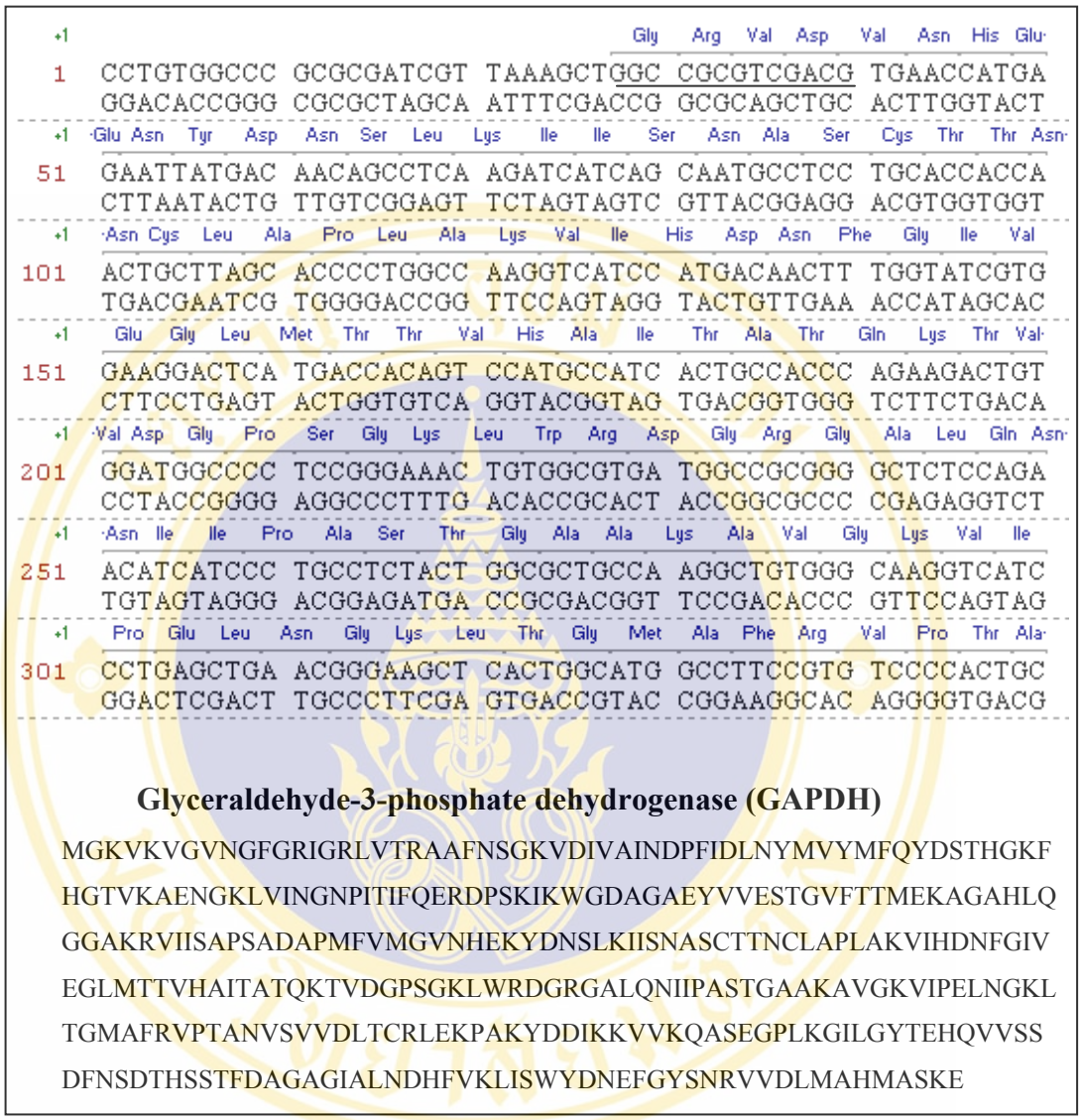


**Figure 51 cDNA insert encoding GAPDH screened by yeast two-hybrid system.**
The figure illustrates cDNA insert sequences of positive clone encoding in-frame GAPDH obtained from yeast two-hybrid screening. The underlined represent adaptor linker for cloning purpose (upper). Human GAPDH composes of 335 amino acids (lower).

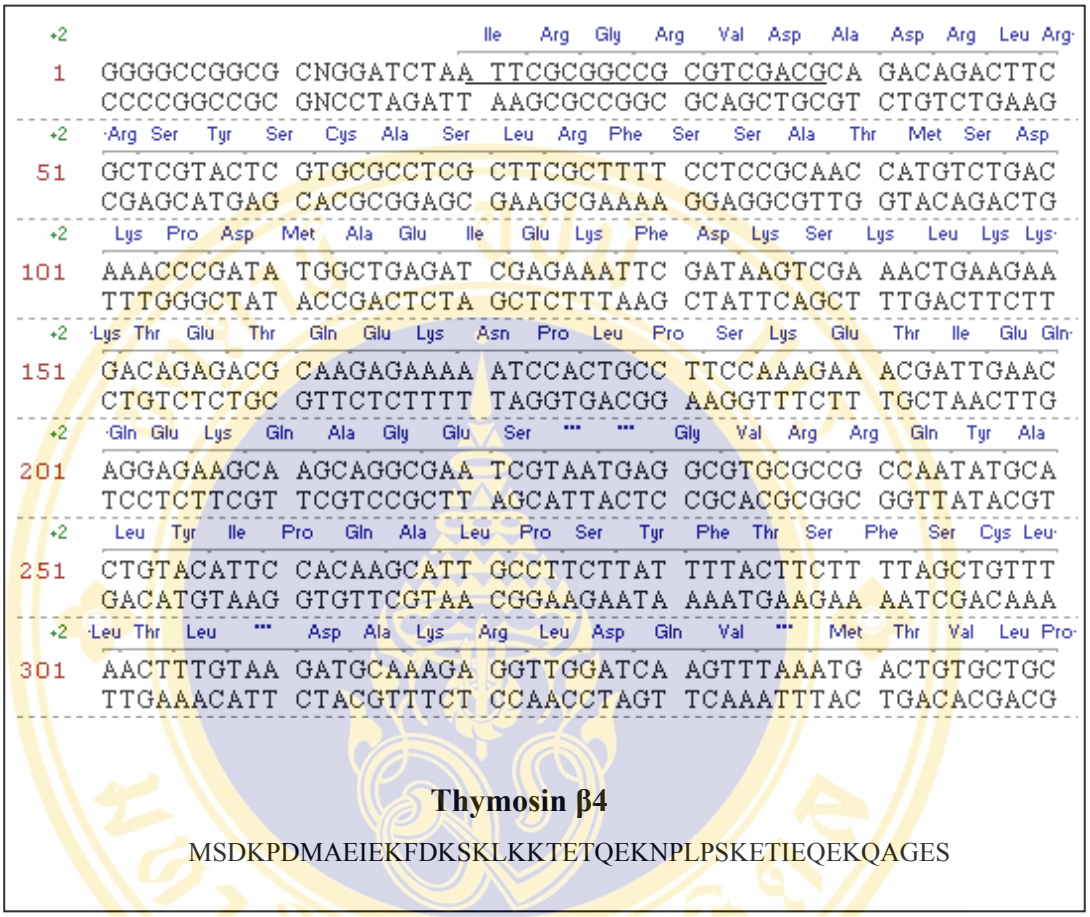


**Figure 52 cDNA insert encoding thymosin β4 screened by yeast two-hybrid system.**

The figure illustrates cDNA insert sequences of positive clone encoding in-frame thymosin β4 obtained from yeast two-hybrid screening. The underlined represent adaptor linker for cloning purpose (upper). Human thymosin β4 composes of 54 amino acids (lower).

## 1. Growth media

### 1.1 Bacterial media

#### 1.1.1 Low salt Luria-Bertani plate (LB plate)

Per liter:

| | | |
|---|---|---|
| Peptone | 10 | g |
| Yeast extract | 5 | g |
| NaCl | 10 | g |
| Agar | 15 | g |

Distilled water was added up to 950 ml.

The mixture was shaken until the solutes dissolved and adjust the volume of solution to 1 liter with distilled water. This media was sterilized by autoclaving for 20 min at 15 psi on liquid cycle.

#### 1.1.2 Low salt Luria-Bertani broth (LB broth)

LB broth medium was made the same way as LB plate, leaving out the agar.

#### 1.1.3 Luria-Bertani media with kanamycin or ampicillin

When the medium cool down to approximately 50 °C, 50 mg/ml kanamycin (100mg/ml ampicillin) was added to LB medium to a final concentration of 50 µg/ml for kanamycin or 100 µg/ml for ampicillin.

#### 1.1.4 SOB broth

To 950 ml of distilled water, add:

| | | |
|---|---|---|
| Peptone | 20 | g |
| Yeast extract | 5 | g |
| NaCl | 0.5 | g |
| 250 mM KCl | 10 | ml |

The mixture was shaken until the solutes dissolved and adjust the pH to 7.0 with 5 N NaOH and adjust the volume of solution to 1 liter with distilled water. This medium was sterilized by autoclaving for 20 min at 15 psi on liquid cycle. After autoclaving, 5 ml of 2 M $MgCl_2$ was added.

#### 1.1.5 SOC broth

Preparation of SOC broth was the same as SOB medium except it contains 20 mM glucose. After the SOB broth has been autoclaved, allowed cooling to 65 °C before adding 20 ml of sterile 1 M glucose.

**1.2 Yeast media**

**1.2.1 YPD plate**

Per liter:

To 950 ml of distilled water, add:

| | | |
|---|---|---|
| Peptone | 20 | g |
| Yeast extract | 10 | g |
| Agar | 20 | g |

The mixture was shaken until the solutes dissolved and adjusted the volume to 1 liter with distilled water. It was sterilized by autoclaving for 20 min at 15 psi on liquid cycle.

**1.2.2 YPD broth**

YPD broth was made the same way as YPD plate, leaving out agar.

**1.2.3 YPDA plate**

For adenine-supplemented YPD (YPDA), add 15 ml of a 0.2% adenine hemisulfate solution per liter of medium (final concentration is 0.003%). Adenine hemisulfate tolerates autoclaving.

**1.2.4 YPDA broth**

YPDA broth was made the same way as YPDA plate, leaving out agar.

**1.2.5 YPDA with kanamycin**

For kanamycin-containing medium, prepare YPD or YPD above. After autoclaved medium has cooled to 55 °C, add 0.2–0.3 ml of 50 mg/ml kanamycin (final concentration10–15 mg/L).

**1.2.6 Yeast nitrogen base without amino acids (YNB) plate**

Per liter:

To 950 ml of distilled water, add:

| | | |
|---|---|---|
| YNB | 7 | g |
| Agar | 20 | g |

The mixture was shaken until the solutes dissolved and adjusted the volume of solution to 1 liter with distilled water. It was sterilized by autoclaving for 20 min at 15 psi on liquid cycle.

**1.2.7 YNB broth**

YNB broth was made the same way as YNB plate, leaving out agar.

### 1.2.8 10X dropout solution

Dissolve all components below with 1 liter distilled water

**Nutrient 10X**

**Concentration**

| | | |
|---|---|---|
| L-Arginine HCl | 200 | mg/L |
| L-Isoleucine | 300 | mg/L |
| L-Lysine HCl | 300 | mg/L |
| L-Methionine | 200 | mg/L |
| L-Phenylalanine | 500 | mg/L |
| L-Threonine | 2000 | mg/L |
| L-Tyrosine | 300 | mg/L |
| L-Uraci | 200 | mg/L |
| L-Valine | 1500 | mg/L |

These components below were made separately.

| | | |
|---|---|---|
| L-Adenine hemisulfate salt | 10 | g/L |
| L-Histidine HCl monohydrate | 10 | g/L |
| L-Leucine | 10 | g/L |
| L-Tryptophan | 10 | g/L |

Dropout supplements were autoclaved and stored at 4 °C for up to 1 year.

### 1.2.9 Synthetic dropout medium (SD)

Per liter:

| SD plates | YNB agar | 40% glucose | 10X dropout solution | Adenine (10 g/L) | Histidine (10 g/L) | Leucine (10 g/L) | Tryptophan (10 g/L) |
|---|---|---|---|---|---|---|---|
| SD/-Trp | 836 ml | 50 ml | 100 ml | 2 ml | 2 ml | 10 ml | - |
| SD/-Leu | 844 ml | 50 ml | 100 ml | 2 ml | 2 ml | - | 2 ml |
| SD/-Trp/-Lue | 846 ml | 50 ml | 100 ml | 2 ml | 2 ml | - | - |
| SD/-Trp/-Leu/-His/-Ade | 850 ml | 50 ml | 100 ml | - | - | - | - |

### 1.2.10 Liquid dropout medium

Liquid dropout medium was made the same way as dropout plates except replacement YNB agar with YNB broth.

**1.2.11 X-α-Gal stock**

Dissolve 5-bromo-4-chloro-3-indolyl-β-D-galactopyranoside in N,Ndimethyl-formamide (DMF) to final concentration 20 mg/ml. It can be stored in the dark at -20 °C.

**1.2.12 Synthetic dropout medium containing X-α-Gal**

Per liter:

The appropriate dropout agar medium 1 liter was prepared and autoclaved for 20 min at 15 psi. Let cool to 55 °C and added 2 ml of X-α-Gal (20 mg/ml).

**2. For transformation of yeast**

**2.1 PEG/LiAc solution** (polyethylene glycol/lithium acetate)

Prepare fresh just prior to use.

| | Final Conc. | To prepare 10 ml of solution |
|---|---|---|
| PEG 4000 | 40% | 8 ml of 50% PEG |
| TE buffer | 1X | 1 ml of 10X TE |
| LiAc | 1X | 1 ml of 10X LiAc |

**2.2 Stock solutions**

**50% PEG 3350** (Polyethylene glycol, avg. mol. wt. = 3,350; Sigma #P-3640) prepare with sterile deionized $H_2O$; if necessary, warm solution to 50 °C to help the PEG go into solution.

**100% DMSO** (Dimethyl sulfoxide; Sigma #D-8779)

**10X TE buffer:** 0.1 M Tris-HCl, 10 mM EDTA, pH 7.5. Autoclave.

**10X LiAc:** 1 M lithium acetate (Sigma #L-6883) Adjust to pH 7.5 with dilute acetic acid and autoclave.

**3. For protein extraction from yeast**

**3.1 Cracking buffer stock solution**

| | To prepare 100 ml: | |
|---|---|---|
| 8M Urea | 48 | g |
| 5% (w/v) SDS | 5 | g |

| | | |
|---|---|---|
| 40 mM Tris-HCl [pH6.8] | 4 | ml of a 1 M stock solution |
| 0.1 mM EDTA* | 20 | ml of a 0.5 M stock |
| 0.4 mg/ml Bromophenol blue | 40 | mg |
| Deionized water | to a final volume of 100 ml | |

* EDTA primarily inhibits metalloproteases.

**3.2 Complete cracking buffer** (complete): The following recipe is sufficient for one protein extract. Prepare only the volume required just before use.

| | To prepare 1.13 ml of complete cracking buffer: | |
|---|---|---|
| Cracking buffer stock solution | 1 | ml (recipe above) |
| β-mercaptoethanol | 10 | ml |
| Protease inhibitor cocktails | | |

**4. For β-galactosidase Filter Assays**

**4.1 Z-buffer**

| | | |
|---|---|---|
| $Na_2HPO_4\ 7H_2O$ | 16.1 | g/L |
| $NaH_2PO_4\ H_2O$ | 5.50 | g/L |
| KCl | 0.75 | g/L |
| $MgSO_4\ 7H_2O$ | 0.246 | g/L |

Adjust to pH 7.0 and autoclave. It can be stored at room temperature for up to 1 year.

**4.2 X-β-gal stock solution**

Dissolve 5-bromo-4-chloro-3-indolyl-β-D-galactopyranoside (X-GAL; #8060-1) in N,N-dimethylformamide (DMF) at a concentration of 20 mg/ml. Store in the dark at –20 °C.

**4.3 Z buffer/X-gal solution**

| | | |
|---|---|---|
| Z buffer | 100 | ml |
| β-mercaptoethanol (Sigma #M-6250) | 0.27 | ml |
| X-gal stock solution | 1.67 | ml |

**5. For SDS-PAGE and immunoblotting**

**5.1 10% SDS-polyacrylamide gel**

| Reagents | 10% Separating gel/15 ml | 4% Stacking gel/5 ml |
|---|---|---|
| Acrylamide/bis-acrylamide mix solution (ml) | 5.00 | 0.67 |
| Separating gel buffer (ml) | 3.75 | - |
| Stacking gel buffer (ml) | - | 1.25 |
| Distilled water (ml) | 6.25 | 3.05 |
| 10% ammonium persulfate (µl) | 75 | 50 |
| TEMED (µl) | 15 | 10 |

Allow the separating gel to polymerize for 30-45 min before pouring the stacking gel on top.

**5.2 Separating gel buffer (4x concentration)**

Per 500 ml:

| | | |
|---|---|---|
| 1.5 M Tris | 91 | g |
| 0.4% SDS | 2 | g |
| pH to 8.7 with HCl | | |

**5.3 Stacking gel buffer (4x concentration)**

Per 100 ml:

| | | |
|---|---|---|
| 0.4 M Tris | 6.05 | g |
| 0.4% SDS | 0.40 | g |
| pH to 6.8 with HCl | | |

**5.4 SDS sample loading buffer (2x concentration)**

Per 100 ml:

| | | |
|---|---|---|
| 20% glycerol | 20 | ml |
| 2% β-mercaptoethanol | 2 | ml |
| 4% SDS | 4 | g |
| 0.13 M Tris | 1.52 | g |
| Bromophenol blue | 1 | mg |
| pH to 6.8 with HCl | | |

**5.5 Reservoir buffer (10x concentration)**

Per liter:

| | | |
|---|---|---|
| 0.125 M Tris | 30.2 | g |
| 0.960 M glycine | 72 | g |
| 0.5% SDS | 5 | g |

pH~ 8.3 when diluted, do not adjust pH

**5.6 Acrylamide stock**

Per 100 ml:

| | | |
|---|---|---|
| 30% acrylamide | 30 | g |
| 0.8% bis-acrylamide | 0.8 | g |

Kept at 4 °C in brown bottle

**5.7 Transblot buffer**

Per liter:

| | | |
|---|---|---|
| 25 mM Tris base | 3.63 | g |
| 192 mM Glycine | 17.28 | mM |
| 20% Methanol | 200 | ml |

**5.8 TBST**

Per liter:

| | | |
|---|---|---|
| 20 mM Tris, pH 7.5 | 2.42 | g Tris base |
| 137 mM NaCl | 8 | g |
| 0.1% Tween-20 | 1 | ml |
| Distilled water | to 1 | liter |

**6. For transfection using calcium phosphate precipitation method**

**6.1 2x HEPES (500 ml)**

| | | |
|---|---|---|
| NaCl | 8 | g |
| $Na_2HPO_4$ (anhydrous) | 0.105 | g |
| HEPES | 6.5 | g |

Distilled water 500 ml

pH to 7.0 and filter sterilize. Store in frozen aliquots, but keep in refrigerator after thawing.

**6.2 2 M $CaCl_2$**

Filter sterilize. Store in frozen aliquots, but keep in refrigerator after thawing.

**7. Solutions and buffers for general used**

**7.1 TE**

| | | |
|---|---|---|
| Tris HCl | 10 | mM |
| EDTA, pH 7.5 | 0.1 | mM |

**7.2 50x TAE**

| | | |
|---|---|---|
| Tris base | 242 | g |
| 0.5 M EDTA, pH 8.0 | 100 | ml |
| Glacial acetic acid | 57.1 | ml |

**7.3 Agarose gel loading dye**

40% sucrose

xylene cyanol

0.5 M EDTA

# BIOGRAPHY

| | |
|---|---|
| **NAME** | Mrs. Thitima Keskanokwong |
| **DATE OF BIRTH** | 1 MAY 1974 |
| **PLACE OF BIRTH** | Burirum, Thailand |
| **INSTITUTIONS ATTENDED** | Khon Kaen University, 1992-1995<br>Bachelor of Science (Biochemistry)<br>Mahidol University, 1997-2001<br>Master of Science (Biochemistry)<br>Mahidol Universtiy, 2002-2007<br>Doctor of Philosophy (Molecular Genetics and Genetic Engineering) |
| **RESEARCH GRANT** | Royal Golden Jubilee Ph.D. Scholarship From Thailand Research Fund (TRF) |

**PUBLICATION:**

1. Keskanokwong T, Shandro HJ, Johnson DE, Kittanakom S, Vilas GL, Thorner P, Reithmeier RA, Akkarapatumwong V, Yenchitsomanus PT, Casey JR. Interaction of Integrin linked Kinase with kAE1 $Cl^-/HCO_3^-$ Exchanger. Journal of Biological Chemistry (in press).

**SCIENTIFIC PRESENTATIONS:**

1. Thitima Keskanokwong, Haley J. Shandro, Saranya Kittanakom, Reinhart A. F. Reithmeier, Pa-thai Yenchitsomanus, Joseph R. Casey and Varaporn Akkarapatumwong. A New Insight Into Anion Exchanger 1 (AE1) Trafficking In Human Kidney. Gordon Research Conference on Membrane Transport Protein, 13-18 Aug 2006, University of New England, Biddeford, Maine, USA.

2. Keskanokwong T, Akkarapatumwong V, Haley J. Shandro, *et al*. Integrin-linked Kinase Promotes Intracellular Processing of Kidney Anion ($Cl^-/HCO_3^-$) Exchanger 1 (kAE1). RGJ-Ph.D. Congress VII, 20-22 April 2006, Jomtien Palm Beach Resort, Pattaya, Chonburi, Thailand.

3. Keskanokwong T, Akkarapatumwong V, Yenchitsomanus P. Identification of protein binding to anion exchanger 1 in human kidney. RGJ-Ph.D. Congress V, 23-25 April 2004, Jomtien Palm Beach Resort, Pattaya, Chonburi, Thailand.